THE UNIVERSITY OF MICHIGAN
COLLEGE OF ENGINEERING
Department of Chemical Engineering

Technical Report

CALORIMETRIC STUDIES ON ARGON AND HEXAFLUORO ETHANE AND A GENERALIZED CORRELATION OF MAXIMA IN ISOBARIC HEAT CAPACITY

Kwan Y. Kim

DRDA Project 003470

Supported by:

NATIONAL SCIENCE FOUNDATION
GRANT NO. GK-24719
WASHINGTON, D.C.

administered through:

DIVISION OF RESEARCH DEVELOPMENT AND ADMINISTRATION ANN ARBOR

January 1974

To my mother, Mrs. Chong Kil Yi

and

My wife, Hae Rim

ACKNOWLEDGEMENTS

I wish to express my appreciation to the following people who contributed to the success of this work:

To Professor John E. Powers, the chairman of my thesis committee, for his guidance and encouragement.

To Professors Dale E. Briggs, James H. Hand and Edgar F. Westrum, Jr., for serving on the doctoral committee.

To Joseph C. Golba who contributed to this work by assisting in all phases of the experiments.

To Andre W. Furtado for many suggestions which involved the present work.

To Takaya Miyazaki for his help during the measurements of C_2F_6. To E. Ruke and H. Senecal of the ORA Instrument Shop and D. Connell of the Chemical Engineering Department for their shop services.

I also wish to acknowledge the following organizations: The National Science Foundation for support of the research and for provision of fellowships; the E. I. du Pont de Nemours & Co. for the donation of Freon-116 used in this work.

Finally, I would like to thank my mother, my wife and my daughter for their faith in me.

TABLE OF CONTENTS

Page

DEDICATION ii

ACKNOWLEDGEMENTS iii

LIST OF TABLES vii

LIST OF FIGURES ix

NOMENCLATURE xiii

ABSTRACT xvi

I. INTRODUCTION 1

II. PRELIMINARY CONSIDERATIONS 3

Thermodynamics of Flow Calorimetry 3

Data Interpretation 8

Thermodynamic Consideration for Basic Data 9

Constructing Equal Area Curve 12

Interpretation of Joule-Thomson Data 13

Thermodynamic Consistency Checks 14

Error Analysis 15

Corresponding States Principle 15

Significance of $C_p(T)$ Maxima 19

Previous Studies on $C_p(T)$ Maxima 22

Choice of Experimental Fluids 23

Previous Experimental Data for Argon 24

Previous Experimental Data for C_2F_6 27

III. CALORIMETRIC DETERMINATIONS WITH ARGON 28

The Recycle Flow System 28

Calorimeters 31

Experimental Measurements 31

Page

Experimental Procedure 40

Material Used 41

Region of Measurements 42

Results 45

C_p and $C_p(T)$ Maxima 48

Isenthalpic and Isothermal Data 53

Enthalpy Changes on Vaporization 56

Heat Leak Check 60

Thermodynamic Consistency Checks 60

Enthalpy Table and Diagram 63

Comparison With Other Published Data 68

IV. CALORIMETRIC DETERMINATIONS WITH HEXAFLUOROETHANE 75

New Recycle Flow System 75

Multipurpose Calorimeter 78

Experimental Measurements 80

Material Used 83

Region of Measurements 84

Determination of Liquid Densities 84

Results 91

C_p and $C_p(T)$ Maxima 91

Isothermal Data 97

Enthalpy Changes on Vaporization 101

Thermodynamic Consistency Checks 101

Enthalpy in the Critical Region 101

Enthalpy Table and Diagram 110

Comparison With Previous Experimental Data 110

Page

V. GENERALIZED CORRELATION FOR $C_p(T)$ MAXIMA 115

Data for Correlation 115

Location of $C_p(T)$ Maxima 119

Magnitude of $C_p(T)$ Maxima 119

Discussion of Results 125

VI. SUMMARY AND CONCLUSION 128

VII. RECOMMENDATIONS FOR FUTURE WORK 129

APPENDIX A. 131

APPENDIX B. 138

APPENDIX C. 149

REFERENCES 169

LIST OF TABLES

Table		Page
II-1.	A List of Fluids Suitable for Use in the Present Equipment	35
III-1.	Composition of Argon	42
III-2.	Isobaric Heat Capacities of Argon	51
III-3.	$C_p(T)$ Maxima Data for Argon	53
III-4.	Joule-Thomson Coefficients of Argon at -240°F	55
III-5.	Enthalpy Difference of -240°F Isotherm Calculated From the Isenthalpic Data	55
III-6.	$\phi(P)$ Maxima Data for Argon	56
III-7.	Isothermal Throttling Coefficients of Argon	58
III-8.	Saturation Data for Argon	60
III-9.	Tabulated Values of Saturation Enthalpy for Argon	65
III-10.	Tabulated Values of Enthalpy for Argon	66
III-11.	Comparison of Isobaric Heat Capacities of Argon	69
IV-1.	Composition of C_2F_6	83
IV-2.	Isobaric Heat Capacities of C_2F_6	92
IV-3.	$C_p(T)$ Maxima Data for C_2F_6	97
IV-4.	$\phi(P)$ Maxima Data for C_2F_6	97
IV-5.	Isothermal Throttling Coefficients of C_2F_6	98
IV-6.	Comparison of Saturation Data for C_2F_6	102
IV-7.	Enthalpy of C_2F_6 Near the Critical Point	107
IV-8.	Critical Constant for C_2F_6	110
IV-9.	Tabulated Values of Saturation Enthalpy for C_2F_6	112
IV-10.	Tabulated Values of Enthalpy for C_2F_6	113
V-1.	Sources of $C_p(T)$ Maxima and C_p^o Data	116

Table Page

V-2. Data Used in the Present Correlation 117

V-3. Critical Constants for the Substances Used in This Work 118

V-4. Comparison of the Data With Values Determined From the Correlation 126

V-5. Mean and Standard Deviations for $(T^M_{exp} - T^M_{calc})$ 127

A-1. Calibration Constants for Platinum Resistance Thermometer 132

A-2. Calibration Data for Thermopiles 133

A-3. Pressure Transducer (high) Calibrations 134

A-4. Pressure Transducer (low) Calibrations 135

A-5. Flow Meter Calibrations 136

A-6. Density Data of C_2F_6 at 0°F 137

B-1. Basic Isobaric Data for Argon 139

B-2. Basic Isothermal Data for Argon 144

B-3. Basic Isobaric Data for C_2F_6 145

B-4. Basic Isothermal Data for Argon 148

C-1. $\overline{C}_p$ Values for Argon 150

C-2. $\overline{\mu}$ Values of Argon 159

C-3. ϕ Values for Argon 159

C-4. Enthalpy Traverse Data for Argon 161

C-5. $\overline{C}_p$ Values for C_2F_6 163

C-6. $\overline{\phi}$ Values for C_2F_6 167

C-7. Enthalpy Traverse Data for C_2F_6 168

LIST OF FIGURES

Figure		Page
II-1.	A Schematic Diagram for a Flow Calorimeter............	4
II-2.	Schematic Diagram Illustrating the Calorimeter assemblies used in this work..........................	5
II-3.	Example of an Isobaric Run............................	11
II-4.	Example of an Isothermal Run..........................	11
II-5.	An Illustration of $C_p(T)$ Curves in the Supercritical Region.	20
II-6.	Plot Showing the Location of $C_p(T)$ Maxima.............	20
III-1.	Flow Diagram of the Recycle-Flow System Used for the Measurements With Argon...............................	29
III-2.	Pressure Transducer (High) Calibration................	34
III-3.	Pressure Transducer (Low) Calibration.................	34
III-4.	A Modified Circuit of Power Input to the Calorimeter..	36
III-5.	Flow Meter Calibration................................	39
III-6.	Comparison of the Present Flow Meter Calibration with a Generalized One by Furtado[18].........................	39
III-7.	Chromatographic Analysis of the Argon Sample from the System..	43
III-8.	Range of Calorimetric Determination on Argon	44
III-9.	Isobaric Heat Capacity for Argon at 286 psia	47
III-10.	Isobaric Heat Capacity for Argon at 457 psia..........	47
III-11.	Isobaric Heat Capacity for Argon at 571 psia	47
III-12.	Isobaric Heat Capacity for Argon at 1143 psia.........	48
III-13.	Isobaric Heat Capacity for Argon at 706 psia	49
III-14.	Isobaric Heat Capacity for Argon at 950 psia..........	49
III-15.	Isobaric Heat Capacity for Argon at 800 psia	49
III-16.	Isobaric Heat Capacity for Argon at 1371 psia	50

Figure Page

III-17. Isobaric Heat Capacity for Argon at 1714 psia 50

III-18. Isobaric Heat Capacity for Argon at 2000 psia 50

III-19. Joule-Thomson Coefficient for Argon at -240°F 54

III-20. Isothermal Throttling Coefficient for Argon at -168.3°F 54

III-21. Isothermal Throttling Coefficient for Argon at -208.9°F 57

III-22. Isothermal Throttling Coefficient for Argon at -191.2°F 57

III-23. Isothermal Throttling Coefficient for Argon at 167°F.. 57

III-24. Isobaric Enthalpy Traverse Across the Two Phase Boundary for Argon at 457 psia. 59

III-25. Isobaric Enthalpy Traverse Across the Two Phase Boundary for Argon at 286 psia........................ 59

III-26. Isobaric Enthalpy Traverse Across the Two Phase Boundary for Argon at 571 psia 59

III-27. Heat Leak Test for the Isobaric Calorimeter. Mean Heat Capacity of Argon as a Function of Reciprocal Flow Rate.. 61

III-28. Thermodynamic Consistency Checks for the Present Calorimetric Data for Argon 62

III-29. H-P-T Diagram for Argon 64

III-30. Comparison of the Present Isobaric Heat Capacities With Those from Walker[60] 73

III-31. Comparision of the Present Isobaric Heat Capacities With Those from Michels *et al.*[38, 39] 73

III-32. Comparison of the Present Isobaric Heat Capacities With Those Calculated from the Equation of State by Gosman *et al.*, [22] 73

III-33. Comparison of the Present Isobaric Heat Capacities in the High Temperature Region with Those From Michels, *et al.*,[38, 39] 74

III-34. Comparison of the Present Enthalpies with the Tabulated Values from IUPAC 74

Figure Page

IV-1. Flow Diagram of the New Recycle-Flow System.......... 76

IV-2. Diagram Illustrating the Principle of the Multipurpose Calorimeter 79

IV-3. Drawing of the Multipurpose Calorimeter Assembly 81

IV-4. Range of Calorimetric Determinations on C_2F_6 85

IV-5. Diagram Illustrating the Measurement of Liquid Density 86

IV-6. Arrangement for the Liquid Density Measurement 88

IV-7. Plot of Liquid Densities for C_2F_6 at 0°F 90

IV-8. Isobaric Heat Capacity for C_2F_6 at 490 psia 93

IV-9. Isobaric Heat Capacity for C_2F_6 at 437 psia........... 94

IV-10. Isobaric Heat Capacity for C_2F_6 at 442 psia 94

IV-11. Isobaric Heat Capacity for C_2F_6 at 247 psia 95

IV-12. Isobaric Heat Capacity for C_2F_6 at 432 psia 95

IV-13. Isobaric Heat Capacity for C_2F_6 at 700 psia........... 95

IV-14. Isobaric Heat Capacity for C_2F_6 at 839 psia 96

IV-15. Isobaric Heat Capacity for C_2F_6 at 1049 psia.......... 96

IV-16. Isobaric Heat Capacity for C_2F_6 at 1398 psia.......... 96

IV-17. Isobaric Heat Capacity for C_2F_6 at 1969 psia 96

IV-18. Isothermal Throttling Coefficient for Argon at 0°F ... 99

IV-19. Isothermal Throttling Coefficient for Argon at 67.5°F. 99

IV-20. Isothermal Throttling Coefficient for Argon at 122°F. 100

IV-21. Isothermal Throttling Coefficient for Argon at 176°F. 100

IV-22. Isothermal Throttling Coefficient for Argon at 247°F. 100

IV-23. Isobaric Enthalpy Traverse Across the Two Phase Boundary for C_2F_6 at 247 psia........................ 103

IV-24. Isobaric Enthalpy Traverse Across the Two Phase Boundary for C_2F_6 at 432 psia 103

Figure Page

IV-25. Thermodynamic Consistency Checks for the Present Calorimetric Data for C_2F_6 104

IV-26. Plots of Enthalpies at $C_p(T)$ Maxima and Average Enthalpies at Saturation Points as Function of Pressure (C_2F_6) 106

IV-27. Plot of Enthalpies for C_2F_6 in the Critical Region ... 106

IV-28. Plot of the Saturation Line Near the Critical Point, $C_p(T)$ Maxima and $\phi(P)$ Maxima 109

IV-29. $\underline{H}$-P-T Diagram for C_2F_6 111

V-1. Plot of $C_p(T)$ Maxima Locations in P_r-T_r Coordinates .. 120

V-2. Plot Showing the Correlation for the Location of $C_p(T)$ Maxima 121

V-3. Plot for the $C_p(T)$ Maxima on $\ell n\ P_r - \ell n\ (C_p^M - C_p^o)/R$ Coordinates 122

V-4. Plot Showing a Correlation for the Magnitude of $C_p(T)$ Maxima on Intermediate Coordinates. 124

V-5. Plot Showing the Final Correlation for the Magnitude of $C_p(T)$ Maxima 124

NOMENCLATURE

a, b, c, d, D	Constants in Equation (V-3)
a, b, c, d	Constants in Equation (IV-1)
a, b	Constants for the viscosity-density isotherm (Equation (III-4))
A, B, C, D	Constants in pressure transducer calibration (Equation III-1))
A, B, C, D	Constants in flow meter calibration (Equation (III-5))
A', B', C', D'	Constants in flow meter calibration (Equation (III-6))
A, B	Constants in Equation (V-1)
B	Second virial coefficient
C_p	Isobaric specific heat capacity
$C_p(T)$ Maximum	Maximum of C_p along isobar
C_p^M	Magnitude of $C_p(T)$ maximum
C_p^o	C_p at zero pressure
$\overline{C}_p$	Mean value of C_p over some temperature interval
d	Deviation defined in Equation (III-9)
E	Voltage
emf	Electromotive force
f	Factor defined in Equation (V-2)
F	Mass flow rate
g	Function defined by Equation (V-3)
h	Plank's constant
$\underline{H}$	Specific enthalpy
k	Boltzmann's constant
k	Constant in Equation (III-8)
m	molecular mass

N	Avogadro's number
P	Pressure
P^M	Pressure of the $C_p(T)$ maximum
Q	Quadrupole moment
$\dot{Q}$	Rate of heat transfer
R	Gas constant
T	Temperature
T^M	Temperature of the $C_p(T)$ maximum
V	Volume
V	Volt
$\dot{W}$	Rate of work done
$X_1, X_2, \ldots, X_n$	Variables in Equation (II-16)
$X_1', X_2', \ldots, X_n'$	Variables in Equation (II-17)
X	Variable in Equation (III-6)
X	Variable defined in Equation (V-3)
X	Variable in Equation (IV-1)
Y	Variable in Equation (IV-1)
Y	Variable in Equation (IV-2)
Z	Compressibility factor
α	Polarizability
α_C	Riedel factor
β	A measure of deviation of intermolecular potential from that of simple fluids
γ	Third parameter defined in Equation (II-24)
ε_0	Intermolecular parameter known as minimum energy

Δ	Difference
μ	Dipole moment
μ	Joule-Thomson coefficient
μ	Viscosity
μ	Micro (10^{-6})
$\bar{\mu}$	Mean value of μ
ρ	Density
σ	Intermolecular parameter known as collision diameter
$\sum$	Summation
ϕ	Isothermal throttling coefficient
$\bar{\phi}$	Mean value of ϕ in some pressure interval
$\phi(P)$ maximum	Maximum of ϕ along isotherm
ω	Acentric factor

Subscripts

C	Critical point property
0	Reference state
r	Reduced property
sat	Saturation property
vap	Vaporization
1	Inlet condition
2	Outlet condition

Conversion Factors for Units Used in This Work

1 atm = 14.696 psia

1 Btu = 1055.87 Joules

1 cu ft = 28317 ml

1 lb = 453.592 g

°R = °F + 459.67

R = 10.73147 psi ft^3/°R - lb mole

ABSTRACT

CALORIMETRIC STUDIES ON ARGON AND HEXAFLUOROETHANE AND A GENERALIZED CORRELATION OF MAXIMA IN ISOBARIC HEAT CAPACITY

by

Kwan Young Kim

Chairman: John E. Powers

The objectives of this research are: (1) To conduct calorimetric measurements on argon and hexafluoroethane. Experimental range for argon covers temperatures between -240°F and 220°F and pressures up to 2000 psia. For hexafluoroethane it covers temperatures between 0°F and 250°F and pressures up to 2000 psia. (2) To develop a generalized correlation for $C_p(T)$ maxima based on the existing $C_p(T)$ maxima and the ones obtained from the present experimental work.

The equipment used in the measurements with argon was a recycle flow system utilizing a Corblin diaphragm compressor for recycling the fluid. Two calorimeters, an isobaric and throttling calorimeter, were used interchangeable in the system. The basic calorimetric measurements were interpreted to yield smoothed values of enthalpy, isobaric heat capacities, maxima of isobaric heat capacity, isothermal throttling coefficients, Joule-Thomson coefficients (with an inversion point at -240°F) and enthalpy changes in vaporization. Enthalpy-pressure-temperature table and diagram are prepared. The data are internally self-consistent to about 0.09%.

Measurements with hexafluoroethane were made at the new recycle flow system with double-acting precision metering pumps and a multipurpose calorimeter which can be used for both isobaric and throttling modes of operation. The data obtained were smoothed values of enthalpy, isobaric heat capacities and their maxima, isothermal throttling coefficients. In addition, extensive measurements of enthalpy in the critical region were made and the critical constants were determined from these measurements. Enthalpy-pressure-temperature table and diagram were prepared. The data were internally self-consistent to about 0.03%.

$C_p(T)$ maxima data obtained in this research and existing data in the literature were used to develop a generalized correlation within the three

parameter corresponding states principle making use of the Riedel factor, α_C, as the third parameter. Correlational effort was divided into two parts: (1) Correlation of locus of $C_p(T)$ maxima and (2) Correlation of magnitude of $C_p(T)$ maxima. The correlation covers satisfactorily the data for substances with widely different physical properties including hydrocarbons, CO_2, and H_2O as well as argon and C_2F_6.

I - INTRODUCTION

Importance of a knowledge of thermal properties for fluids in a wide range of temperature and pressure has been well acknowledged by many engaged both in industrial and theoretical fields. To both designers and engineers in charge of process operation and maintenance, having sufficient thermal property data for their working fluids is essential because it is directly related to the economic and operational concerns. In the field of thermodynamic research, accurate thermal property data are needed in testing theories of fluid behavior or in correlating these data.

In the past, however, people in the area of experimental research on thermodynamic properties were mainly concerned with the measurements of PVT behavior of fluids. Consequently, while PVT data are available for many substances in wide temperature and pressure ranges, thermal property data are available only for a few substances, especially at elevated pressures. Obtaining the thermal properties from the PVT, however, requires differentiation and integration steps, which would cause errors and sometimes they are too significant to be acceptable. Therefore, it is desirable to obtain the thermal property data directly from calorimetric measurements.

The Thermal Properties of Fluids Laboratory at the University of Michigan has been the source of thermal property data for a number of hydrocarbons, nitrogen and their mixtures for the past decade with a recycle-flow calorimetric facility capable of producing accurate data for wide ranges of pressure and temperature. Recently, a new facility has been developed and tested for its performance in the course of Ph.D. thesis work by Miyazaki.[34] The new facility turns out to be simpler and more economical to operate, and it is capable of producing highly accurate data.

As noted earlier, thermal property data and C_p data in particular are scarce in the region of elevated pressures and especially in the supercritical region where most rapid changes in C_p occur. This region includes the neighborhood of $C_p(T)$ maxima curve, the loci of C_p maxima on isobars, mathematically those satisfying $(\partial C_p/\partial T)_p = 0$, projected on

P-T plane. Therefore, most of the existing correlations for C_p, which are based on the C_p values derived from PVT data, give worse predictions in this region. For example, some C_p values in the vicinity of the $C_p(T)$ maxima curve estimated from the generalized correlation by Edmister [14] (which is based on PVT data for hydrocarbons) differ from the direct C_p data[18, 34, 61] by as high as 100%. It is felt that a correlation of $C_p(T)$ maxima will contribute significantly to the improvement of existing C_p correlation and, it can be an important first step to developing a new generalized C_p correlation to be based on the direct C_p data.

Therefore the objectives of the present research are (1) to contribute to the existing knowledge of the thermal properties of fluids by obtaining accurate data of some pure fluids (argon and hexafluoroethane) through carefully conducted experiments with the available calorimetric facilities, and (2) to make contributions in the area of predicting thermal property data by obtaining extensive $C_p(T)$ maxima as well as C_p data and correlating them with existing $C_p(T)$ maxima data in the literature.

II - PRELIMINARY CONSIDERATIONS

Before undertaking the research, a study was made on the information applicable to the present investigation, and the results are presented in this section. The first part of this section is devoted to a review of thermodynamic relations fundamental to the description of flow calorimeters, such as the ones used in the present experiments. A discussion is also made on the techniques applied to interpreting the basic data to obtain smoothed enthalpy and its derivatives such as C_p, ϕ and μ. The second part of the section presents a review of the matters relevant to the present goal of correlating the $C_p(T)$ maxima. The corresponding states principle is chosen as the framework of the correlation because it has been recognized as one of the most useful tools in the area of thermodynamic correlations. In a comparative test of calorimetric enthalpy data with existing prediction methods, Powers[42] demonstrates that the corresponding states correlations yield highly accurate estimates of enthalpy for CH_4, C_3H_8, N_2 and He in most of the P-T region where comparisons are made. In another case Furtado[18] confirms the corresponding states principle as a successful means for predicting and representing the enthalpy of ethane.

The last part of the section presents a discussion on the choice of experimental fluids, argon and C_2F_6, among others. Some other fluids which could be subjected to the experimental investigation in the existing facility are presented as the future reference. It also presents a review of the previous data on argon and C_2F_6, which are relevant to the present investigation.

Thermodynamics of Flow Calorimetry

The principle of the flow calorimeters, such as the ones used in the present work, can be illustrated with the following simple schematic:

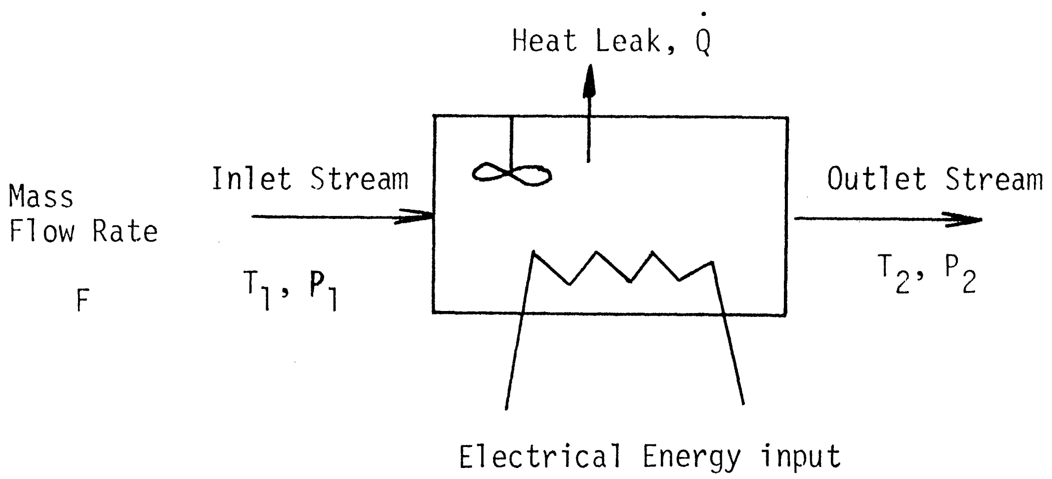

Figure II-1. A Schematic Diagram for a Flow Calorimeter

At a steady state operation of a nonreacting fluid, the first law of thermodynamics gives the following relation for the calorimeter with negligible potential and kinetic energy effects:

$$\underline{H}_2 - \underline{H}_1 = (\dot{Q} - \dot{W})/F \qquad \text{(II-1)}$$

where $\underline{H}$ = specific enthalpy of the fluid
$\dot{Q}$ = the rate of heat leak
$\dot{W}$ = the rate of electric energy input
F = the mass flow rate

The schematic drawing for the calorimeter assembly used in the measurements of argon is presented in Figure II-2(a). The calorimeter, C, is encased in a metal container (D) which is evacuated to a few micron vacuum to minimize convection heat transfer between the calorimeter and its container. Differential thermopiles are placed between the inlet (A) and outlet (B) junctions to measure the temperature difference across the calorimeter. Pressure taps are connected to these junctions for inlet and outlet pressure measurements. The calorimeter assembly is immersed in a constant temperature bath maintained at the inlet

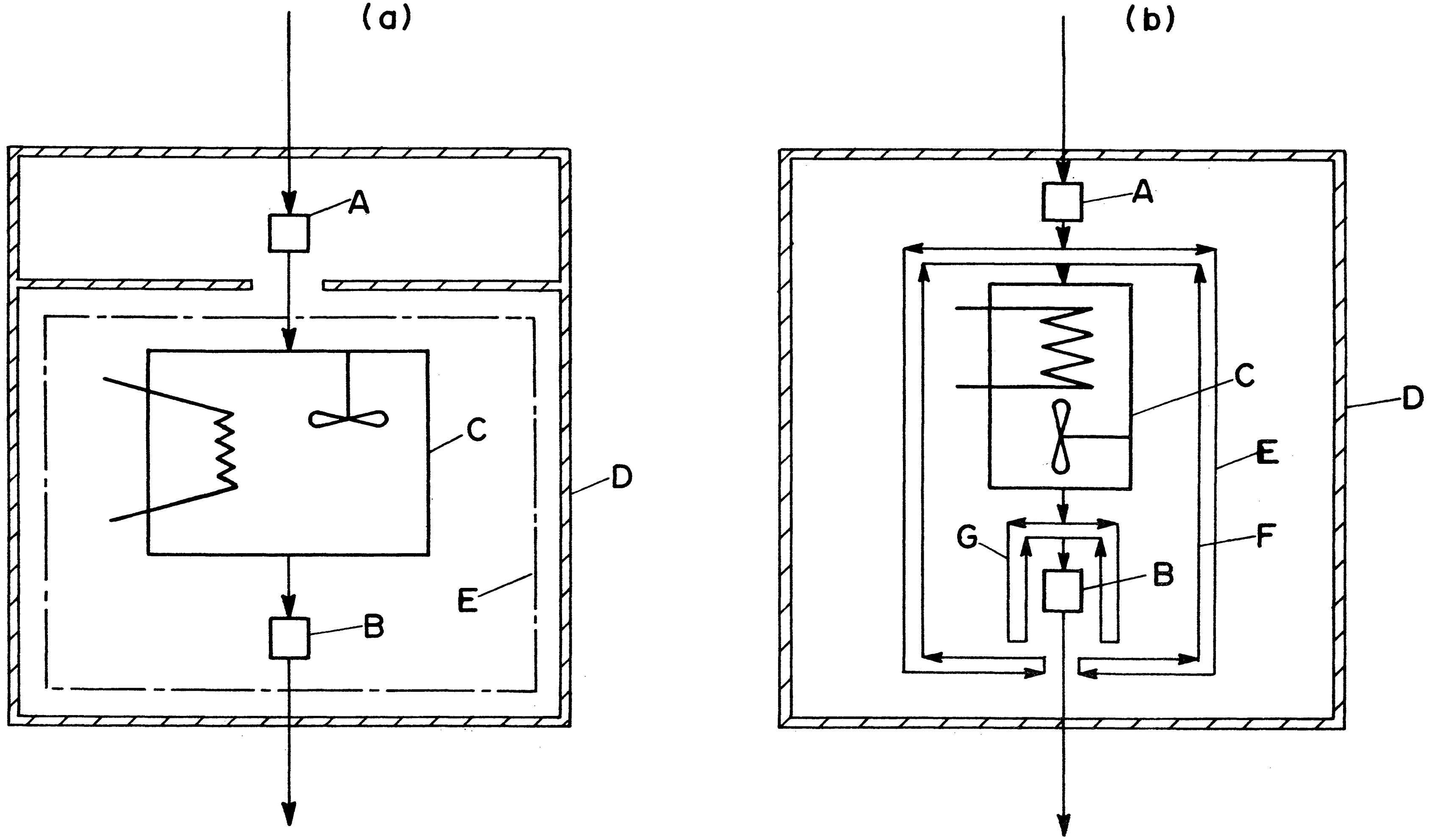

Figure II-2. Schematic diagram illustrating the calorimeter assemblies used in this work.

temperature, T_1. The inlet junction is separated from the calorimeter by a mechanical partition in order to prevent the radiation from the calorimeter. The calorimeter and the outlet junction are surrounded by a radiation shield (E) wrapped with heating wire, a so-called guard heater. For nonisothermal operations, electrical energy is added to the guard heater and is adjusted until a differential thermocouple between the shield and the calorimeter, as monitored by a galvanometer, indicates zero temperature difference. In this case $\dot{Q}$ should be practically zero.

A schematic drawing for the calorimeter assembly used for the measurements of C_2F_6 is presented in Figure II-2(b). In this case, the calorimeter (C) and the outlet junction (B) are surrounded by the coils (E and F) through which the fluid enters the calorimeter. The outlet junction (B) is again surrounded by the coil (G), through which the fluid from the calorimeter flows. Most of the heat radiated from the calorimeter to the coils E and F is absorbed by the fluid stream, which travels to the calorimeter, and consequently heat loss $\dot{Q}$ should become very small.

When the calorimeter is operated in such a way that $\dot{Q}$ becomes negligibly small, Equation (II-1) reduces to

$$\underline{H}_2 - \underline{H}_1 = \frac{-\dot{W}}{F} . \qquad \text{(II-2)}$$

For the pure fluid, which is the case of the present investigation, in the absence of unusual force fields,

$$\underline{H}_1 = \underline{H}(T_1, P_1)$$

$$\underline{H}_2 = \underline{H}(T_2, P_2)$$

Since $\underline{H}$ is a point function, Equation (II-2) can be rewritten as

$$[\underline{H}(T_1, P_2) - \underline{H}(T_1, P_1)] + [\underline{H}(T_2, P_2) - \underline{H}(T_1, P_2)] = \frac{-\dot{W}}{F} . \qquad \text{(II-3)}$$

The first and second square brackets represent respective isothermal and isobaric changes of enthalpy. As C_p and ϕ are defined as

$$C_p = \left(\frac{\partial \underline{H}}{\partial T}\right)_P \qquad \phi = \left(\frac{\partial \underline{H}}{\partial P}\right)_T \qquad \text{(II-4)}$$

Equation (II-3) can be rewritten as

$$\int_{P_1}^{P_2} \phi(T_1, P)\, dP + \int_{T_1}^{T_2} C_p(T, P_2)\, dT = \frac{-\dot{W}}{F} \qquad \text{(II-5)}$$

Equations (II-3) and (II-5) are valid within a single phase. In case of measurements across the phase boundary, it is necessary to use the more general form:

$$\int_{P_1}^{P_{sat}} \phi(T_1, P)\, dP + \int_{T_1}^{T_{sat}} C_p(T, P_2)\, dT + \Delta\underline{H}_{vap}$$

$$+ \int_{P_{sat}}^{P_2} \phi(T_1, P)\, dP + \int_{T_{sat}}^{T_2} C_p(T, P_2)\, dT = \frac{-\dot{W}}{F} \qquad \text{(II-6)}$$

where $\Delta\underline{H}_{vap}$ is the enthalpy change by vaporization at T_{sat} and P_{sat}. It can be seen from Equation (II-5) that the calorimeter can be specified so only one term in the left hand side of the equation is dominant. For example, the pressure drop across the isobaric calorimeter is made as small as possible so that the second term is dominant. Thus, the measurements of electrical energy input, $\dot{W}$, and flow rate yield an integral average of C_p between the temperatures T_1 and T_2. In the isothermal calorimeter a sizeable pressure drop is made as the fluid is throttled through a capillary coil of fixed length and diameter. An adjustable quantity of electrical energy is added to the fluid stream to maintain T_2 as close to T_1 as possible. In this case the first term should dominate over the second and the electrical energy input provides us with an integral average of ϕ between the pressures P_1 and P_2.

In cases where a pressure drop causes a rise in the fluid temperature, an isothermal operation is not possible as it requires the removal of energy from the throttled fluid. It is then necessary to operate the calorimeter in the isenthalpic mode. No electrical energy is added in this case and the guard heater is heated to bring the shield temperature to that of the calorimeter outlet section so as to reduce $\dot{Q}$ to essentially zero. Then Equation (II-5) simplifies to

$$\int_{T_1}^{T_2} C_P(T, P_2)\, dT = -\int_{P_1}^{P_2} \phi(T_1, P)\, dP \tag{II-7}$$

or

$$\bar{C}_P(T_1, T_2; P_2) \cdot (T_2 - T_1) = -\bar{\phi}(T_1; P_1, P_2) \cdot (P_2 - P_1). \tag{II-8}$$

Therefore, the measurements of T_1, P_1, T_2 and P_2 define the mean adiabatic Joule-Thomson coefficient as

$$\bar{\mu}(T_1, T_2; P_1, P_2) \equiv \frac{T_2 - T_1}{P_2 - P_1} = \frac{-\bar{\phi}(T_1; P_1, P_2)}{\bar{C}_P(T_1, T_2; P_2)} \tag{II-9}$$

Data Interpretation

Practically it is not possible to avoid pressure changes and temperature changes, however small, completely from the actual isobaric and isothermal operations. During a series of isobaric (or isothermal) measurements inlet pressures (or inlet temperatures) can change slightly from the reference pressure (or temperature) depending on the operation condition. Therefore, those effects should be compensated from the basic data before C_P or ϕ values are determined.

Thermodynamic Consideration for Basic Data

If the reference pressure for an isobaric run is P_0, then every data point in the run at slightly different inlet pressure P_1 must be corrected to P_0. The small pressure drop $(P_1 - P_2)$ must also be compensated. The desired enthalpy difference can be expressed as

$$\underline{H}(T_2, P_0) - \underline{H}(T_1, P_0) = \{\underline{H}(T_2, P_2) - \underline{H}(T_1, P_1)\} + \{\underline{H}(T_2, P_0) - \underline{H}(T_2, P_2)\} + \{\underline{H}(T_1, P_1) - \underline{H}(T_1, P_0)\} . \qquad \text{(II-10)}$$

The first term is the actual measured enthalpy difference [see Equation (II-5)] and the others are correction terms. Equation (II-10), when rewritten in terms of the appropriate enthalpy derivatives, becomes

$$\underline{H}(T_2, P_0) - \underline{H}(T_1, P_0) = \left(\frac{-\dot{W}}{F}\right) + \int_{P_2}^{P_0} \phi(T_2, P)\, dP + \int_{P_0}^{P_1} \phi(T_1, P) dP. \qquad \text{(II-11)}$$

Therefore, the mean heat capacity over the interval between T_2 and T_1 may be determined as

$$\overline{C}_P(T_1, T_2; P_0) = \frac{1}{T_2 - T_1} \left[\left(\frac{-\dot{W}}{F}\right) + \int_{P_2}^{P_0} \phi(T_2, P)\, dP + \int_{P_0}^{P_1} \phi(T_1, P)\, dP \right]$$

Similarly, for an isothermal run with T_0 as the reference temperature, we have

$$\underline{H}(T_0, P_2) - \underline{H}(T_0, P_1) = \frac{-\dot{W}}{F}\Big) + \int_{T_2}^{T_0} C_p(T, P_2)\, dT + \int_{T_0}^{T_1} C_p(T, P_1)\, dT. \qquad \text{(II-13)}$$

The mean isothermal throttling coefficient over the interval P_2 and P_1 may be determined as

$$\bar{\phi}(T_0; P_1, P_2) = \frac{1}{P_2 - P_1} \left[\left(\frac{-\dot{W}}{F}\right) + \int_{T_2}^{T_0} C_p(T, P_2)\, dT + \int_{T_0}^{T_1} C_p(T, P_1)\, dT \right]. \qquad \text{(II-14)}$$

As an isobaric run (see Figure II-3) consists of a series of measurements where the inlet conditions are held fairly constant, the corrected basic data may be differenced with additional corrections for small inlet temperature variations. Suppose we choose two data points i and j with inlet temperatures T_{1i} and T_{1j}, and outlet temperatures T_{2i} and T_{2j}, respectively. If T_0 is the reference inlet temperature of the run, then the mean heat capacity over the interval between T_{2i} and T_{2j} is given by

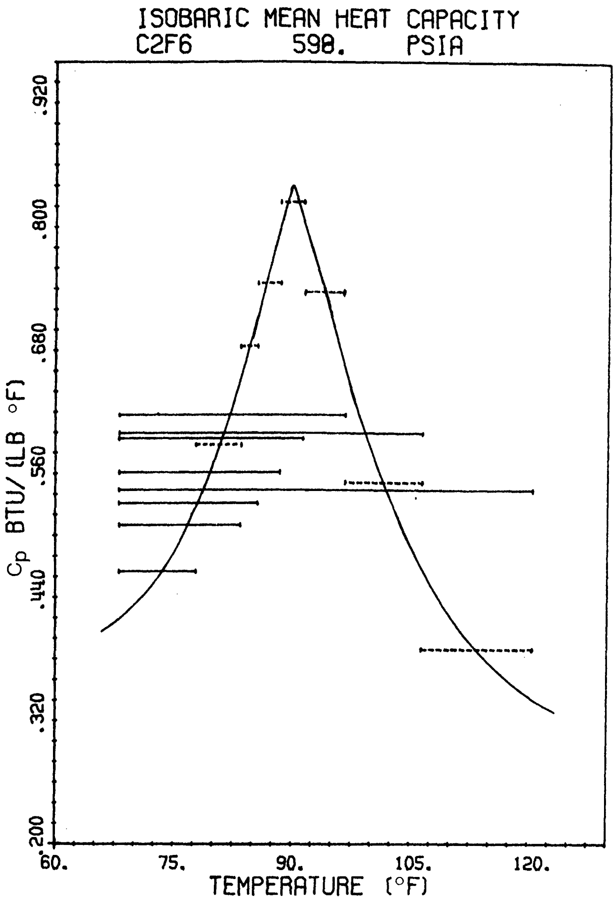

Figure II-3. Example of an isobaric run.

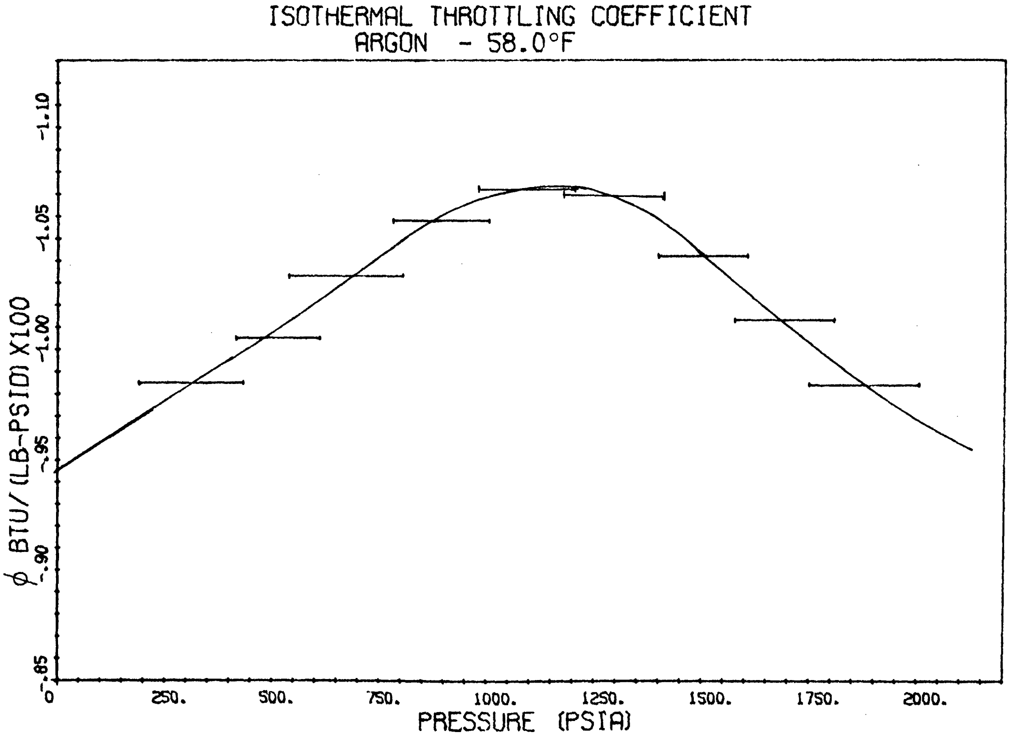

Figure II-4. Example of an isothermal run.

$$\begin{aligned}\bar{C}_P(T_{2i}, T_{2j}; P_0) &= \left(\frac{T_{2j} - T_{1j}}{T_{2j} - T_{2i}}\right) \bar{C}_P(T_{1j}, T_{2j}; P_0) \\ &- \left(\frac{T_{2i} - T_{1i}}{T_{2j} - T_{2i}}\right) \bar{C}_P(T_{1i}, T_{2i}; P_0) + \left(\frac{T_0 - T_{1i}}{T_{2j} - T_{2i}}\right) \bar{C}_P(T_{1i}, T_0; P_0) \\ &- \left(\frac{T_0 - T_{1j}}{T_{2j} - T_{2i}}\right) \bar{C}_P(T_{1j}, T_0; P_0). \end{aligned} \tag{II-15}$$

The mean heat capacities given by Equation (II-12) are solid horizontal lines while those in Equation (II-15) are dotted lines, as shown in Figure II-3. A smoothed heat capacity curve is drawn along the entire isobar under the constraint that the area under the horizontal lines is equal to the area under the smoothed curve. The mean isothermal throttling coefficients given by Equation (II-14) are shown in Figure II-4. A smoothed ϕ curve is constructed along the entire isotherm with the same "equal area" constraint that is imposed on C_P.

Constructing Equal Area Curve

Constructing equal area curves for C_P and ϕ from the basic data is the most crucial part of the data reduction since it is the data interpreted from the curves that constitute the result of the whole experimental activity. Several techniques related to this matter appear in the works of previous investigators.[3, 18, 34, 61] An excellent review on the merits and deficiencies of those techniques are presented in Furtado's work.[18] The most reliable technique at the present time appears to be the one proposed by Furtado,[18] and it is adopted for use in the present work. A detailed description of the technique can be found in the original work, and it need not be elaborated here. Instead, an outline of the technique is introduced briefly.

This technique, so-called computer aided graphical technique, employs a graphic curve fitting method and machine computation as a tool to check the fittability of a drawn curve to the basic data. A smoothed curve of C_P vs T (or ϕ vs P) is manually constructed according to the Simpson's rule technique.[3] The curve is made on a large sized graph of the corrected basic and differenced data plotted as horizontal lines. From the curve, point values of C_p or ϕ were selected at proper intervals so these values could adequately represent the shape of the curve. The functional relationship in the interval between any two successive points is represented by successive five point Lagrange interpolation polynomials.[6] The desired interval is arranged to lie between the third and fourth of the five points whenever possible. The integral over each interval is computed to obtain enthalpy differences using Gauss-Legendre quadrature.[6] The area under the curve is also computed over the intervals corresponding to the basic and differenced data and compared with the experimental ones. These comparisons provide a check on the graphical technique and indicate regions where adjustments are necessary. In this work, the final curves are made to fit the corrected basic data within 0.2% deviation. Though all the integrations and interpolations over the curve were done by machine computation, the repeated manual construction of the curves and preparation of the input data to the computer alone made this procedure one of the most time consuming procedures in this work.

Interpretation of Joule-Thomson Data

In this investigation only a single run of isenthalpic measurements is made with argon, which is illustrated in Figure (III-19), where the average value of Joule-Thomson coefficient, μ, is plotted over the pressure interval for each data point. It should be pointed out that the successive data points do not lie on the same isenthalpic curve when the inlet pressure is changed and the inlet temperature remains constant throughout the run. Strictly speaking, the point value of μ cannot be obtained from the equal area curve through the data points. However, as Yesavage[61] suggested, if the temperature difference, $T_2 - T_1$, is small and μ is not a strong function of temperature, which is the case with the present measurements, the plot of μ vs P may be approximated by an equal area curve as shown in the figure.

The isenthalpic data can be interpreted to yield an enthalpy isotherm corresponding to the inlet temperature of the run. From Equation (II-9) $\bar{\phi}(T_1; P_1, P_2)$ can be obtained from an experimental determination of $\bar{\mu}$ and an estimate of $\bar{C}_p(T_1, T_2; P_2)$. Then the point values of $\phi(T_1, P)$ can be determined by constructing the equal area curve through $\bar{\phi}$ data using the technique described earlier.

Thermodynamic Consistency Checks

When the experimental isotherms and isobars form a network of closed loops, as shown in Figure (III-28), for example, then the isothermal and isobaric data obtained over a loop can be checked for self-consistency. We chose the enthalpy loop from -58°F to 167°F and from 286 psia to 1143 psia for explanation on how the loop check is accomplished. The enthalpy changes between the grid points are obtained from the integrals of the C_p or ϕ curves discussed earlier in this section. For example,

$$35.09 = \int_{-58°F}^{167°F} C_p(T, P = 1143 \text{ psia})\, dT$$

$$-3.27 = \int_{286 \text{ psia}}^{1143 \text{ psia}} \phi(T = 167°F, P)\, dP$$

As enthalpy is a state function, the algebraic sum of all enthalpy differences around the loop, $\sum \Delta H_i$, should be exactly equal to zero. In practice, it is a finite value (in this case -0.09 Btu/lb when the sum is taken along the clock-wise path). The actual sum divided by the sum of the absolute values of the enthalpy differences, percent deviation $\equiv \sum \Delta H_i / \sum |\Delta H_i| \times 100$, can serve as a measure of the thermodynamic consistency of the data. In this case inconsistency of the loop is $-0.09/76.81 \times 100 = -0.117\%$. It is necessary to adjust enthalpy differences between grid points optimally so that the percent deviation of each loop becomes exactly zero. In the particular case examined, the final enthalpy change from -58°F to 167°F at 1143 psia needs an addition of 0.096 Btu/lb to the original 35.09 Btu/lb. Adjustments for the other arms of the loop are also given in the parenthesis.

In order to avoid a concentration of errors in the small end loop, the largest loop (-240°F to 167°F, and from 286 psia to 2000 psia) is balanced first and bounds are established on the total acceptable variations for the individual arms. Then, the smaller constituent loops are balanced within these constraints. The bottom loops are fabricated with zero pressure enthalpy differences calculated with the ideal gas heat capacity, C_p^o, from the literature. Particularly for argon, the zero enthalpy changes can be obtained exactly as C_p^o is $(5/2)R$, in accordance with the kinetic theory of monoatomic molecules. Therefore, the bottom loops can provide an opportunity to check the data with the exact values. As the entire network is balanced, the smoothed C_p and ϕ values for the individual arms are now readjusted by increasing or decreasing uniformly to conform to the final enthalpy adjustment assigned to the given arm.

Error Analysis

A comprehensive error analysis of the basic measurements and reduced data has been undertaken by the previous investigators.[25, 36, 37, 18] As pointed out by Furtado,[18] estimation of the accuracy of the basic enthalpy data based on the errors involved in the major experimental measurements is at best approximate in view of the highly variable dependence of the enthalpy on temperature and pressure. Furthermore, the precise contribution of unsteady state and mass leakage is almost always uncertain. It is suggested[61, 18] that the most reliable index for the accuracy of the results is the observed discrepancy between the original and adjusted values of the enthalpy difference for each arm of every enthalpy loop for any given system.

Corresponding States Principle

The corresponding state principle has been stated in many ways by many people, although the basic theoretical idea behind each statement is the same as the one introduced by Van der Waals about one hundred years ago. We may here adopt the one from Reid and Sherwood,[48] that "all substances would have the same equation of state when expressed in terms of dimensionless (or reduced) system variables". Let

$$F(X_1, X_2, \ldots, X_n) = 0 \qquad \text{(II-16)}$$

be a universal function with n system variables describing the state of all pure fluids (we purposely restrict to pure substances only for the present discussion). These variables should be external thermodynamic variables as P, V and T and also internal variables pertaining to molecular or atomic properties.

Now suppose we render dimensionless X_1 to X_n by dividing them by X_1', ..., X_n', respectively, where X_1', ..., X_n' are some arbitrary constants. Then we may rewrite Equation (II-16) as

$$F\left(\frac{X_1}{X_1'}, \ldots, \frac{X_n}{X_n'}\right) = 0 \qquad \text{(II-17)}$$

As for those dimensionless variables Bird and Brock[4] suggested the following:

$$F\left(\frac{P\overline{V}}{NkT}, \frac{\overline{V}}{N\sigma^3}, \frac{kT}{\varepsilon_0}, \frac{\mu^2}{\varepsilon_0\sigma^3}, \frac{Q^2}{\varepsilon_0\sigma}, \frac{\alpha}{\sigma^3}, \frac{h}{\sigma(m\varepsilon_0)^{1/2}}, \beta\right) = 0 \qquad \text{(II-18)}$$

where k = Boltzmann's constant
h = Plank's constant
m = molecular mass
σ = intermolecular potential parameter known as collision diameter
ε_0 = intermolecular potential parameter known as minimum energy
μ = dipole moment
Q = quadrupole moment
β = a measure of deviation of intermolecular potential from that of simple fluids
α = polarizability
N = Avogadro's number

Since ε_0 and σ are usually unknown, they are conveniently replaced by experimentally measurable quantities; ε_0/k by critical temperature, T_C, and $N\sigma^3$ by V_C, critical volume. There are theoretical grounds for those replacements. Since T_C is a measure of the kinetic energy at the state when liquid and vapor states are identical, we may expect proportionality between T_C and minimum energy of a molecule, ε_0. As σ is a distance parameter, we also expect proportionality between σ^3 and V_C. The dimensionless group, $h/\sigma(m\varepsilon_0)^{1/2}$, is for the quantum effect. Except for such quantum gases as Ne, He, H_2, etc., this effect is accounted for only at very low temperatures; therefore, we generally exclude this group from the equation.

Through the preceding arguments, Equation (II-18) reduces to

$$F\left(\frac{PV}{NkT}, \frac{V}{V_C}, \frac{T}{T_C}, \frac{\mu^2}{V_C kT_C}, \frac{Q^2}{V_C{}^5 kT_C}, \frac{\alpha}{V_C}, \beta\right) = 0 \qquad \text{(II-19)}$$

It is desirable to replace V/V_C by P/P_C, as P_C data are generally more reliable than V_C data.[48] Introduction of P/P_C in place of V/V_C, however, is accompanied by Z_C, critical compressibility factor, since

$$\frac{V}{V_C} = \frac{Z}{Z_C} \cdot \frac{T}{T_C} \cdot \frac{P_C}{P} \qquad \text{(II-20)}$$

where $Z = PV/NkT$.

Therefore, we must add to Equation (II-19) one more variable as a price for V/V_C elimination. Hence, we have Equation (II-21),

$$F\left(\frac{Z}{Z_C}, \frac{P}{P_C}, \frac{T}{T_C}, \frac{\mu^2}{V_C kT_C}, \frac{Q^2}{V_C{}^5 kT_C}, \frac{\alpha}{V_C}, \beta\right) = 0 \qquad \text{(II-21)}$$

which expresses a basic relation for the corresponding states principle (CSP) with eight dimensionless variables as parameters. For convenience, we may rewrite Equation (II-21) in the Z explicit function as

$$Z = Z(T_r,\ P_r,\ Z_C,\ \frac{\mu^2}{V_C kT_C},\ \frac{Q^2}{V_C{}^5 kT_C},\ \frac{\alpha}{V_C}\ ,\ \beta) \qquad \text{(II-22)}$$

Note that $P_r = P/P_C$, $T_r = T/T_C$

Although it is desirable that either Equation (II-21) or (II-22) be an analytical expression, it can be instead a tabulation of data or a generalized chart drawn from smoothed data.

In practice, however, all of the variables in Equation (II-22) are seldom accounted for. The simplest form of CSP has only two parameters

$$Z = Z(P_r,\ T_r) \qquad \text{(II-23)}$$

which implies the compressibility factor as a function of T_r and P_r only. A certain group of molecules called simple fluids such as Ar, Kr, Xe, CH_4, which have spherically symmetric structures, was experimentally observed to conform to Equation (II-23).

In an attempt to improve two parameter CSP in such a way to cover more than simple fluids, people in the field of thermodynamic correlations have worked out three parameter CSP by introducing the third parameter, γ, as

$$Z = Z(T_r,\ P_r,\gamma) \qquad \text{(II-24)}$$

Comparing Equation (II-24) with Equation (II-22), we may see that γ should be equivalent to lumped contribution of the five parameters in Equation (II-22). Efforts have been made by a number of researchers to fit γ to some macroscopically measurable quantities. Riedel[46] related the third parameter to measured values of the slope of the reduced vapor pressure at the critical point. His parameter, designated as α_C, is expressed as

$$\alpha_C = \left(\frac{d\ \ell n\ P_r}{d\ \ell n\ T_r}\right)_{\substack{T_r = 1 \\ P_r = 1}} \tag{II-25}$$

where P_r = reduced vapor pressure.

Pitzer and coworkers[43] introduced a third parameter called acentric factor, ω, as

$$\omega = -1 - (\log P_r)_{T_r = 0.7} \tag{II-26}$$

Although addition of the third parameter significantly improved the performance of the two parameter CSP, it is not satisfactory enough to cover the fluids with polarity or appreciable asymmetry in their intermolecular force fields, such as H_2O, NH_3, alcohols, etc. A few attempts have been made to improve the three parameter CSP through the addition of parameters. An excellent review on the multiparameter CSP appears in an article by Leland and Chappelear.[30] However, as indicated by Leland and Chappelear, the current state of the extent and accuracy of the measurements related to the potential parameters makes it difficult to generalize CSP beyond the three parameter correlation.

Significance of $C_p(T)$ Maxima

For pure substances the isobaric heat capacity may be expressed as

$$C_p = C_p(T, P) \tag{II-27}$$

If a C_p vs T plot is made along an isobar in the supercritical region, it exhibits a peak called $C_p(T)$ maximum. The peak becomes sharper as the pressure is closer to the critical pressure, P_C, and eventually becomes infinite when the pressure equals P_C. Figure II-5 illustrates some of C_p vs T plots for argon in the supercritical region. As shown in the figure, $C_p(T)$ maximum is characterized by the magnitude, C_p^M,

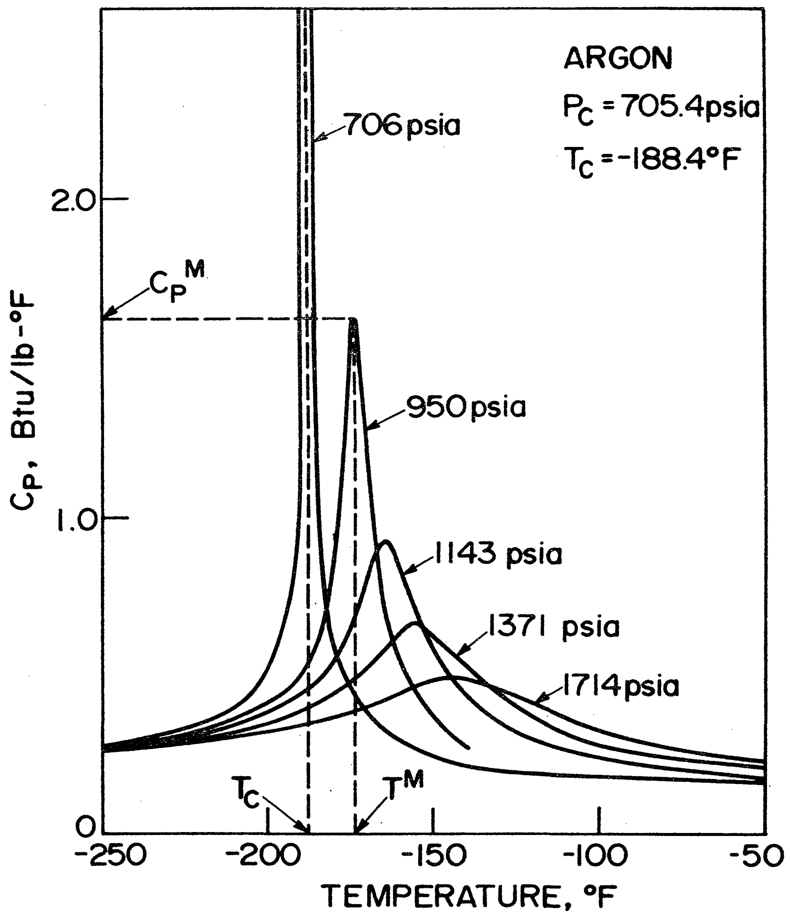

Figure II-5. An illustration of Cp(T) curves in the super critical region.

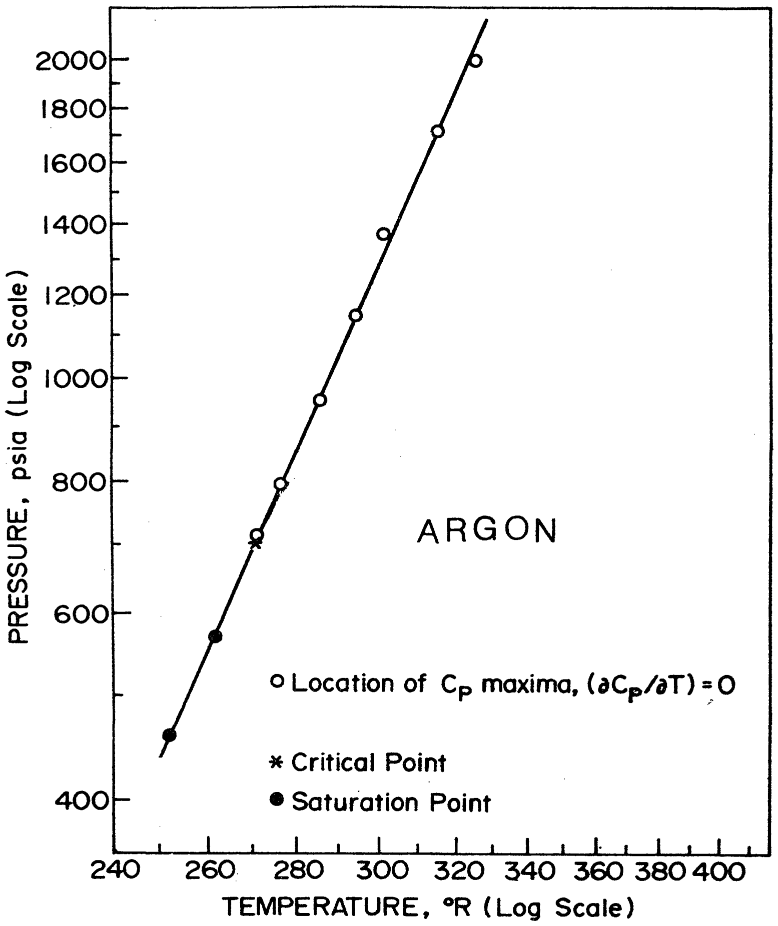

Figure II-6. Plot showing the location of Cp(T) maxima.

and location, T^M, for the peak of a given pressure. If T^M vs P plot is made on a P-T plane, as shown in Figure II-6, the plot demonstrates a curve similar to the vapor pressure curve in the subcritical region. It was suggested by Kaganir[26] and Jakob[25] and later substantiated by the experimental results of Sirota, et al.[51] that the slope of the vapor pressure curve at the critical point is the same as that of the curve formed by the loci of $C_p(T)$ maxima (called $C_p(T)$ maxima curve). Therefore, they once regarded the $C_p(T)$ maxima curve as an extension of the vapor pressure curve into the supercritical region.

The existence of rapid changes in C_p along the $C_p(T)$ maxima curve made a few researchers speculate that there might be a structural change in fluids at the supercritical region, and the $C_p(T)$ maximum curve might be the boundary between "vapor-like" and "liquid-like" phases[51, 52]. However, there is insufficient information on the physical nature of the maxima and the existence of phase transition is still questionable.

Nevertheless, the knowledge of location and the magnitude of $C_p(T)$ maxima would be of great importance to the formulation of any C_p correlation. There are several existing correlations for $(C_p - C_p{}^o)$ by several investigators. Lydersen, et al.[27] established generalized charts for $(C_p - C_p{}^o)$ from their generalized compressibility table. Sherwood[53] established $(C_p - C_p{}^o)$ correlation from the generalized enthalpy tables by Curl and Pitzer.[5] There are generalized $(C_p - C_p{}^o)$ charts by Edmister[14] and by Weiss and Joffe.[59] All these correlations are based in PVT data, not C_p data. The thermodynamic relation, as described by Equation (II-28)

$$C_p(T, P) - C_p{}^o(T) = T \int_0^P \left(\frac{\partial^2 V}{\partial T^2}\right) dP \qquad \text{(II-28)}$$

shows that in order to obtain C_p data, PVT data should be differentiated twice, followed by an integration either numerically or graphically, which would introduce sometimes significant errors. Especially in a $C_p(T)$ maxima region where rapid changes in C_p occur, reliability of C_p's derived from PVT's are quite questionable. Even for the regions excluding the neighborhood of critical point, according to Weise and Joffe[59], errors encountered may be as high as 50 to 100%. Therefore, direct determinations of C_p as well as $C_p(T)$ maxima in this region of poorest definition would contribute significantly to the improvement of existing correlations as well as to the development of new generalized C_p correlations.

Previous Studies on $C_p(T)$ Maxima

Because of experimental difficulties involved in the measurements of calorimetric data, direct C_p data in the supercritical region are available for only a few substances. Consequently $C_p(T)$ maxima data are found among only those substances. Most of the data are from several researchers in the U.S.S.R. and the previous workers of the Thermal Properties of Fluids Laboratory (TPFL) at the University of Michigan. Sirota and his coworkers[51, 52] report $C_p(T)$ maxima of H_2O from their extensive work on C_p measurements in the supercritical region. $C_p(T)$ maxima of CO_2 were obtained by Rivikin and Gukov[47]. The data obtained through experimental measurements at TPFL include $C_p(T)$ maxima for CH_4[25], C_2H_6[18, 34], C_3H_8[61], and N_2[35]. In addition, the data have been obtained for a number of binary mixtures of CH_4 - C_2H_6[18], C_2H_6 - C_3H_8[18], CH_4 - C_3H_8[36, 37], and CH_4 - N_2[37], and a ternary mixture of CH_4 - C_2H_6 - C_3H_8[18].

There are few investigations related to correlations for $C_p(T)$ maxima. Sirota, _et al._[51] observed from their experimental $C_p(T)$ maxima data of water that the location of the peak could be expressed in the simple expression

$$\ln P_r = \alpha_c\left(1 - \frac{1}{T_r}\right) \qquad \text{(II-29)}$$

where P_r = reduced pressure

T_r = reduced temperature at which the peak locates

Powers[45] has suggested, based on his study of the $C_p(T)$ maxima data obtained from the University of Michigan, the following equation for the location of $C_p(T)$ maxima:

$$\ln P_r = \alpha_C \ln T_r \qquad \text{(II-30)}$$

Choice of Experimental Fluids

It was felt that for a fluid to be suitable for the experiment planned at TPFL it should meet the following criteria:

1. It should be nontoxic and physiologically inert.
2. It should be chemically stable.
3. Its critical temperature and pressure should lie well within the operating range of the equipment.
4. It should be available as a relatively pure material.

The first criterion is the concern of life hazard to persons engaged in the experiments in case of mass leaks from the equipment. Since the measurements usually take a long period of time, there could be a chance of prolonged gas exposure to the human beings involved. Therefore, even at a low level of concentration, a toxic gas can inflict injuries to the human body. It was decided that the fluids belonging to, or are equivalent to, groups one through four of Underwriter's Laboratory Classification[58] be excluded from further considerations. For example, fluids otherwise suitable for our investigation, such as SiF_4 and BF_3, were rejected.

The second criterion concerns possible decomposition of a fluid within the system. This may result in erronous data and, furthermore, lead to such dangerous situations as explosions, line pluggings, etc. The third criterion aims to eliminate the fluids with critical constants out of the operating range of the present equipment (temperatures between -240°F and 300°F and pressures up to 2000 psia). With such fluids, measurements cannot be made both in the subcritical and the supercritical regions. Among the fluids satisfying this criterion, those with relatively low critical constants are preferable because the measurements in the supercritical region will be emphasized in the present work.

The fourth criterion concerns the impurity level in the sample to be used for the experiment. It would be ideal to use a sample free of impurities. Practically, however, every commercially available sample contains impurities varying from the level of less than 0.001% to as high as 10% depending on the substances. It is desirable to choose the sample with an impurity level lower than 0.1%; however, up to 0.5% impurity could be acceptable if the content of impurities is known and the corrections could be made.

Table II-1 gives a list of some of the fluids which were considered for our use. Excluded from the table are the ones already used in the previous works at TPFL (such as CH_4, C_2H_6, C_3H_8 and N_2). The list consists of the simple molecules (Ar, Kr, Xe), fluorocarbons, a couple of olefins and CO_2. It was intended that one simple molecule and one fluorocarbon be chosen for the present investigation, and argon and C_2F_6 (Freon-116) were finally chosen among them. The choice of C_2F_6, among other fluorocarbons was in accordance with the interest of the du Pont de Nemours & Co., which donated C_2F_6 with high purity (99.9%). It is to be noted that while argon is a simple fluid with $\alpha_C = 5.98$, C_2F_6, the fluorine analog of ethane, is a substance with $\alpha_C = 7.19$, a comparatively high value. Therefore, the choice of the substances with widely different α_C values for the calorimetric measurements may furnish information which could help establish the third parameter effect on the $C_p(T)$ maxima correspondence.

Previous Experimental Data for Argon

A comprehensive literature search for the thermodynamic data published up to 1964 is found in a publication of NBS[23]. It includes more than 400 sources for the data not only of thermodynamic but also

TABLE II-1

A LIST OF FLUIDS SUITABLE FOR USE IN THE PRESENT EQUIPMENT

Substance		Molecular Weight	Tc (°F)	Pc (psia)
Ar		39.94	-188.6	705.4
Kr		83.7	- 82.8	798
Xe		131.3	- 38.1	853
CCl_2F_2	(Freon-12)	120.93	233.6	596.9
$CClF_3$	(Freon-13)	104.47	83.9	561
$CBrF_3$	(Freon-13B1)	148.93	152.6	575
CF_4	(Freon-14)	88.01	- 50.2	543
$CHClF_2$	(Freon-22)	86.48	204.8	721.9
CHF_3	(Freon-23)	70.02	78.6	701
$CClF_2$-CF_3	(Freon-115)	154.48	175.9	453
C_2F_6	(Freon-116)	138.02	67.1	437
C_4F_8	(Freon-C318)	200.04	239.6	403.6
C_2H_4		28.05	49.9	742
C_3H_6		42.08	197.5	668
CO_2		44.01	87.9	1071

mechanical and transport properties. There are only a few cases in which direct measurements of thermal properties have been made. Roebuck and Osterberg[49] have determined the Joule-Thomson coefficients with the highest initial pressure being 200 atm and initial temperatures ranging from -150°C to 300°C. The specific heats of the saturated solid and liquid have been reported by Eucken[15, 16] and Clusius[7,8] who conducted low temperature calorimetric measurements. They have determined the latent heats of fusion and vaporization at the triple point and normal boiling point.

Walker[60] has determined C_p of argon for pressures from 10 to 40 atm and temperatures from -240°F to -140°F from calorimetric measurements with a bomb-type nonflow calorimeter. Reliability of Walker's data are somewhat questionable because the measurements involved heat capacities of the calorimeter which were usually higher than those of the sample except for the peak region. According to his analysis, the overall accuracy of data was ±0.7%.

Compilations of thermodynamic properties of argon may be traced back to the work of Michels, et al.[39] who calculated and tabulated C_p, H and S as well as other thermodynamic properties at temperatures between 0 and 150°C and pressures up to 1050 atm. Later Michels and coworkers[38] extended the compilation to temperatures down to -140°C. Din[10] has prepared thermodynamic tables and a Mollier diagram from the data published up to 1952. His work covered temperatures between 90 and 240°K and pressures up to 5000 atm. A similar work has been done by Hilsenrath, et al.[24] The most recent compilation is the one prepared by Angus and Armstrong[1] under the auspices of the International Union of Pure and Applied Chemistry (IUPAC), covering temperatures from 85 to 1100°K and pressures up to 1000 bar. It is a collation of two recent tables, one by Gosman, et al.[22] of NBS and the other by Vasserman, et al.[56, 57] of Odessa Institute of Marine Engineers, U.S.S.R. The two sets of tables are to a large extent based on the same data. Angus and Armstrong noted that agreement between the values of the properties listed in the two tables, with the exception of the heat capacities, is within the range comparable to the experimental errors.

Previous Experimental Data for C_2F_6

A literature survey reveals few sources for the thermodynamic properties of hexafluoroethane. Pace and Aston[41] have determined the heat capacity of saturated solid and liquid from 11.2 to 195.0°K from calorimetric measurements. They have also measured the vapor pressures of the solid and the liquid to the normal boiling point (194.87°K) as well as the heat of vaporization and saturated vapor density at 273.16°K. A compilation of thermodynamic properties of hexafluroethane has been issued by Freon Products Division of E. I. du Pont de Nemours & Co.[17] The ranges of the compilation are temperatures from -150°F to 460°F and pressures up to 460 psia. Values of the ideal gas heat capacity determined from spectroscopic analysis are found in the literature.[9, 54]

III - CALORIMETRIC DETERMINATIONS WITH ARGON

This section presents the descriptions of the experimental equipment and procedure and presentation and discussion of the results. The equipment used in the present work was originally designed and constructed by Faulkner.[19] It has been subjected to improvements and modifications by previous workers[25, 35, 36, 37, 61, 18] and is well documented in their Ph.D. theses. Therefore, the facility is described here only briefly. Emphasis is put on the modifications and calibrations of measuring instruments which were done during the present investigation. Experimental results are presented in the form of tabulation of the basic data $\underline{H}$, $\overline{C}_p$, $\overline{\phi}$, and $\overline{\mu}$ as well as the smoothed values of C_p, ϕ and μ. Plots of C_p, ϕ and μ along the isotherms and $\underline{H}$-P-T diagram are presented. These data are checked for thermodynamic consistency and compared with values from the literature.

The Recycle Flow System

A flow diagram of the system is shown in Figure III-1. It is fundamentally a recycle flow system designed to supply a fluid at a constant measured rate to a calorimeter at a designated temperature and pressure. The fluid is compressed to a pressure higher than that at which measurements are to be made (usually 4 ~ 500 psi higher than the calorimeter inlet pressure) by means of a two-stage Corblin diaphragm compressor operating at a constant volumetric rate (~4 SCFM). The fluid, after passing through the scavenger bomb containing heated copper fillings which absorb any oxygen in the stream, is throttled approximately to a preselected pressure through the compressor throttle valve (CT). The flow is then divided into two streams: one stream bypasses to the inlet buffer through the bypass throttle valves (BT) and the other (called the main stream) proceeds to the calorimeter. Eventually these two streams merge at the inlet buffer at about 80 psig and recycle to the compressor.

The main stream enters a cylinder called the high pressure buffer which serves to stabilize the fluctuation of the flow pressure. The fluid then either passes through the cooling water coil (when the desired temperature

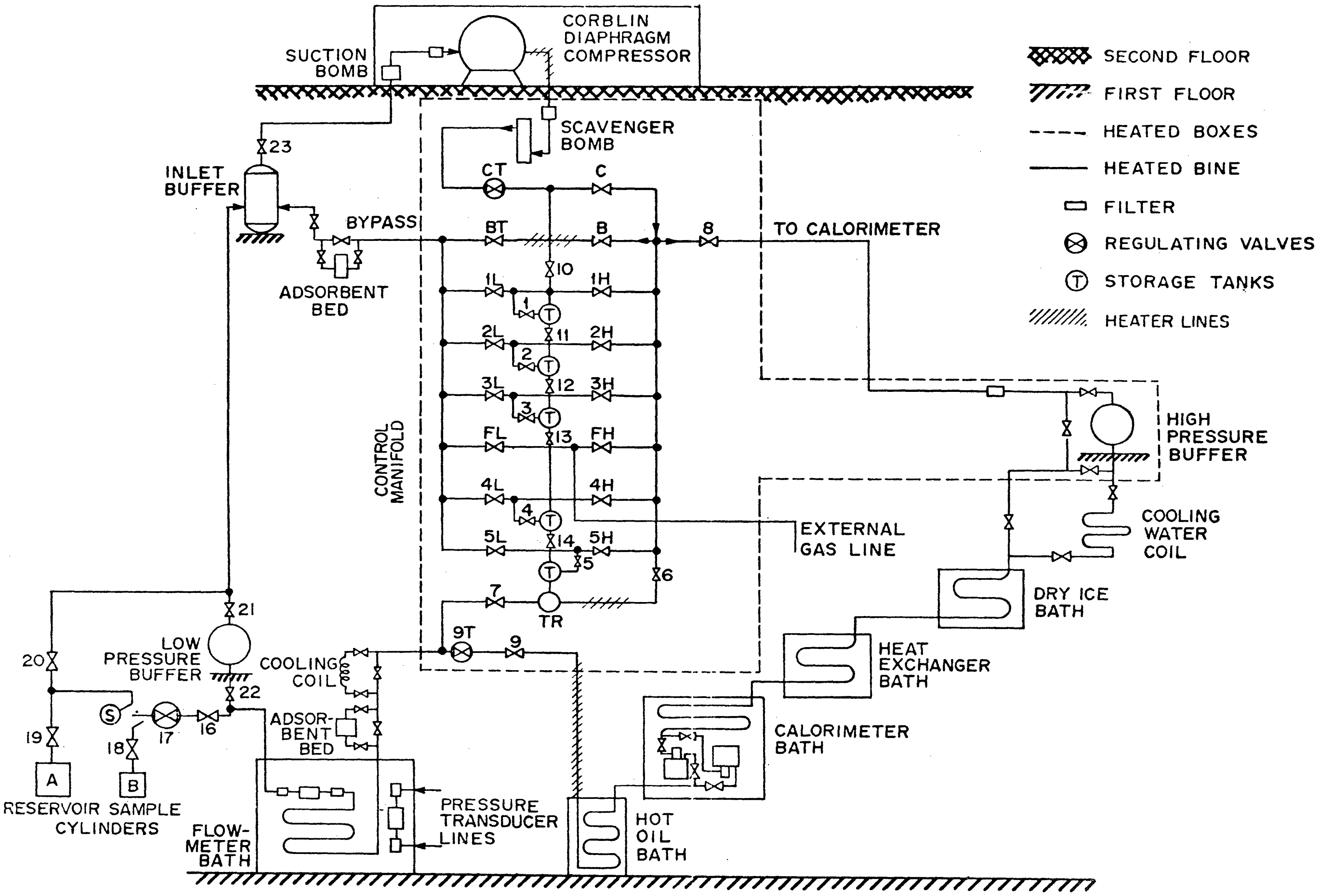

Figure III-1. Flow diagram of the recyle-flow system used for the measurements with argon.

is lower than room temperature) or proceeds directly to the dry ice bath. The dry ice bath contains 175 feet of 3/16 in. O.D. copper tubing which serves to bring the fluid temperature down to about -100°F, if necessary, when the bath is filled with a dry ice-acetone mixture. The stream next enters the heat exchanger bath containing 325 feet of 3/16 in. O.D. copper tubing immersed in a bath fluid which is maintained to within ±1°F of the calorimeter inlet temperature using a controlled immersion heater. It then enters the calorimeter bath containing 100 feet of 3/16 in. O.D. copper tubing for a final temperature conditioning for the calorimeter. Originally both the isothermal and isobaric calorimeters were placed in the bath and the stream was directed to either one of the calorimeters depending on the type of the measurements by manipulating the four cryogenic valves inside the bath. However, it was found out after Furtado's measurements that a small portion of the stream could bypass to the inactive calorimeter as some of the cryogenic valves failed to shut completely. Since it was difficult to prevent the bypass completely during the run, it was decided that the inactive calorimeter be removed from the bath and inlet and outlet lines to the calorimeter were plugged.

The calorimeter bath is well stirred and temperatures are controlled to within ±0.05°F of a desired temperature. Isopentane (temperatures below -50°F) and Dow-Corning silicone oil (temperatures above -50°F) are used as bath fluids for both the calorimeter and heat exchanger baths. At below ambient temperatures, the bath fluid is cooled by liquid nitrogen passing through the cooling coil immersed in the bath. The liquid nitrogen is supplied from externally located 160-liter dewars and its flow is regulated by adjusting a valve located in the nitrogen vent line outside the bath. The measurements of the inlet pressure and temperature, the changes in temperature and pressure across the calorimeter, and the electrical energy input are made as the fluid passes through the calorimeter. After leaving the calorimeter, the condensed part of the fluid, if any, is completely vaporized as it passes through the hot oil bath and returns to the control manifold where it is throttled to 80 psig through the calorimeter throttle valve (9T).

The fluid then enters the flowmeter bath where the flow meter is located. The bath is filled with water and the temperature is maintained at 27 ±0.05°C by a 100 watt tubular heater controlled by a mercury contact switch. The fluid passes through 50 feet of 3/8 in. O.D. copper tubing for the temperature conditioning before entering the calibrated Meriam flow meter. Micron filters are located on the inlet and outlet side of the meter to remove entrapped particles from the stream. The fluid passes through another 50 feet of copper tubing after the flow rate is measured and returns to the compressor via the inlet buffer. Two bypassable absorbent beds are located in the bypass stream to the inlet buffer and in the inlet stream to the flow meter bath. These beds, designated to remove oil and moisture in the stream, consist of layers of molecular sieves 3A and 4A, activated charcoal and drierite. A twelve foot double pipe water cooling coil is placed in the flow meter stream before the absorbent bed. There are five storage tanks located in a heated air bath. These tanks serve to adjust the pressure for the recycling system.

Calorimeters

The isobaric and isothermal calorimeters used in this work are the same ones used by Furtado.[18] The isobaric calorimeter was originally designed by Faulkner[19] and it is modified by previous workers.[25, 61, 18] The isothermal or throttling calorimeter was designed by Mather[37] and it also has been subjected to modifications by previous workers.[61, 18] An excellent description of the original design and modifications to those calorimeters can be found in Furtado's thesis.[18]

Experimental Measurements

Detailed descriptions for the experimental measurements and the measuring instruments are found in the theses of Jones,[25] Manker,[36] and Mather[37] and are discussed here only briefly with an emphasis on the changes made during the present investigation.

The major measurements in this experiment can be listed as the following:

1. Temperature at the inlet to the calorimeter.
2. Temperature rise through the isobaric calorimeter.
3. Temperature difference between the isothermal calorimeter inlet and outlet.
4. Pressure at the inlet to the calorimeter.
5. Pressure drop through the isobaric calorimeter.
6. Pressure drop through the throttling calorimeter.
7. Electrical energy input to the calorimeters.
8. Mass flow rate.

(1) The temperature at the inlet to the calorimeter is assumed to be the calorimeter bath temperature, which is measured using a platinum resistance thermometer. The calibration of the thermometer was made by NBS (June, 1968) and the calibration constants are given in Table A-1 of Appendix A. The accuracy of the bath temperature measurement is 0.04°F.

(2) The temperature rise through the isobaric calorimeter is measured with duplicate six-function copper-constantant thermopiles calibrated by NBS. Calibration data are fitted to fourth degree polynomials by the least square method. The calibration data and the constants of least square fits are given in Table A-2 of Appendix A.

(3) The temperature difference between the isothermal calorimeter inlet and outlet is measured with a 15 junction copper-constantan thermopile calibrated by NBS. The calibration equation for the thermopile was obtained by Furtado[18] and its constants as well as the calibration data are shown in Table A-2 of Appendix A.

(4) Pressures at the inlet to the calorimeter are measured by the Mansfield and Green (M & G) dead weight gage (with a gas to oil pressure transmitter and an electronic null detector) which is sensitive to imbalances as low as 0.05 psi. The resolution of the dead weight gage is 0.2 psig. According to Furtado,[18] who tested the instrument against a calibration standard Model 2400 Ruska dead weight gage, discrepancies between the two sources are within 0.1% over the pressure range from 250 to 2000 psia.

(5) The pressure drops through the isobaric calorimeter are measured using a 40 inch high pressure mercury manometer enclosed in a heated air box to prevent liquid holdup in the lines in case of low temperature operation. Normally the pressure drops never exceed 1 psi. Accuracy of the measurement is ±0.05 inches of mercury.

(6) The pressure drop through the throttling calorimeter is measured using two strain gage type absolute transducers installed on the inlet (high pressure) and outlet (low pressure) pressure taps by Furtado.[18] Originally a strain gage differential transducer (Sensotec Model ZD) with an operating range from 0 to 250 psid up to 2000 psia line pressure was installed for the measurement. However, at the beginning of the isothermal run a significant mass leak was detected through the metal gasket which was deteriorated by corrosion due to prolonged immersion in the flow meter bath. As a result, the differential transducer was sent back to the manufacturer for repair and in the meantime all of the isothermal runs had to be made with the absolute transducers. Each pressure transducer was calibrated against the M&G dead weight gage three times, at the beginning, middle and last period of the isothermal measurements. The results are plotted in Figures III-2 and III-3. For both high and low pressure transducers the following equation well fits the data:

$$E = A + BP + CP^2 + DP^3 \qquad \text{(III-1)}$$

where E = EMF transduced by the transducer, μV

P = gage pressure, psig.

The constants A, B, C and D for each transducer as well as the calibration data are presented in Tables A-3 and A-4 of Appendix A. Average deviations for the equations from the data are 0.025% for the low pressure transducer and 0.020% for the high pressure one.

(7) The electrical energy input to the calorimeters is supplied by a DC power supply (KEPCO Model SM325-2MX) capable of delivering up to 2.0 amps at 325 volts within 0.01% voltage regulation. The power input

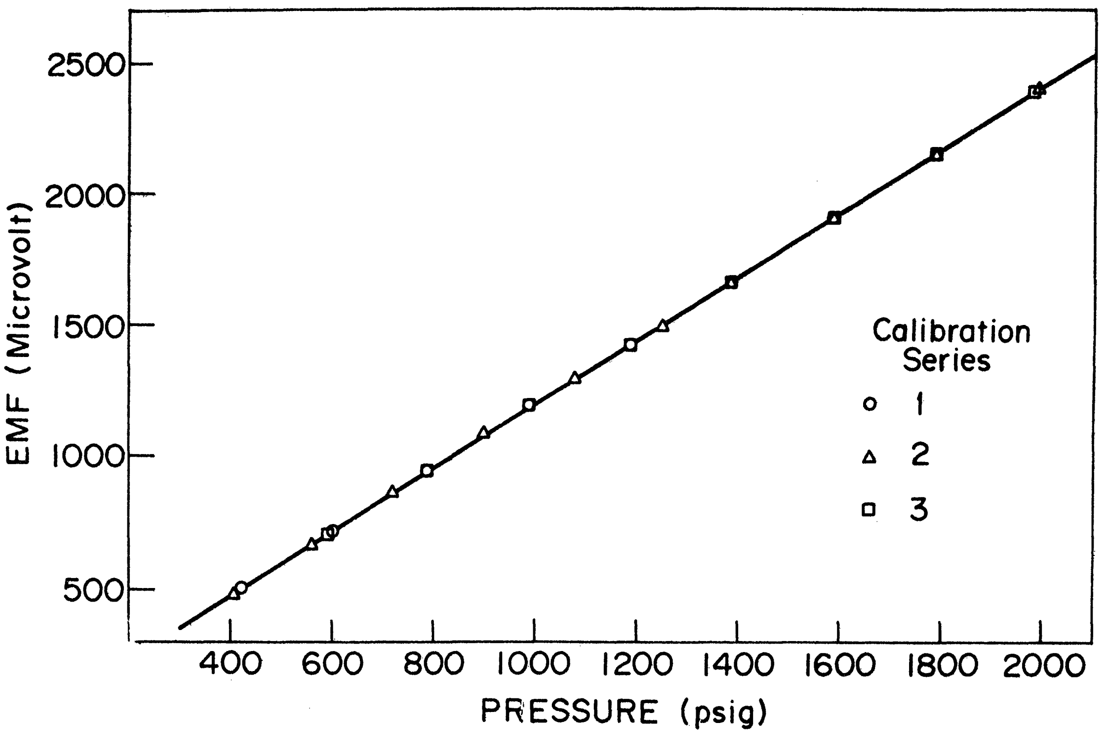

Figure III-2. Pressure transducer (high) calibration.

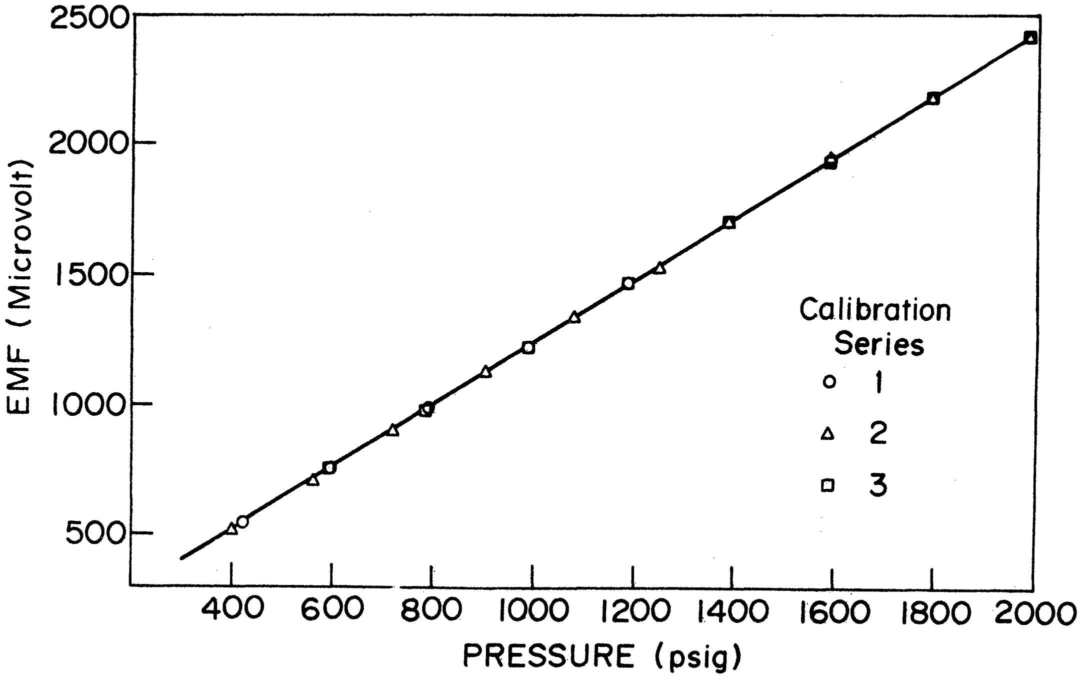

Figure III-3. Pressure transducer (low) calibration.

is measured by a K-3 potentiometer using standard resistors to scale down the voltage to the range of the potentiometer. A wiring diagram for the power measurement circuit appears in Yesavage's thesis.[61] During isothermal measurements it is necessary to make fine adjustments to the power input of the calorimeter heater so that the temperature difference between the inlet and outlet of the calorimeter can be maintained as small as possible. However, it was found from past experience that maintaining the outlet temperature within ±0.02°F (5μV) of the inlet temperature by manual adjustment of a potentiometer attached to the power supply alone was difficult. To accommodate this, the circuit for the isothermal calorimeter was modified by adding a 40-turn Helipot for fine adjustment of its power input. The modified circuit is shown in Figure III-4. The coarse adjustment of the power is made with the potentiometer attached to the power supply (not shown in the drawing). Then the fine adjustment is done by regulating the R_4 setting. The switch S_2 serves as a bypass if necessary. The power input to the calorimeter heater, R_C, is determined by simultaneous measurements of E_1 and E_3. According to Yesavage[61] the accuracy of the power input determination is within ±0.05%.

(8) The mass flow rate is calculated from the pressure drop across the Meriam flow meter, the density and the viscosity of the fluid at the flow meter. The pressure drop is measured to ±0.001 inches by a 20-inch precision water manometer. The density of the fluid is estimated at the flow meter inlet pressure, as measured to ±0.01 inches by a 180 inch mercury manometer, and the flow meter bath temperature using the virial equation truncated after the second virial coefficient:

$$\frac{PV}{RT} = 1 + B/V \tag{III-2}$$

where V = molar volume of the fluid
P = flow meter inlet pressure
T = temperature of the flow meter bath
B = second virial coefficient of the fluid.

The second virial coefficient, B, for argon at temperatures close to the flow meter bath temperature (27°C) can be expressed, based on the data

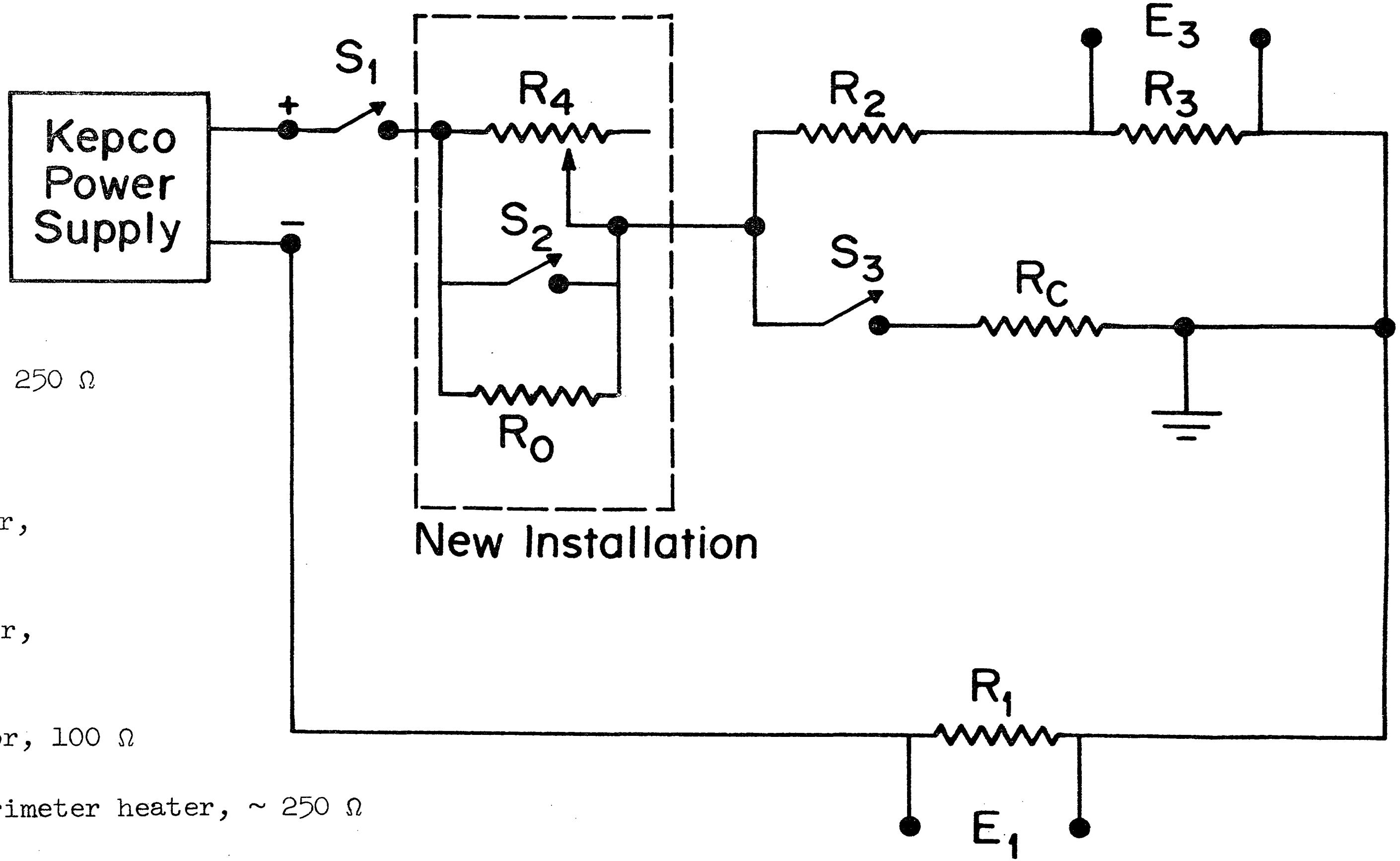

LEGEND

S_1, S_2, S_3	Switches
R_4	40-turn Helipot, 250 Ω
R_0	Resistor, 10 Ω
R_1	Standard resistor, 0.1 Ω
R_2	Standard resistor, 20,000 Ω
R_3	Standard resistor, 100 Ω
R_c	Isothermal calorimeter heater, ~ 250 Ω
E1	EMF across R1 (measured with K-3 potentiometer)
E3	EMF across R3 (measured with K-3 potentiometer)

Figure III-4. A modified circuit of power input to the calorimeter.

by Dymond and Smith,[12] as

$$B = 55.73 - 21534.6/T \tag{III-3}$$

Here B is in cc/g-mole and T is in °K. The viscosity of argon was estimated from the correlation for the viscosity-density isotherm reported by Flynn et al.[20] as

$$\mu = a + b\rho \tag{III-4}$$

where ρ = mass density of argon

a and b were obtained from their data as a = 0.6671 (T-298.16) + 225.3, b = 0.100 (T-298.16) + 109.0. Here T is in °K, a in μpoise, and b in μpoise - cc/g.

The flowmeter is calibrated by a direct method involving the weighing of the condensed fluid collected in a liquid nitrogen cooled sampling tank in a specified time interval. The apparatus and procedure of the calibration have been described by Jones[25] and a modified version for the procedure is later described in detail by Furtado.[18] The flow rates used in the present experimenta are between 0.04 and 0.30 lb/min; however, for most of the cases flow rates are around 0.2 lb/min. As a calibration equation, the following form is used in the present work:

$$\frac{\rho \Delta P}{\mu F} = A + B\left(\frac{F}{\mu}\right) + C\left(\frac{F}{\mu}\right)^2 + D\left(\frac{F}{\mu}\right)^3 \tag{III-5}$$

where ΔP = pressure drop across the flow meter

F = mass flow rate.

This equation has been used by previous workers at the Laboratory.[25, 35, 36, 37, 61, 18] Furtado[18] discussed the following alternative to the equation.

$$\frac{10F}{\sqrt{\rho \Delta P}} = A' + B'X + C'X^2 + D'X^3 \qquad \text{(III-6)}$$

where $X = \ln\left(\frac{\rho \Delta P}{\mu^2} \times 10^3\right)$

He observed from his calibrations for ethane, ethane-propane and methane-ethane mixtures that at low flow rates [$F/\mu < 0.002$ (lb/min/μ poise)] Equation (III-5) was preferable to Equation (III-6), while Equation (III-6) was better at intermediate and high flow rates. Flow meter calibration results for argon were found to be satisfactorily fitted to Equation (III-5) as the upper limit for F/μ was only 0.0012 (lb/min/μ poise) due to the high value of argon viscosity (roughly twice as high as that of ethane). The plot of calibration data (Table A-5 in Appendix A) is shown in Figure III-5. The standard deviation of the data is 0.14%.

It is interesting to compare the present calibration with those for other systems since the calibration should be independent of system fluids if their densities and viscosities are accurately estimated, assuming there is no change in the flow meter characteristics with time. Furtado[18] reported that a single curve could represent the calibrations for his ethane and all of the binary systems of methane-ethane and ethane-propane within 0.25% deviation for the range up to $F/\mu = 2.2 \times 10^{-3}$ (lb/min/micropoise). A comparison of the present calibration with his generalized one is made in Figure III-6. There is, however, a uniform discrepancy of 2.2% between them which indicates errors involved in the estimation of viscosity and/or density. It is unlikely that this discrepancy is due to the errors in density estimation since both for argon and hydrocarbons density can be accurately estimated at the flow meter condition (27°C at 85 psig). Therefore, it is concluded that the discrepancy is due to incorrect estimations of viscosity either of argon or the hydrocarbons (or both). The viscosity of argon, however, is determined from Equation (III-4) which was derived from the direct experimental data while that of hydrocarbons was estimated from the prediction method of Lee, *et. al.*[31] Assuming that there is uniform error in the estimation

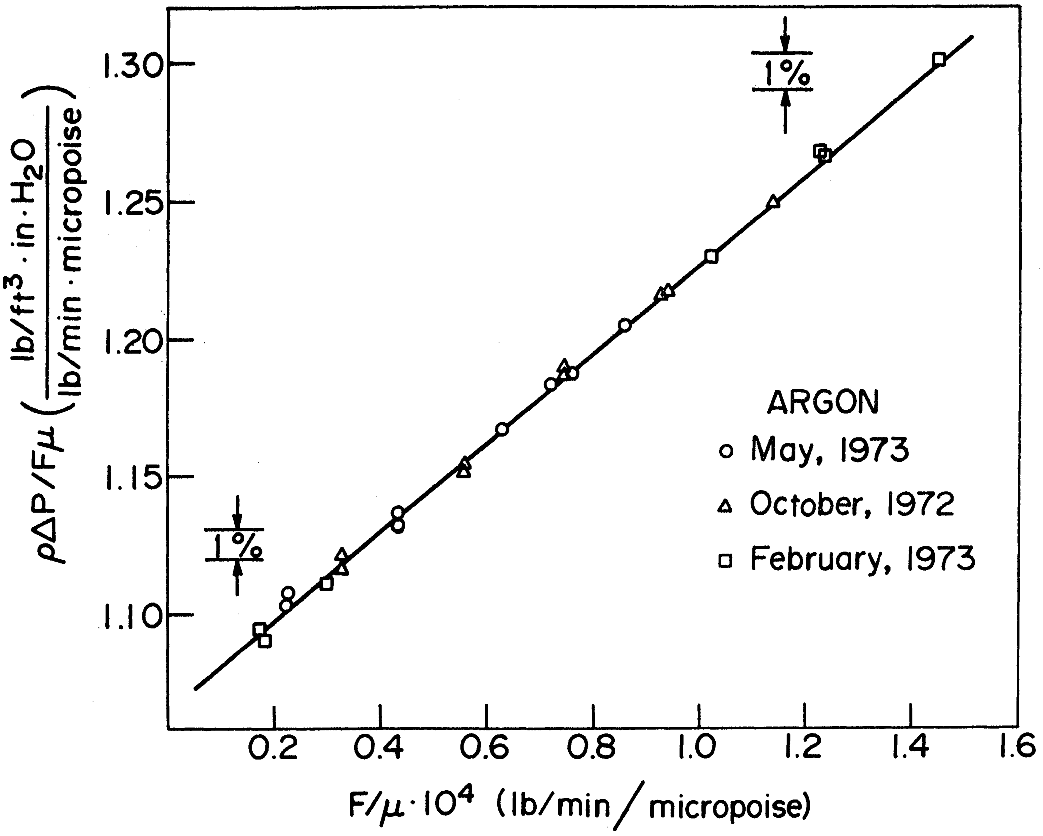

Figure III-5. Flow meter calibration.

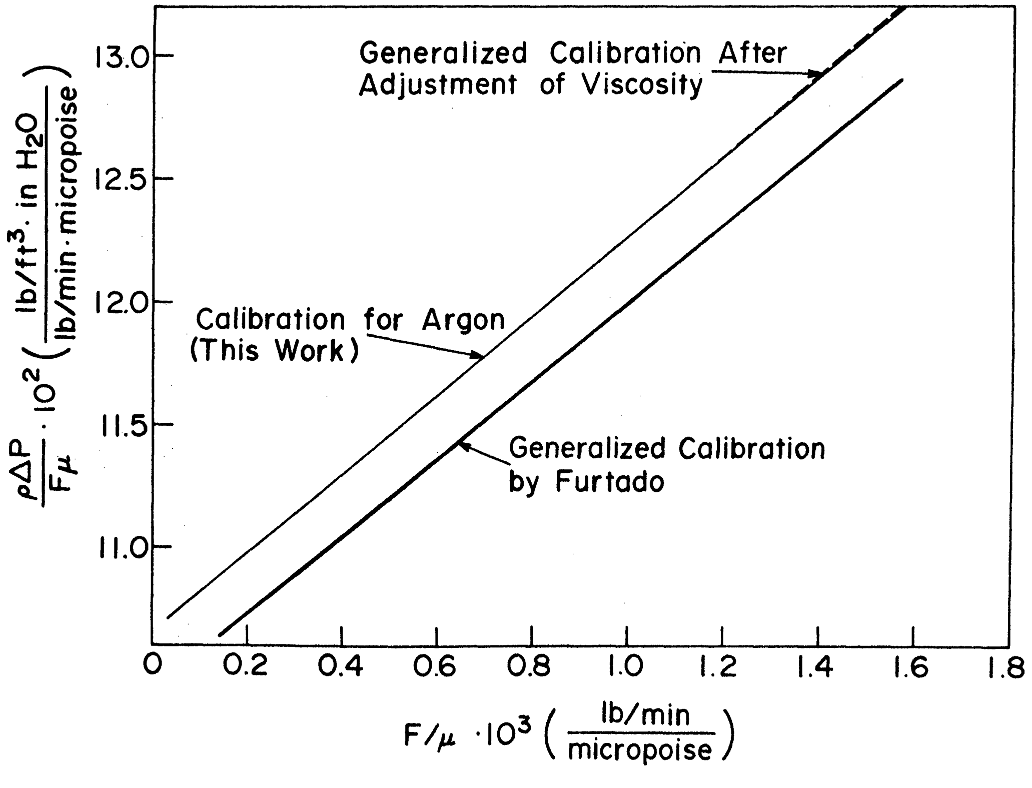

Figure III-6. Comparison of the present flow meter calibration with a generalized one by Furtado.[18]

of viscosity of the hydrocarbons, the generalized calibration is adjusted with uniform increase of 2.2% in viscosity, which lifts the original curve to a new one (see Figure III-6). The agreement between the argon and the adjusted calibrations is well within 0.1%, which is remarkable since it is better than fitting abilities of both equations to their calibration data.

All of the electrical or electrically transduced measurements are made on a K-3 potentiometer (Leeds and Northrup Co.) using standard resistors to scale down voltages to the range of the potentiometer. The circuit for the potentiometer and calibration data for the resistors are essentially the same as the ones given in the Jones' thesis.[25] During the present investigation 2-volt rechargeable storage cells which had been used for the power source to the potentiometer were replaced by a Leeds and Northrup power supply (#099034). This replacement eliminates the need for recharging the cell and frequent standardizations to compensate for the voltage drop of the cells due to depletion. In addition emf of the standard cell for the potentiometer was carefully checked by the procedures suggested in the manual and the standard cell setting on the potentiometer was adjusted accordingly.

Experimental Procedure

An excellent procedure for the acquisition of the basic data is presented in Furtado's work[18] and is applicable to the present work. Therefore, the operating procedure is not described in detail here. Instead, a brief discussion is made on some careful measurements taken during the present experiment.

(1) Usually the first data point of an experimental run is measured when it appears that the flow system reaches its steady state. This is judged by the indications of the dead weight pressure balance and the calorimeter thermocouple emf when other control elements were functioning properly. Nevertheless, past experiences showed that the first data points were frequently subjected to errors due to unsteady state effect. To remedy this, every first point was repeated again 30 minutes later to check the unsteady state effect. If the result shows

an appreciable change in the values, which indicate an unsteady state behavior of the system, then the same procedure is repeated again until the consecutive values reproduce each other within experimental uncertainty.

(2) After the first point consecutive measurements are spaced at least 45 minutes apart so that a period of more than ten minutes is allowed from the time the system shows steady state to the final measurement.

(3) Mass leaks from the system are checked at the beginning of the equipment operation. During the measurements, if a leak is suspected, further measurements are postponed until the source is found and the leak stopped.

(4) An average calorimeter bath temperature variation over a given run is controlled within the variation of ±0.05°F (as compared to ±0.1°F shown in previous investigations[37, 61, 18]). Inlet pressure variations for a run are regulated within ±1.0 psia (as compared to ±2.0 psia reported by previous investigators[37, 61, 18]) and they are further regulated within ±0.3 psia for the measurements in the vicinity of $C_p(T)$ maxima.

Material Used

The material used in the present investigation is UHP grade argon (99.999%) of Matheson Gas Co. Before the sample is charged, the entire recycle system is first evacuated (the last fluid in the system was a ternary mixture of 85% CH_4 - 10% C_2H_6 - 5% C_3H_8) to about 100 micron of vacuum. It is then filled with technical grade argon (99.9%) up to 200 psia and the gas circulated through the system for 24 hours. The system is evacuated again to about 100 micron of vacuum before the sample is charged to the system.

Once the sample is charged it is circulated through the system about 24 hours and a portion of it is taken into a standard cylinder for composition analysis. As a primary check for possible impurities, the sample from the standard cylinder was subjected to a gas-solid chromatographic analysis. A specific column capable of separating argon, N_2

and CH_4 was made with six foot 1/4 in. O.D. copper tubing filled with Linde molecular sieve 5A, which was dried at 600°F for an hour in a furnace as suggested in the literature.[33] The result of the analysis using the column (the column and a thermal conductivity detector are immersed in the flow meter bath at 27°C and helium is used as a carrier gas) is presented in Figure III-7. As shown in the figure, no impurities are detected through the chromatographic analysis. Later the sample is analyzed by mass spectrometry at the University of Michigan and its analysis is in Table III-1.

TABLE III-1

Composition of Argon

CO_2	0.002%
N_2	0.003%
CH_4	0.005%
Ar(by difference)	99.990%
	100.000%

Molecular weight of sample 39.945

Region of Measurements

The range of experimental determinations is shown on a P-T plane as Figure III-8. The horizontal and vertical lines represent isobaric and isothermal runs. Each run is numbered in the chronological order of the investigation. The numbers with "R" designate isothermal runs and one isenthalpic run (48R). The vapor pressure curve is drawn in the diagram to indicate the phase corresponding to each run. The dotted line drawn from the critical point represents an estimate of the locus of $C_p(T)$ maxima. Some of the isobaric runs are designated with more than one number as they are subjected to more than one measurement. In some cases the measurements are repeated for the entire temperature ranges, in others they are repeated only for specific temperature ranges where the accuracy of the data is in question. Since the primary interest

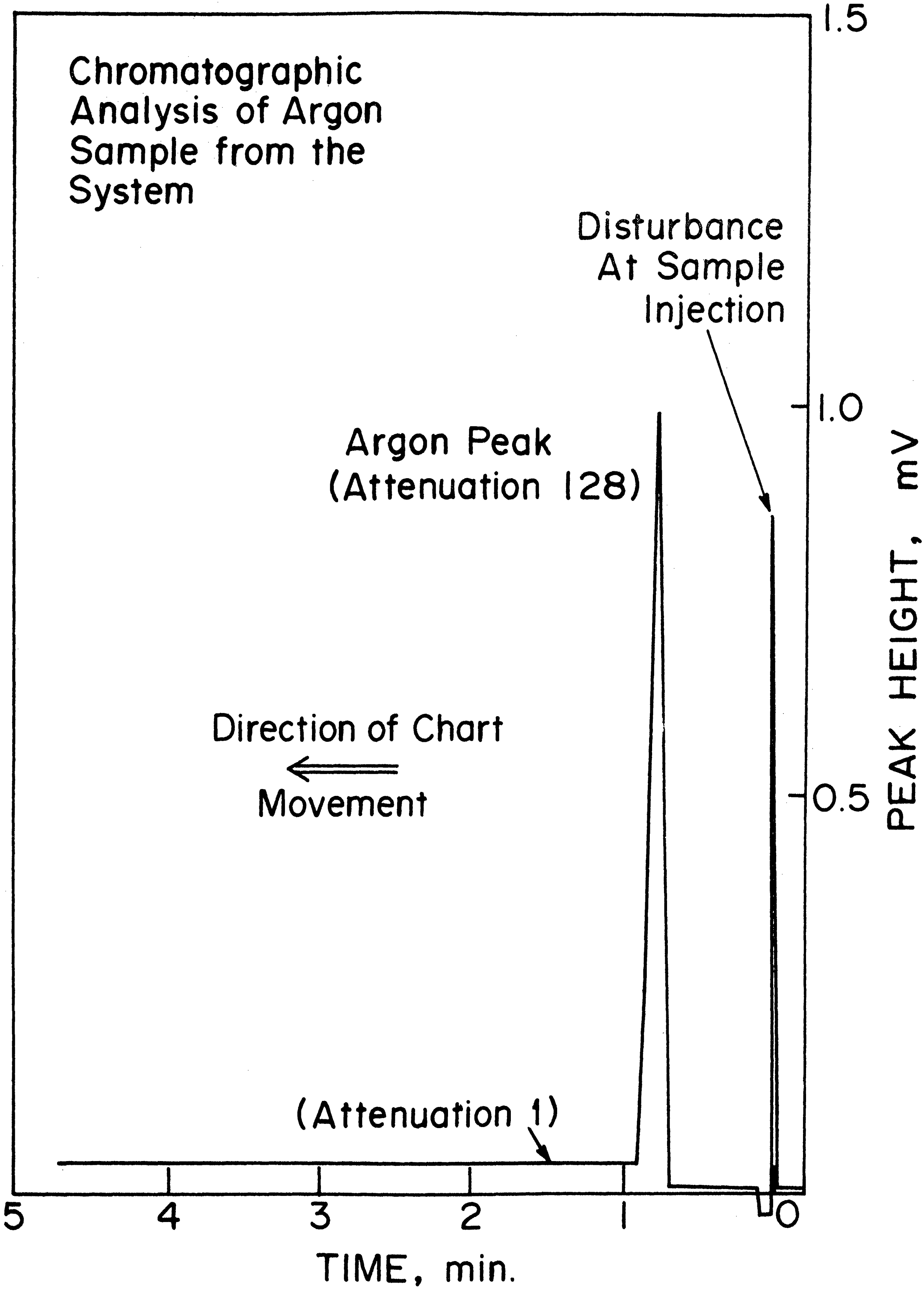

Figure III-7. Chromatographic analysis of the argon sample from the system.

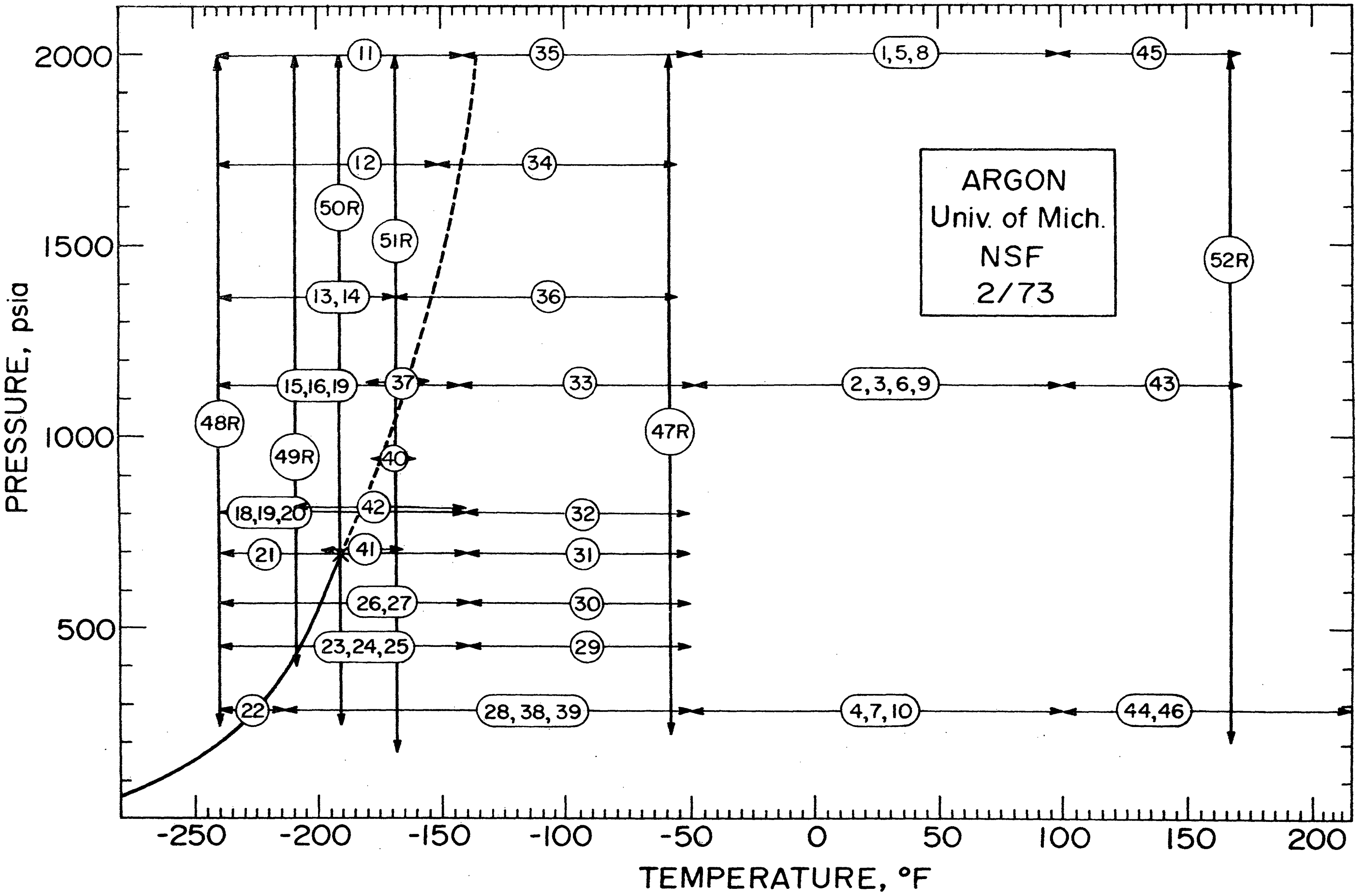

Figure III-8. Range of calorimetric determination on argon.

was in C_p measurements in the region of $C_p(T)$ maxima and vapor pressure curve, as many isobaric runs were planned as possible in this region. In the supercritical region isobaric runs are made at 706, 800, 950, 1143, 1371, 1714 and 2000 psia. In the subcritical region measurements were made at 286, 457 and 571 psia. Except for 950 and 2000 psia, those pressures were chosen in such a way that their reduced values are the same as those of the propane runs conducted by Yesavage,[61] thus forming a set of corresponding states between two systems. As will be seen later, the pressure levels for the measurements of C_2F_6 are also made in the same way.

Extensive measurements were made in the gas region at 286 psia and in the supercritical regions at 1143 psia and 2000 psia. In all, seven isobaric runs were made for seven C_p maxima determinations and three isobaric runs were made across the two phase boundary which gave the enthalpy changes on vaporization as well as the heat capacity of liquid and gas phases. One isenthalpic run at -240°F and five isothermal runs at -208.9°F, -191.2°F, -168.3°F, -58°F and 167°F were made to obtain isothermal changes of enthalpy. Those runs are designed to establish a network of enthalpy loops with the isobaric runs so that the thermodynamic consistency of the data could be established. It should be mentioned here that because of the experimental difficulty encountered during isothermal measurements across the two phase boundary, the isothermal run at -208.9°F (49R) could not be extended to the gas phase region. The basic data for argon are presented in Tables B-1 (isobaric) and B-2 (isenthalpic and isothermal) of Appendix B.

Results

C_p and $C_p(T)$ Maxima

From the isobaric measurements of enthalpy, C_p values were determined by the method described in Section II. For the 286 psia isobar (see Figure III-9), measurements were extended to a higher temperature region (up to 220°F) where the thermodynamic behavior of argon is closer to that of ideal gas than any other region of the present measurements.

For the isobars at 457 psia (Figure III-10) and 571 psia (Figure III-11) C_p values for both liquid and gas phases were determined.

A typical isobar in the supercritical region (1143 psia) is illustrated in Figure III-12. The data extend from -250°F to 190°F. The C_p value increases sharply as the temperature approaches the location of the peak (designated T^M), where C_p reaches the maximum value (designated C_p^M) and then decreases rapidly as the temperature increases. At higher temperatures C_p changes only slightly with temperature. In this case T^M is determined as 165.0°F with uncertainty of ±0.2°F and C_p^M as 0.935 ±0.003 Btu/lb-°F. Figure III-13 shows an isobar at 706 psia which is less than 1 psia above the critical pressure (P_C = 705.4 psia from Grigor and Steele[21]). The $C_p(T)$ curve, as shown in Figure III-13, forms a very sharp peak exceeding 10 Btu/lb-°F (cf. C_p^0 = 0.1244 Btu/lb-°F). T^M for this curve is -188.6°F with an uncertainty of ±0.2°F (the critical temperature by Grigor and Steel[21] is -188.61°F). T^M was determined by repeated measurements with small outlet temperature increments between successive data points as represented by the short dotted lines in the vicinity of the peak.

The plot of the isobaric run at 950 psia (Figure III-14) clearly defines an equal area curve in the vicinity of the $C_p(T)$ maximum. This run was made particularly to determine the peak. The temperature increments between successive measurements were made smaller than 2°F. $C_p(T)$ curves at 800, 1371, 1714 and 2000 psia are also shown in Figures III-15, III-16, III-17 and III-18, respectively. C_p values for each isobar are tabulated in Table III-2 and $C_p(T)$ maxima data are listed in Table III-3. $\overline{C}_p$ values are listed in Table C-1 of Appendix C.

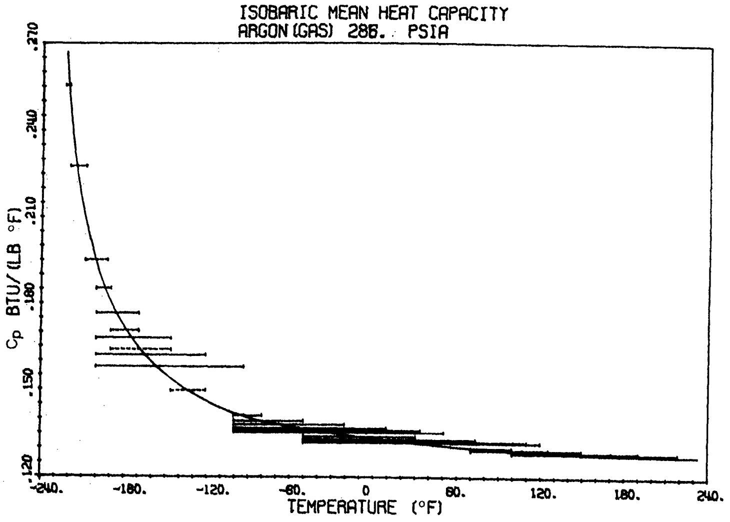

Figure III-9. Isobaric heat capacity for argon at 286 psia.

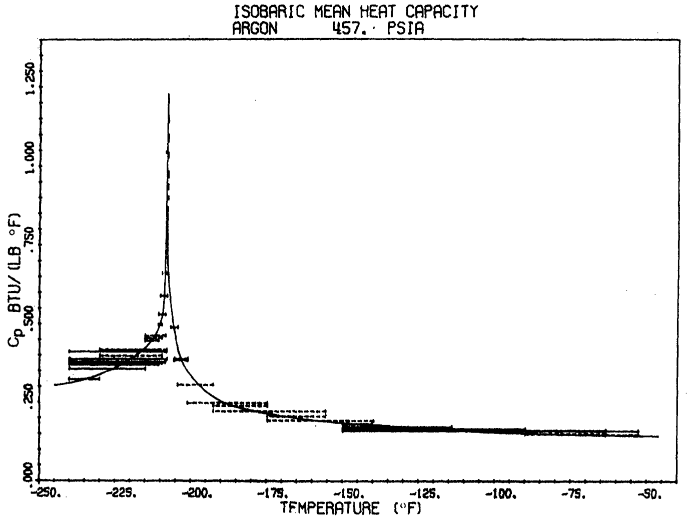

Figure III-10. Isobaric heat capacity for argon at 457 psia.

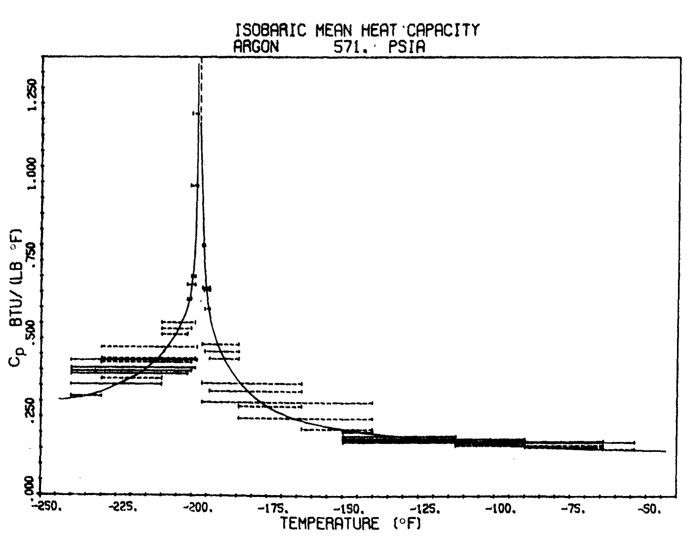

Figure III-11. Isobaric heat capacity for argon at 571 psia.

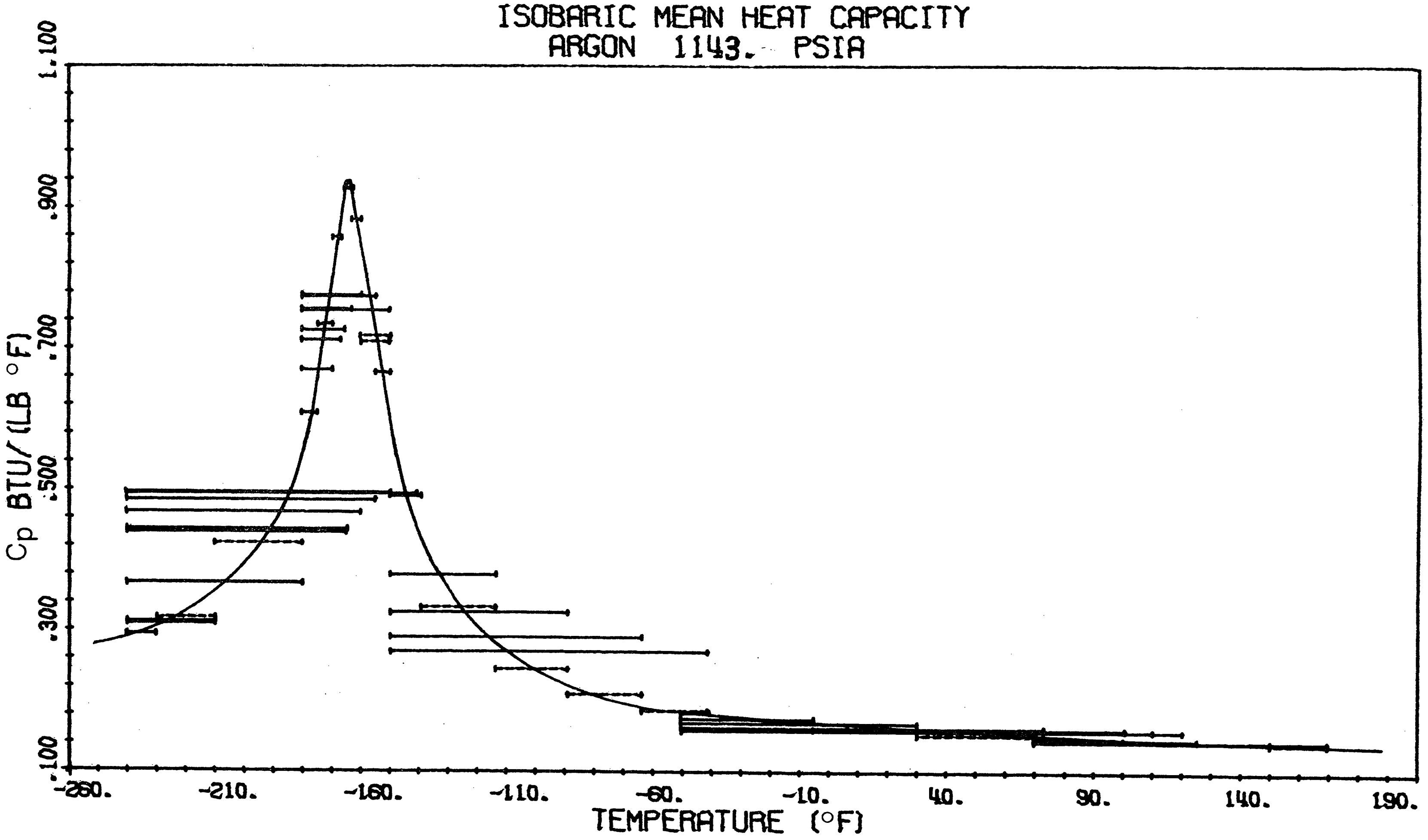

Figure III-12. Isobaric heat capacity for argon at 1143 psia.

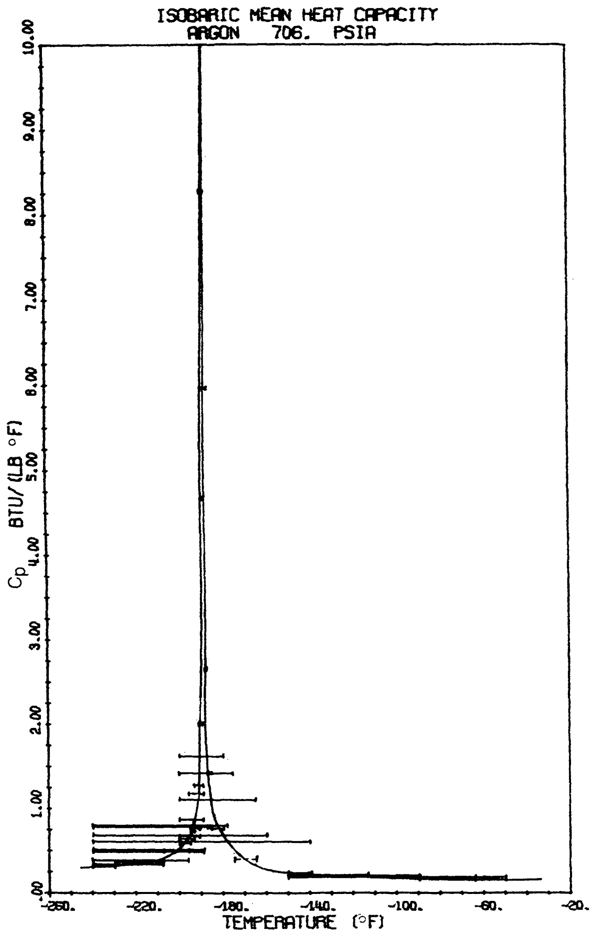

Figure III-13. Isobaric heat capacity for argon at 706 psia.

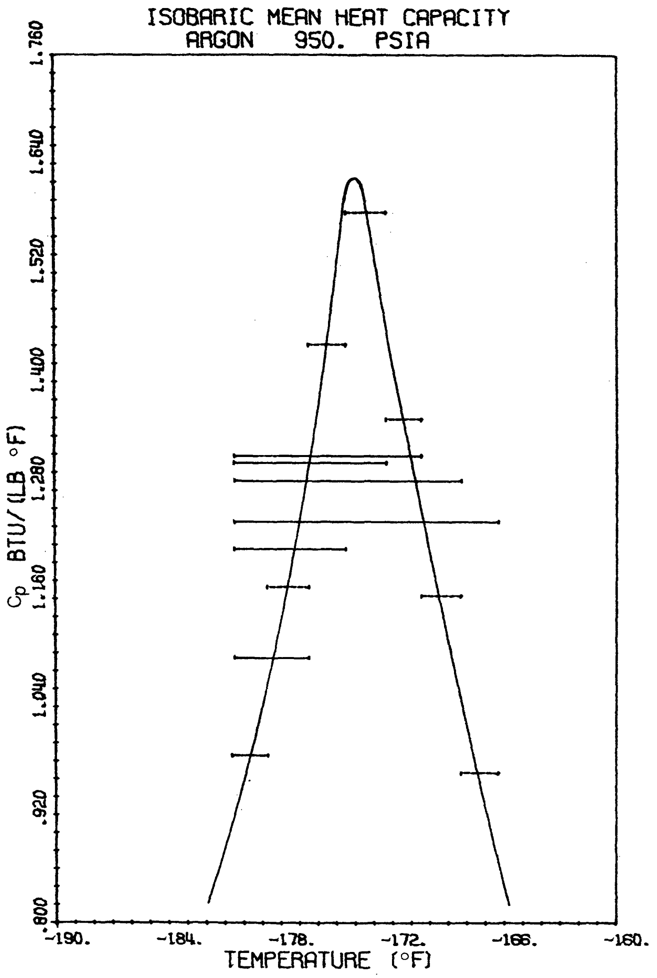

Figure III-14. Isobaric heat capacity for argon at 950 psia.

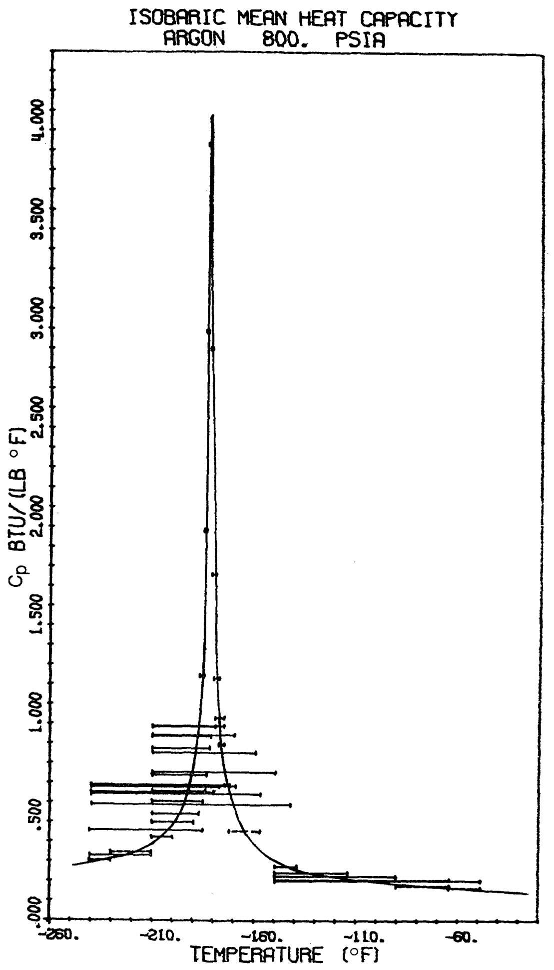

Figure III-15. Isobaric heat capacity for argon at 800 psia.

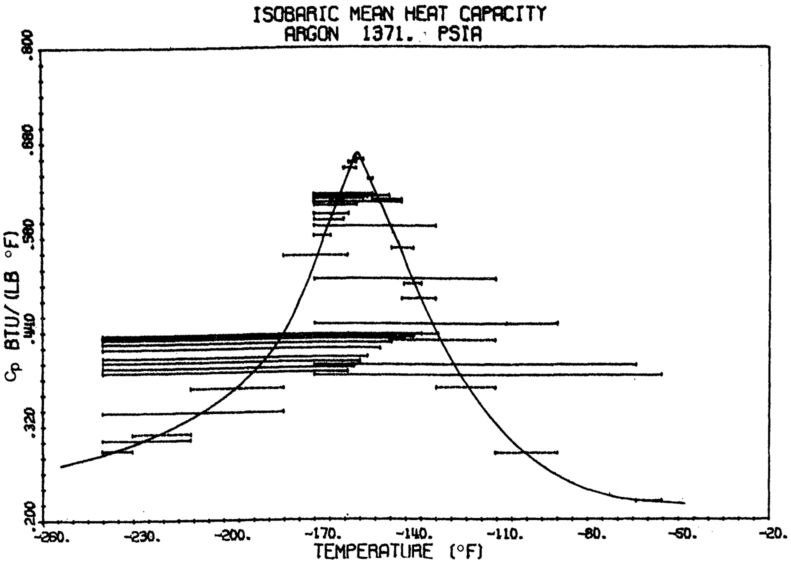

Figure III-16. Isobaric heat capacity for argon at 1371 psia.

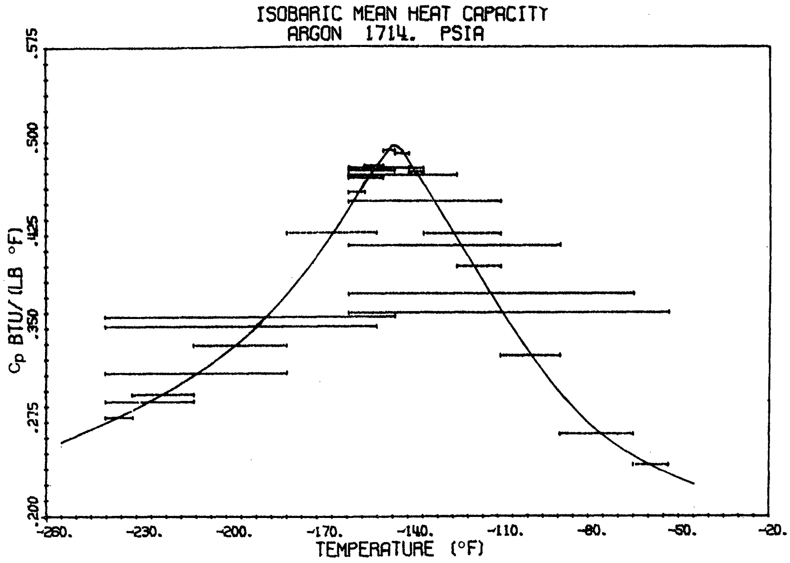

Figure III-17. Isobaric heat capacity for argon at 1714 psia.

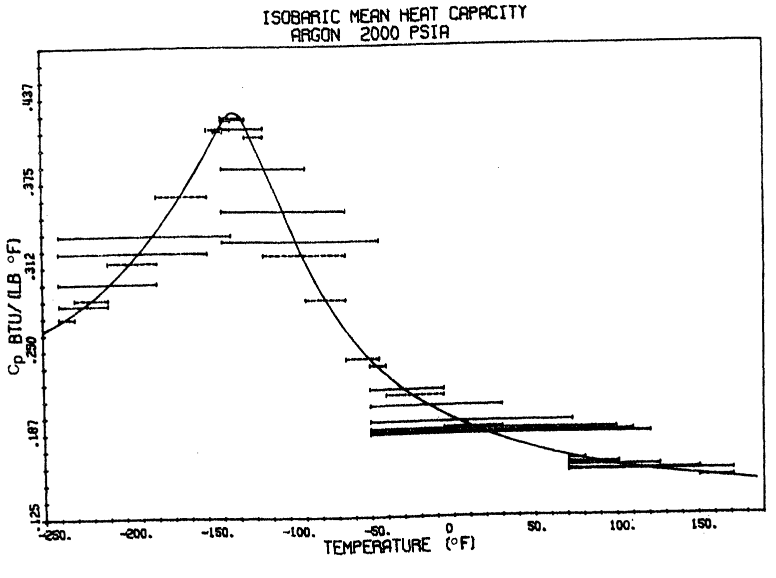

Figure III-18. Isobaric heat capacity for argon at 2000 psia.

TABLE III-2

ISOBARIC HEAT CAPACITIES OF ARGON

Pressure = 286. psia		Pressure = 457. psia		Pressure = 571. psia		Pressure = 706. psia		Pressure = 800. psia	
Temperature (°F)	C_p (Btu/lb-°F)	Temperature (°F)	C_p (Btu/lb-°F)	Temperature (°F)	C_p (Btu/lb-°F)	Temperature (°F)	C_p (Btu/lb-°F)	Temperature (°F)	C_p (Btu/lb-°F)
-230.	0.2922	-240.	0.3090	-240.	0.3044	-250.	0.2924	-250.	0.2705
-220.	0.2457	-230.	0.3378	-230.	0.3281	-240.	0.3035	-240.	0.2946
-210.	0.2152	-220.	0.3880	-220.	0.3691	-230.	0.3236	-230.	0.3204
-200.	0.1923	-215.	0.4250	-210.	0.4362	-220.	0.3558	-220.	0.3435
-190.	0.1787	-210.	0.4750	-205.	0.5139	-210.	0.3970	-210.	0.3850
-180.	0.1705	-209.	0.5000	-200	0.6649	-200.	0.5226	-200.	0.4793
-170.	0.1640	-208.5	0.7250	-199.	0.9358	-195.	0.7004	-195.	0.6072
-160.	0.1586	-206.	0.5373	-198.5	2.2660	-193.	0.8255	-190.	0.8000
-150.	0.1544	-202.	0.3620	-197.5	1.0600	-191.	1.0750	-188.	0.9095
-140.	0.1510	-198.	0.3020	-196.	0.7620	-190.	1.3410	-186.	1.1500
-130.	0.1482	-194.	0.2717	-194.	0.5216	-189.	2.7390	-184.	2.1930
-120.	0.1460	-190.	0.2528	-190.	0.4360	-188.6.	10.1000	-183.	3.7600
-110.	0.1441	-185.	0.2389	-180.	0.3112	-187.9	9.0450	-182.6	4.0570
-100.	0.1424	-180.	0.2276	-170.	0.2544	-187.	1.9400	-182.	3.2560
- 80.	0.1398	-170.	0.2100	-160.	0.2270	-185.	1.2170	-181.	2.4120
- 60.	0.1378	-160.	0.1961	-140.	0.1983	-183.	0.7862	-180.	1.6780
- 40.	0.1359	-140.	0.1759	-120.	0.1794	-180.	0.5800	-178.	1.1510
- 20.	0.1344	-120.	0.1638	-100.	0.1680	-175.	0.4274	-175.	0.7930
0.	0.1333	-100.	0.1551	- 80.	0.1594	-170.	0.3691	-170.	0.5513
20.	0.1324	- 80.	0.1508	- 60.	0.1515	-160.	0.2899	-160.	0.3600
40.	0.1316	- 60.	0.1475			-140.	0.2214	-150.	0.2960
70.	0.1306					-120.	0.2030	-140.	0.2660
100.	0.1295					-100.	0.1850	-120.	0.2187
130.	0.1288					- 80.	0.1745	-100.	0.1945
160.	0.1283					- 60.	0.1620	- 80.	0.1740
190.	0.1281					- 40.	0.1530	- 60.	0.1614
220.	0.1278							- 40.	0.1630

TABLE III-2 (Concluded)

Pressure = 950. psia		Pressure = 1143. psia		Pressure = 1371. psia		Pressure = 1714. psia		Pressure = 2000. psia	
Temperature (°F)	C_p (Btu/lb-°F)	Temperature (°F)	C_p (Btu/lb-°F)	Temperature (°F)	C_p (Btu/lb-°F)	Temperature (°F)	C_p (Btu/lb-°F)	Temperature (°F)	C_p (Btu/lb-°F)
-180.	0.9640	-250.	0.2846	-250.	0.2714	-250.	0.2626	-250.	0.2608
-178.	1.1260	-230.	0.3025	-230.	0.2959	-230.	0.2866	-230.	0.2797
-176.	1.3520	-210.	0.3466	-210.	0.3270	-210.	0.3107	-210.	0.2994
-174.	1.6270	-200.	0.3863	-200.	0.3538	-190.	0.3447	-190.	0.3225
-172.	1.4400	-190.	0.4437	-190.	0.3898	-180.	0.3712	-180.	0.3383
-170.	1.2140	-180.	0.5477	-180.	0.4324	-170.	0.4037	-170.	0.3532
-168.	1.0360	-170.	0.8150	-170.	0.5334	-160.	0.4463	-160.	0.3745
-166.	0.8444	-167.	0.8995	-160.	0.6295	-150.	0.4830	-150.	0.3938
		-165.	0.9350	-158.	0.6490	-146.	0.4929	-140.	0.4185
		-163.	0.9004	-156.	0.6624	-144.	0.4947	-136.	0.4235
		-160.	0.8387	-154.	0.6490	-142.	0.4929	-134.	0.4248
		-150.	0.5905	-150.	0.6171	-140.	0.4890	-130.	0.4217
		-140.	0.4294	-140.	0.5344	-130.	0.4572	-120.	0.4086
		-130.	0.3464	-130.	0.4333	-120.	0.4155	-100.	0.3512
		-120.	0.3000	-120.	0.3638	-100.	0.3296	- 80.	0.2932
		-100.	0.2400	-100.	0.2800	- 80.	0.2714	- 60.	0.2565
		- 80.	0.2101	- 80.	0.2370	- 60.	0.2380	- 40.	0.2319
		- 60.	0.1935	- 60.	0.2224			- 20.	0.2121
		- 30.	0.1763					0.	0.1988
		0.	0.1637					30.	0.1831
		30.	0.1562					60.	0.1715
		60.	0.1518					90.	0.1636
		90.	0.1468					120.	0.1580
		120.	0.1441					150.	0.1534
		150.	0.1409					180.	0.1497
		180.	0.1387						

TABLE III-3

$C_p(T)$ Maxima Data For Argon

Pressure (psia)	T^M (°F)	C_p^M (Btu/lb-°F)
706	-188.6 ±0.2	>10.0
800	-182.6 ±0.2	4.057 ±0.014
950	-174.0 ±0.2	1.627 ±0.004
1143	-165.0 ±0.2	0.935 ±0.003
1371	-158.9 ±0.5	0.649 ±0.002
1714	-144.0 ±0.8	0.4947 ±0.0015
2000	-134.0 ±1.0	0.4248 ±0.0010

Isenthalpic and Isothermal Data

One isenthalpic run was made at -240°F and the basic data were plotted (see Figure III-19) to obtain the values of μ. It is observed that the curve goes through the inversion point ($\mu = 0$ at $P = 425$ psia). The values are listed in Table III-4. Table III-5 presents isothermal enthalpy changes at -240°F which were obtained from the isenthalpic data using the method discussed in Section II. A typical isothermal run (-168.3°F) is illustrated in Figure III-20. The equal area curve is drawn through the basic isothermal data using the method discussed in Section II. Note that all the ϕ values are negative. This curve is extrapolated to the zero pressure value calculated from the thermodynamic relation

$$\phi\ (T,\ P = 0) = B - T\left(\frac{dB}{dT}\right) \qquad \text{(III-7)}$$

where B is the second virial coefficient.

B from Gosman, et al.[21] (expressed in an equation form) was used for the calculation. The $-\phi$ value increases sharply as the pressure approaches the peak location ($P \approx 950 \pm 25$ psia), where $-\phi$ reaches its maximum (0.06915 ±0.00069 Btu/lb-psid), and then it decreases rapidly as the pressure passes the peak. At higher pressures ϕ changes only slightly

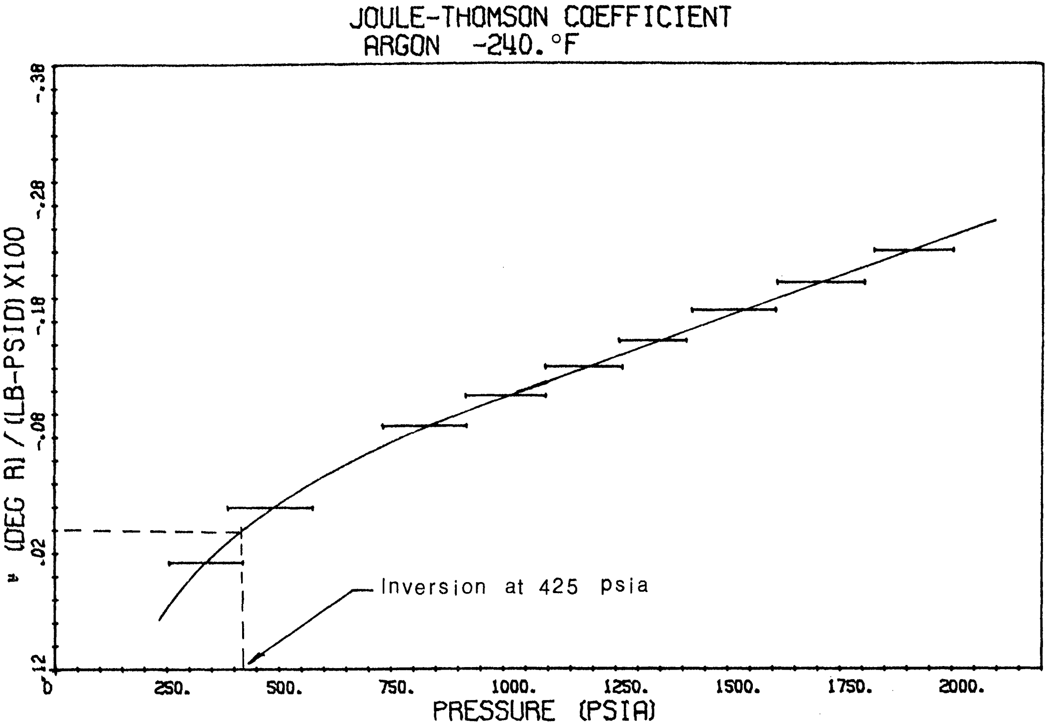

Figure III-19. Joule-Thomson coefficient for argon at -240°F.

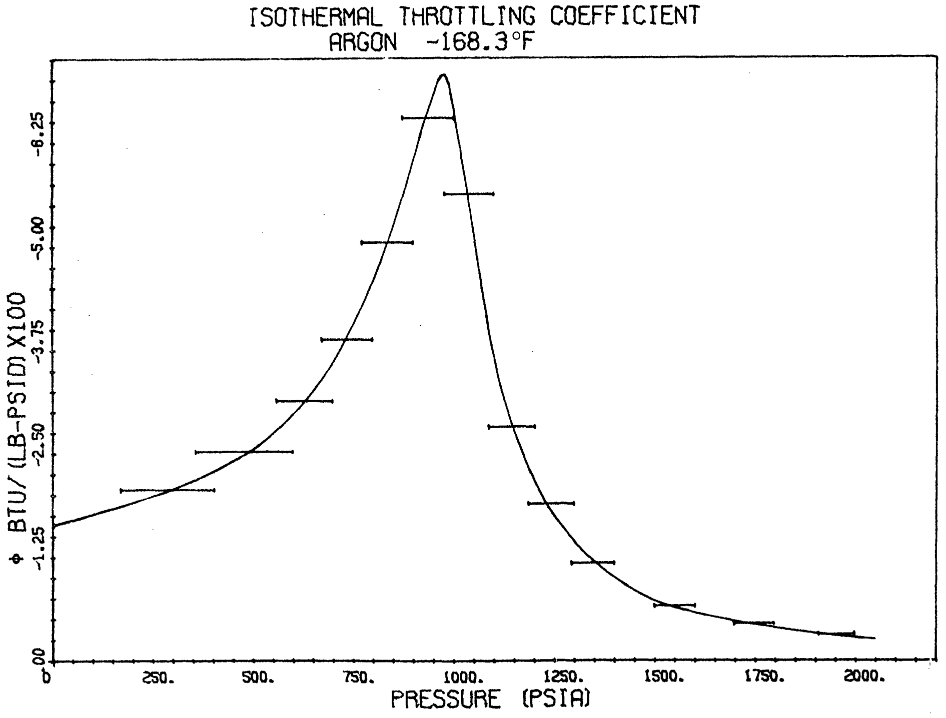

Figure III-20. Isothermal throttling coefficient for argon at -168.3°F.

TABLE III-4

JOULE-THOMSON COEFFICIENTS OF ARGON AT -240.°F

Pressure (psia)	μ x 100 (°F/psid)
250.	0.0700
300.	0.0434
400.	0.0033
500.	-0.0245
600.	-0.0471
800.	-0.0850
1000.	-0.1140
1200.	-0.1427
1400.	-0.1722
1600.	-0.1992
1800.	-0.2248
2000.	-0.2515

TABLE III-5

ENTHALPY DIFFERENCE OF -240.°F ISOTHERM CALCULATED FROM THE ISENTHALPIC DATA

Pressure (psia)	$\underline{H}$ (Btu/lb)
2000.	0
1714.	-0.18
1371.	-0.37
1143.	-0.47
800.	-0.58
706.	-0.60
571.	-0.62
457.	-0.63
286.	-0.62

with pressure. The other isotherms at -208.9°F, -191.2°F and 167°F are also illustrated in Figures III-21, III-22 and III-23, respectively. Another $\phi(P)$ maximum was determined from the -58°F isotherm as shown in Figure II-4 ($-\phi = 0.01073 \pm 0.00005$ Btu/lb-psid at $P = 1200 \pm 50$ psia). Values for $\phi(P)$ maxima are listed in Table III-6. The ϕ values of the isotherms are presented in Table III-7. Values for $\bar{\mu}$ and $\bar{\phi}$ are listed in Tables C-2 and C-3 of Appendix C.

TABLE III-6

$\phi(P)$ Maxima Data for Argon

Temperature (°F)	Pressure (psia)	$-\phi \times 100$ (Btu/lb-psid)
-168.0	950 ±20	6.915 ±0.069
- 58.0	1200 ±50	1.0725 ±0.0054

Enthalpy Changes on Vaporization

A typical plot of enthalpy vs temperature across the two phase boundary (457 psia) is shown in Figure III-24. Enthalpy change on vaporization is determined from the enthalpy difference between the upper and lower break points. It was observed that the phase transistion is isothermal within ±0.02°F (note that the sample used in the measurement is 99.9% argon). Enthalpy traverses for 286 and 571 psia appear in Figures III-25 and III-26. The data for these plots are presented in Table C-4 of Appendix C. The latent heats and saturation temperatures determined in this work are presented in Table III-8 together with literature values for comparison.

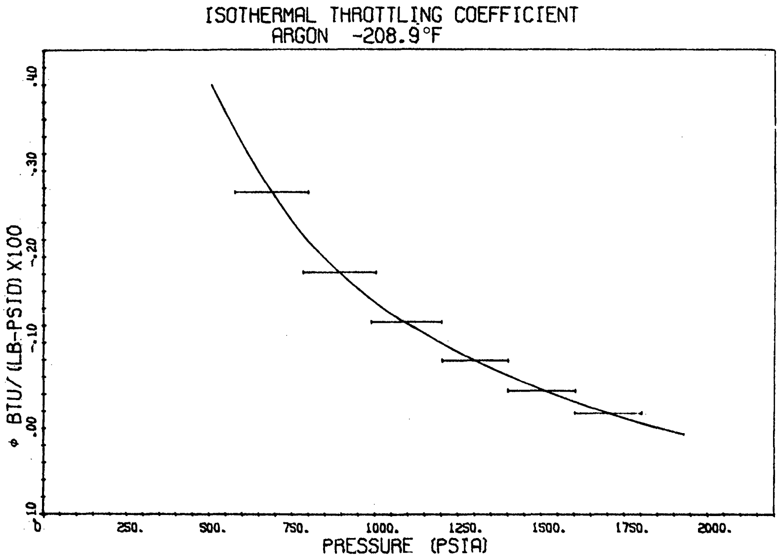

Figure III-21. Isothermal throttling coefficient for argon at -208.9°F.

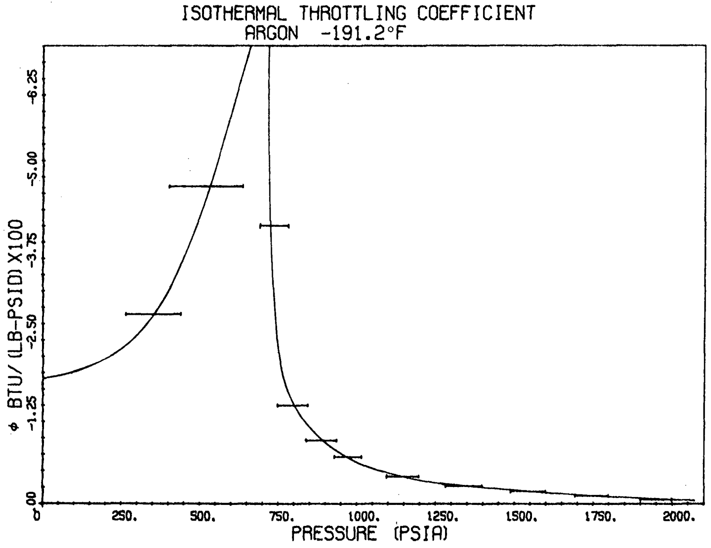

Figure III-22. Isothermal throttling coefficient for argon at -191.2°F.

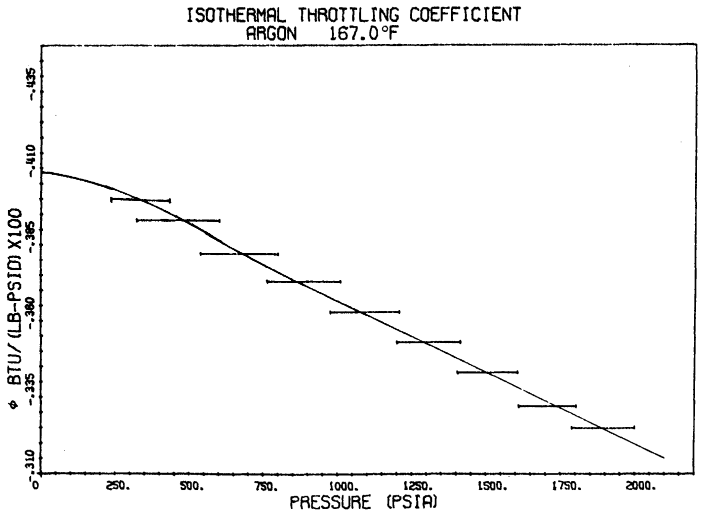

Figure III-23. Isothermal throttling coefficient for argon at 167°F.

TABLE III-7

ISOTHERMAL THROTTLING COEFFICIENTS OF ARGON

Temperature = -209.°F		Temperature = - 191.°F		Temperature = -168.°F		Temperature = -58.°F		Temperature = 167.°F	
Pressure (psia)	- Φ x 100 (Btu/lb-psid)	Pressure (psia)	- Φ x 100 (Btu/lb-psid)	Pressure (psia)	- Φ x 100 (Btu/lb-psid)	Pressure (psia)	- Φ x 100 (Btu/lb-psid)	Pressure (psia)	- Φ x 100 (Btu/lb-psid)
550.	0.3690	0.	1.8900	0.	1.6410	0.	0.9450	0.	0.4037
600.	0.3284	100.	2.0800	100.	1.7620	200.	0.9741	200.	0.4103
700.	0.2646	200.	2.3400	200.	1.8990	400.	0.9953	400.	0.3969
800.	0.2180	300.	2.6400	300.	2.0840	600.	1.0220	600.	0.3863
900.	0.1739	400.	3.1400	400.	2.2950	800.	0.0510	800.	0.3761
1000.	0.1474	500.	4.1700	500.	2.5670	900.	1.0600	1000.	0.3668
1200.	0.0994	580.	6.0510	600.	2.9740	1000.	1.0670	1200.	0.3572
1400.	0.0603	660.	8.2820	700.	3.5890	1100.	1.0710	1400.	0.3475
1600.	0.0297	740.	2.0400	800.	4.5280	1200.	1.0725	1600.	0.3373
1800.	0.0078	780.	1.6230	900.	6.2000	1300.	1.0670	1800.	0.3280
2000.	0.0077	820.	1.3030	930.	6.8070	1400.	1.0560	2000.	0.3203
		900.	0.9002	950.	6.9150	1600.	1.0270		
		1000.	0.6359	985.	6.7040	1800.	0.9928		
		1100.	0.4633	1000.	6.4700	2000.	0.9620		
		1200.	0.3657	1100.	3.7500				
		1400.	0.2390	1200.	2.2100				
		1600.	0.1660	1300.	1.3650				
		1800.	0.1050	1400.	0.9940				
		2000.	0.05485	1600.	0.5841				
				1800.	0.4071				
				2000.	0.2964				

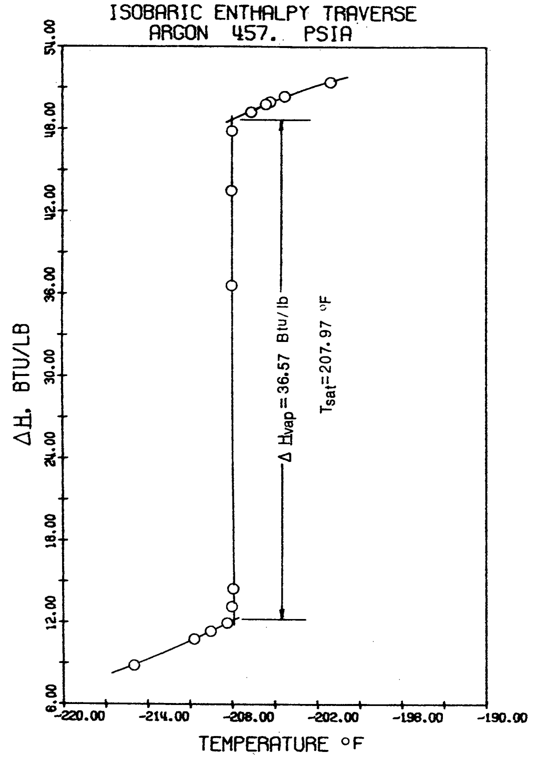

Figure III-24. Isobaric enthalpy traverse across the two phase boundary for argon at 457 psia.

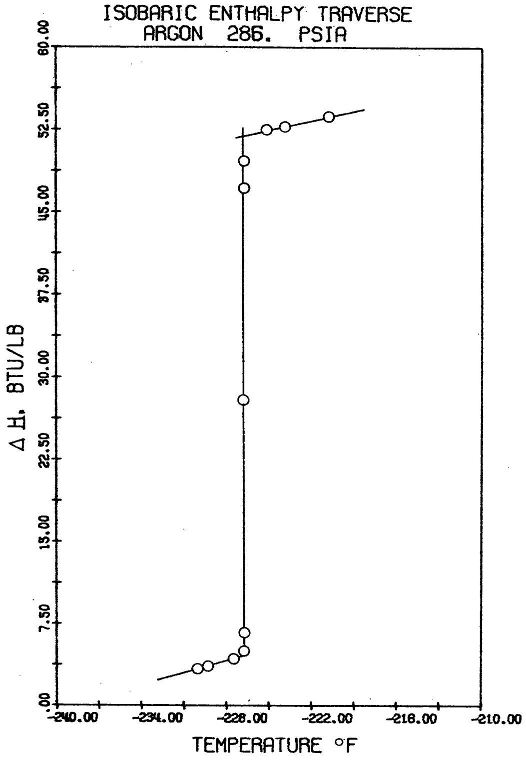

Figure III-25. Isobaric enthalpy traverse across the two phase boundary for argon at 286 psia.

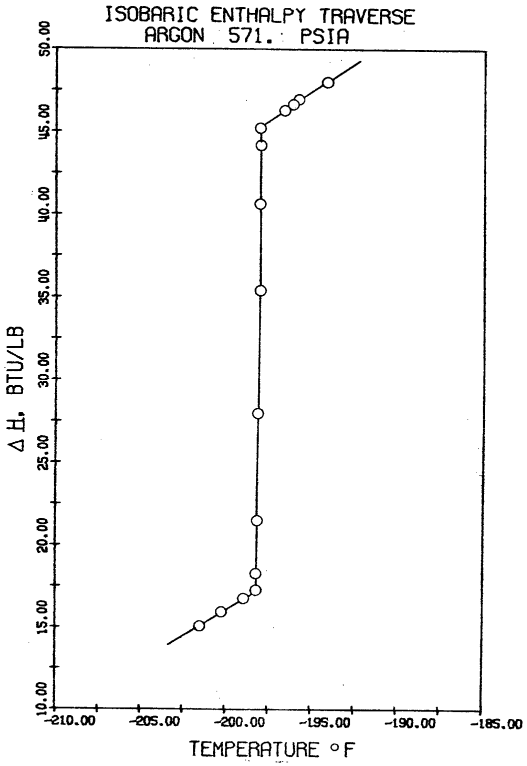

Figure III-26. Isobaric enthalpy traverse across the two phase boundary for argon at 571 psia.

TABLE III-8

Saturation Data for Argon

Pressure (psia)	Latent Heat (Btu/lb)		Saturation Temp. (°F)	
	This Work	Gosman *et al.*[22]	This Work	Gosman *et al.*[22]
286	47.66 ±0.05	47.53	-226.74 ±0.02	-226.75
457	36.57 ±0.05	36.66	-207.97 ±0.02	-207.94
571	27.68 ±0.05	27.55	-198.00 ±0.04	-198.17

Heat Leak Check

As discussed in Section II, the calorimeters used in this work are designed and operated in such a way that the heat leak from the calorimeters $\dot{Q}$ can be reduced to an insignificant level during the non-isothermal operation. Accordingly, $\dot{Q}$ is neglected from the enthalpy measurements. A series of isobaric enthalpy determinations were made at four different flow rates with the same inlet and outlet conditions to establish whether or not the calorimeter was adiabatic.[40, 36, 37, 61, 18] As the result $(\Delta \underline{H}/\Delta T)$ vs $1/F$ plot is made on Figure III-27, where ΔT is the temperature difference across the calorimeter. The plot indicates that the mean heat capacity is independent of the flow rate, which confirms $\dot{Q}$ is insignificant if not zero.

Thermodynamic Consistency Checks

The consistency checks between isobaric and isothermal measurements of argon are presented in Figure III-28. Isobaric and isothermal enthalpy differences between the experimental isotherms and isobars appear on each of the related intervals (all the values are in Btu/lb). Numbers in parentheses represent the adjustments required for every loop to be balanced. (A more detailed explanation is in Section II). The average and maximum inconsistencies in terms of the percent deviation are 0.09 and 0.34, respectively. Accuracies of the present isobaric and isothermal data are estimated at 0.2% and 0.4%, respectively.

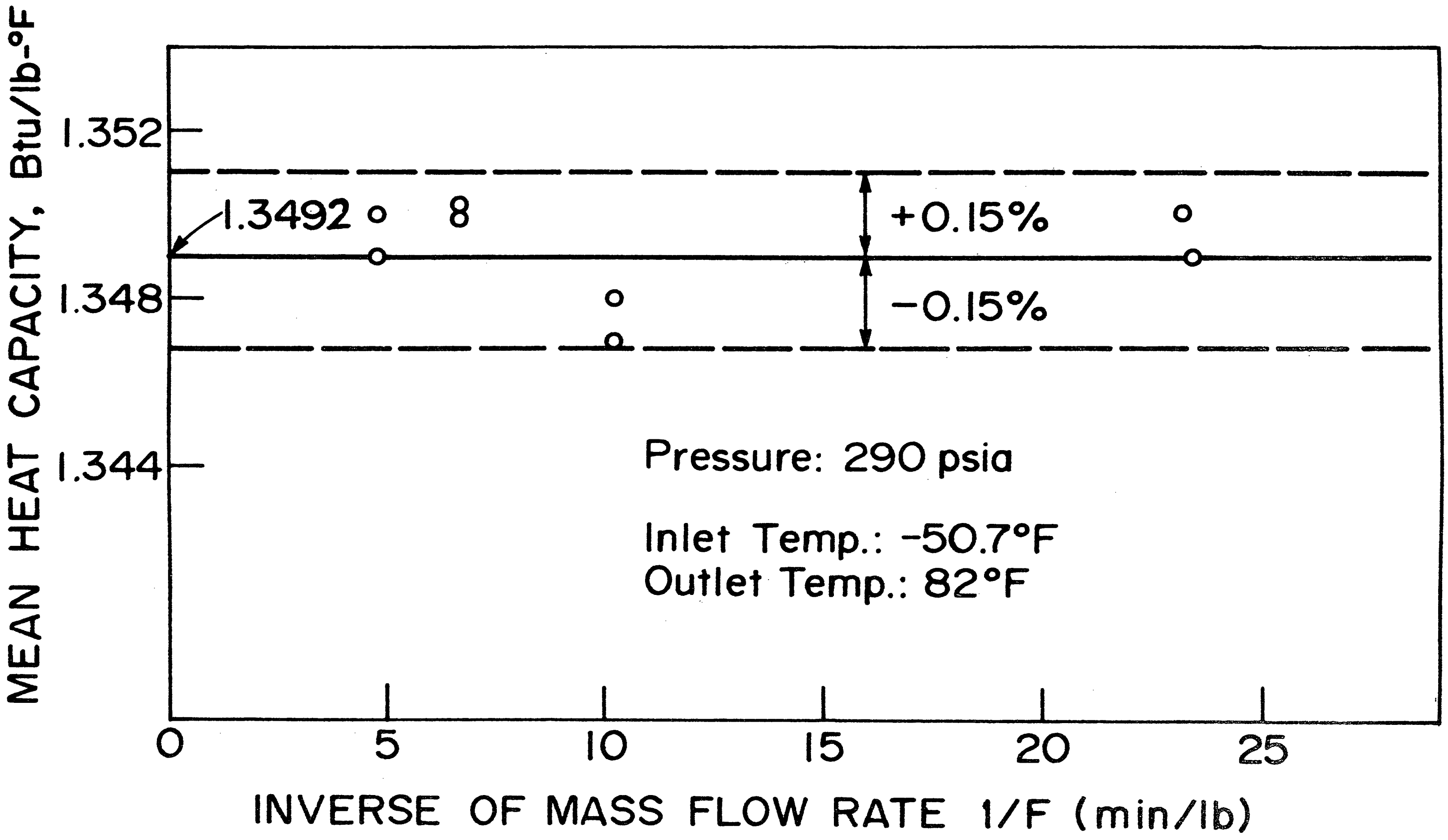

Figure III-27. Heat leak test for the isobaric calorimeter. Mean heat capacity of argon as a function of reciprocal flow rate.

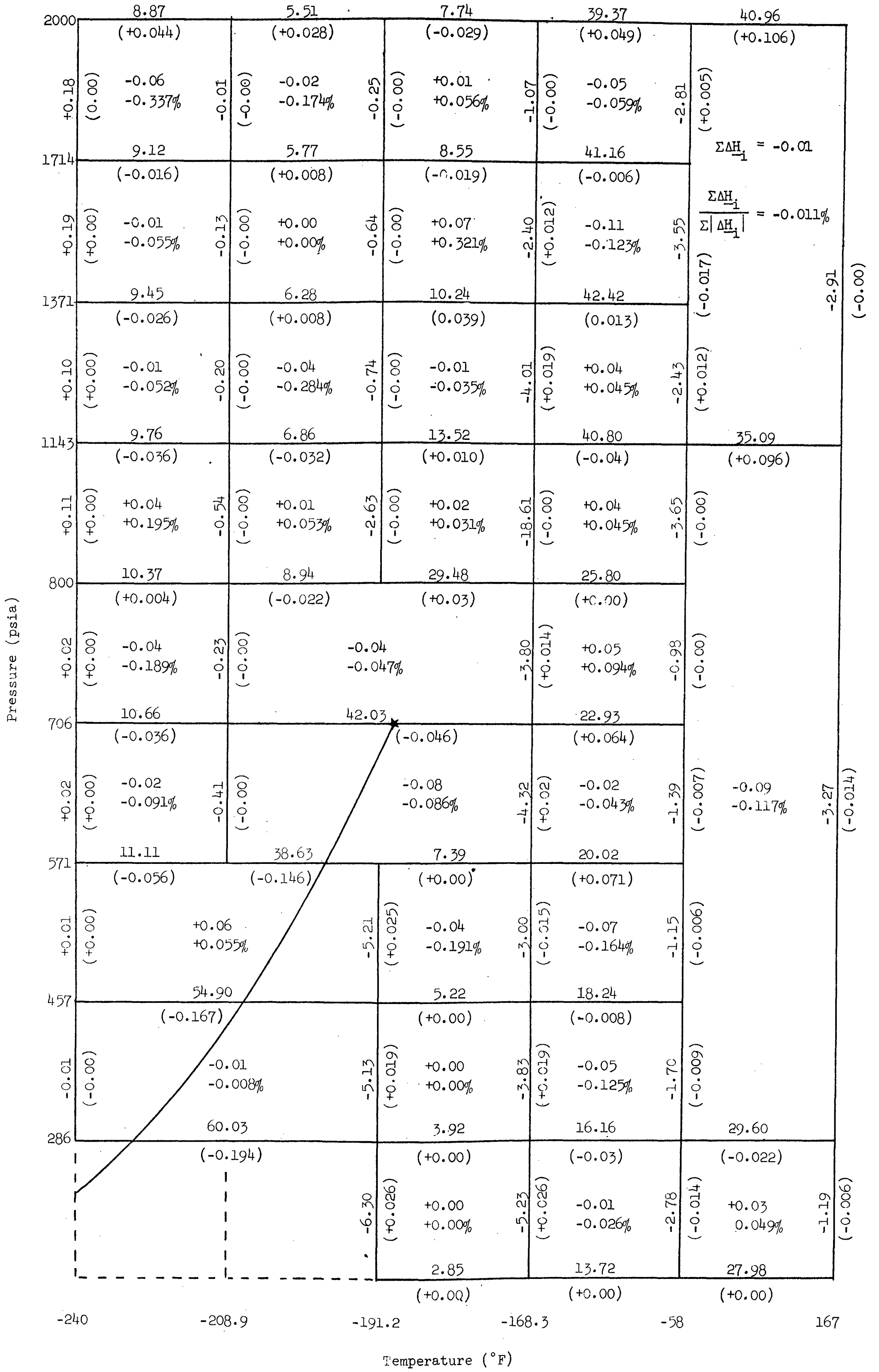

Figure III-28. Thermodynamic consistency checks for the present calorimetric data for argon.

Enthalpy Table and Diagram

The enthalpy diagram presented in Figure III-29 represents the enthalpy of argon at any point within the region of the present measurements as defined in Figure III-8. The diagram is prepared mainly by the data obtained from the present investigation and the zero enthalpy value calculated from the knowledge of $C_p{}^o$ (= 5/2R). Saturation enthalpies were obtained by smoothing the values given by Gosman[22] with the ones determined from the present experiment. Table III-9 lists those smoothed enthalpy values at saturation. Table III-10 tabulates enthalpy values at regular intervals of temperature and pressure, including those for the measured isotherms. The reference selected for the enthalpy of argon is $\underline{H}$ = 0 for the perfect crystal at 0°R. This reference has been taken by several investigators[10, 22] as calorimetric data for solid argon are available down to a low temperature. Din[10] calculated the enthalpy of the saturated liquid at 1 atm (87.28°K) from the ideal crystal at zero temperature to be 2972.46 J/mole (32.011 Btu/lb). This value was obtained by integrating and summing the calorimetric data of Clusius[7] extending from 10°K to the normal boiling point (87.28°K) and adding to it a value based on the Debye relationship:

$$C_p = kT^3 \tag{III-8}$$

between 0°K and 10°K, K being a constant evaluated from the C_p values close to 10°K. Gosman[22] later set the enthalpy for the ideal gas at 87.28°K to be 237.9316 J/g (102.355 Btu/lb) based on Din's value.

In this work, the enthalpy values along the 0 psia isobar were obtained by adding to the Gosman's value zero enthalpy changes from 87.28°K based on $C_p{}^o$ = 5/2R. Those values, then, specified the reference enthalpy for every experimental isotherm at 0 psia. Therefore, the enthalpy of the ideal gas at -240°F is obtained as in the following:

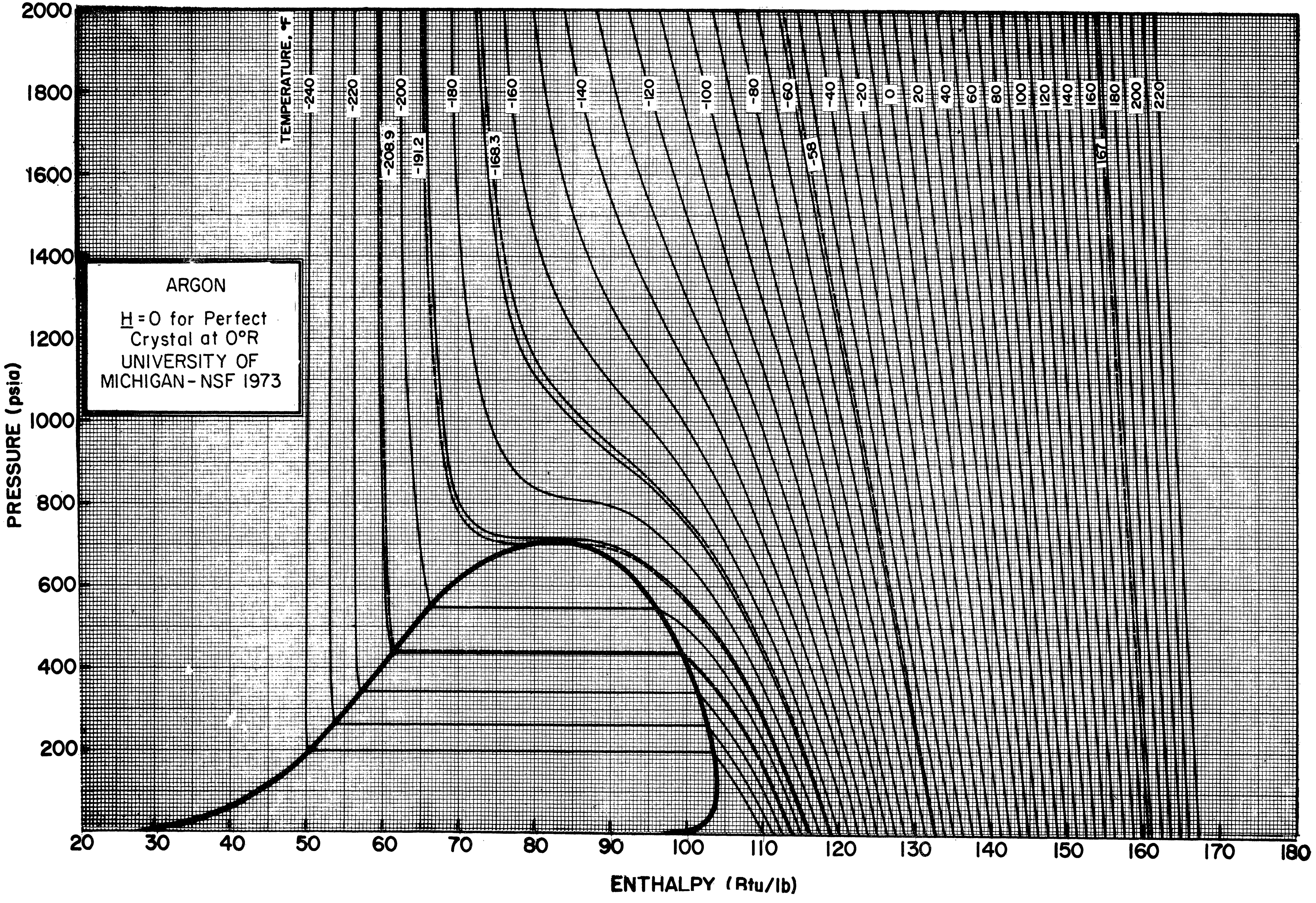

Figure III-29. H-P-T Diagram for Argon.

TABLE III-9

TABULATED VALUES OF THE SATURATION ENTHALPY FOR ARGON

Pressure (psia)	Saturation Temperature (°F)	Saturated Liquid (Btu/lb)	Saturated Vapor (Btu/lb)	Latent Heat (Btu/lb)
100	-261.6	44.1	103.9	59.8
200	-239.6	50.7	103.5	52.8
286	-226.74	54.8	102.5	47.7
300	-225.0	55.4	102.2	46.8
400	-213.6	59.9	100.3	40.4
457	-207.97	62.3	98.9	36.6
500	-204.1	64.2	97.6	33.4
571	-198.0	67.4	95.1	27.7
600	-196.0	69.2	93.8	24.6
700	-189.0	79.8	86.0	6.2

Note: $\underline{H}$ = 0 for the perfect crystal at 0.°R

TABLE III-10

TABULATED VALUES OF ENTHALPY FOR ARGON

Temperature (°F)	Pressure (psia) 0	100	200	300	400	500	600	700	800	900	1000
-240.	110.14	107.08	50.12	50.10	50.09	50.09	50.11	50.12	50.14	50.17	50.20
-230.	111.38	108.71	105.25	53.50	53.25	53.23	53.15	53.04	53.20	53.03	53.10
-220.	112.63	110.23	107.78	103.51	56.74	56.50	56.48	56.46	56.47	56.37	56.28
-210.	113.87	111.52	109.00	105.78	101.52	60.73	60.32	60.23	60.10	59.96	59.80
-208.9	114.00	111.70	109.23	105.98	101.76	61.17	60.75	60.53	60.49	60.30	60.20
-200.	115.11	113.03	110.70	107.95	103.70	100.03	65.74	64.90	64.31	63.87	63.51
-191.2	116.21	113.95	111.28	109.60	106.71	102.99	97.85	87.40	69.45	68.17	67.50
-190.	116.36	114.20	112.00	109.75	106.97	103.42	98.43	90.15	70.48	68.73	67.90
-180.	117.60	115.71	113.67	111.44	108.98	106.15	102.67	97.83	89.20	76.50	74.10
-170.	118.84	117.02	115.22	113.10	110.94	108.48	105.70	102.23	98.05	91.50	85.27
-168.3	119.06	117.30	115.55	113.51	111.28	108.97	106.21	102.80	98.30	92.77	86.75
-160.	120.09	118.45	116.71	114.79	112.79	110.55	108.09	105.31	102.36	98.80	94.55
-150.	121.33	119.93	118.27	116.48	114.69	112.73	110.54	108.22	105.63	102.73	99.72
-140.	122.58	121.28	119.80	118.22	116.42	114.50	112.50	110.48	108.45	106.22	103.78
-130.	123.82	122.49	121.01	119.51	117.95	116.25	114.55	112.75	110.99	109.10	107.07
-120.	125.06	124.98	122.62	121.23	119.72	118.04	116.50	114.84	113.27	111.47	109.60
-110.	126.31	125.13	123.78	122.48	121.08	119.72	118.24	116.73	115.39	113.72	112.10
-100.	127.55	126.30	125.15	123.82	122.10	121.28	119.98	118.60	117.40	115.97	114.50
- 90.	128.79	127.15	126.49	125.28	124.09	122.82	121.67	120.45	119.29	117.80	116.50
- 80.	130.04	128.94	127.90	126.76	125.11	124.49	123.28	122.17	121.08	119.74	118.52
- 70.	131.28	130.24	129.21	128.12	127.03	126.00	124.95	123.90	122.78	121.53	120.45
- 60.	132.52	131.50	130.48	129.49	128.48	127.45	126.43	125.39	124.42	123.26	122.21
- 58.	132.77	131.71	130.78	129.80	128.80	127.80	126.78	125.76	124.75	123.70	122.67
- 50.	133.77	132.90	131.93	130.95	129.99	129.01	128.00	127.00	126.02	125.08	124.05
- 40.	135.01	134.05	133.17	132.22	131.77	130.44	129.49	128.56	127.63	126.72	125.80
- 30.	136.25	135.42	143.50	133.68	132.75	131.92	130.99	130.15	129.32	128.43	127.52
- 20.	137.50	136.18	135.81	135.00	134.20	133.39	131.51	131.70	130.89	130.05	129.22
- 10.	138.74	137.97	137.17	136.41	135.52	134.77	134.00	133.22	132.43	131.67	130.85
0.	139.99	139.23	138.49	136.72	136.98	136.20	135.47	134.70	133.45	133.20	132.96
10.	141.23	140.49	139.24	139.00	138.29	137.55	136.81	136.15	135.43	134.72	133.90
20.	142.47	141.72	141.02	140.41	139.70	138.99	138.28	137.60	136.91	136.25	135.53
30.	143.72	143.02	142.41	141.72	141.04	140.45	139.74	139.08	138.39	137.77	137.18
40.	144.96	144.24	143.59	143.01	142.43	141.76	141.10	140.50	139.85	139.23	138.67
50.	146.20	145.51	144.95	144.32	143.73	143.12	142.51	141.96	141.30	140.70	140.17
60.	147.45	147.83	146.25	145.67	145.05	144.50	142.43	143.30	142.73	142.18	141.56
70.	148.69	148.05	147.50	147.00	146.45	145.79	145.27	144.72	144.15	143.58	143.03
80.	149.93	149.30	138.74	148.18	147.67	147.08	146.58	146.03	145.57	145.00	144.50
90.	151.18	150.57	150.06	149.59	149.10	148.53	148.06	147.04	146.97	146.52	146.02
100.	152.42	151.82	151.32	150.82	150.32	149.90	149.42	148.95	148.36	147.94	147.47
110.	153.66	153.03	152.55	152.09	151.70	151.21	150.72	150.25	149.75	149.30	148.90
120.	154.91	154.40	153.96	153.46	152.95	152.47	151.99	151.50	151.13	150.55	150.21
130.	156.15	155.71	155.22	154.75	154.29	153.82	153.30	152.83	152.50	152.00	151.55
140.	157.40	157.00	156.50	156.04	155.64	155.20	154.72	154.22	153.87	153.47	153.02
150.	158.64	158.23	157.78	157.41	156.98	156.50	156.01	155.63	155.23	154.75	154.35
160.	159.88	159.35	158.99	158.52	158.20	157.76	157.43	156.99	156.59	156.10	155.72
167.	160.75	160.25	159.95	159.50	159.00	158.62	158.23	157.80	157.48	157.05	156.70
170.	161.13	160.68	160.28	159.93	159.51	159.15	158.75	158.40	157.95	157.08	157.23
180.	162.37	161.99	161.53	161.12	160.73	160.43	159.98	159.53	159.29	158.81	158.50
190.	163.61	163.18	162.80	162.48	162.02	161.68	161.30	160.98	160.63	160.30	159.99
200.	164.86	164.50	164.07	163.77	163.48	163.05	162.72	162.43	161.97	161.68	161.28
210.	166.10	165.65	165.30	164.99	164.70	164.32	164.00	163.72	163.31	168.00	162.70
220.	167.34	167.00	166.59	166.28	165.99	165.57	165.35	164.94	164.64	169.27	164.00

DATUM: H = 0 for perfect crystal at 0°R.
Unit for H is Btu/lb.

TABLE III-10 (Concluded)

Temperature (°F)	Pressure (psia)									
	1100	1200	1300	1400	1500	1600	1700	1800	1900	2000
-240.	50.25	50.30	50.32	50.37	50.43	50.48	50.54	50.60	50.66	50.72
-230.	53.10	53.20	53.23	53.26	53.28	53.30	53.42	53.46	53.49	53.53
-220.	56.24	56.24	56.25	56.25	56.26	56.26	56.27	56.27	56.28	56.36
-210.	59.70	59.52	59.48	59.45	59.42	59.40	59.43	59.38	59.35	59.30
-208.9	60.02	59.98	59.92	59.77	59.78	59.75	59.77	59.72	59.72	59.75
-200.	63.25	63.00	62.78	62.60	62.50	62.48	62.47	62.47	62.44	62.35
-191.2	67.00	66.51	66.20	65.93	65.66	65.50	65.46	65.28	65.30	65.20
-190.	67.98	67.98	66.77	66.48	66.23	66.01	65.92	65.73	65.57	65.57
-180.	72.67	71.70	70.95	70.34	69.95	69.55	69.40	69.20	69.00	68.82
-170.	80.55	77.22	76.22	75.10	74.46	73.82	73.28	72.92	72.51	72.28
-168.3	81.98	78.98	77.20	76.00	75.08	74.50	74.03	73.53	73.05	72.80
-160.	89.84	85.80	82.96	80.85	79.45	78.27	77.48	76.80	76.26	75.66
-150.	96.05	92.62	89.60	87.01	85.12	83.58	82.30	81.32	80.50	79.81
-140.	101.16	98.22	95.42	92.98	90.78	88.96	87.32	85.95	84.72	83.90
-130.	104.95	102.33	99.95	97.73	95.72	93.84	92.07	90.66	89.40	88.13
-120.	106.73	105.72	103.20	102.72	99.93	98.22	96.55	95.03	93.68	92.28
-110.	110.49	108.71	106.78	105.08	103.50	101.97	100.48	99.02	97.61	96.26
-100.	113.00	111.97	109.81	108.22	106.68	105.15	103.80	102.95	101.10	99.91
- 90.	115.17	113.68	112.18	110.75	109.44	108.05	106.78	105.55	104.42	103.27
- 80.	117.27	116.00	114.70	113.28	112.01	110.82	109.70	108.52	107.44	106.33
- 70.	119.27	118.18	116.98	115.76	114.15	113.48	112.30	111.22	110.15	109.13
- 60.	121.10	120.02	118.99	117.95	116.87	115.80	114.83	113.80	112.77	111.75
- 58.	121.55	120.48	119.30	118.26	117.30	116.32	115.40	114.45	113.48	112.45
- 50.	123.07	121.07	121.10	120.05	119.00	117.78	117.00	116.05	115.20	114.23
- 40.	124.90	123.99	123.05	122.20	121.24	120.34	119.48	118.52	117.18	116.62
- 30.	126.68	125.80	124.98	124.04	123.22	122.36	121.49	120.54	119.72	118.89
- 20.	128.43	127.58	126.75	125.98	125.18	124.32	123.50	122.70	121.90	121.05
- 10.	130.06	129.33	128.52	126.78	127.01	126.22	125.47	124.68	123.92	123.14
0.	131.70	130.99	130.23	129.49	128.74	128.02	127.29	126.56	125.94	125.16
10.	133.25	132.53	131.90	131.17	130.48	129.82	129.10	128.47	127.73	127.12
20.	134.94	134.22	133.55	132.95	132.24	131.60	130.95	130.25	129.62	129.02
30.	136.35	135.80	135.22	134.56	133.99	133.35	132.72	132.15	131.50	130.08
40.	138.00	137.45	136.80	136.23	135.60	135.04	134.49	133.97	133.28	132.69
50.	139.55	139.00	138.44	137.82	137.25	136.70	136.08	135.52	134.98	134.44
60.	141.23	140.51	139.99	139.45	138.92	138.82	137.78	137.24	136.72	136.17
70.	142.52	142.01	141.50	141.01	140.48	139.97	139.55	138.93	138.85	137.86
80.	143.99	143.50	142.98	142.48	142.00	141.50	141.00	140.50	140.03	139.53
90.	145.52	145.02	144.52	144.03	143.55	143.05	142.57	142.10	141.63	141.15
100.	146.98	146.50	146.00	145.04	145.10	144.62	143.19	143.80	143.30	142.77
110.	148.42	147.95	147.50	147.01	146.57	146.15	145.70	145.23	144.35	144.37
120.	149.80	149.30	148.95	148.50	148.01	147.57	147.19	146.76	146.45	145.95
130.	151.18	150.77	150.33	149.95	149.50	149.08	148.67	148.25	147.82	147.51
140.	152.62	152.23	151.34	151.48	151.01	150.60	150.23	149.86	149.49	149.01
150.	153.98	153.58	153.20	152.80	152.51	152.08	151.24	151.90	151.00	150.61
160.	155.30	154.98	154.61	154.23	153.47	153.52	153.23	152.89	152.51	152.11
167.	156.32	155.98	155.70	155.33	155.00	154.70	154.37	154.00	153.20	153.30
170.	156.82	156.49	156.17	155.82	155.49	155.09	154.83	154.49	154.11	153.77
180.	158.23	157.92	157.52	157.23	156.95	156.55	156.25	155.97	155.60	155.27
190.	159.60	159.27	158.96	158.55	157.76	157.99	157.19	157.43	157.05	156.74
200.	161.01	160.63	160.32	160.01	159.72	159.45	159.05	158.82	158.50	158.22
210.	162.40	162.00	161.22	161.47	161.12	160.83	160.52	160.24	160.00	159.68
220.	163.72	163.47	163.18	162.85	162.57	162.28	162.00	161.70	161.48	161.14

DATUM: $\underline{H} = 0$ for perfect crystal at 0°R.
Unit for $\underline{H}$ is Btu/lb.

	$\underline{H}$ (Btu/lb)
Perfect Crystal at 0°R	0
Saturated liquid at 1 atm and -302.57°F	32.011[a]
Latent heat at -302.57°F	69.671[b]
Pressure effect on enthalpy (from 1 atm to 0)	0.673[b]
Ideal gas enthalpy (-302.57°F to -240°F)	7.781[c]
	110.136

[a] Estimation made by Din[10]

[b] Calculated by Gosman et al.[22]

[c] Based on $C_p{}^o = 5/2R$

Comparison With Other Published Data

In order to make a comparison between the isobaric heat capacity, data of this work and those of Walker,[60] the latter was smoothed to obtain the values along the isobars of the present measurements. Thirty-five points were compared covering a temperature range from -250°F to -140°F and a pressure range from 286 psia to 1371 psid. A comparison was made against the smoothed values of C_p which Michels et al.[38, 39] derived from their accurate PVT data. One hundred thirty three points were compared covering temperatures from -229°F to 220°F and pressures up to 2000 psia. Finally, a comparison is made with C_p values, which were calculated from the equation of state proposed by Gosman, et al.[22] Since Gosman, et al.[22] did not compile C_p values in their table, the writer had to carry out the computation for those values using an expression for C_p derived from their equation of state. Values of 155 points are included in the comparison of temperatures ranging from -240°F to 60°F and pressures up to 2000 psia. Results of these comparisons are presented in tabular form in Table III-11.

Tabulations of such comparisons are useful but are difficult in assessing the overall trend for the comparisons. Therefore, topographical deviation diagrams, as shown in Figures III-30, III-31 and III-32,

TABLE III-11

COMPARISONS OF ISOBARIC HEAT CAPACITIES OF ARGON

Temperature (°F)	Pressure = 286. psia			
	C_p (Btu/lb-°F)			
	This Work	Walker	Michels	Gosman
-220.	0.2457		0.2310	0.2321
-210.	0.2152		0.2050	0.2062
-200.	0.1923		0.1890	0.1897
-190.	0.1787		0.1770	0.1790
-180.	0.1705		0.1700	0.1703
-170.	0.1640		0.1630	0.1644
-160.	0.1586		0.1566	0.1587
-150.	0.1544		0.1528	0.1556
-140.	0.1510		0.1481	0.1515
-130.	0.1482		0.1498	0.1487
-120.	0.1460		0.1472	0.1466
-110.	0.1441		0.1445	0.1440
-100.	0.1424		0.1427	0.1435
- 80.	0.1398		0.1397	0.1401
- 60.	0.1378		0.1375	0.1371
- 40.	0.1359		0.1355	0.1349
- 20.	0.1344		0.1342	0.1351
0.	0.1333		0.1331	0.1335
20.	0.1324		0.1322	0.1325
40.	0.1316		0.1314	0.1304
70.	0.1306		0.1303	0.1294
100.	0.1295		0.1294	
130.	0.1288		0.1237	
160.	0.1283		0.1282	
190.	0.1281		0.1278	
220.	0.1278		0.1274	

Temperature (°F)	Pressure = 457. psia			
	C_p (Btu/lb-°F)			
	This Work	Walker	Michels	Gosman
-240.	0.3090	0.310		
-230.	0.3378	0.336		
-220.	0.3880	0.380		
-215.	0.4250	0.417		
-210.	0.4750	0.474		0.5406
-202.	0.3620	0.382	0.2419	0.3519
-190.	0.2528	0.275	0.2662	0.2639
-185.	0.2389	0.246		0.2447
-180.	0.2276	0.219		0.2302
-170.	0.2100		0.2079	0.2092
-160.	0.1961		0.1952	0.1948
-140.	0.1759		0.1760	0.1761
-120.	0.1638		0.1646	0.1644
-100.	0.1551		0.1569	0.1567
- 80.	0.1508		0.1506	0.1512
- 60.	0.1475		0.1466	0.1465

Temperature (°F)	Pressure = 571. psia			
	C_p (Btu/lb-°F)			
	This Work	Walker	Michels	Gosman
-230.	0.3281	0.325		
-220.	0.3691	0.363		
-210.	0.4362	0.433	0.4292	0.4285
-200.	0.6649	0.680		1.5765
-196.	0.7620	0.720		0.6616
-190.	0.4360	0.486		0.4337
-180.	0.3112	0.355		0.3128
-170.	0.2544	0.297		0.2607
-160.	0.2270	0.261	0.2760	0.2308
-140.	0.1983		0.1977	0.1975
-120.	0.1794		0.1790	0.1790
-100.	0.1680		0.1676	0.1677
- 80.	0.1594		0.1589	0.1596
- 60.	0.1515		0.1534	0.1537

TABLE III-11 (Continued)

Temperature (°F)	Pressure = 706. psia C_p (Btu/lb-°F) This Work	Walker	Michels	Gosman
-250.	0.2924			0.2763
-240.	0.3035	0.297		0.2904
-230.	0.3236	0.316		0.3102
-220.	0.3558	0.348	0.3400	0.3401
-210.	0.3970	0.399	0.3910	0.3925
-200.	0.5226	0.527	0.5110	0.5151
-190.	1.341			1.6075
-185.	1.217			1.081
-180.	0.5800			0.6037
-175.	0.4274	0.543		0.4541
-170.	0.3691	0.455	0.6057	0.3780
-160.	0.2899	0.344	0.3923	0.2987
-140.	0.2214		0.2454	0.2310
-120.	0.2030		0.2014	0.2002
-100.	0.1850		0.1821	0.1820
- 80.	0.1745		0.1699	0.1703
- 60.	0.1620		0.1622	0.1623
- 40.	0.1530		0.1557	0.1561

Temperature (°F)	Pressure = 800. psia C_p (Btu/lb-°F) This Work	Walker	Michels	Gosman
-240.	0.2946			0.2870
-220	0.3435		0.3230	0.3314
-210.	0.3850		0.3660	0.3746
-200.	0.4793		0.4500	0.4614
-190.	0.8000			0.7622
-184.	2.193			2.5414
-180.	1.678			1.745
-175.	0.7930			0.7976
-170.	0.5513		0.5760	0.5527
-160.	0.3600		0.3810	0.3753
-150.	0.2960		0.3090	0.3020
-140.	.2660		0.2680	0.2616
-120.	0.2187		0.2213	0.2174
-100.	0.1945		0.1937	0.1935
- 80.	0.1740		0.1784	0.1787
- 60.	0.1614		0.1689	0.1683
- 40.	0.1630		0.1609	0.1611

Temperature (°F)	Pressure = 1143. psia C_p (Btu/lb-°F) This Work	Walker	Michels	Gosman
-250.	0.2846			0.2670
-230.	0.3025			0.2903
-210.	0.3466		0.3300	0.3328
-200.	0.3863		0.3650	0.3709
-190.	0.4437		0.4300	0.4358
-180.	0.5477		0.5210	0.5667
-170.	0.8150		0.7830	0.8221
-165.	0.9350		0.9079	0.8864
-160.	0.8387		0.7771	0.8129
-150.	0.5905		0.5745	0.5785
-140.	0.4294		0.4545	0.4326
-130.	0.3464		0.3670	0.3508
-120.	0.3000		0.3194	0.3008
-100.	0.2400		0.2475	0.2443
- 80.	0.2101		0.2147	0.2135
- 60.	0.1935		0.1963	0.1942
- 30	0.1763		0.1760	0.1762
0	0.1637		0.1647	0.1648
30	0.1562		0.1571	0.1569
60	0.1518		0.1514	0.1511
90	0.1468		0.1471	
120	0.1441		0.1439	
150	0.1409		0.1413	
180	0.1387		0.1389	

TABLE III-11 (Concluded)

Temperature (°F)	Pressure = 1371. psia C$_p$ (Btu/lb-°F) This Work	Walker	Michels	Gosman
-230.	0.2959	0.290		0.2827
-210.	0.3270	0.326	0.3100	0.3157
-200.	0.3538	0.357	0.3360	0.3418
-190.	0.3898	0.395	0.3750	0.3804
-180.	0.4324	0.429	0.420	0.4405
-170.	0.5334	0.545	0.5370	0.5347
-160.	0.6295	0.640	0.6562	0.6350
-158.	0.6490		0.6680	0.6447
-156.	0.6624		0.6652	0.6481
-154.	0.6490		0.6477	0.6453
-150.	0.6171	0.737	0.6126	0.6236
-140.	0.5344	0.587	0.5251	0.5248
-130.	0.4333		0.4484	0.4310
-120.	0.3638		0.3852	0.3634
-100.	0.2800		0.2884	0.2827
- 80.	0.2370		0.2413	0.2392
- 60.	0.2224		0.2159	0.2182

Temperature (°F)	Pressure = 1714. psia C$_p$ = (Btu/lb-°F) This Work	Walker	Michels	Gosman
-250.	0.2626			0.2577
-230.	0.2866			0.2738
-210.	0.3107		0.2840	0.2977
-190.	0.3447		0.3280	0.3364
-180.	0.3712		0.3610	0.3656
-170.	0.4037		0.4050	0.4036
-160.	0.4463		0.4490	0.4482
-150.	0.4830		0.4780	0.4844
-146.	0.4929		0.4800	0.4910
-144.	0.4947		0.4810	0.4918
-142.	0.4929		0.4820	0.4910
-140.	0.4890		0.4831	0.4887
-130.	0.4572		0.4648	0.4580
-120.	0.4155		0.4174	0.4125
-100.	0.5296		0.3362	0.3300
- 80.	0.2714		0.2774	0.2751
- 60.	0.2380		0.2441	0.2399

Temperature (°F)	Pressure = 2000. psia C$_p$ (Btu/lb-°F) This Work	Walker	Michels	Gosman
-250.	0.2608			0.2541
-230.	0.2797			0.2677
-210.	0.2994		0.2840	0.2867
-190.	0.3225		0.3080	0.3146
-180.	0.3383		0.3200	0.3336
-170.	0.3532		0.3253	0.3565
-160.	0.3745		0.3195	0.3824
-150.	0.3938		0.3362	0.4072
-140.	0.4185		0.3625	0.4226
-136.	0.4235		0.3731	0.4244
-134.	0.4248		0.3768	0.4241
-130.	0.4217		0.3752	0.4213
-120.	0.4086		0.2712	0.4035
-100.	0.3512		0.3473	0.3473
- 80.	0.2932		0.2968	0.2957
- 60.	0.2565		0.2627	0.2580
- 40.	0.2319		0.2327	0.2314
- 20.	0.2121		0.2140	0.2121
0.	0.1988		0.1987	0.1979
30.	0.1831		0.1832	0.1822
60.	0.1715		0.1719	0.1719
90.	0.1636		0.1643	
120.	0.1580		0.1584	
150.	0.1534		0.1536	
180.	0.1497		0.1493	

are prepared for summarizing the results. The deviation, d, in the diagrams are defined as

$$d = \frac{C_p \text{ (This Work)} - C_p \text{ (Literature)}}{C_p \text{ (This Work)}} \times 100 \qquad \text{(III-9)}$$

Lines corresponding to zero percent deviation are sketched in much the same manner one might draw a contour line from survey determinations on a topographic map. In a similar manner contour lines corresponding to ±1%, ±5% and ±10% deviation were sketched in. Suitable coding was developed to distinguish these regions as illustrated in the figures. Comparisons, as shown in these diagrams, reveal that in the lower temperature region the present data agree better with Walker's values than those from the other two sources. In the region of temperatures higher than -70°F the deviations of both Gosman and Michels show less than 1%. In temperatures higher than 0°F a comparison of the present data with the values from Michels is presented more specifically in Figure III-33. In the lower pressure region agreements are excellent (deviations are less than 0.2%).

Smoothed values of the present enthalpy data (Table III-8) are compared with tabulated values by IUPAC.[1] IUPAC values are also based on $\underline{H} = 0$ for perfect crystal at the absolute zero temperature ($\underline{H}$ of saturated vapor at 87.28°K coincides with that of Din's compilation[10] (237.543 J/g) which is based on the perfect crystal at 0°K). Comparisons were made at ninety-four points covering the temperature range from -240°F to 220°F and the pressure range from 0 to 2000 psia. Care was taken to include points near the two-phase and critical regions. The results of comparisons are illustrated as a topographical diagram in Figure III-34. Discrepancies between two sources never exceed 0.5 Btu/lb and for more than half of the region they are less than 0.2 Btu/lb. The average absolute deviation of all 94 points is 0.2 Btu/lb.

Finally, the present heats of vaporization are compared with those from Gosman, et al.[22] (see Table III-8). The latter, according to Gosman, et al. were calculated using their vapor pressure equation and equation of state. The discrepancies in the latent heats between two sources are within ±0.5%, while the present saturation temperatures agree within experimental errors with Gosman's values.

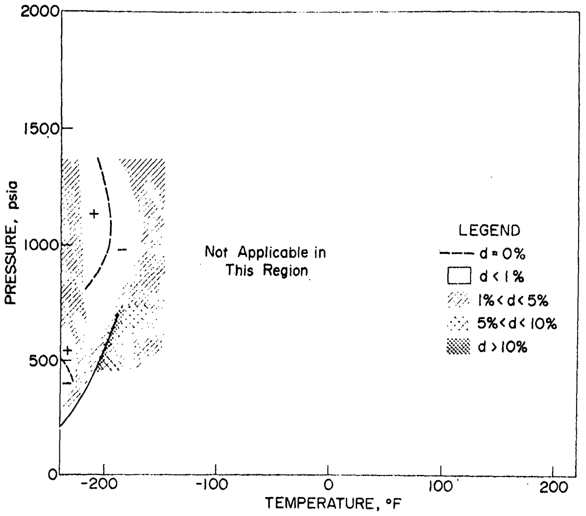

Figure III-30. Comparison of the present isobaric heat capacities with those from Walker.[60]

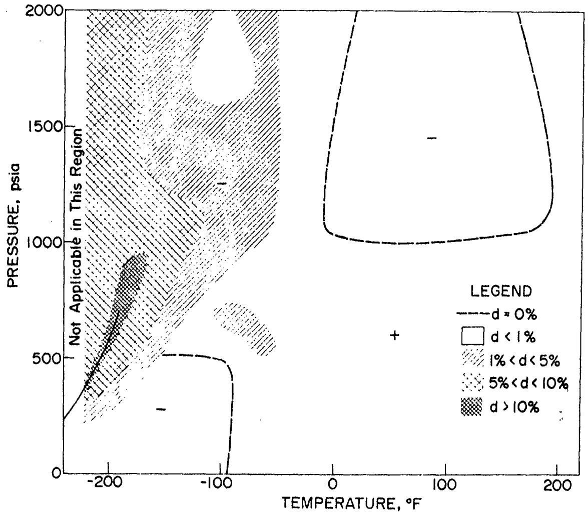

Figure III-31. Comparison of the present isobaric heat capacities with those from Michels et al.[38,39]

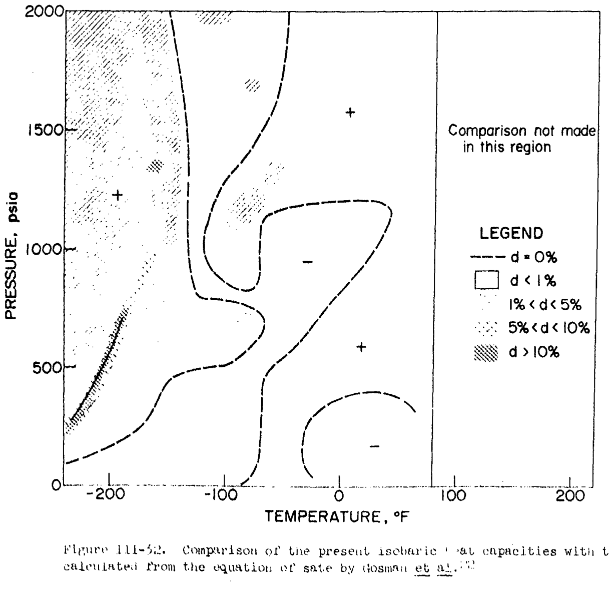

Figure III-32. Comparison of the present isobaric heat capacities with those calculated from the equation of sate by Gosman et al.[illegible]

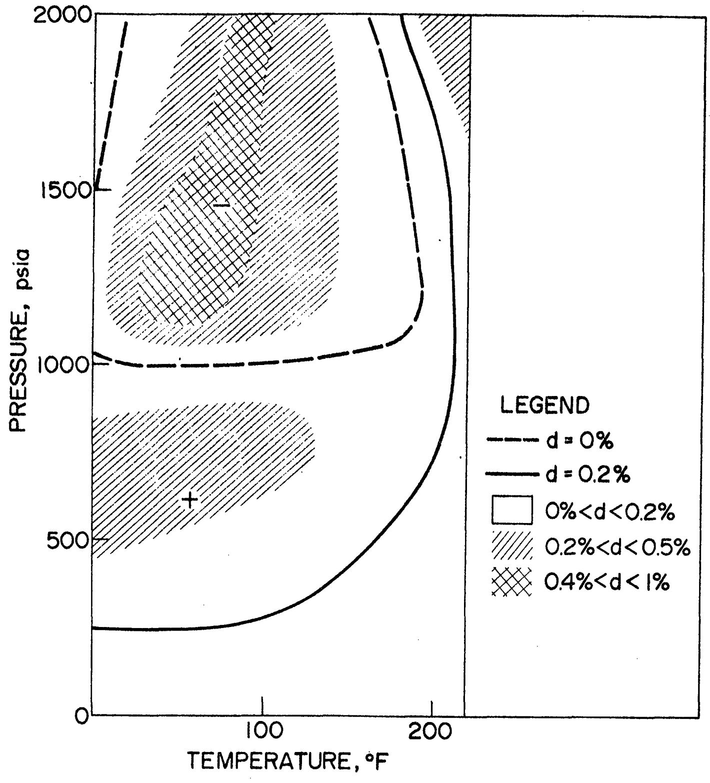

Figure III-33. Comparison of the present isobaric heat capacities in the high temperature region with those from Michels et al.[38,39]

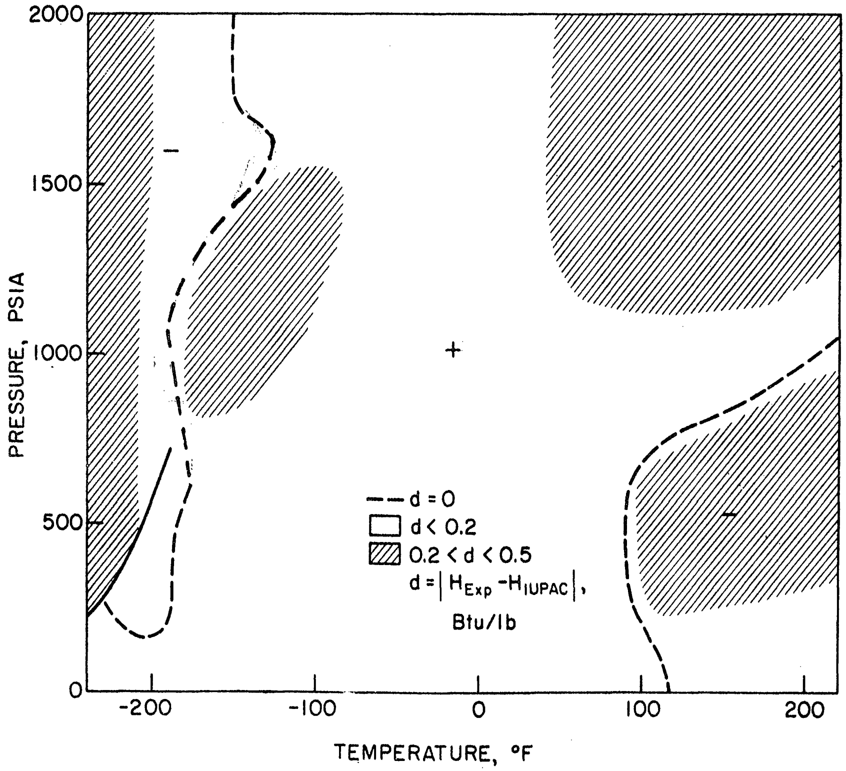

Figure III-34. Comparison of the present enthalpies with the tabulated values from IUPAC.

IV - CALORIMETRIC DETERMINATIONS WITH HEXAFLUOROETHANE

As the new recycle flow system, designed and constructed by Miyazaki,[34] has been successfully operated with ethane, it was decided that calorimetric measurements with C_2F_6 be conducted at the new system. The operation of the new facility is simpler and more economical than that of the existing one as the new facility has a single calorimeter which can be used both for isobaric and isothermal (and isenthalpic) modes of operation. In addition the flow rate of the system fluid is maintained constant during the operation by a pair of double-acting precision metering pumps which provide a constant flow through the system. Detailed descriptions of the facility and important aspects of equipment design can be found in Miyazaki's thesis.[34] Therefore, only a brief description of the experimental equipment will be presented in the first part of this section. The rest of the section is devoted to presentation and discussion of the experimental results.

New Recycle Flow System

A schematic diagram of the system is shown in Figure IV-1. Like the existing facility described before, it is a recycle flow system designed to supply a fluid at a constant flow rate to a calorimeter at a predetermined temperature and pressure. The constant flow of the system fluid is provided by a pair of identical precision metering pumps (P-1A and P-1B), one of which discharges the fluid in the liquid phase as a precisely machined plunger moves down at a constant speed while the other takes in the fluid as the other plunger moves up at the same constant speed. When the plungers reach the ends of the cylinders (upper and lower ends, respectively), the so-called "switch-back" system reverses the moving directions of the plungers and the discharging pump becomes the in-take pump and vice versa. The flow direction of main stream to the calorimeter is, however, maintained constant with a set of four solenoid values (V1, V2, V3, and V4). When the pump P-1A is discharging, V1 and V4 are open, while V2 and V3 are closed; when P-1B is discharging V2 and V3 are open and V1 and V4 are closed. In order to prevent possible bypass flow in case there are leaks through the closed valves due to

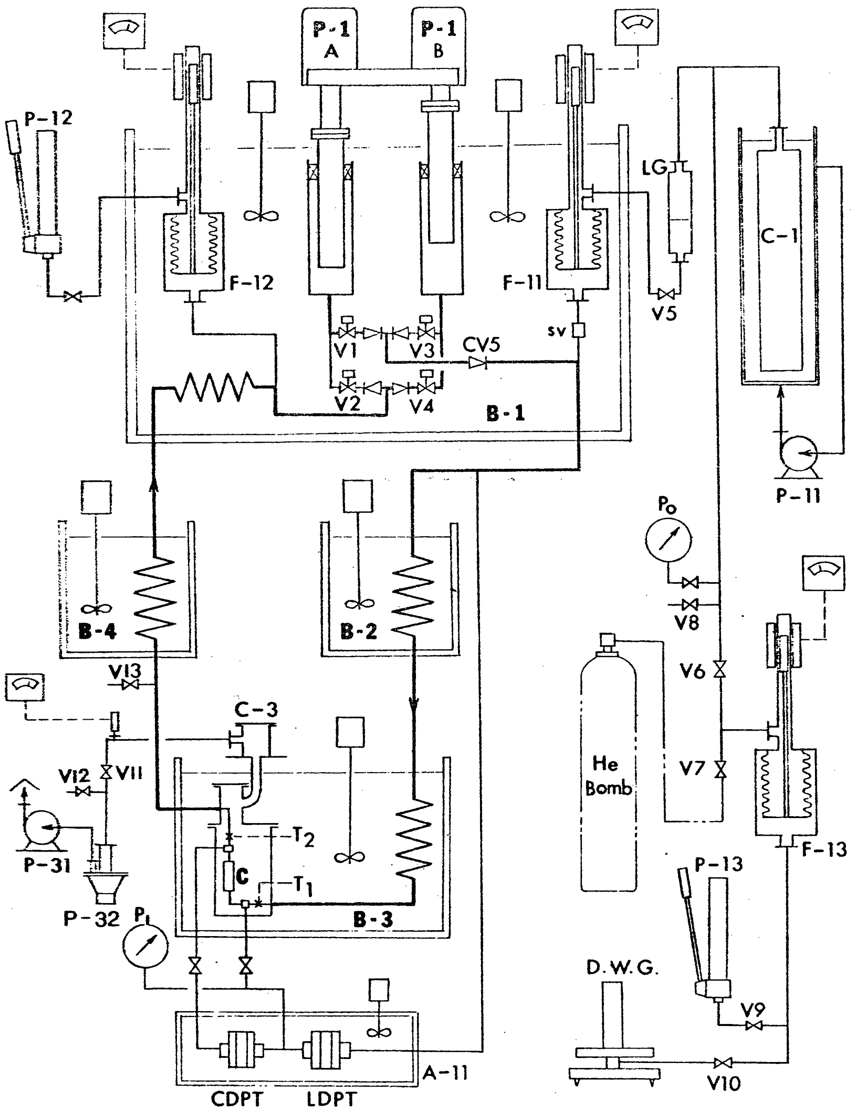

P-1A and P-1B	Metering pumps
☐⋈	Solenoid valve
◁	Check valve
⋈	Shut-off valve
B-1	Pump bath
B-2	Pre-conditioning bath
B-3	Calorimeter bath
B-4	Post-conditioning bath
A-11	Air box
F-11, F-12, F-13	Bellows
LG	Level gage
P-12, P-13	Oil pumps (manual)
P-11	Water circulation pump
P-31	Vacuum pump
P-32	Diffusion pump
P_1, P_o	Heise pressure gages
D.W.G.	Ruska dead weight gage
C	Calorimeter
C-3	Calorimeter vacuum pot
CDPT	Calorimeter differential pressure transducer
LDPT	Line differential pressure transducer
SV	Safety valve
T1	Inlet thermometer
T2	Outlet thermometer
C-1	Helium cylinder

Figure IV-1. Flow diagram of the new recycle-flow system incomplete closing of stems, a check valve is installed in a series with each of those solenoid valves. All the valves and the pump cylinders are immersed in the pump bath (B-1) fluid which maintains a constant temperature by a pair of controlled immersion heaters. Throughout the present measurements the bath temperature is maintained at 0 ±0.05°F (Dow-Corning silicon oil is used as the bath fluid).

The system fluid, discharged from the pump bath, enters the preconditioning bath (B-2) containing 1/8-in. O.D. stainless steel tubing immersed in the bath fluid, which is maintained to within ±1°F of the calorimeter bath temperature using a linear temperature controller (Bayley Instrument, Model 21). Then it enters the calorimeter bath (B-3) containing a coil of 1/8-in. O.D. tubing for a final temperature conditioning for the calorimeter. The calorimeter bath temperature is controlled by Thermotrol 1053 (Hallakainen Instrument) within ±0.02°F of a desired temperature. The measurements of the inlet temperature and pressure, and the changes in temperature and pressure across the calorimeter and the electric energy input are made as the fluid passes through the calorimeter. After leaving the calorimeter, the fluid enters the postconditioning bath (B-4), which is identical to the preconditioning bath (B-2). Passing through the bath, the fluid is conditioned to within ±1°F of the pump bath temperature and finally enters the pump bath and one of the metering pump cylinders.

One of the distinguished features in the system is a pressure controlling mechanism employing a set of bellows and a buffer cylinder (C-1) filled with helium. One of the bellows (F-11) serves to balance the system pressure with the helium pressure of the cylinder (C-1). The bellows is filled with oil and the oil-helium interface is visualized by a reflection type high pressure level gage (LG). The cylinder (C-1) is immersed in a controlled water bath which serves to maintain the helium temperature constant. Generally the valve V5 is closed when the system is not in operation. It is also closed when it is necessary to change the system pressure. In this case another bellows (F-12) is used to set the fluid pressure by compressing or expanding by way of the manual oil pump, P-12. Adjustment of helium pressure to that of the system is made by introducing higher pressure helium from the He Bomb or venting it out through V8, if necessary. Fluctuation in the system pressure during the operation is compensated by a slight movement of the bellows (F-11). Thus, the system pressure is maintained the same as the helium pressure of the cylinder (C-1).

The other bellows (F-13), together with the manual oil pump (P-13), is to be used when it is necessary to increase the helium pressure above the pressure of the bomb. The position of each of the bellows is monitored by a reading of emf transduced from linear displacement transducers. A specially designed safety valve, SV, serves to prevent excessive expansion of F-11 caused by mass leak from the system during the operation. When the bellows expands to a certain point, the safety valve closes by itself and thus prevents further depletion of the fluid pressure from the shell side of the bellows. The valve, V-13, serves either as an entrance or a vent for the system fluid.

Multipurpose Calorimeter

The calorimeter used in this experiment is the one Miyazaki developed in the course of his thesis work.[34] It is designed to operate in both isobaric and throttling modes. Figure IV-2 schematically illustrates the principle of the calorimeter. The calorimeter consists of 3/16 in. O.D. tubing (1) and a coaxial capillary tubing of about 0.03 in. I.D. (2). This small tubing is surrounded by electrical heating wire with glass fiber insulation (3). The heating wire extends a length of 30" (A). The shut-off valve (5) is connected by a 1/16 in. O.D. tubing (8) in which 0.02" piano wire (9) is inserted. One end of the wire is attached to an externally located adjuster (11) which can thrust down the wire to make the shut-off valve closed. When the valve is closed, the path of the stream is restricted to the capillary tubing which causes a pressure drop of between 25 psid and 150 psid depending on the flow rate and condition of the flow. Thus, the isothermal or isenthalpic measurements can be made in this way. In the isothermal measurements, electrical energy is transferred from the heating wire to the stream in the capillary tubing to maintain the temperature of outgoing fluid the

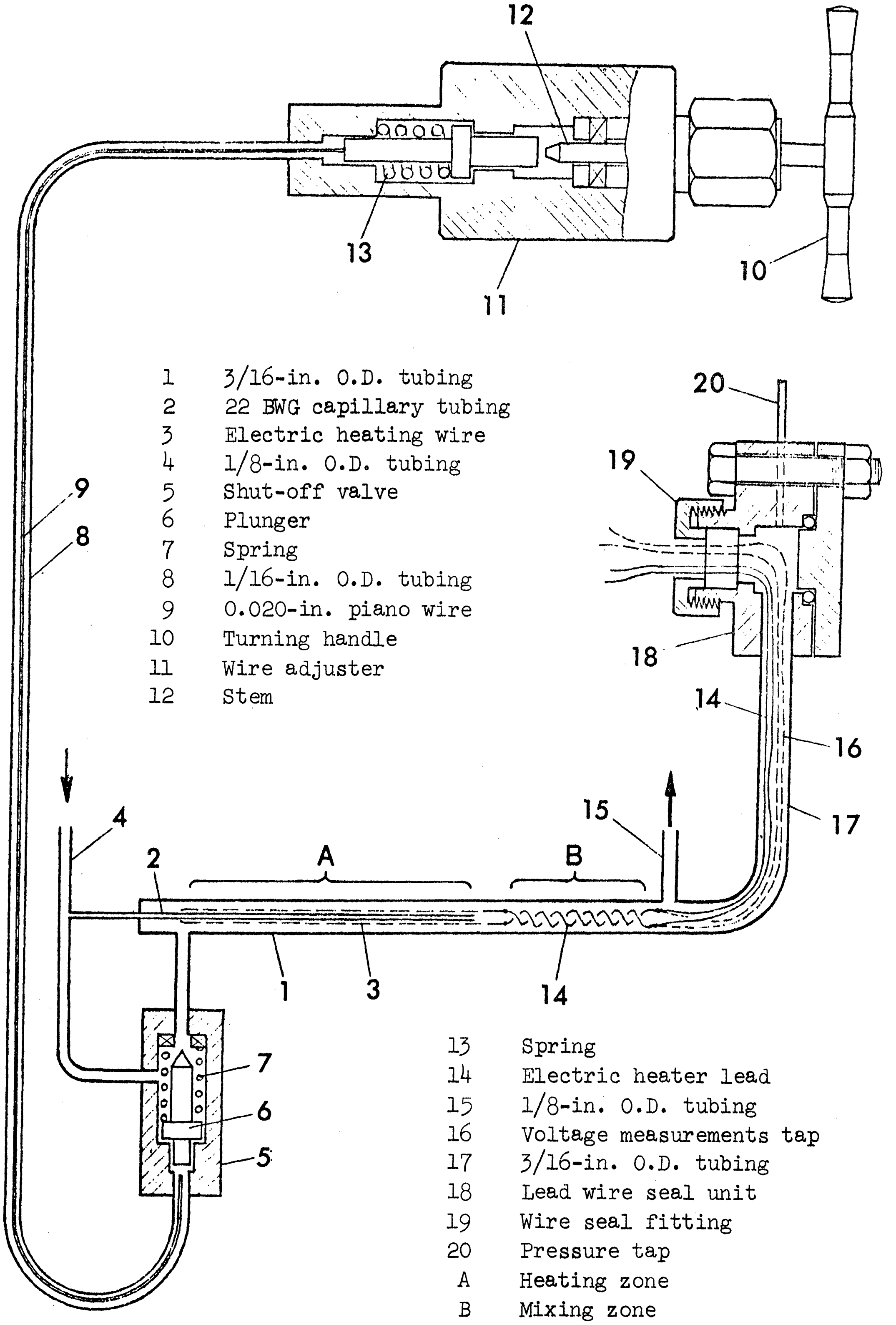

1	3/16-in. O.D. tubing
2	22 BWG capillary tubing
3	Electric heating wire
4	1/8-in. O.D. tubing
5	Shut-off valve
6	Plunger
7	Spring
8	1/16-in. O.D. tubing
9	0.020-in. piano wire
10	Turning handle
11	Wire adjuster
12	Stem
13	Spring
14	Electric heater lead
15	1/8-in. O.D. tubing
16	Voltage measurements tap
17	3/16-in. O.D. tubing
18	Lead wire seal unit
19	Wire seal fitting
20	Pressure tap
A	Heating zone
B	Mixing zone

Figure IV-2. Diagram illustrating the principle of the multipurpose calorimeter same as that of the incoming one. When the valve is open, most of the stream passes through the annulus and pressure drop across the calorimeter becomes smaller (order of 0.1 psid). In this case, the calorimeter can be operated in the isobaric mode. After the heating section (A), the stream passes through the section B of 20" length filled with twisted lead wires for the heater, which serve as baffles for mixing the stream. The mixed stream then leaves the calorimeter through the outgoing line (15). The lead wires and the voltage measurement taps (16) are led to the outside through the sealed unit (18).

The actual calorimeter assembly is shown in Figure (IV-3). For easier understanding of the drawing in Figure IV-3, the reader is advised to refer to Figure II-2(b) as well as Figure IV-2. Comparing Figure II-2(b) and Figure IV-3, one can see that A and B in Figure II-2(b) correspond to T1 and T2 in Figure IV-3. E, F and G in Figure II-2(b) are the coils wrapped by radiation shields R1, R2 and R3, respectively, in Figure IV-3. The calorimeter and shut-off valve, which have been explained in Figure IV-2, are shown in Figure IV-3 as items 5 and 6. Radiation shield R4 on the coil leading to the exit is installed to reduce the conduction heat loss along the calorimeter outlet pressure tap, 4. Y is a small piece of metal which serves as a thermal contact between the pressure tap and the outgoing tube to reduce the temperature gradient on the pressure tap. Similarly, a thermal contact is made at X between the inlet tube and the piano wire lead, which was explained in Figure IV-2. The broken line (2) indicates a radiation shield with guard heater. It was installed as an additional guard in case the heat loss could not be satisfactorily prevented by the inner shields. It was observed in most cases that the temperature difference between the guard shield and R1 was small (less than 0.1°C) without adding power to the guard heater.

Experimental Measurements

For a detailed description of experimental measurements and accuracies involved in the measuring instruments, the reader is referred to Miyazaki's thesis.[34] The major measurements of the experiments are as follows:

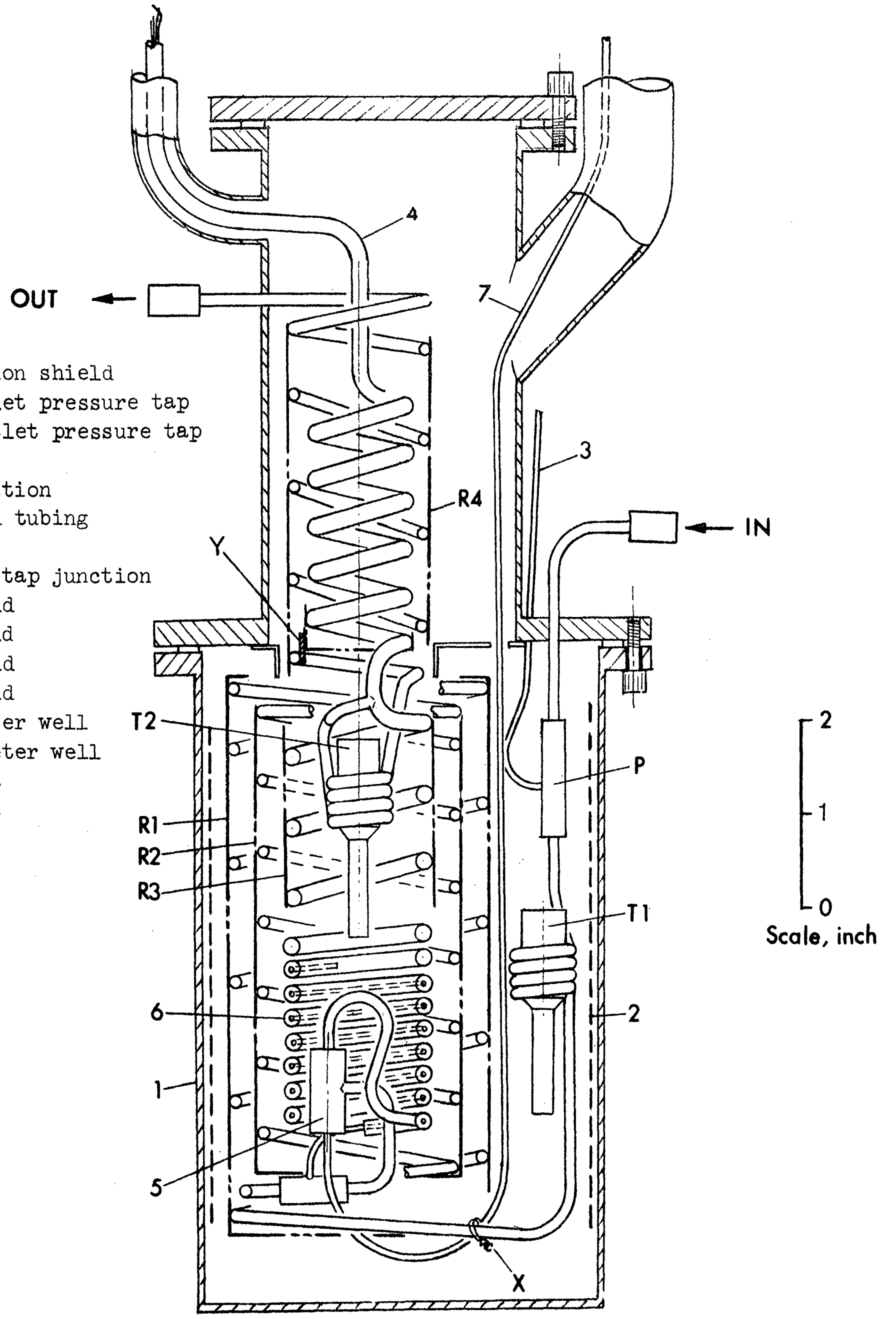

1	Vacuum pot
2	Guarded radiation shield
3	Calorimeter inlet pressure tap
4	Calorimeter outlet pressure tap
5	Shut-off valve
6	Calorimeter section
7	Piano wire lead tubing
P	Inlet pressure tap junction
R1	Radiation shield
R2	Radiation shield
R3	Radiation shield
R4	Radiation shield
T1	Inlet thermometer well
T2	Outlet thermometer well
X	Thermal contact
Y	Thermal contact

Figure IV-3. Drawing of the multipurpose calorimeter assembly

1. The calorimeter inlet and outlet temperatures are measured by a quartz crystal thermometer (Hewlett-Packard, Model 28D1A). Corrections were made on the thermometer readings as suggested by Miyazaki.[34] The thermometer has a resolution of 0.0001°C and a factory calibration gives accuracy of ±0.02°C. In addition a six junction copper-constantan thermopile is placed between the inlet and outlet measuring points to make independent measurements of the temperature differences. According to Miyazaki,[34] for measurements of the outlet temperatures, the thermopile readings are more reliable than the quartz thermometer readings, especially when the temperature differences are small across the calorimeter. Therefore, the outlet temperatures were determined from the thermopile readings and the inlet temperatures were measured with the quartz thermometer. The emf of the thermopile is measured using a K-5 potentiometer. A calibration equation for the thermopile is given in Miyazaki's thesis.[34]

2. The electrical energy input to the calorimeter is supplied by a DC power supply (KEPCO Model PVS100-IMG) capable of delivering up to 1 ampere at 100 volts. It is measured by a K-5 potentiometer using standard resistors to scale down the voltage to the range of the potentiometer.

3. The calorimeter inlet pressure is determined from the measurement of helium pressure of the cylinder, C-1, (refer to Figure IV-1) using a dead weight gage (Ruska Instrument, Model 2400), with a resolution of 0.1 psi. The gage actually measures the oil pressure balanced by the helium pressure exerted by the bellows, F-13. In order to compensate for the spring effect of the bellows, it is adjusted to its equilibrium position, as monitored by the null indicator, before the measurement. A small inbalance in pressure between the system fluid and helium, as indicated by the position indicator for the bellows, F-11, is corrected using the calibration made by Miyazaki.[34] In addition,

the line pressure drop between the bellows (F-11) and the inlet to the calorimeter is measured using a differential pressure transducer (LDPT) so that the calorimeter inlet pressure can be calculated accurately.

4. The pressure drop across the calorimeter is measured using a differential pressure transducer. A calibration was prepared by Miyazaki.[34] According to Miyazaki, the data fit the calibration equation within ±0.15%.

5. The volumetric flow rate is determined by the pump displacement speed together with a knowledge of the cross-sectional area of the plunger, which is corrected for the thermal contraction at the pump bath temperature. In the present investigation the pump speeds are set at values corresponding to 12 and 14.2 c.c./min.

Material Used

The material used in the experiment is an extra pure grade donated by the Freon Division of du Pont de Nemours and Co. Before the sample was charged, the system was evacuated to 100 micron pressure. The system was flushed with the sample several times in a similar method as described in Section III. A sample, after the experiment was finished, was taken from the system and sent to a Freon Products Laboratory of du Pont Co. for analysis. The result of the analysis is presented in Table IV-1.

TABLE IV-1

Composition of C_2F_6

C_2F_6	99.980%
Air	0.014
Freon 12 (CCl_2F_2)	0.003
Others*	0.003
	100.000%

(*Possibly, CO, CF_4, C_2F_5H, $C_2Cl_3F_6$ and H_2O)

Molecular weight of the sample: 138.01

Region of Measurements

Calorimetric studies on C_2F_6 covered the temperatures from 0°F to 250°F and pressures from 247 to 1969 psia as shown on a P-T plane in Figure IV-4. Each run is numbered in the chronological order of investigation. The vapor pressure curve is drawn in the diagram to indicate the phase corresponding to each run. In the supercritical region emphasis is placed on isobaric measurements in the $C_p(T)$ maxima region, which includes the runs at 490, 598, 700, 839, 1049 and 1398 psia. Extended measurements are made at 247 and 1969 psia. The pressures, except for 598 and 1969 psia, were chosen in such a way that their reduced values are the same as those for the experimental isobars in the argon measurements (and propane measurements[61]). An isobaric run was made at 432 psia, which according to du Pont Co.[11], is the critical pressure. An enthalpy vs temperature plot constructed from the measurements (Figure IV-24) shows a significant enthalpy change indicating the pressure was significantly below the critical pressure. In an attempt to locate the true critical point, a series of isobaric enthalpy traverse runs in the critical region were added to the original plan. These are presented in Figure IV-4. The pressure levels selected for those measurements are (in descending order) 442, 437, 436, 433.5, 432, 427 and 418 psia. In addition, enthalpy traverse runs were made at 376 and 247 psia.

Isothermal changes in enthalpy were measured along the five isotherms: 0, 67.6, 122, 176 and 247°F. The basic data for C_2F_6 are presented in Tables B-3 (isobaric) and B-4 (isothermal) of Appendix B.

Determination of Liquid Densities

As already discussed, the volumetric flow rate could be estimated accurately from a knowledge of the speed of the metering pump displacement and the cross-sectional area of the pump cylinder. For the calculation of mass flow rate, however, it is necessary to know the density of the liquid inside the pump cylinder. In a previous investigation with ethane,[34] liquid densities were estimated from the available data which were believed to be accurate. For C_2F_6, however, density data

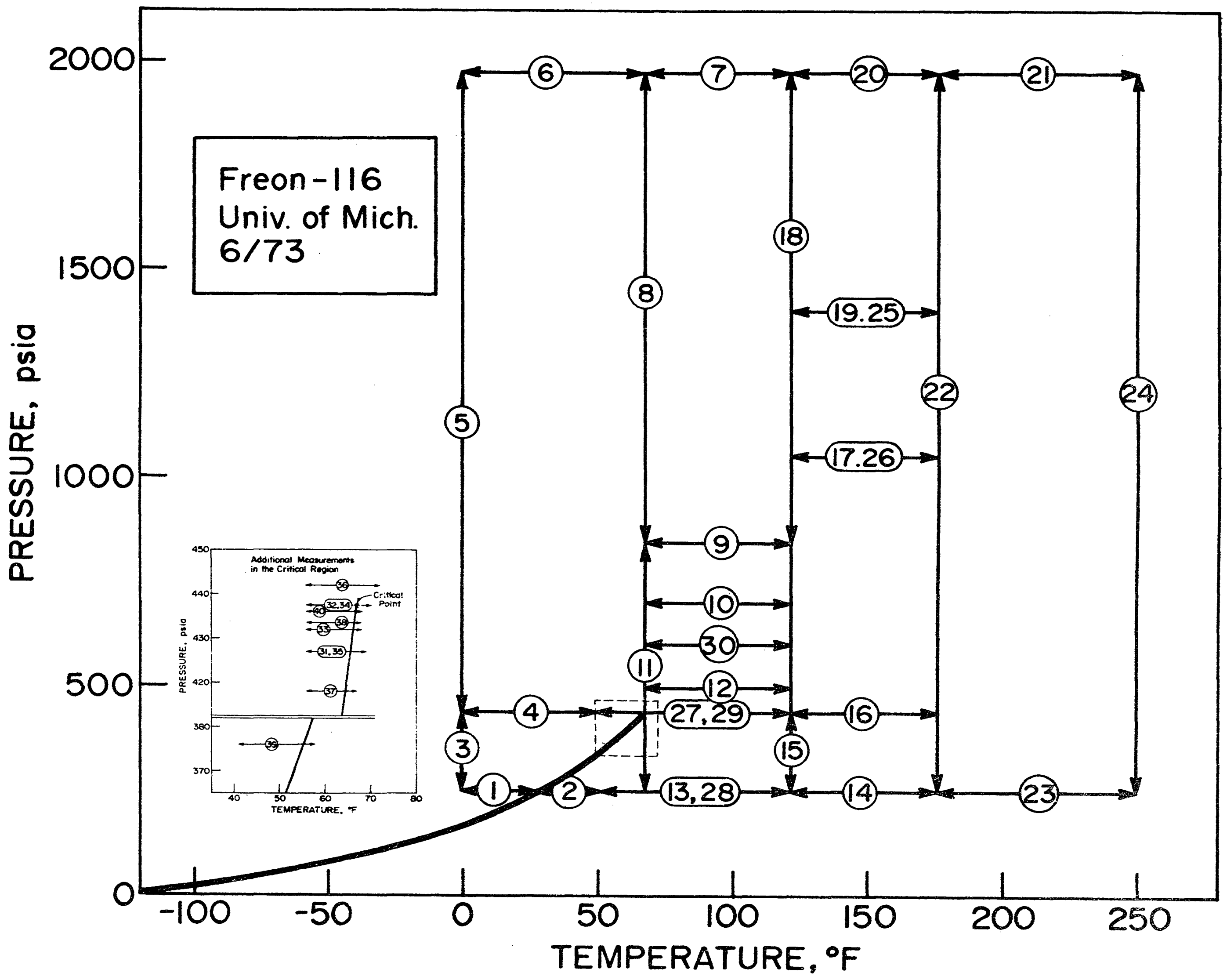

Figure IV-4. Range of calorimetric determinations on C_2F_6.

in the sub-cooled region were not available in the literature. Therefore, a new technique had to be developed in order to determine the necessary liquid densities experimentally.

The technique involves a simple principle which can be described below:

Consider a cylinder with a piston containing a liquid at temperature T_0 and pressure P_0 (see Figure IV-5). Suppose a portion of the liquid is discharged into an empty tank by opening a throttling valve connected to the cylinder. Then, the valve is closed and the position of the piston is adjusted until the pressure inside the cylinder is restored to P_0. Suppose that the temperature of the liquid is maintained at T_0 throughout the procedure.

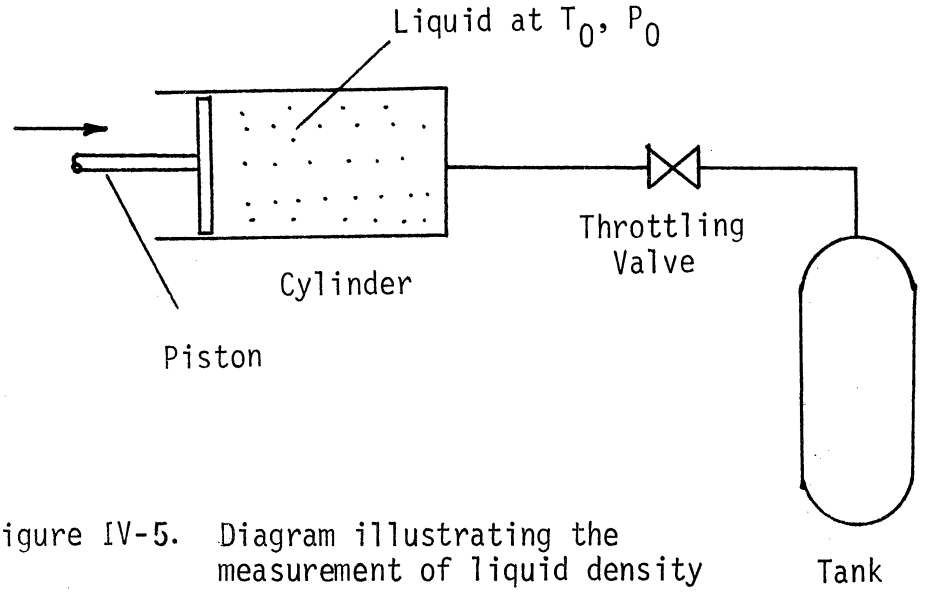

Figure IV-5. Diagram illustrating the measurement of liquid density

Then, the density of the liquid, $\rho(T_0, P_0)$, is determined from the knowledge of volume displacement by the piston and the mass of the liquid inside the tank as

$$\rho\ (T_0, P_0) = \frac{m}{\Delta V}$$

where m = mass of the liquid collected in the tank
ΔV = volume displacement by the piston.

In the actual measurement of the density, one metering pump is used as a cylinder with piston in Figure IV-5. Since the pump has a scale which reads the piston position to ±0.0025 mm, the volume displacement can be estimated to ±0.005 cc.(total volume displacement is about 100 cc). The temperature of the liquid inside the cylinder can be maintained constant as the pump bath serves to keep the pump cylinder at the desired temperature. A sufficiently long period of time (between one and two hours) is allowed after the bath starts to control at the temperature so the liquid inside the cylinder reaches a steady temperature very close to, if not at, the bath temperature. In the present measurement, the bath temperature is maintained at 0°F, well below the saturation temperature for the lowest isobaric run (247 psia). The liquid temperature is assumed to be the same as the bath temperature as measured by the thermocouple immersed in the bath fluid. Figure IV-6 illustrates schematically the actual arrangement of the equipment used for this work. One of the sample bombs used in the calibration for the flow meter in the previous recycle system was used as the tank collecting the fluid from the cylinder. As shown in the figure, part of the line connecting the cylinder (P-1A) and the throttling valve (VA) had to be exposed to room temperature since it was practically impossible to immerse the sampling tank into the pump bath. However, the external line, and hence the hold-up of the fluid exposed to the ambient air was reduced as small as possible (total volume of the fluid exposed to the air was less than 10 cc). As a consequence, the rest of the recycle system was disconnected during this density calibration.

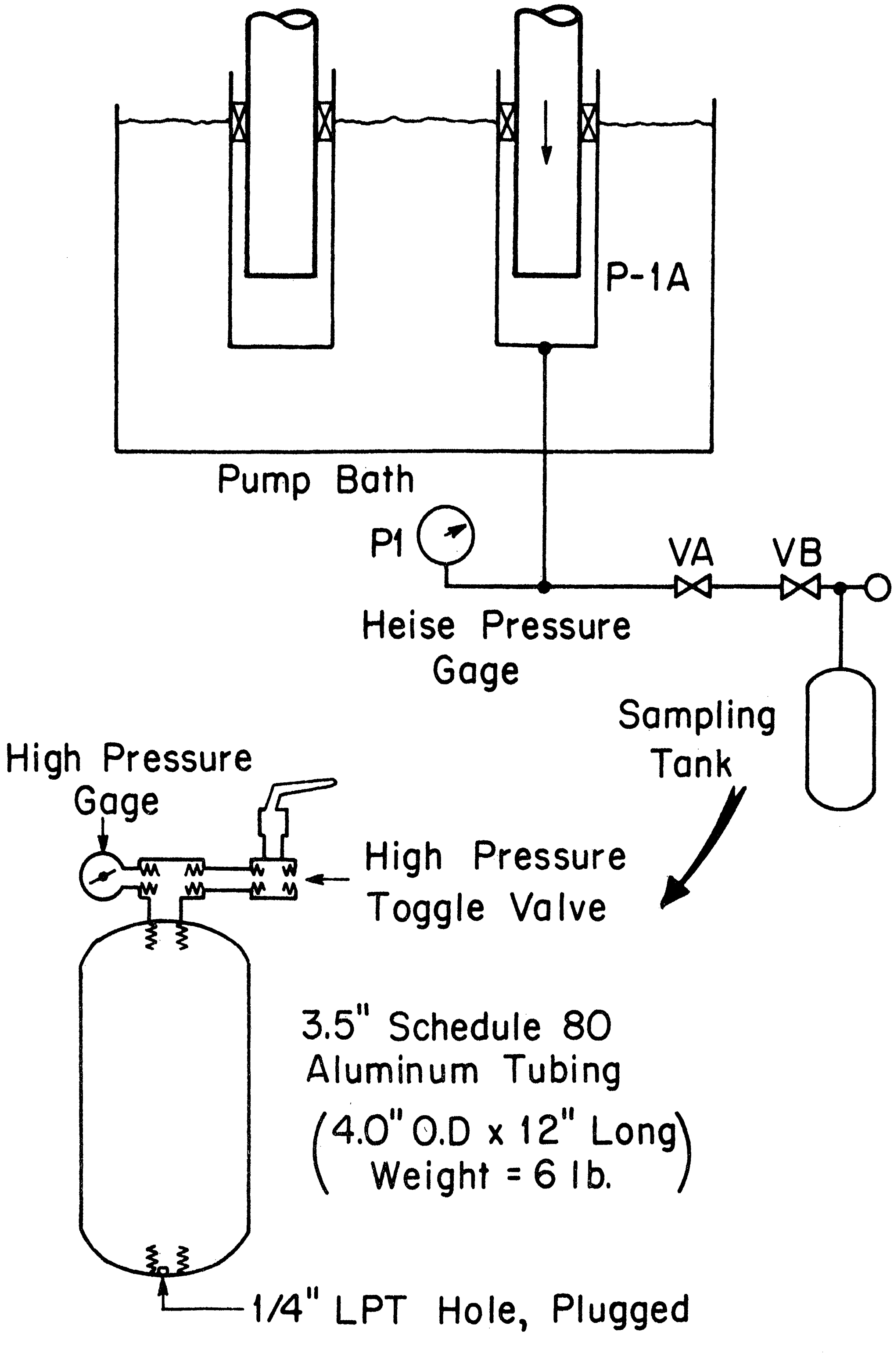

Figure IV-6. Arrangement for the liquid density measurement.

The bellows (F-11 of Figure IV-1) had to be disconnected from the line since it could provide a variable volume during the measurement. As the result the pressure of the fluid in the system could not be determined by the dead weight gage. Instead, the Heise gage (P1) was connected for measurements of the fluid pressure. The pressure could be read with the Heise gage within ±1 psi accuracy, which would affect errors somewhere between 0.004 and 0.01% on the measured densities depending on the pressure. Since these errors were tolerable for the present work, using the Heise gage for the pressure readings was considered justifiable.

In the present measurement the liquid was discharged while the pump piston was moving down continuously. In the meantime the opening of the throttle valve (VA in Figure IV-6) was manually adjusted so that the fluid pressure, as monitored by the Heise gage (P1), stayed constant at the initial pressure, P_0. After filling, the toggle valve (VB) is closed; the pump is stopped. Finally, the position of the piston is adjusted until the pressure settles to the initial pressure, P_0. Usually about an hour is allowed between pump shut-off and the final settling-down to make sure the fluid inside the cylinder reaches an equilibrium condition. The fluid accumulated inside the tank was determined by directly weighing the tank before and after the calibration procedure. In a typical measurement, about 120 grams of the fluid are collected (resolution of the balance used for the measurements is 0.001 g).

The whole procedure is repeated for various pressures to obtain a series of density data at 0°F. Those data, together with the saturation density in the literature, are plotted against pressure, as shown in Figure IV-7. The densities are fitted to an equation as

$$Y = A + BX + CX^2 + DX^3 \qquad \text{(IV-1)}$$

where Y = density of C_2F_6, g/cc
X = pressure, psia

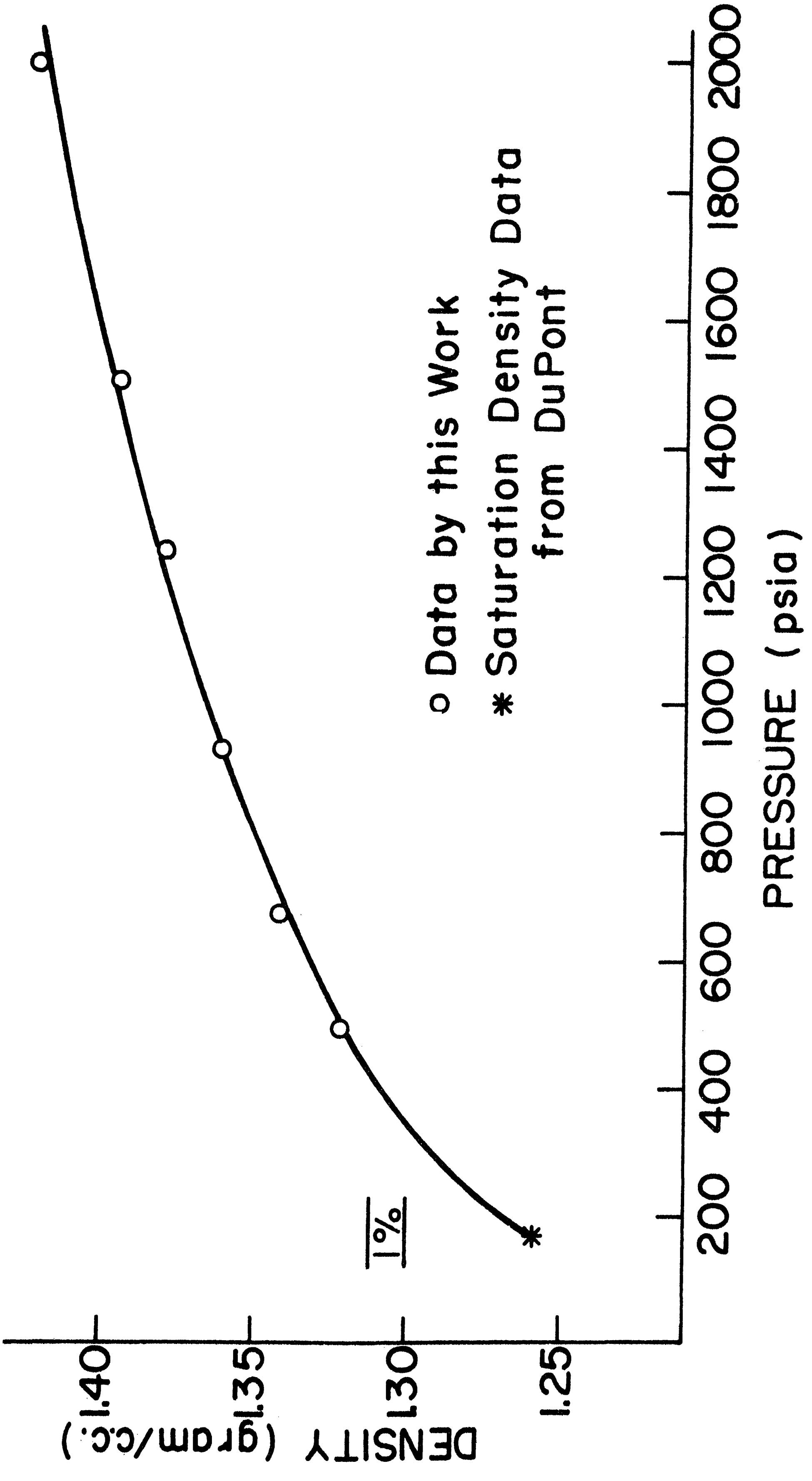

Figure IV-7. Plot of liquid densities for C_2F_6 at 0°F.

The constants in Equation (IV-1) together with the density data are listed in Table A-6 of Appendix A. The equation fits the data within 0.05%. It is important to realize that the same equipment (the metering pump) and the same condition were used in the density measurements and the actual experiments. Thus, the technique used here establishes a means for the absolute flow calibration. Although the density data represented by Equation (IV-1) should be precise, for the specific purpose of this investigation it is not imperative that the data also be accurate.

Results

C_p and $C_p(T)$ Maxima

C_p values are determined from isobaric measurements of enthalpy using the method described in Section II. The values so determined are listed in Table IV-2. A typical isobar (490 psia) in the supercritical region is illustrated in Figure IV-8. The isobars, designed to determine $C_p(T)$ maxima at 437 and 442 psia, are shown in Figures IV-9 and IV-10, respectively. The value of $C_p(T)$ maximum for 437 psia is indeterminate because the pressure is very close to, if not at, the critical pressure (refer to Figure IV-28). At 442 psia the value of $C_p(T)$ maximum is obtained at 68.0°F as 11.64 Btu/lb-°F (cf. $C_p{}^o$ at the corresponding temperature is 0.18 Btu/lb-°F). The other $C_p(T)$ vs T plots are presented in Figures IV-11, IV-12, IV-13, IV-14, IV-15, IV-16 and IV-17. All of the $C_p(T)$ maxima obtained in the present work are listed in Table IV-3. The basic measurements are listed in Table C-5 of Appendix C.

TABLE IV-2

ISOBARIC HEAT CAPACITIES of C_2F_6

Pressure = 247. psia		Pressure = 432. psia		Pressure = 490. psia		Pressure = 598. psia		Pressure = 700. psia	
Temperature (°F)	C_p (Btu/lb-°F)	Temperature (°F)	C_p (Btu/lb-°F)	Temperature (°F)	C_p (Btu/lb-°F)	Temperature (°F)	C_p (Btu/lb-°F)	Temperature (°F)	C_p (Btu/lb-°F)
0.	0.2960	0.	0.2950	64.	0.3697	70.	0.4310	70.	0.3744
10.	0.3080	10.	0.3060	70.	0.7095	80.	0.5732	80.	0.4177
20.	0.3290	20.	0.3150	72.	0.9093	86.	0.7378	90.	0.4869
25.	0.3515	30.	0.3260	74.	1.6350	89.6	0.8365	96.	0.5436
28.	0.3103	40.	0.3480	74.8	2.2920	92.	0.7815	100.	0.5761
34.	0.2779	50.	0.4050	75.1	2.3930	96.	0.6789	101.4	0.5800
40.	0.2658	60.	0.5405	75.4	2.2960	100.	0.5812	104.	0.5640
60.	0.2414	63.	0.7945	76.	2.0320	106.	0.4729	108.	0.5322
80.	0.2320	65.	1.2140	77.	1.6050	112.	0.3980	114.	0.4900
100.	0.2295	66.	1.4660	78.	1.2160	120.	0.3429	120.	0.4568
120.	0.2291	68.	0.9787	80.	0.8744				
140.	0.2295	70.	0.7600	85.	0.5412				
160.	0.2300	74.	0.5190	90.	0.3997				
180.	0.2303	80.	0.3900	100.	0.3547				
200.	0.2307	90.	0.3230	110.	0.3148				
220.	0.2311	100.	0.3000	120.	0.2779				
250.	0.2324	120.	0.2694						
		140.	0.2550						
		160.	0.2500						
		180.	0.2488						

Pressure = 839. psia		Pressure = 1049. psia		Pressure = 1398. psia		Pressure = 1969. psia	
Temperature (°F)	C_p (Btu/lb-°F)	Temperature (°F)	C_p (Btu/lb-°F)	Temperature (°F)	C_p (Btu/lb-°F)	Temperature (°F)	C_p (Btu/lb-°F)
70.	0.3364	120.	0.3772	120.	0.3282	0.	0.2780
80.	0.3569	130.	0.3839	130.	0.3323	20.	0.2800
90.	0.3818	134.	0.3868	140.	0.3365	40.	0.2826
100.	0.4137	136.	0.3880	150.	0.3405	60.	0.2858
110.	0.4457	138.	0.3868	160.	0.3427	80.	0.2893
114.	0.4586	144.	0.3815	162.	0.3428	100.	0.2929
117.	0.4666	150.	0.3758	164.	0.3427	120.	0.2965
120.	0.4511	160.	0.3654	170.	0.3413	140.	0.3009
		170.	0.3551	176.	0.3386	160.	0.3050
		176.	0.3490			180.	0.3088
						200.	0.3112
						205.	0.3115
						210.	0.3112
						230.	0.3090
						250.	0.3060

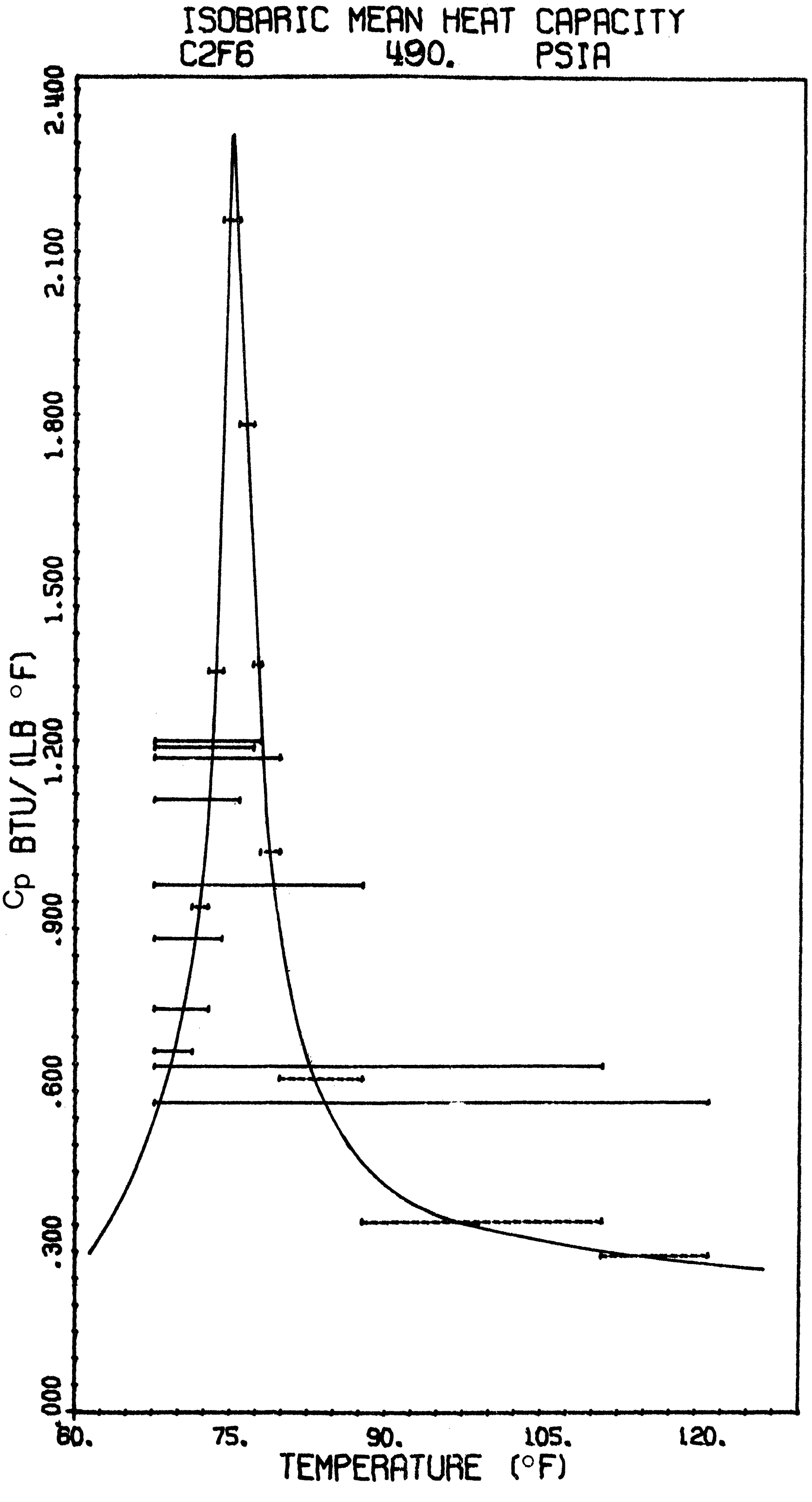

Figure IV-8. Isobaric heat capacity for C_2F_6 at 490 psia.

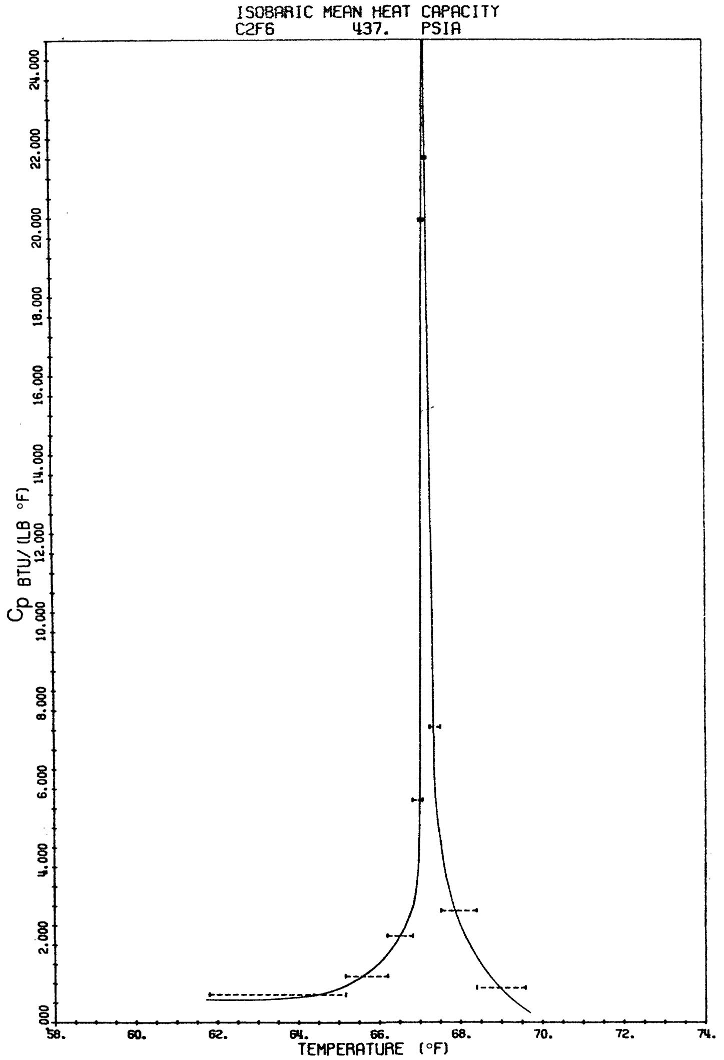

Figure IV-9. Isobaric heat capacity for C_2F_6 at 437 psia.

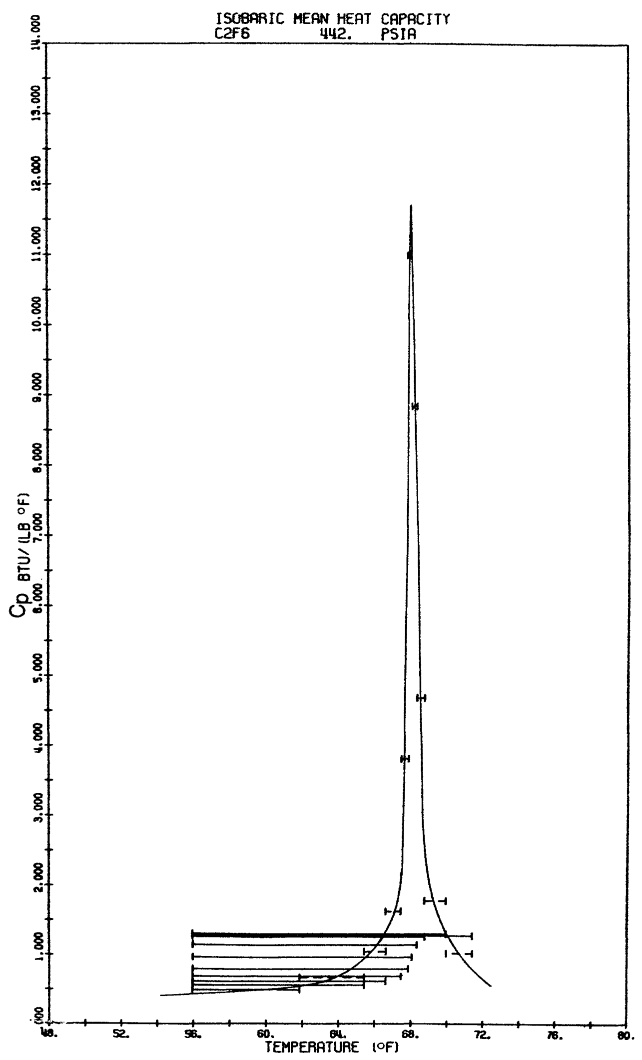

Figure IV-10. Isobaric heat capacity for C_2F_6 at 442 psia.

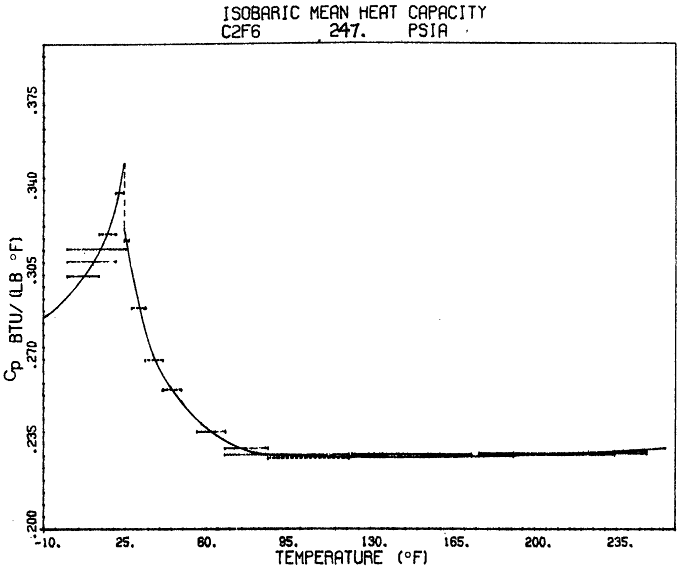

Figure IV-11. Isobaric heat capacity for C_2F_6 at 247 psia.

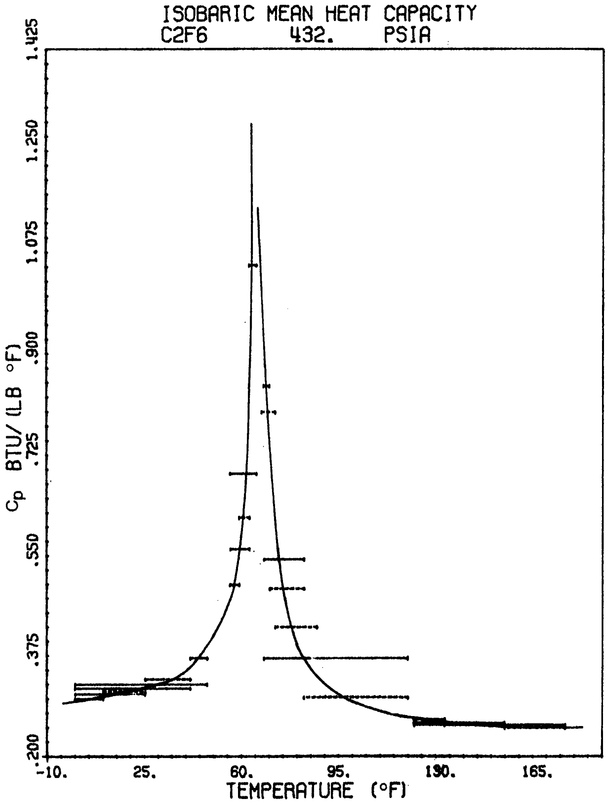

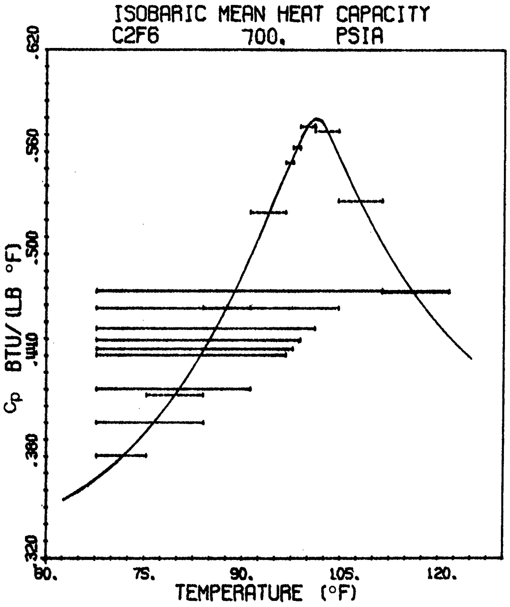

Figure IV-12. Isobaric heat capacity for C_2F_6 at 432 psia.

Figure IV-13. Isobaric heat capacity for C_2F_6 at 700 psia.

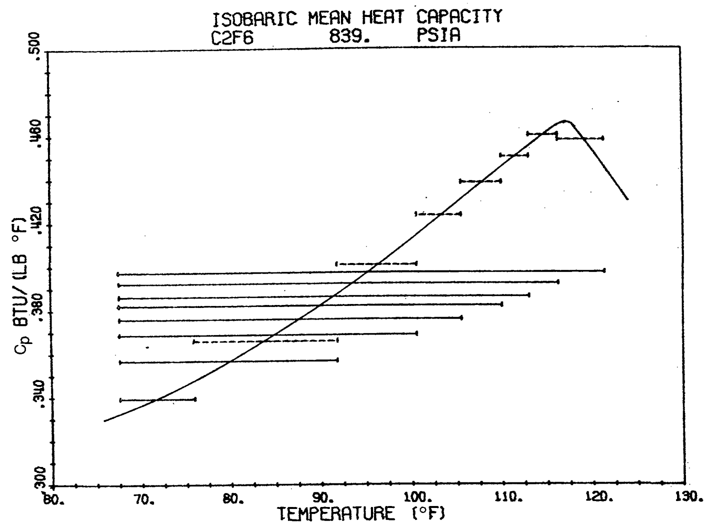

Figure IV-14. Isobaric heat capacity for C_2F_6 at 839 psia.

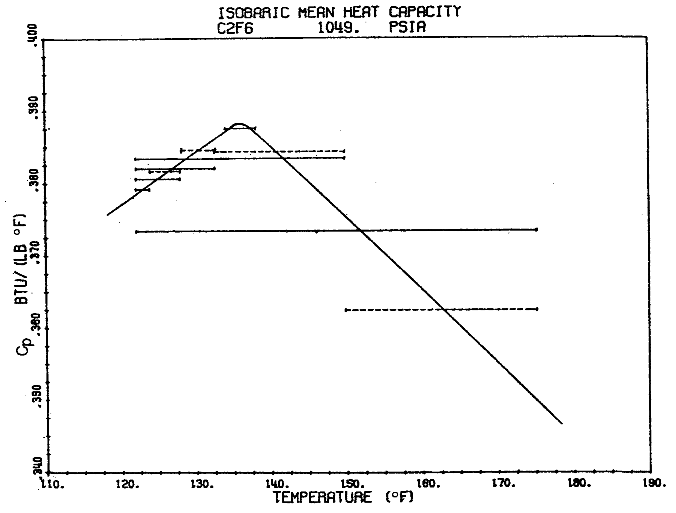

Figure IV-15. Isobaric heat capacity for C_2F_6 at 1049 psia.

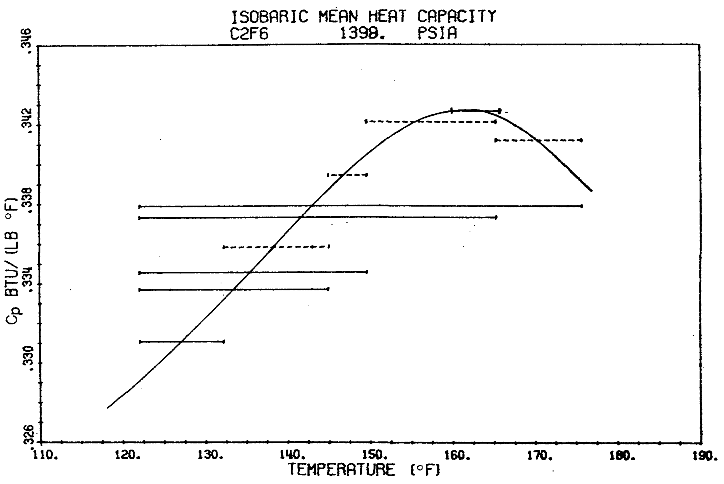

Figure IV-16. Isobaric heat capacity for C_2F_6 at 1398 psia.

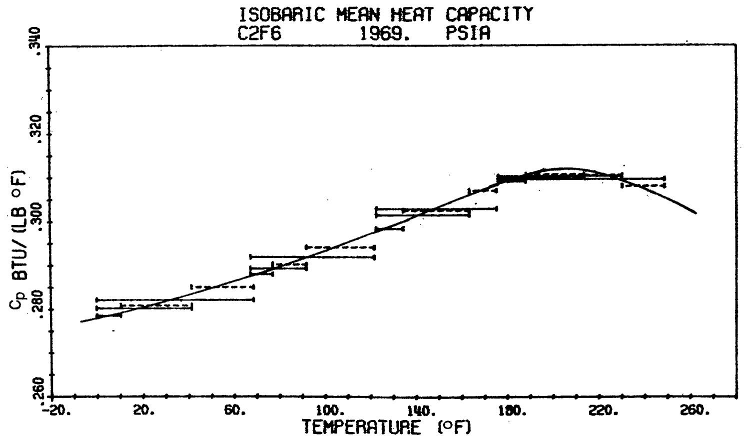

Figure IV-17. Isobaric heat capacity for C_2F_6 at 1969 psia.

TABLE IV-3

$C_p(T)$ Maxima Data for C_2F_6

Pressure (psia)	T^M (°F)	C_p^M (Btu/lb-°F)
437	67.10 ±0.1	>25.0
442	68.0 ±0.1	11.64 ±0.4
490	75.1 ±0.1	2.343±0.01
598	89.6 ±0.2	0.8365 ±0.002
700	101.4 ±0.3	0.5800 ±0.001
839	117.0 ±0.5	0.4666 ±0.001
1049	136.0 ±1.0	0.388 ±0.007
1398	162.0 ±1.5	0.3428 ±0.0007
1969	205.0 ±2.0	0.3115 ±0.0005

Isothermal Data

ϕ values for all of the experimental isotherms were determined using the methods described in Section II. These are presented in Table IV-5. $\phi(P)$ maxima data are presented in Table IV-4. Plots made for the isotherms at 0, 67.6, 122, 176 and 247°F are shown in Figures IV-18, IV-19, IV-20, IV-21 and IV-22, respectively. An inversion point (0°F at 865 psia) is observed in Figure IV-18. The basic data are listed in Table C-6 of Appendix C.

TABLE IV-4

$\phi(P)$ Maxima Data for C_2F_6

Temp. (°F)	Pressure (psia)	$-\phi \times 100$ (Btu/lb-psid)
122	645 ±20	4.352 ±0.044
176	770 ±40	1.990 ±0.010
247	840 ±40	1.250 ±0.006

TABLE IV-5

ISOTHERMAL THROTTLING COEFFICIENTS OF C_2F_6

Temperature = 0.°F		Temperature = 67.6°F		Temperature = 122.°F		Temperature = 176.°F		Temperature = 247.°F	
Pressure (psia)	- Φ x 100 (Btu/°F-psid)	Pressure (psia)	- Φ x 100 (Btu/°F-psid)	Pressure (psia)	- Φ x 100 (Btu/°F-psid)	Pressure (psia)	- Φ x 100 (Btu/°F-psid)	Pressure (psia)	- Φ x 100 (Btu/°F-psid)
200.	0.1190	0.	2.6800	0.	1.9600	0.	1.2500	0.	0.6950
300.	0.0930	200.	3.2250	200.	2.1360	200.	1.4780	200.	0.8277
400.	0.0532	300.	3.9400	400.	2.4900	400.	1.7110	400.	0.9900
600.	0.0250	360.	5.2450	500.	3.0150	600.	1.9090	600.	1.1410
800.	0.0053	400.	6.9600	600.	4.0300	700.	1.9710	700.	1.2120
865.	0.0000	460.	5.5410	630.	4.2730	750.	1.9890	800.	1.2480
1000.	-0.0100	500.	2.5980	645.	4.3520	770.	1.9900	840.	1.2500
1200.	-0.0168	600.	1.1340	660.	4.3220	800.	1.9800	900.	1.2400
1400.	-0.0340	700.	0.5989	700.	4.0990	900.	1.8900	1000.	1.1880
1600.	-0.0436	800.	0.3224	800.	3.1200	1000.	1.7100	1200.	1.0270
1800.	-0.0520	1000.	0.1683	900.	1.9700	1200.	1.2560	1400.	0.8620
2000.	-0.0616	1200.	0.1300	1000.	1.2680	1400.	0.8540	1600.	0.7040
		1400.	0.1100	1200.	0.6866	1600.	0.6000	1800.	0.5670
		1600.	0.0900	1400.	0.3993	1800.	0.4500	2000.	0.4430
		1800.	0.0700	1600.	0.2307	2000.	0.3221		
		2000.	0.0630	1800.	0.1709				
				2000.	0.1150				

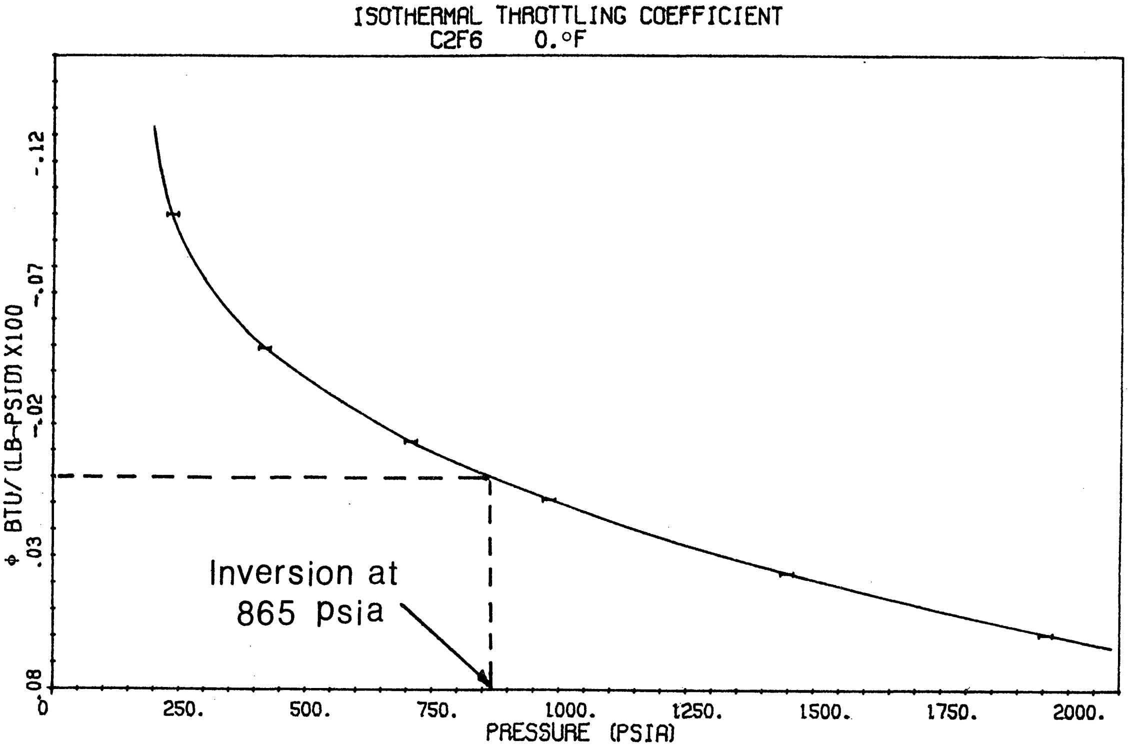

Figure IV-18. Isothermal throttling coefficient for argon at 0°F.

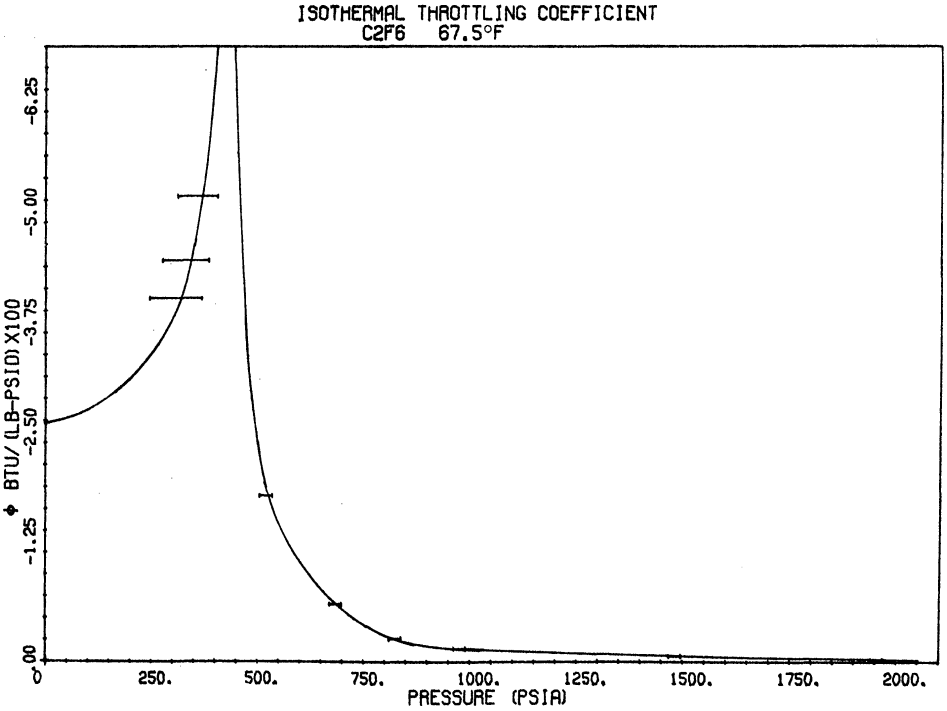

Figure IV-19. Isothermal throttling coefficient for argon at 67.5°F.

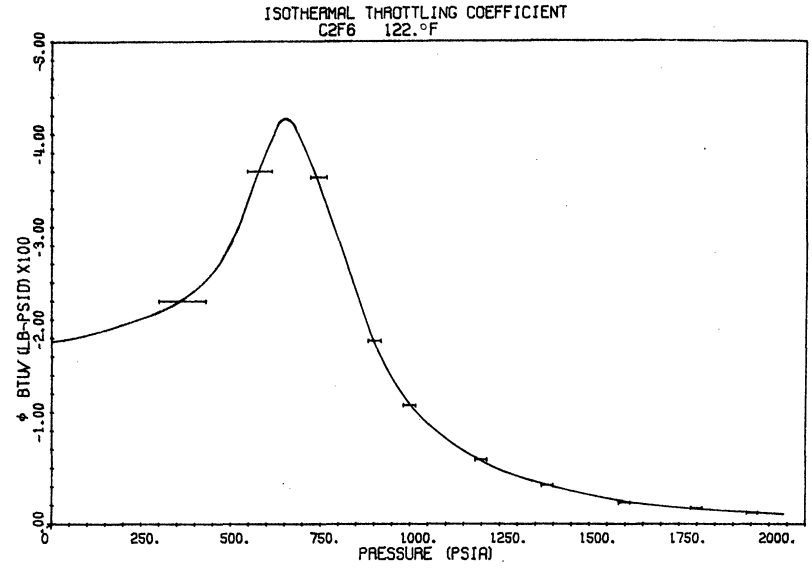

Figure IV-20. Isothermal throttling coefficient for argon at 122°F.

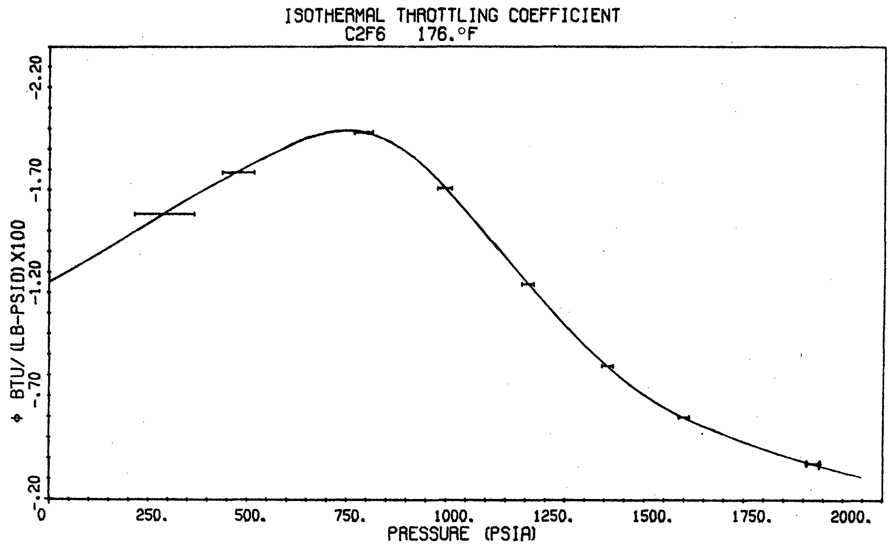

Figure IV-21. Isothermal throttling coefficient for argon at 176°F.

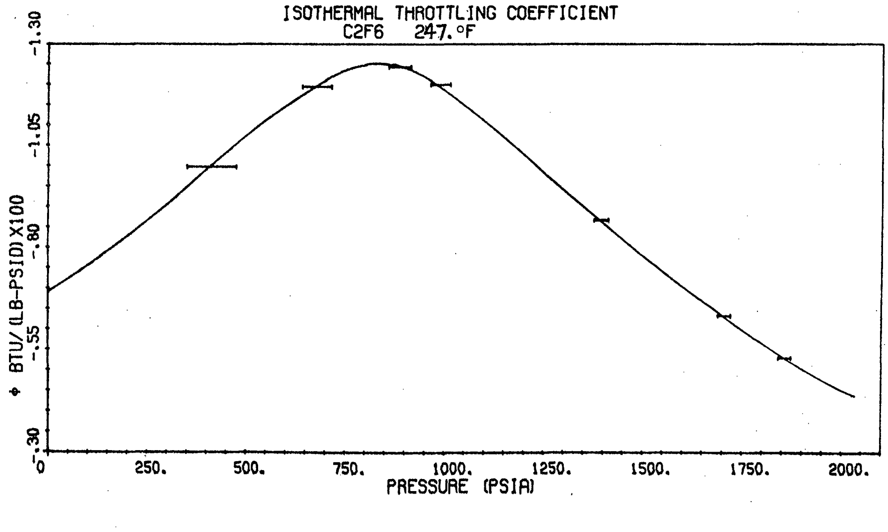

Figure IV-22. Isothermal throttling coefficient for argon at 247°F.

Enthalpy Changes on Vaporization

A typical plot of enthalpy change vs temperature across the two phase boundary is shown in Figure IV-23. The enthalpy change on vaporization is determined from the enthalpy difference between the upper and lower break points. The enthalpy traverse at 432 psia is also presented here in Figure IV-24 which shows the latent heat of 7.7 Btu/lb. Basic data for those plots appear in Table C-7 of Appendix C. The saturation temperatures and latent heats determined from the present measurements are summarized in Table IV-6 together with literature values for comparison.

Thermodynamic Consistency Checks

The consistency checks between isobaric and isothermal measurements of C_2F_6 are presented in Figure IV-25. The average and maximum inconsistencies are 0.03% and 0.10% respectively. The accuracy of the isobaric and isothermal data is estimated at 0.05% and 0.10%, respectively.

Enthalpy in the Critical Region

As discussed earlier in this section, a series of isobaric enthalpy determinations have been made in the critical region (see the enclosed square in Figure IV-4). These runs were planned primarily for the sake of determining an accurate value for the critical pressure, when it became apparent that the true critical pressure is higher than 432 psia (the value obtained from the literature[11]). It is, however, unprecedented that the critical constants are to be determined from the enthalpy measurements in the critical region. Also unprecedented are the present measurements of enthalpy change in vaporization at pressures only a few psi below the critical point. Even for the fluids which have been subjected to extensive calorimetric investigations, such as H_2O and CO_2, enthalpies are seldom measured in the critical neighborhood. (For H_2O, the enthalpy values at 220 Kg/cm^2 (P_C = 225 Kg/cm^2) are the only ones ever determined in the closest range of the critical pressure.) Obviously the measurements

TABLE IV-6

COMPARISON OF SATURATION DATA FOR C_2F_6

Pressure (psia)	Saturation Temperature (°F)		Latent Heat (Btu/lb)	
	This Work	Du Pont	This Work	Du Pont
247.	25.30 ± 0.02	25.27	29.40 ± 0.05	29.10
376.	55.35 ± 0.02	55.85	15.26 ± 0.05	16.42
418.	64.35 ± 0.02	64.61	10.20 ± 0.05	9.60
427.	65.52 ± 0.02	66.53	8.84 ± 0.05	2.95
432.	65.96 ± 0.02	67.50	7.70 ± 0.05	1.00
433.5	66.30 ± 0.02	---	6.70 ± 0.05	---
436.	66.70 ± 0.02	---	4.50 ± 0.05	---

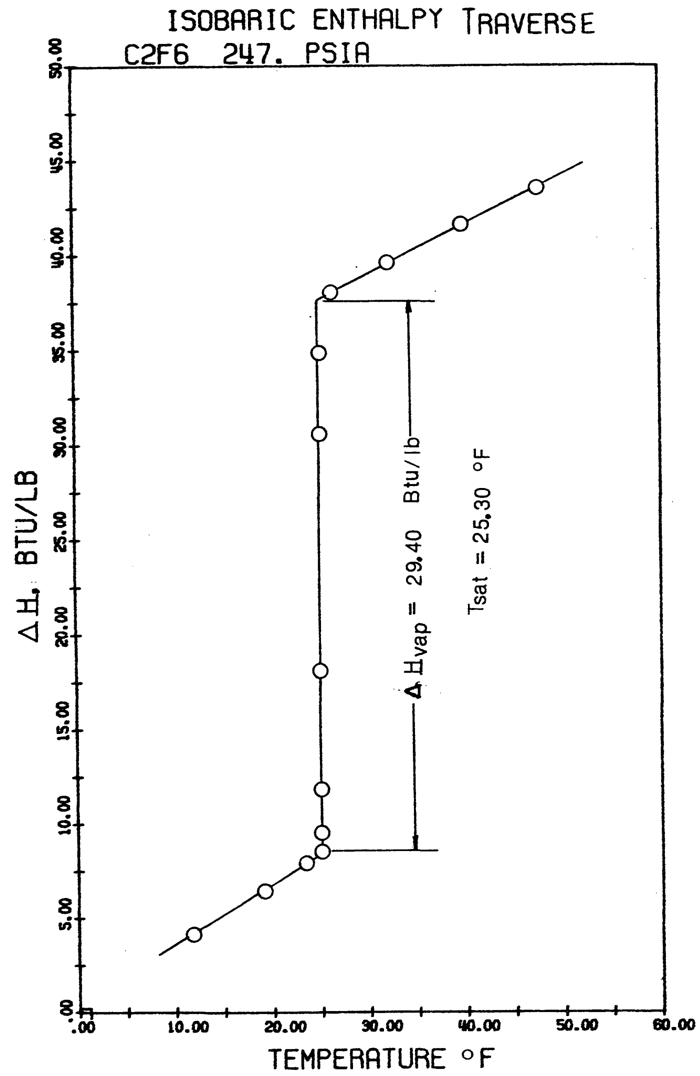

Figure IV-23. Isobaric enthalpy traverse across the two phase boundary for C_2F_6 at 247 psia.

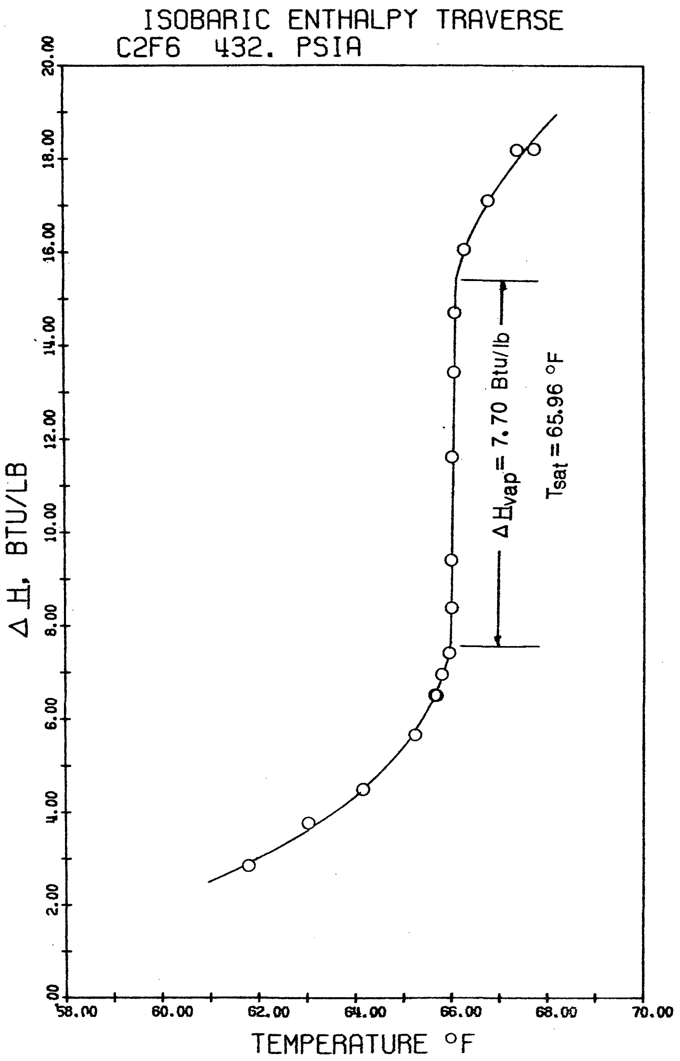

Figure IV-24. Isobaric enthalpy traverse across the two phase boundary for C_2F_6 at 432 psia.

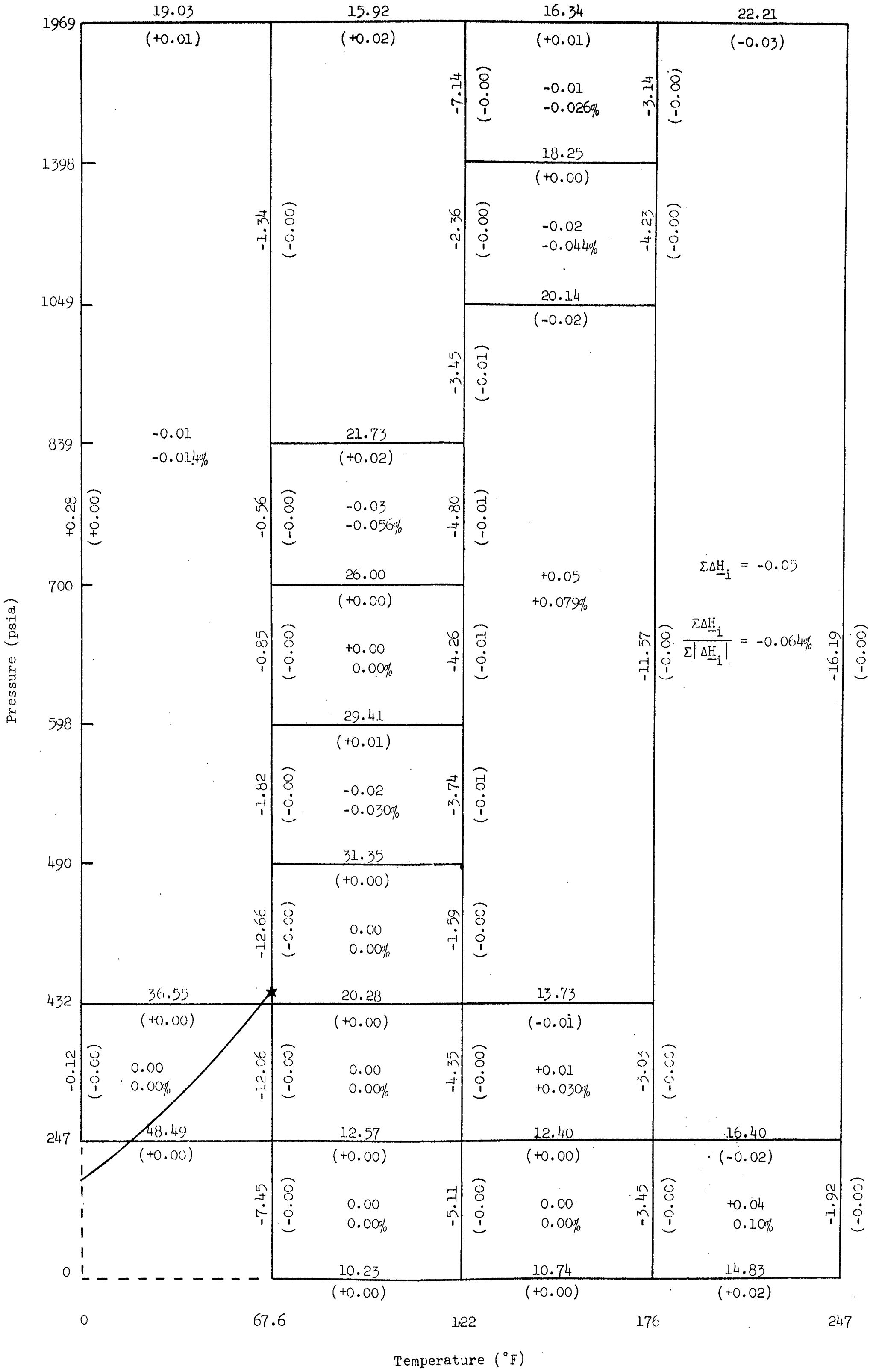

Figure IV-25. Thermodynamic consistency checks for the present calorimetric data for C_2F_6.

of enthalpy in the critical region alone can be a significant contribution in the knowledge of thermodynamics for C_2F_6 - as well as other substances.

As illustrated in Figure IV-4, seven isobaric runs were made in the critical region, which consist of about one hundred measured points along those isobars. Since each run yields a set of isobaric enthalpy differences as determined from its inlet temperature and pressure, it is necessary to establish a reference which serves to relate every set of measured enthalpy differences to the enthalpy values from a common basis. For the common basis of C_2F_6 enthalpies, $\underline{H}$ = 0 at 0°F and 0 psia, is chosen arbitrarily but conveniently since the enthalpy on any experimental isobar or isotherm can be easily calculated from the point through the enthalpy network in Figure IV-25. In order to establish the reference for the enthalpies in the critical region, enthalpy values at the location of $C_p(T)$ maxima and values of average saturation enthalpy (average of the saturated liquid and vapor enthalpies at a given pressure) are estimated from the common basis and those are plotted versus pressure, as shown in Figure IV-26. According to Powers,[45] this plot would form a smooth curve which could serve to provide reference enthalpies for the isobaric runs in the critical region, and consequently enthalpies for all the data points of the runs. Determination of the enthalpy values for those points then makes it possible to construct the saturation boundary in $\underline{H}$-T diagram, as illustrated in Figure IV-27, and thus to determine the critical pressure as 437 ±0.5 psia (cf. 432 psia in the literature[11]) by inspection of the boundary. Table IV-7 presents the values of enthalpy near the critical point.

In order to determine the critical temperature the saturation data in the critical region are plotted on log P - log T coordinates, as shown in Figure IV-28. The saturation line is fitted as a straight line to the data pointsbased on the general observation[46] that the vapor pressure is linear with the saturation temperature on a log-log scale near the critical point. From this plot and the critical pressure determined earlier, the critical temperature is determined as 526.8 ±0.1°R (cf. 527.17°R in the literature[11]) as illustrated in Figure IV-28. Plotted in Figure IV-28 are loci of $C_p(T)$ and $\phi(P)$ maxima, determined

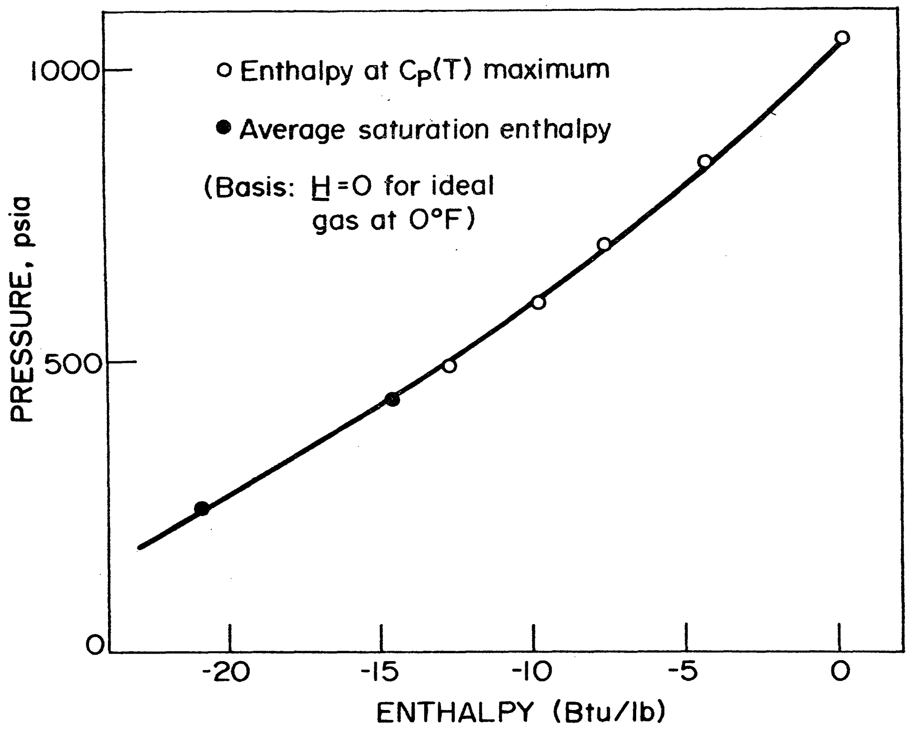

Figure IV-26. Plot of enthalpies at Cp(T) maxima and average enthalpies at saturation points as function of pressure (C_2F_6).

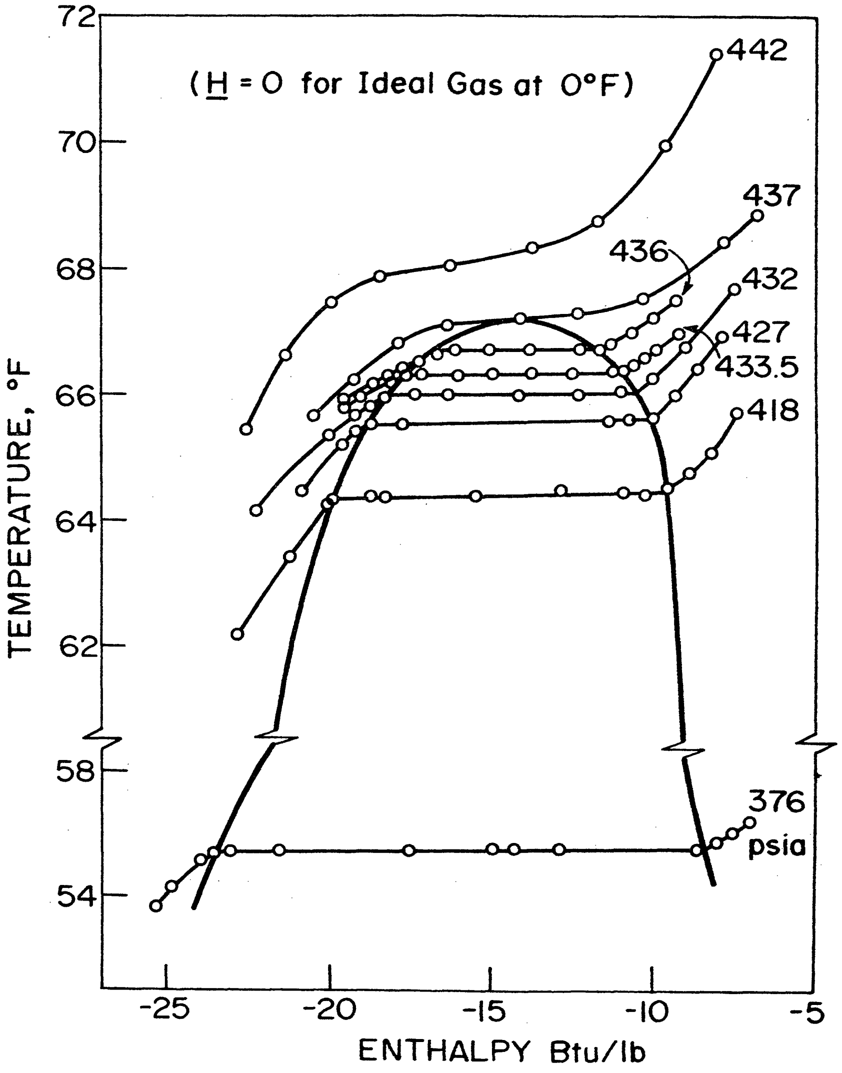

Figure IV-27. Plot of enthalpies for C_2F_6 in the critical region.

TABLE IV-7

ENTHALPY OF C_2F_6 NEAR THE CRITICAL POINT

Pressure = 376 psia		Pressure = 418. psia		Pressure = 427. psia		Pressure = 432. psia	
Temperature (°F)	$\underline{H}$ (Btu/lb)	Temperature (°F)	$\underline{H}$ (Btu/lb)	Temperature (°F)	$\underline{H}$ (Btu/lb)	Temperature (°F)	$\underline{H}$ (Btu/lb)
53.55	-25.311	62.13	-22.841	64.48	-20.858	64.15	-22.222
54.25	-24.747	63.41	-21.194	65.18	-19.608	65.32	-20.060
55.10	-23.892	64.23	-20.030	65.40	-19.162	65.60	19.214
55.32	-23.514	64.30	-19.881	65.51	-18.701	65.65	-19.211
55.36	-22.980	64.36	-18.734	65.52	-17.736	65.77	-18.765
55.36	-21.500	64.36	-18.272	65.57	-11.383	65.91	-18.305
55.41	-17.535	64.38	-15.474	65.60	-10.717	65.96	-17.340
55.47	-14.942	64.47	-12.856	65.63	-10.037	65.96	-16.317
55.50	-14.258	64.44	-10.946	65.98	- 9.344	65.97	-14.102
55.44	-12.846	64.42	-10.279	66.41	- 8.635	66.00	-12.274
55.52	- 8.615	64.54	- 9.599	66.90	- 7.911	66.05	-11.005
55.69	- 8.015	64.75	- 8.905			66.24	-10.047
56.05	- 7.546	65.07	- 8.196			66.74	- 9.001
56.35	- 7.055	65.73	- 7.470			67.33	- 7.530
56.45	- 7.055						

Note: $\underline{H}$ = 0 for ideal gas at 0.°F

TABLE IV-7 (Concluded)

Pressure 433.5 psia		Pressure 436. psia		Pressure = 437. psia		Pressure = 442. psia	
Temperature (°F)	$\underline{H}$ (Btu/lb)	Temperature (°F)	$\underline{H}$ (Btu/lb)	Temperature (°F)	$\underline{H}$ (Btu/lb)	Temperature (°F)	$\underline{H}$ (Btu/lb)
65.79	6.576	65.90	-19.533	65.67	-20.464	65.43	-22.537
65.95	7.022	66.15	-18.627	66.21	-19.216	66.62	-21.290
66.08	7.483	66.29	-18.152	66.83	-17.835	67.46	-19.910
66.18	7.957	66.39	-17.663	67.08	-16.324	67.86	-18.399
66.27	8.447	66.51	-17.159	67.19	-14.106	68.06	-16.182
66.29	8.951	66.62	-16.640	67.27	-12.287	68.34	-13.730
66.28	10.003	66.70	-16.109	67.53	-10.338	68.76	-11.738
66.31	11.113	66.70	-15.000	68.40	- 7.852	69.96	- 9.617
66.33	12.281	66.72	-13.829	68.85	- 6.800	71.41	- 8.130
66.30	13.509	66.72	-12.285				
66.37	14.794	66.71	-11.643				
66.35	15.125	66.78	-11.316				
66.46	15.459	67.02	-10.651				
66.59	15.797	67.23	- 9.972				
66.73	16.137	67.50	- 9.280				
66.96	16.830						

Note: $\underline{H}$ = 0 for ideal gas at 0.°F

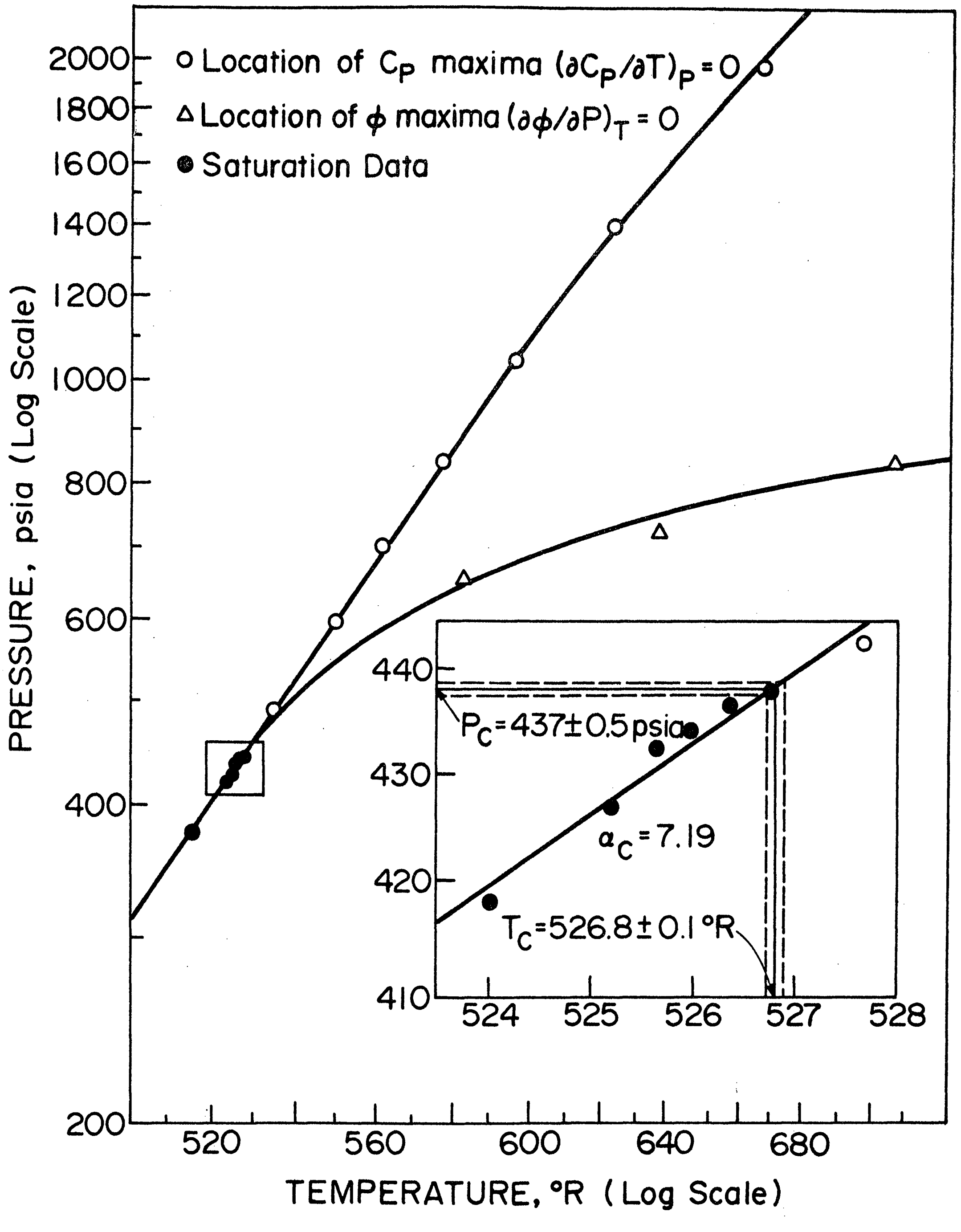

Figure IV-28. Plot of the saturation line near the critical point, Cp(T) maxima and Φ(P) maxima for C_2F_6.

in the present investigation. The line of $C_p(T)$ maxima, as discussed in Section II, demonstrates a smooth extension of the saturation line into the supercritical region. It is interesting to observe that the line of $C_p(T)$ maxima is curved slightly downward at higher pressures. An α_C value of 7.19 is obtained from the slope of the line at the critical point. The $\phi(P)$ maxima are found to lie along the curve which separates further from the line of $C_p(T)$ maxima as the pressure increases. Table IV-8 lists the critical constants both from this work and the literature for comparison.

TABLE IV-8

Critical Constants for C_2F_6

	T_C(°R)	P_C (psia)	α_C
du Pont*	527.17	432	7.05**
This Work	526.8 ±0.1	437 ±0.5	7.19

*Reference 11.

**Value determined from the normal boiling point data using the method suggested by Riedel[46]

Enthalpy Table and Diagram

Enthalpies determined in the present investigation are presented as a diagram illustrated in Figure IV-30. Table IV-9 presents the saturation enthalpies. The enthalpy values of the measured isobars are presented at regular intervals of temperature, including those for the measured isotherms, in Table IV-10. The reference chosen for the enthalpy table is $\underline{H} = 0$ for the ideal gas at 0°F. The zero enthalpies are calculated from $C_p^{\,o}$ in the literature.[54]

Comparison With Previous Experimental Data

Comparison of the present saturation data with those from du Pont Co. are presented in Table IV-6. Significant discrepancies shown in latent heats in the critical region are a consequence of differences in values of critical constants as shown in Table IV-5. There are,

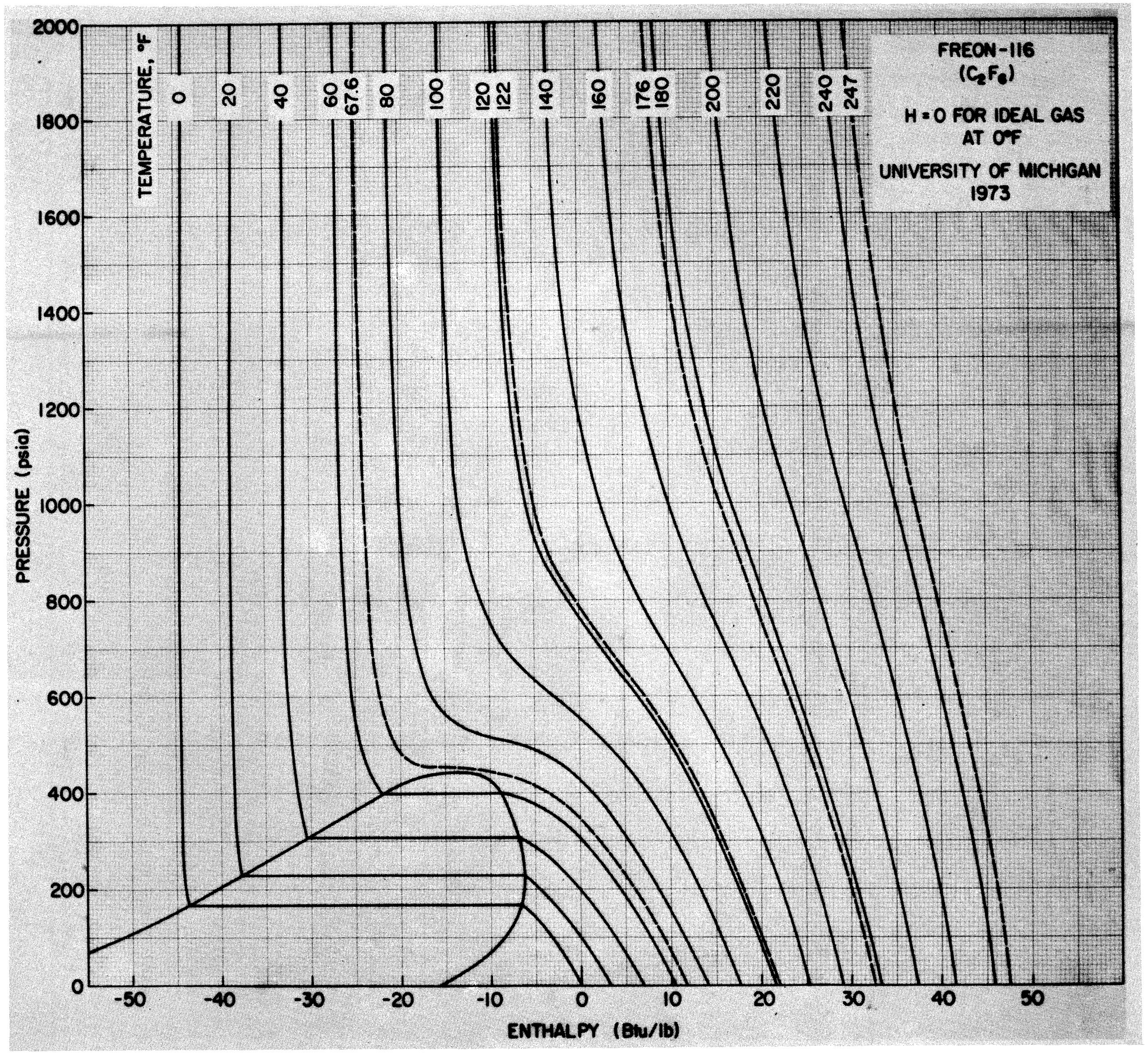

Figure IV-29. H-P-T Diagram for C_2F_6.

TABLE IV-9

TABULATED VALUES OF SATURATION ENTHALPY FOR C_2F_6

Pressure (psia)	Temperature (°F)	Enthalpy (Btu/lb)		
		Saturated		Latent Heat
		Liquid	Vapor	
247.	25.30	-35.61*	- 6.21	29.40
376.	55.35	-23.61	- 8.35	15.26
418.	64.35	-19.77	- 9.57	10.20
427	65.52	-18.83	- 9.99	8.84
432.	65.96	-18.09	-10.39	7.70
433.5	66.30	-17.54	-10.84	6.70
436.	66.70	-16.38	-11.88	4.50

*$\underline{H}$ = 0 for ideal gas at 0.°F

TABLE IV- 10

TABULATED VALUES OF ENTHALPY FOR C_2F_6

Temperature (°F)	Pressure (psia)									
	0	247	432	490	598	700	839	1049	1398	1969
0	0.00	-44.19	-44.31	-44.34	-44.37	-44.39	-44.40	-44.38	-44.30	-44.03
20	3.42	-38.00	-38.21	-38.51	-38.71	-38.76	-38.78	-38.78	-38.74	-38.53
40	6.86	- 2.51	-31.66	-31.97	-32.52	-32.72	-32.79	-32.84	-32.86	-32.87
60	10.37	2.60	-23.29	-23.96	-25.26	-25.86	-26.22	-26.50	-26.80	-27.16
67.6	11.75	4.30	- 7.76	-20.42	-22.24	-23.09	-23.65	-24.07	-24.52	-24.99
80	14.01	7.22	- 0.31	- 5.35	-16.40	-18.21	-19.36	-20.16	-20.79	-21.39
100	17.64	11.83	6.29	4.08	- 2.29	- 8.37	-11.69	-13.84	-14.77	-15.57
120	21.56	16.43	11.97	10.36	6.47	2.01	- 2.79	- 6.29	- 8.44	- 9.64
122	21.98	16.87	12.52	10.93	7.18	2.91	- 1.90	- 5.45	- 7.81	- 9.05
140	25.40	21.00	17.22	15.81	12.80	9.51	5.61	1.46	- 1.82	- 3.66
160	29.25	25.60	22.26	21.07	18.69	16.19	12.99	8.96	4.98	2.41
176	32.72	29.27	26.24	25.20	23.20	21.22	18.48	14.67	10.44	7.30
180	33.30	30.00	27.08	26.09	24.21	22.31	19.67	15.99	11.73	8.52
200	37.40	34.66	32.12	31.27	29.72	28.15	25.91	22.58	18.35	14.72
220	41.60	39.32	37.16	36.39	35.07	33.71	31.74	28.73	24.73	20.94
240	45.88	43.99	42.20	41.48	40.26	39.00	37.19	34.48	30.74	26.98
247	47.57	45.65	43.95	43.28	42.12	40.92	39.20	36.69	33.12	29.48

Note: $\underline{H}$ = 0 for ideal gas at 0°F.
Unit for $\underline{H}$ is Btu/lb.

however, good agreement between the two sources for the saturation data at 247 psia.

V - GENERALIZED CORRELATION FOR $C_p(T)$ MAXIMA

This section is devoted to correlating experimental $C_p(T)$ maxima data now available both from the literature and the present calorimetric investigations. $C_p(T)$ maxima, as noted in an earlier section of this thesis, is characterized by the temperature of the peak, T^M, and the magnitude, C_p^M, for a given pressure and therefore, the correlation efforts are conveniently divided into two parts:

1. A correlation for locations of the peak (the correlation between the pressure, P^M, and T^M).
2. A correlation for magnitudes of the peak [the correlation between P^M and $(C_p^M - C_p^o)$].

In the second part of the correlation, the objective is chosen as $(C_p^M - C_p^o)$, where C_p^o is zero pressure heat capacity, instead of C_p^M with the following reasons: Most of the existing C_p correlations are expressed in terms of $(C_p - C_p^o)$; $(C_p - C_p^o)$ is more directly related to the other thermodynamic functions than C_p. As discussed in Section II, this work was attempted within the principle of the corresponding states. A further discussion will follow the rest of this section.

Data for the Correlation

The sources of $C_p(T)$ maxima data, as reviewed in Section II, are summarized in Table V-1. It is to be noted that the most extensive data are available from H_2O. Included in the table are data for C_6H_6 and C_6H_{12} which were determined from the enthalpy data of Lenoir, et al.[29] using the method employed in previous sections. Their enthalpy measurements were not made carefully in the peak region and consequently the C_p maxima obtained were crude compared to the other data. Nevertheless, data were added to the present work because it was desirable to add the cyclic hydrocarbons into the scope of the present correlation. The data used in this work were presented in terms of reduced values in Table V-2. The critical constants used in the data reduction are listed in Table V-3.

TABLE V-1

SOURCES OF Cp(T) MAXIMA AND Cp° DATA

Substance	Molecular Weight*	No. of Data	Source	Source of Cp°
methane	16.13	6	Jones (25)	Rossini (50)
ethane	30.07	9	Furtado (18), Miyazaki (34)	Rossini (50)
propane	44.05	3	Yesavage (61)	Rossini (50)
argon	39.95	6	This work	Cp° = 5/2 R
nitrogen	28.01	1	Mage (35)	Hilsenrath (24)
water	18.02	14	Sirota (51,52)	Rossini (50)
carbon dioxide	44.01	6	Rivikin (47)	Rossini (50)
hexafluoroethane	138.01	8	This work	Texas A&M Univ. (54)
benzene	78.06	2	Lenoir (29)	Rossini (50)
cyclohexane	84.16	1	Lenoir (29)	Rossini (50)

*Based on the materials used in the sources.

TABLE V-2

DATA USED IN THE PRESENT CORRELATION

Substance	P (psia)	Pr	T^M(°R)	T^M_r	$\frac{Cp^M-Cp^\circ}{R}$	Source
CH_4	680	1.012	344.2	1.003	450.6	Jones (25)
	800	1.191	354.4	1.033	53.12	Jones (25)
	1000	1.488	369.2	1.076	19.37	Jones (25)
	1200	1.786	380.7	1.109	12.50	Jones (25)
	1500	2.231	394.2	1.149	8.48	Jones (25)
	2000	2.976	414.7	1.208	5.70	Jones (25)
C_2H_6	750	1.059	554.9	1.010	229.6	Miyazaki (34)
	800	1.130	560.4	1.024	105.5	Miyazaki (34)
	820	1.158	563.4	1.025	82.78	Miyazaki (34)
	900	1.271	572.0	1.041	46.33	Miyazaki (34)
	1000	1.412	580.9	1.057	27.69	Furtado (18)
	1250	1.765	602.7	1.096	14.97	Furtado (18)
	1500	2.118	620.9	1.130	11.26	Furtado (18)
	1750	2.471	634.2	1.154	8.90	Furtado (18)
	2000	2.824	655.7	1.200	7.10	Furtado (18)
C_3H_8	700	1.134	678.7	1.020	106.8	Yesavage (61)
	1000	1.620	716.7	1.077	21.32	Yesavage (61)
	1200	1.944	740.7	1.117	14.53	Yesavage (61)
N_2	2000	4.073	287.7	1.269	4.47	Mage (35)
Ar	800	1.134	277.1	1.022	79.06	This work
	950	1.347	285.7	1.054	30.21	This work
	1143	1.620	294.7	1.087	16.30	This work
	1371	1.944	303.7	1.120	10.81	This work
	1714	2.430	315.7	1.165	7.44	This work
	2000	2.835	325.7	1.201	6.03	This work
H_2O	3271	1.019	1168.1	1.003	1111.0	Sirota (51,52)
	3414	1.064	1174.6	1.008	331.0	Sirota (51,52)
	3556	1.108	1181.1	1.014	186.8	Sirota (51,52)
	3911	1.219	1196.9	1.027	88.07	Sirota (51,52)
	4267	1.330	1211.9	1.040	52.77	Sirota (51,52)
	4978	1.551	1239.4	1.064	34.34	Sirota (51,52)
	5689	1.773	1264.6	1.085	24.91	Sirota (51,52)
	6400	1.995	1287.1	1.105	19.82	Sirota (51,52)
	7112	2.216	1307.6	1.122	16.58	Sirota (51,52)
	8534	2.660	1343.1	1.153	12.81	Sirota (51,52)
	9956	3.103	1375.1	1.180	10.58	Sirota (51,52)
	11378	3.543	1399.4	1.201	9.15	Sirota (51,52)
	12801	3.990	1416.9	1.216	8.19	Sirota (51,52)
	14223	4.433	1432.4	1.229	7.44	Sirota (51,52)
CO_2	1280	1.195	561.5	1.026	73.44	Rivikin (47)
	1430	1.334	570.9	1.043	39.62	Rivikin (47)
	1707	1.593	585.9	1.070	22.53	Rivikin (47)
	2145	2.002	605.5	1.106	13.76	Rivikin (47)
	2857	2.667	632.9	1.145	8.95	Rivikin (47)
	3556	3.319	660.9	1.171	6.98	Rivikin (47)
C_2F_6	442	1.011	527.6	1.002	796.0	This work
	490	1.121	534.8	1.015	150.0	This work
	598	1.368	549.3	1.043	44.46	This work
	700	1.602	561.1	1.065	27.16	This work
	839	1.920	576.7	1.095	19.03	This work
	1049	2.400	595.7	1.131	13.27	This work
	1398	3.199	621.7	1.180	9.78	This work
	1969	4.506	660.7	1.266	6.98	This work
C_6H_6	800	1.120	1028.7	1.017	130.00	Lenoir (29)
	1000	1.400	1063.7	1.051	33.39	Lenoir (29)
C_6H_{12}	800	1.360	1048.7	1.053	37.27	Lenoir (29)

TABLE V-3

CRITICAL CONSTANTS FOR THE SUBSTANCES USED IN THIS WORK

Substance	Critical Temperature (°R)	Critical Pressure (psia)	α_c
methane	343.2	672.0	5.86
ethane	549.7	708.2	6.28
propane	665.7	617.4	6.54
argon	271.1*	705.6*	5.76
nitrogen	226.7	491.0	5.98
water	1165.1	3208.6	7.39
carbon dioxide	547.6	1071.3	6.71**
hexafluoroethane	526.8***	437.5***	7.19***
benzene	1011.8	714.4	6.83
cyclohexane	995.8	588.0	6.85

*Grigor and Steele(21)

**Vukalovich and Altunin(55)

***This work

Otherwise, data from Reid and Sherwood(48)

Location of $C_p(T)$ Maxima

Figure V-1 demonstrates a plot of the reduced temperature, $T_r^M = T^M/T_C$, vs reduced pressure, $P_r^M = P^M/P_C$, which includes the values presented in Table V-2. All data points do not fall on a single curve with this particular choice of the coordinates as the points of different gases, as characterized by values of α_C, diverge from each other as illustrated by a set of curves for different values of α_C (6, 6.5 and 7.0). This divergence shows that a two parameter corresponding states principle does not hold satisfactorily for the location of $C_p(T)$ maxima and therefore an extension to at least a three parameter corresponding states principle seems to be necessary.

In this work, using α_C as a third parameter, the following equation is proposed as a correlation for loci of $C_p(T)$ maxima:

$$\ln P_r^M = \alpha_C \left[A\left(1 - \frac{1}{T_r^M}\right) + B \ln T_r^M\right] \qquad \text{(V-1)}$$

where A = 0.3414
B = 0.6586

A and B are determined by the least square fit with equal weight on each data point. In fact, Equation (V-1) is a linear combination of the two previous equations [Equations (II-29) and (II-30)] suggested by Sirota, et al.(51) and Powers,[45] respectively. Figure V-2 demonstrates the correlation of the data on new coordinates, X-Y, where $X = \ln P_r$, $Y = \alpha_C\,[0.3414\,(1 - 1/T_r) + 0.6586 \ln T_r]$. The data points were observed to fall closely on a straight line representing Equation (V-1).

Magnitude of $(C_p^M - C_p^o)$

Figure V-3 shows a plot of $(C_p^M - C_p^o)/R$ vs P_r^M on a log-log scale. The data of the different gases diverge from each other because of the need for a three parameter, rather than a two parameter CSP. It seems that this divergence is somehow related to α_C since the substances with higher α_C values show higher $(C_p^M - C_p^o)/R$ values than those with lower α_C values when compared at the same level of P_r^M. Thus, α_C is introduced

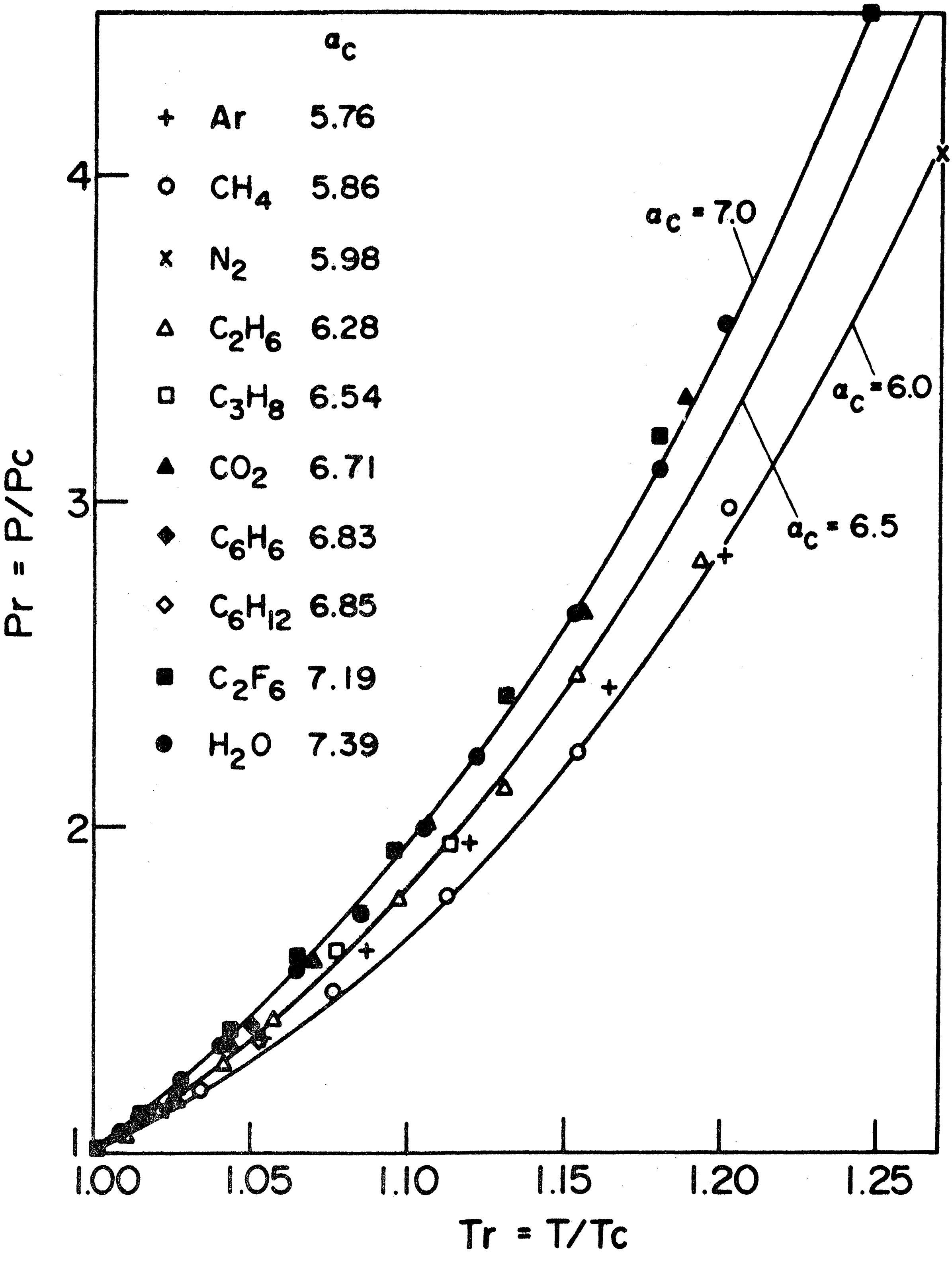

Figure V-1. Plot of Cp(T) maxima locations in Pr-Tr coordinates.

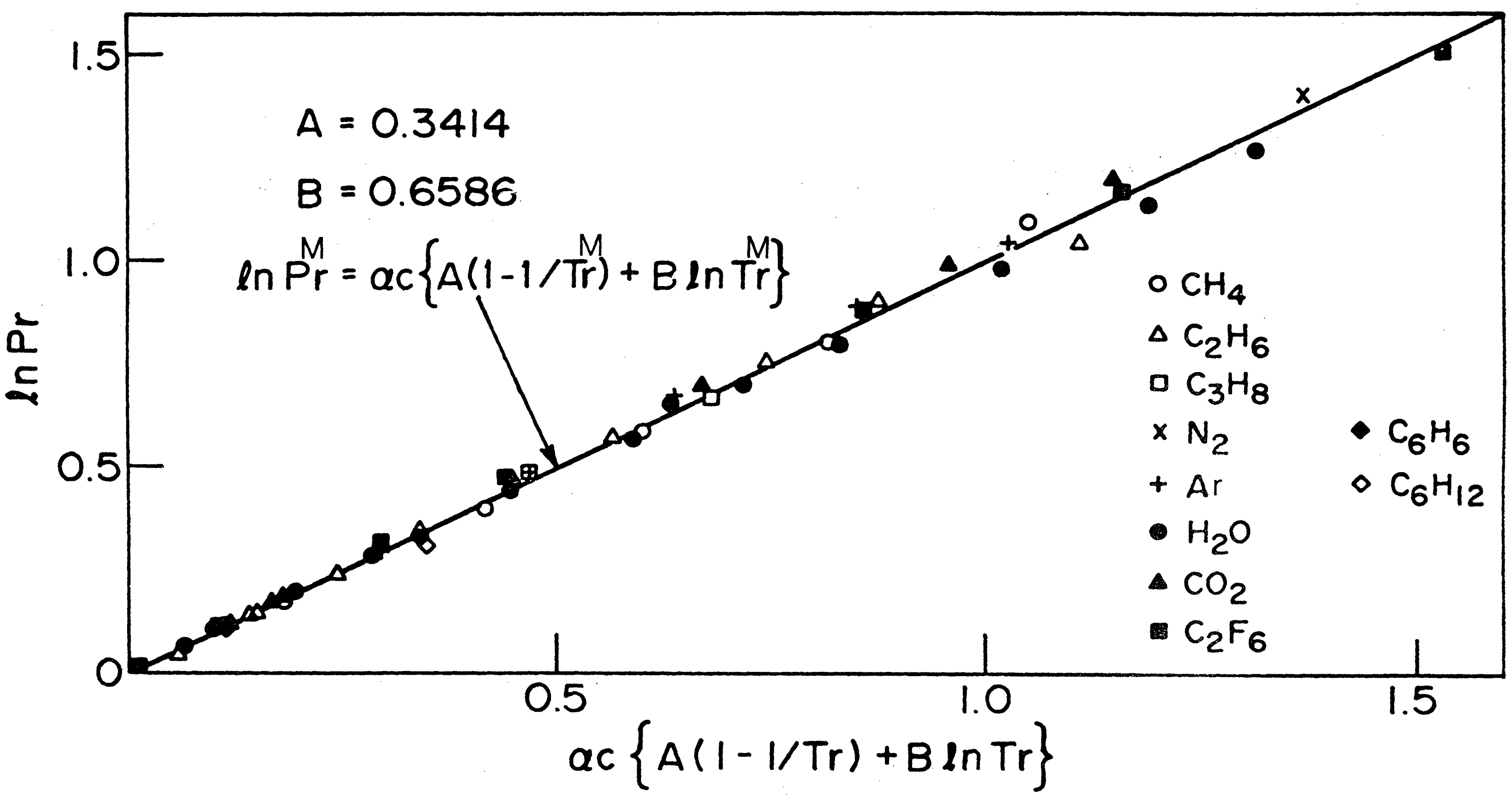

Figure V-2. Plot showing the correlation for the location of Cp(T) maxima.

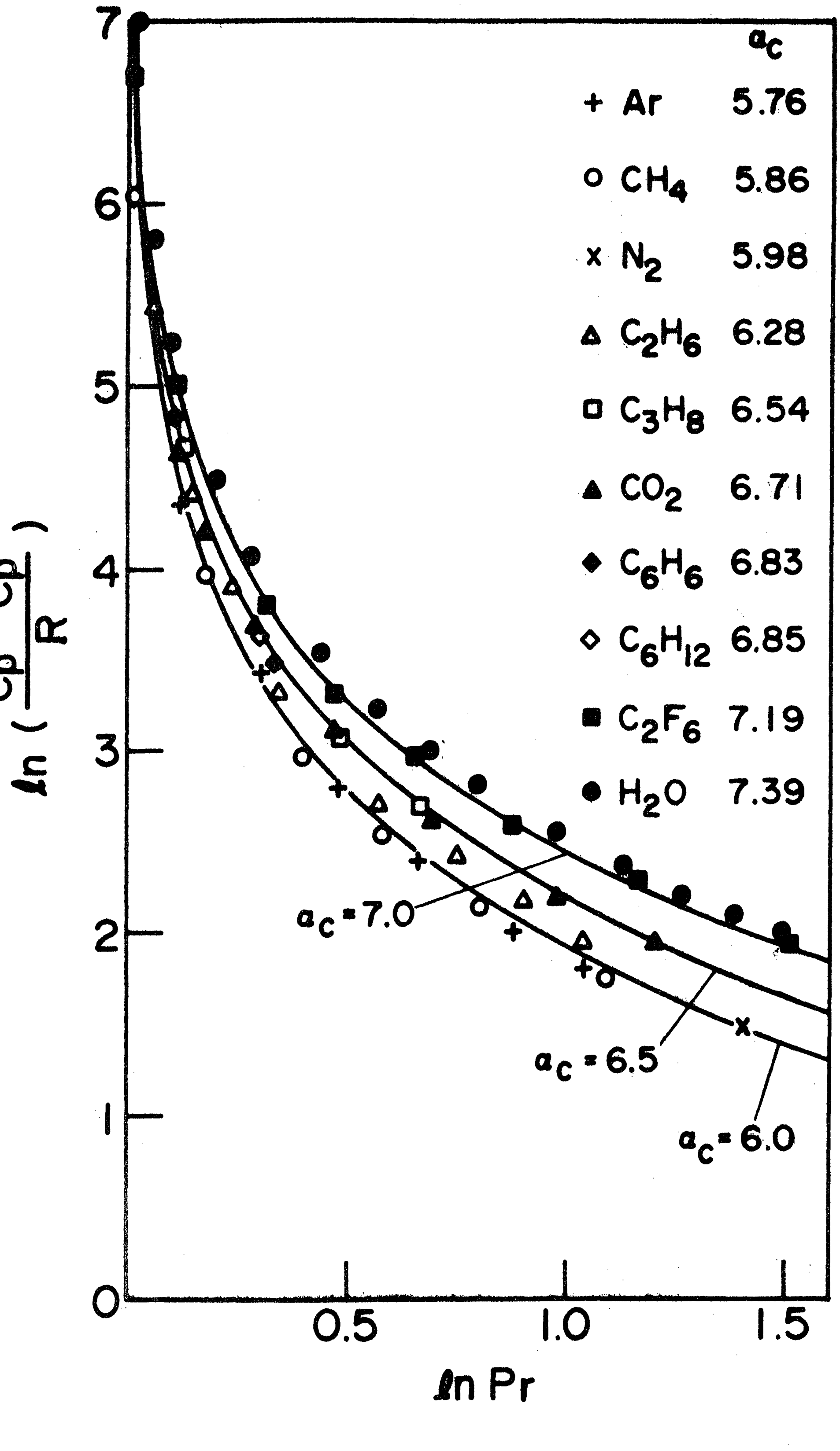

Figure V-3. Plot for the Cp(T) maxima on $\ln Pr - \ln\left(\frac{Cp^M - Cp^\circ}{R}\right)$ coordinates.

as a third parameter in this part of the correlation. The correlational effort is focused on the selection of a proper ordinate which will make the data points fall on a single curve. As the first step $[(\alpha_C/(y + a)]$ was taken, where $y = \ln[(C_p^M - C_p^o)/R]$ and a is an arbitrary constant. The particular choice of the ordinate is intended to make the correlation zero at the origin, which is more convenient than infinity in correlating the data analytically. α_C in the numerator is designed to reduce the discrepancy between the plots of different gases. With a = 1.2 the data plotted in the new coordinates is shown in Figure V-4. Compared to Figure V-3, the new plot shows better correlation of data points especially in the region of high P_r. In the intermediate region for P_r, the data between different gases still are not gathered closely to each other.

To compensate for this discrepancy, the ordinate is modified again by introducing a factor f as

$$Y = \frac{\alpha_C}{y + 1.2} (1 + f) \qquad \text{(V-2)}$$

where $f = \dfrac{(7 - \alpha_C)}{9(1 + 3X^{1.8})}$

The mapping of the data on the final coordinates is presented in Figure V-4. The points are observed to be correlated closely into a single curve (average absolute deviation of the points to the curve is 1.5%) which can be represented as

$$g(X) = ae^{-D/X} + bX + CX^2 + dX^3 \qquad \text{(V-3)}$$

where a, b, c, and d are constants determined by the least square method as below:

a = 0.9106
b = 1.9045
c =-1.2774
d = 0.4239

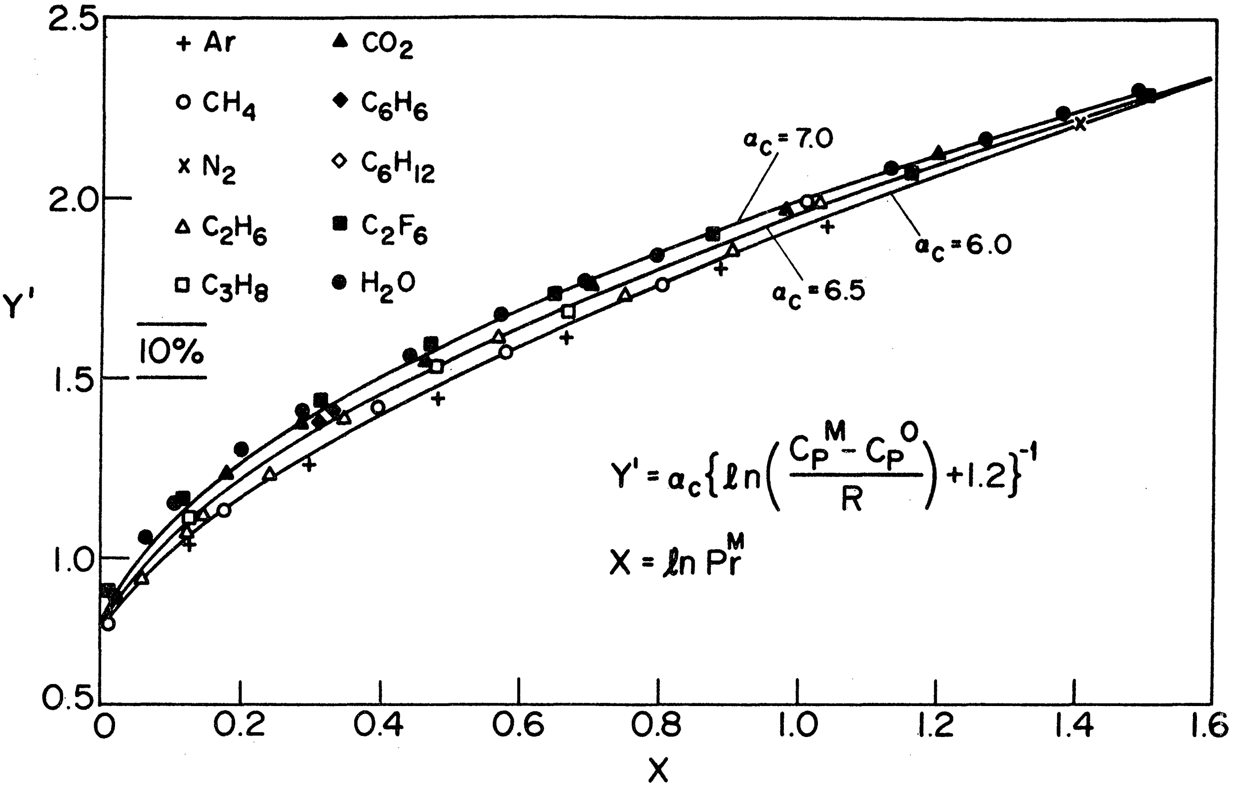

Figure V-4. Plot showing a correlation for the magnitude of Cp(T) maxima on intermediate coordinate.

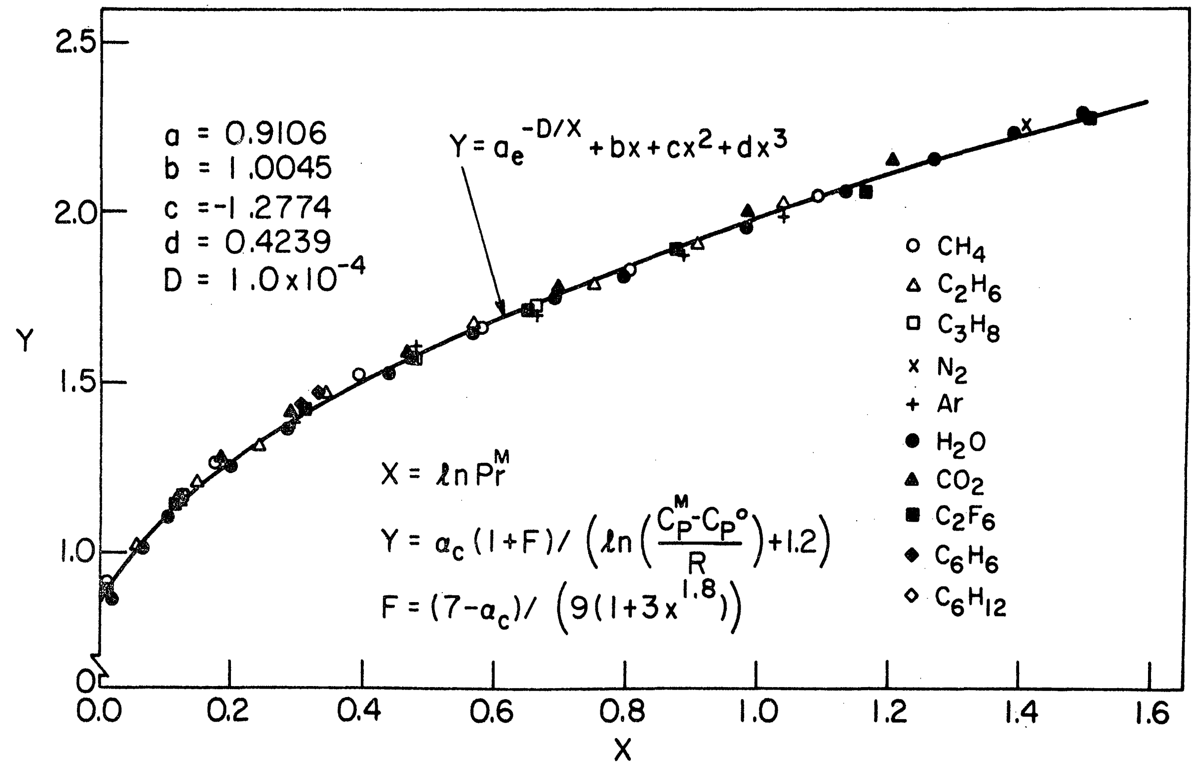

Figure V-5. Plot showing the final correlation for the magnitude of Cp(T) maxima.

The factor, $e^{-D/X}$, in the equation is added so that g(0) = 0. D is chosen as 10^{-4}, an arbitrary small number, which makes the first term essentially the same as a, even for X corresponding to the data nearest to the critical point. The final correlation, therefore, can be expressed as

$$\ln\left(\frac{C_P^M - C_P^o}{R}\right) = \frac{\alpha_C}{g(X)}\left[1 + \frac{7 - \alpha_C}{9(1 + 3X^{1.8})}\right] -1.2 \qquad \text{(V-4)}$$

where $X = \ln P_r^M$

$g(X)$ = a function given by Equation (V-3)

Discussion of Results

In order to evaluate the performance of Equation (V-1) values of T^M were calculated for given pressures and compared with experimental values. They are presented in Table V-4. The average absolute deviation, in terms of temperature difference, is 2°R and in terms of % deviation is 0.3. It is to be noted from the table that in most cases the deviations were within the range of errors associated with experimental T^M values. Those error ranges were estimated from the original experimental C_p data from which the maxima were determined. Usually larger errors were observed in the determination of T^M's at higher reduced pressures where the $C_p(T)$ curves showed broad maxima. Included in Table V-4 are the values of T^M calculated using Equations (II-29) and (II-30). The mean and standard deviations for each set of calculated values from the experimental ones are presented in Table V-5 for comparison. This comparison confirms that Equation (V-1) correlates the data better than the other equations.

TABLE V-4

COMPARISON OF THE DATA WITH VALUES DETERMINED FROM THE CORRELATION

Substance	Pressure (psia)	T^M_{exp} (°R)	$T^M_{cal(1)}$ **		$T^M_{cal(2)}$ ***		$T^M_{cal(3)}$ ****		$\left(\frac{Cp^M-Cp^\circ}{R}\right)_{exp}$	$\left(\frac{Cp^M-Cp^\circ}{R}\right)_{cal}$	
CH_4	680	344.2 ± 0.5	343.9	(-0.3)*	343.9	(-0.3)*	343.9	(-0.3)*	450.6 ± 22.5	467.3	(16.7)*
	800	354.4 ± 0.7	353.6	(-0.8)	353.7	(-0.7)	353.6	(-0.8)	53.12 ± 1.59	56.99	(3.87)
	1000	369.2 ± 1.5	367.3	(-1.9)	368.2	(-1.0)	367.6	(-1.6)	19.37 ± 0.19	19.43	(0.07)
	1200	380.7 ± 1.5	378.9	(-2.8)	380.9	(0.2)	379.5	(-1.2)	12.50 ± 0.09	12.47	(-0.03)
	1500	394.2 ± 1.5	393.6	(-0.6)	395.7	(-1.5)	394.9	(0.7)	8.48 ± 0.04	8.56	(0.08)
	2000	414.7 ± 3.0	413.4	(0.7)	421.7	(9.0)	415.9	(3.2)	5.70 ± 0.03	5.75	(0.05)
C_2H_6	1000	580.9 ± 0.5	580.7	(-0.2)	581.7	(7.8)	581.1	(1.2)	229.6 ± 4.6	239.6	(10.0)
	1250	602.7 ± 0.5	601.8	(-1.0)	604.4	(1.7)	602.6	(-0.1)	105.5 ± 1.6	107.1	(1.6)
	1500	620.9 ± 1.0	619.5	(-1.4)	624.3	(3.4)	621.0	(0.1)	82.78 ± 0.83	84.84	(2.06)
	1750	634.2 ± 1.0	634.9	(0.7)	642.2	(8.0)	637.2	(3.0)	46.33 ± 0.37	44.22	(-2.11)
	2000	655.7 ± 2.0	648.5	(-7.2)	658.6	(2.9)	651.6	(-4.2)	27.69 ± 0.14	27.56	(-0.13)
	750	554.9 ± 0.4	554.7	(-0.2)	554.8	(-0.1)	554.8	(-0.1)	14.97 ± 0.07	15.34	(0.37)
	800	560.4 ± 0.5	560.5	(0.1)	560.6	(0.2)	560.5	(0.1)	11.26 ± 0.05	11.18	(-0.08)
	820	563.4 ± 0.5	562.7	(-0.7)	562.8	(-0.6)	562.8	(-0.6)	8.90 ± 0.04	8.87	(-0.03)
	900	572.0 ± 0.8	571.1	(-0.9)	571.5	(-0.5)	571.2	(-0.8)	7.10 ± 0.03	7.37	(0.27)
C_3H_8	700	678.7 ± 1.5	678.6	(-0.1)	678.7	(0.0)	678.7	(0.0)	106.8 ± 2.1	112.6	(5.8)
	1000	716.7 ± 3.0	716.6	(-0.1)	718.7	(2.0)	717.3	(0.7)	21.32 ± 0.11	20.49	(-0.83)
	1200	740.7 ± 5.0	736.9	(-3.8)	741.0	(0.3)	738.3	(-2.5)	14.53 ± 0.07	14.36	(-0.17)
N_2	2000	287.7 ± 8.0	286.7	(-1.0)	296.3	(8.6)	289.4	(1.7)	4.47 ± 0.02	4.49	(0.02)
Ar	800	277.1 ± 0.2	277.1	(0.0)	277.2	(0.1)	277.1	(0.0)	79.06 ± 0.32	83.09	(4.03)
	1143	294.7 ± 0.2	294.8	(0.1)	295.9	(1.2)	295.1	(0.4)	30.21 ± 0.09	28.83	(1.38)
	1371	303.7 ± 0.5	304.3	(0.6)	306.5	(2.8)	305.0	(1.3)	16.30 ± 0.06	14.73	(-1.57)
	1714	315.7 ± 0.8	316.3	(0.6)	320.5	(4.8)	317.6	(1.9)	10.81 ± 0.03	10.20	(-0.61)
	2000	325.7 ± 1.0	324.9	(-0.8)	331.0	(5.3)	326.7	(1.0)	7.44 ± 0.02	7.21	(-0.23)
	950	285.7 ± 0.2	285.5	(-0.2)	285.9	(0.2)	285.6	(-0.1)	6.03 ± 0.02	5.85	(-0.18)
H_2O	3271	1168.1 ± 0.1	1168.2	(0.1)	1168.2	(0.1)	1168.3	(0.2)	1111.0 ± 44.4	992.2	(-118.8)
	3414	1174.6 ± 0.4	1174.9	(0.3)	1175.0	(0.4)	1175.0	(0.4)	331.0 ± 6.6	300.0	(-31.0)
	3556	1181.1 ± 0.5	1181.5	(0.4)	1181.6	(0.5)	1181.6	(0.5)	186.8 ± 0.9	176.7	(-10.1)
	3911	1196.9 ± 1.0	1196.8	(-0.1)	1197.2	(0.3)	1196.9	(0.0)	88.07 ± 0.44	78.12	(-9.95)
	4267	1211.9 ± 1.4	1211.0	(-0.9)	1211.9	(0.0)	1211.4	(-0.5)	52.77 ± 0.16	49.68	(-3.09)
	4978	1239.4 ± 1.8	1236.5	(-2.9)	1238.8	(-0.6)	1237.2	(-2.2)	34.34 ± 0.03	30.67	(-3.67)
	5689	1264.6 ± 2.5	1259.0	(-5.6)	1263.0	(-1.6)	1260.4	(-4.2)	24.91 ± 0.02	23.41	(-1.50)
	6400	1287.1 ± 2.0	1279.3	(-7.8)	1285.2	(-1.9)	1281.3	(-5.8)	19.82 ± 0.02	19.31	(-0.51)
	7112	1307.6 ± 2.7	1297.6	(-10.0)	1305.8	(-1.8)	1300.3	(-7.3)	16.58 ± 0.02	16.48	(-0.10)
	8534	1343.1 ± 3.0	1330.0	(-13.1)	1342.9	(-0.2)	1334.1	(-9.0)	12.81 ± 0.01	12.65	(-0.16)
	9956	1375.1 ± 3.5	1358.1	(-17.0)	1376.0	(-0.9)	1363.6	(-11.6)	10.58 ± 0.01	10.27	(-0.31)
	11378	1399.4 ± 3.5	1382.8	(-16.6)	1406.0	(6.58)	1389.9	(-9.5)	9.15 ± 0.01	8.81	(-0.34)
	12801	1416.9 ± 5.0	1405.1	(-11.84)	1433.6	(16.7)	1413.5	(-3.4)	8.19 ± 0.01	7.95	(-0.24)
	14223	1432.4 ± 4.0	1425.2	(-7.2)	1459.1	(26.8)	1435.2	(2.8)	7.44 ± 0.01	7.55	(0.11)
CO_2	1280	561.5 ± 0.2	562.3	(0.8)	562.5	(1.0)	562.4	(0.9)	73.44 ± 2.93	75.72	(2.28)
	1430	570.9 ± 0.2	571.6	(0.7)	572.2	(1.3)	571.8	(0.9)	39.62 ± 1.19	40.37	(0.75)
	1707	585.9 ± 0.4	586.9	(1.0)	588.4	(2.5)	587.4	(1.5)	22.53 ± 0.45	22.76	(0.23)
	2145	605.5 ± 0.5	607.3	(1.8)	610.8	(5.3)	608.4	(2.9)	13.76 ± 0.21	14.68	(0.92)
	2857	632.9 ± 2.0	633.7	(0.9)	641.3	(8.4)	636.1	(3.2)	8.95 ± 0.09	9.55	(0.60)
	3556	660.9 ± 2.0	654.8	(-6.1)	666.8	(5.87)	658.4	(-2.5)	6.98 ± 0.07	7.22	(0.24)
C_2F_6	442	527.6 ± 0.1	527.5	(-0.1)	527.6	(0.0)	527.6	(0.0)	796.0 ± 15.9	804.9	(8.9)
	490	534.8 ± 0.1	535.2	(0.4)	535.2	(0.4)	535.2	(0.4)	150.0 ± 0.8	151.5	(1.5)
	598	549.3 ± 0.2	550.3	(1.0)	550.9	(1.6)	550.6	(1.3)	44.46 ± 0.09	41.99	(-2.47)
	700	561.1 ± 0.3	562.4	(1.3)	563.6	(2.5)	562.8	(1.7)	27.16 ± 0.05	26.75	(-0.41)
	839	576.7 ± 0.5	576.8	(0.1)	579.4	(2.7)	577.7	(1.0)	19.03 ± 0.04	19.02	(-0.01)
	1049	595.7 ± 1.0	595.0	(-0.7)	599.8	(4.1)	596.5	(0.8)	13.27 ± 0.03	13.54	(0.27)
	1398	621.7 ± 1.5	619.2	(-2.5)	628.4	(6.7)	622.0	(0.3)	9.78 ± 0.02	9.14	(-0.64)
	1969	660.7 ± 2.0	649.4	(-11.3)	666.2	(5.5)	654.3	(-6.4)	6.98 ± 0.01	6.97	(-0.01)
C_6H_6	800	1028.7 ± 5.0	1028.7	(0.0)	1028.8	(0.1)	1028.8	(0.1)	130.0 ± 19.5	139.29	(9.29)
	1000	1063.7 ± 8.0	1062.8	(-0.9)	1064.2	(0.5)	1063.4	(-0.3)	33.39 ± 1.67	34.64	(1.25)
C_6H_{12}	800	1048.7 ± 15.0	1041.5	(-7.2)	1042.6	(-6.1)	1042.0	(-6.7)	37.27 ± 1.86	38.93	(1.66)

*Number in parentheses represents (calc. value - exp. value).

**Calculations from $\ln P^M_r = \alpha_c \ln T^M_r$.

***Calculations from $\ln P^M_r = \alpha_c \left(1 - \frac{1}{T^M_r}\right)$.

****Calculations from $\ln P^M_r = \alpha_c \left\{0.3414 \left(1 - \frac{1}{T^M_r}\right) + 0.6586 \ln T^M_r\right\}$.

TABLE V-5

Mean and Standard Deviations of $(T^M_{exp} - T^M_{calc})$

	Present Correlation	Eq. II-29	Eq. II-30
Mean Deviation (°R)	-0.5	-2.2	+3.0
Standard Deviation (°R)	3.0	5.0	5.5

To examine the performance of Equation (V-4) $(C_p{}^M - C_p{}^o)/R$ values were calculated from the equation for given pressures and compared with the experimental ones (Table V-4). The errors associated with the experimental values, as presented in the table, have been estimated from the original data for $C_p(T)$ plots from which the maxima was determined. Generally, larger errors were observed in the determination of $C_p{}^M$ values at the pressures close to the critical values where the $C_p(T)$ curves exhibit steep maxima. This was in contrast to the case of T^M, in which T^M was less susceptible to error in this region since the peak locations, on the other hand, are more clearly defined at the sharp peaks than at the smooth ones shown in the higher pressure region. Consequently, higher deviations of the calculated values from the experimental ones were observed in the region near the critical point. The mean and standard deviations of the calculated values from the experimental ones were 1.5% and 5.0% respectively. The relatively high standard deviation probably resulted from the uncertainty of the data especially in the critical region, not from the lack of the fittability of the present correlation. Considering the present correlation includes substances which have widely different α_c values, and notably a polar substance as H_2O, it is felt that the results were satisfactory.

VI - SUMMARY AND CONCLUSIONS

1. Calorimetric data for argon were obtained from the isobaric, isothermal and isenthalpic measurements using the recycle flow system originally designed by Faulkner.[19] The measurements covered the liquid, two-phase, and gaseous regions at temperatures from -240°F to 220°F and at pressures from 286 to 2000 psia. Particular emphasis was placed on the measurements of C_p and $C_p(T)$ maxima in the supercritical region. These data were interpreted to yield C_p, ϕ and μ and further processed to yield enthalpy values. Enthalpy diagrams and tables were prepared. Thermodynamic consistency checks showed that the data were self-consistent to ±0.09%. The accuracy of the isobaric and isothermal data was believed to be 0.2% and 0.4% respectively.

2. Calorimetric data for Freon-116 (C_2F_6) were obtained from the experimental measurements of isobaric and isothermal changes on enthalpy using the new recycle flow system designed by Miyazaki.[34] The measurements covered the liquid, two-phase, and gaseous regions at temperatures from 0°F to 247°F and at pressures between 247 and 1969 psia. Particular emphasis was placed on the measurements of isobaric latent heats of vaporization near the critical point to determine the critical pressure and temperature and C_p and $C_p(T)$ maxima in the supercritical region. Thermodynamic consistency checks showed that the data were self-consistent to ±0.03%. The accuracy of the isobaric and isothermal data was believed to be 0.05% and 0.1%, respectively.

3. From the $C_p(T)$ maxima data obtained from this research together with the ones available from the literature a generalized correlation for the $C_p(T)$ maxima was developed within the framework of the corresponding states principle. The correlation was divided into the two parts: (1) the correlation for the location of the maxima and (2) the correlation for the magnitude of the maxima. The correlation was found to predict the locations and magnitudes of maxima within ±2°F and ±5% errors, respectively.

VII - RECOMMENDATIONS FOR FUTURE WORK

1. As soon as the calorimetric investigation was finished, the old recycle system of the thermal properties of Fluids Laboratory had ceased to operate. At the time of preparing this thesis, it had been dismantled to clear the site for another research activity. There are, however, many fine instruments which can still be used in the new system as replacements wherever and whenever needed. Among them are KEPCO D.C. power supplies, bath controllers (used for the calorimeter and heat exchanger baths) and the pressure transducers. There are many miscellaneous items which should be useful in the future. Therefore, all of these should be reserved.

2. Some suggestions as to the improvements of the new recycle-flow system are in order:

(a) Mass leaks were frequently observed through the gland packing of the metering pump cylinders when the pump cylinders were cooled down at the start-up of the system. Those leaks, which were caused by insufficient temperature compensation of the packings, were arrested by tightening the bolts of the packing rods. However, once the measurements were finished and the pump bath was allowed to warm up (as was the case with the present work) the cylinders could be subjected to more than normal strain due to the thermal expansion. This could be harmful to the precision pumps in the long run. Therefore, some measure should be taken to maintain the pump bath at a constant temperature on a 24 hour basis. This could possibly be done by installing a refrigeration unit which could be operated at relatively low costs.

(b) It would be desirable to have a valve on the line before the calorimeter so the calorimeter could be isolated from the pump bath when it is necessary to repair or replace some parts of the calorimeter.

(c) Replacing the Heise gage on the helium line with the one which could read the pressure of at least 2000 psig is recommended. The present gage reads only to 1000 psig.

3. The present mechanism of lifting and lowering the pump bath should be improved. Installation of a motorized gear or a hydraulic lifter would be desirable if possible.

4. Prediction of location and magnitude of $C_p(T)$ maxima, which has been accomplished through the correlation of the data could be of value in establishing a new generalized correlation of C_p data in the maxima region. It is recommended that an effort be extended to correlate the existing C_p data which have been obtained from calorimetric measurements.

APPENDIX A

CALIBRATION DATA

TABLE A-1

CALIBRATION CONSTANTS FOR PLATINUM RESISTANCE THERMOMETER

α = 3.9261045×10^{-3}
δ = 1.4916703
β = 0.1101088
R_o = 25.5548

where

$$t = \frac{1}{\alpha}\left(\frac{R_t}{R_o} - 1\right) + \delta\left(\frac{t}{100} - 1\right)\frac{t}{100} + \beta\left(\frac{t}{100} - 1\right)\left(\frac{t}{100}\right)^3$$

t = temperature, °C
R_t = resistance of the thermometer at t°C
R_o = resistance of the thermometer at 0°C

TABLE A-2

CALIBRATION DATA FOR THERMOPILES

Temperature (°C)	6 Junctions		Temperature (°C)	15 Junctions,
	TP-A	TP-B		TP-C
-196.	-33338	-33327	-182.85	- 79856
-183.	-31996	-31986	-110.	- 54995
-100.	-20342	-20332	0.	0
- 80.	-16781	-16779	50.	30800
- 60.	-12956	-12955	100.	64665
- 40.	- 8880	- 8876	148.89	100316
- 20.	- 4555	- 4554		
0.	0	0		
20.	4775	4776		
40.	9762	9762		
60.	14950	14945		
80.	20328	20322		
100.	25878	25875		
120.	31607	31602		
140.	37494	37491		
160.	43543	43536		

Note: Reference junctions at 0.°C. EMF is in μV.

Calibrations are fitted to the equation

$$E = At + Bt^2 + Ct^3 + Dt^4$$

where E = EMF, μV

t = temperature, °C

The constants are

	A	B	C x 10^3	D x 10^7
TP-A	233.34	0.27630	-0.22327	0.71210
TP-B	233.29	0.27643	-0.22306	0.68403
TP-C	583.08	0.69165	-0.57190	1.27582

TABLE A-3

PRESSURE TRANSDUCER (HIGH) CALIBRATIONS

X (psig)	Y_{EXP} (μv)	Y_{CAL} (μv)	X (psig)	Y_{EXP} (μv)	Y_{CAL} (μv)	X (psig)	Y_{EXP} (μv)	Y_{CAL} (μv)
1987.4	2387.94	2388.45	1986.1	2387.48	2386.88	1983.8	2383.72	2384.12
1789.7	2150.66	2150.91	1789.0	2149.77	2150.07	1786.9	2147.83	2147.55
1590.7	1911.49	1911.82	1590.9	1911.54	1912.06	1587.4	1908.47	1907.86
1390.0	1670.41	1670.67	1392.6	1673.31	1673.80	1386.0	1665.99	1665.87
1190.7	1431.43	1431.21	1251.1	1503.52	1503.82	1184.7	1423.64	1424.00
988.8	1188.17	1188.62	1081.2	1299.37	1299.70	988.7	1188.46	1188.50
789.3	948.57	948.93	904.1	1087.12	1086.92	784.4	942.89	943.03
595.6	716.40	716.21	719.6	865.56	865.26	588.9	708.19	708.17
417.9	502.55	502.74	560.4	674.01	673.90			
			405.3	487.51	487.60			

$$Y_{CAL} = A + BX + CX^2 + DX^3$$

$A = 0.7360$ $\qquad B = 1.2012$

$C = 2.830 \times 10^{-7}$ $\qquad D = -6.810 \times 10^{-11}$

$$\left| \frac{Y_{EXP} - Y_{CAL}}{Y_{EXP}} \right|_{\text{average}} = 0.02\%$$

TABLE A-4

PRESSURE TRANSDUCER (LOW) CALIBRATIONS

X (psig)	Y_{EXP} (μv)	Y_{CAL} (μv)	X (psig)	X_{EXP} (μv)	Y_{CAL} (μv)	X (psig)	Y_{EXP} (μv)	Y_{CAL} (μv)
1988.0	2421.04	2421.14	1986.7	2420.28	2419.57	1982.9	2414.71	2415.08
1790.5	2185.46	2185.44	1789.3	2183.67	2184.03	1786.5	2180.73	2180.70
1593.6	1949.49	1949.86	1592.7	1948.14	1948.86	1587.5	1942.67	1942.64
1389.4	1705.11	1705.25	1392.8	1708.51	1709.26	1385.5	1700.99	1700.58
1191.6	1467.62	1467.86	1250.9	1538.52	1539.08	1183.8	1458.34	1458.50
989.5	1224.47	1225.18	1082.1	1336.06	1336.37	988.3	1223.36	1223.76
789.5	984.77	985.10	906.1	1125.01	1125.08	782.9	977.09	977.14
595.7	751.99	752.36	719.8	901.83	901.34	589.2	744.59	744.62
418.0	539.41	539.24	557.9	706.89	707.05			
			404.3	523.11	522.89			

$$Y_{CAL} = A + BX + CX^2 + DX^3$$

$A = 39.004$ $\qquad$ $B = 1.1942$

$C = 7.236 \times 10^{-6}$ $\qquad$ $D = -2.6122 \times 10^{-9}$

$$\left| \frac{Y_{EXP} - Y_{CAL}}{Y_{EXP}} \right|_{\text{average}} \doteq 0.025\%$$

TABLE A-5

FLOW METER CALIBRATIONS

X	Y	Y_{CAL}	X	Y	Y_{CAL}	X	Y	Y_{CAL}
0.2259	0.11039	0.11008	0.3279	0.11156	0.11169	0.1737	0.10952	0.10927
0.2269	0.11008	0.11009	0.3292	0.11223	0.11171	0.1830	0.10904	0.10941
0.4332	0.11318	0.11340	0.5580	0.11547	0.11547	0.2983	0.11108	0.11122
0.4341	0.11317	0.11342	0.5582	0.11533	0.11547	0.3011	0.11108	0.11126
0.6272	0.11673	0.11662	0.7450	0.11876	0.11860	1.0197	0.12329	0.12319
0.6281	0.11667	0.11664	0.7446	0.11898	0.11860	1.0219	0.12300	0.12323
0.7226	0.11835	0.11823	0.9323	0.12174	0.12175	1.2336	0.12678	0.12664
0.7573	0.11857	0.11881	0.9368	0.12183	0.12182	1.2344	0.12656	0.12665
0.8588	0.12045	0.12052	1.1367	0.12499	0.12510	1.4494	0.12993	0.12990

$X = (F/\mu) \times 10^3$: (lb/min)(μpoise)

$Y = (\rho\Delta P)/(F\mu)$: $(\text{lb/ft}^3)(\text{in. } H_2O)/(\text{lb/min})/(\mu\text{poise})$

$$Y_{CAL} = A + BX + CX^2 + DX^3$$

$A = 0.10670$ $B = 14.2716$ $C = 3466.40$ $D = -1.56576 \times 10^6$

$$\left| \frac{Y - Y_{CAL}}{Y} \right|_{\text{average}} = 0.14\%$$

TABLE A-6

DENSITY DATA OF C_2F_6 AT 0.°F

X (psia)	Y (g/cc)	Y_{CAL} (g/cc)
165.9	1.25905	1.25931
492.8	1.32165	1.32056
676.3	1.34120	1.34178
932.3	1.36010	1.36105
1243.3	1.37779	1.37671
1506.3	1.39091	1.39127
1980.3	1.42060	1.41991

$$Y_{CAL} = A + BX + CX^2 + DX^3$$

$A = 1.21322$

$B = 3.13492 \times 10^{-4}$

$C = -22.5504 \times 10^{-8}$

$D = 63.6379 \times 10^{-12}$

$$\left|\frac{Y - Y_{CAL}}{Y}\right|_{\text{average}} = 0.05\%$$

APPENDIX B

EXPERIMENTAL DATA

TABLE B-1

BASIC ISOBARIC DATA FOR ARGON

Run No.	Inlet Press. (psia)	Inlet Temp. (°F)	Outlet Temp. (°F)	Power (Btu/min)	Flow (lb/min)	Corr. (Btu/lb)	$\Delta \underline{H}p$ (Btu/lb)	$\left(\frac{\Delta \underline{H}}{\Delta T}\right)_p$ (Btu/lb-°F)
10.02	288.8	-50.34	-4.65	1.455	0.23485	-0.006	6.189	0.1355
10.03	289.3	-50.32	30.23	2.530	0.23414	-0.005	10.799	0.1341
10.04	289.1	-50.35	73.26	3.843	0.23372	-0.004	16.438	0.1330
10.05	289.5	-50.46	100.46	4.660	0.23336	-0.004	19.965	0.1323
10.06	288.7	-50.43	110.16	4.945	0.23278	-0.003	21.241	0.1323
10.07	288.5	-50.51	119.93	5.240	0.23275	-0.003	22.512	0.1321
22.02	286.0	-240.00	-230.06	0.852	0.25411	0.0	3.351	0.3371
22.03	286.0	-240.00	-226.73	1.690	0.25285	-0.0	6.684	0.5037
22.04	285.5	-240.00	-229.24	0.922	0.25350	-0.0	3.637	0.3380
22.05	286.3	-240.00	-227.51	1.088	0.25408	-0.0	4.282	0.3428
22.06	285.6	-240.00	-226.75	1.262	0.25275	-0.0	4.994	0.3769
22.07	286.0	-240.00	-226.75	7.475	0.15028	-0.001	49.739	3.7539
22.08	285.6	-240.00	-226.72	7.129	0.15003	-0.175	47.341	3.5648
22.09	286.1	-240.00	-225.14	7.928	0.15060	-0.016	52.630	3.5417
22.10	286.3	-240.00	-223.91	7.982	0.15071	-0.016	52.948	3.2907
22.11	286.2	-240.00	-220.71	8.105	0.15070	-0.019	53.766	2.7873
38.01	285.9	-200.29	-189.87	0.426	0.21998	-0.007	1.931	0.1853
38.02	285.5	-200.29	-169.48	1.198	0.21970	-0.006	5.447	0.1768
38.03	285.3	-200.30	-146.36	1.988	0.21919	-0.006	9.062	0.1680
38.04	285.5	-200.30	-121.14	2.816	0.21922	-0.005	12.841	0.1622
38.05	285.3	-200.29	-93.61	3.692	0.21904	-0.005	16.850	0.1579
39.01	285.3	-100.53	-80.23	0.560	0.19502	-0.004	2.867	0.1412
39.02	285.7	-100.48	-50.42	1.368	0.19584	-0.004	6.980	0.1394
39.03	285.7	-100.49	-20.76	2.155	0.19568	-0.004	11.007	0.1380
39.04	285.6	-100.46	9.37	2.942	0.19562	-0.003	15.037	0.1369
39.05	285.5	-100.49	33.78	3.573	0.19548	-0.003	18.274	0.1361
39.06	285.3	-100.55	50.58	4.009	0.19567	-0.003	20.484	0.1355
44.02	285.5	70.26	99.50	0.931	0.24443	-0.004	3.804	0.1301
44.03	285.9	70.26	125.68	1.761	0.24490	-0.004	7.186	0.1297
44.04	285.5	70.28	149.46	2.510	0.24490	-0.004	10.244	0.1294
46.01	285.5	99.95	170.73	2.018	0.22139	-0.003	9.114	0.1288
46.02	285.7	99.75	190.13	2.576	0.22159	-0.003	11.624	0.1286
46.03	285.1	99.71	218.28	3.369	0.22111	-0.003	15.233	0.1285
23.01	457.2	-240.09	-229.98	0.614	0.18831	-0.0	3.263	0.3228
23.02	457.3	-240.08	-215.03	1.676	0.18843	-0.0	8.896	0.3551
23.03	457.3	-240.08	-210.65	2.045	0.18845	-0.001	10.851	0.3687
23.04	456.9	-240.09	-209.52	2.147	0.18828	-0.001	11.402	0.3730
23.05	457.3	-240.08	-208.35	2.261	0.18855	-0.003	11.987	0.3778
23.06	457.1	-240.08	-207.87	2.348	0.18831	-0.001	12.468	0.3871
23.07	457.3	-240.11	-207.99	2.487	0.18860	-0.001	13.188	0.4106
23.08	457.5	-240.00	-207.97	6.954	0.18969	-0.003	36.659	1.1445
23.09	457.3	-240.00	-207.96	8.192	0.18790	-0.004	43.594	1.3606
24.01	457.3	-240.00	-205.25	9.006	0.17849	-0.390	50.069	1.4408
24.02	457.5	-240.00	-206.64	8.879	0.17837	-0.386	49.390	1.4805
25.01	457.4	-240.00	-205.53	7.184	0.14409	-0.013	49.847	1.4461
25.02	456.9	-240.00	-207.97	6.922	0.14391	-0.012	48.088	1.5013
25.03	457.0	-240.00	-204.25	7.277	0.14390	-0.014	50.558	1.4142
25.05	457.2	-240.00	-201.00	7.432	0.14404	-0.013	51.583	1.3226

TABLE B-1 (Continued)

Run No.	Inlet Press. (psia)	Inlet Temp. (°F)	Outlet Temp. (°F)	Power (Btu/min)	Flow (lb/min)	Corr. (Btu/lb)	ΔHp (Btu/lb)	$\left(\frac{\Delta H}{\Delta T}\right)_p$ (Btu/lb-°F)
29.01	455.9	-149.84	-140.31	0.361	0.20817	-0.013	1.719	0.1804
29.02	454.9	-149.86	-114.05	1.276	0.20781	-0.012	6.130	0.1712
29.03	457.5	-149.89	-89.82	2.132	0.21493	-0.011	9.910	0.1650
29.04	457.7	-149.85	-63.46	2.982	0.21487	-0.008	13.870	0.1605
29.05	457.1	-149.86	-52.75	3.321	0.21482	-0.006	15.453	0.1591
26.01	571.6	-240.00	-229.91	0.620	0.19449	-0.0	3.188	0.3160
26.02	571.3	-239.96	-209.97	2.060	0.19433	-0.001	10.601	0.3535
26.03	572.2	-239.93	-201.49	2.901	0.19467	-0.001	14.902	0.3877
26.04	571.7	-239.82	-200.19	3.054	0.19444	-0.002	15.707	0.3963
26.05	571.3	-239.89	-198.87	3.242	0.19425	-0.003	16.689	0.4068
26.06	571.4	-240.01	-198.23	3.511	0.19442	-0.002	18.055	0.4321
27.01	571.6	-240.00	-196.56	8.101	0.17461	-0.034	46.358	1.0672
27.02	571.4	-240.00	-197.97	7.909	0.17478	-0.005	45.244	1.0765
27.03	571.4	-240.00	-197.99	7.731	0.17474	-0.005	44.236	1.0530
27.04	571.3	-240.00	-195.74	8.216	0.17463	-0.031	47.014	1.0622
27.05	571.5	-240.00	-194.10	8.385	0.17463	-0.025	47.991	1.0456
27.06	571.1	-240.00	-196.01	8.167	0.17460	-0.038	46.738	1.0625
30.01	571.3	-149.97	-140.23	0.426	0.21258	-0.010	1.993	0.2047
30.02	570.9	-149.92	-112.83	1.502	0.21234	-0.009	7.063	0.1904
30.03	572.1	-149.94	-89.92	2.331	0.21283	-0.008	10.946	0.1824
30.04	571.5	-149.89	-64.22	3.192	0.21292	-0.007	14.986	0.1749
30.05	571.5	-149.90	-53.89	3.709	0.22416	-0.006	16.542	0.1723
21.01	706.2	-239.90	-229.87	0.676	0.21529	-0.0	3.138	0.3129
21.02	707.2	-239.89	-207.46	2.416	0.21547	-0.0	11.213	0.3458
21.03	707.6	-239.89	-188.83	5.380	0.21530	-0.024	24.963	0.4889
21.04	707.4	-239.90	-188.57	5.718	0.21482	-0.043	26.574	0.5177
21.05	708.5	-239.95	-195.70	3.706	0.21564	-0.002	17.184	0.3883
21.06	709.0	-239.86	-187.19	8.951	0.21576	-0.132	41.354	0.7852
21.07	709.0	-239.87	-185.86	9.181	0.21550	-0.045	42.558	0.7880
21.08	704.8	-239.84	-177.87	10.433	0.21029	-0.019	49.593	0.8003
21.09	707.0	-239.92	-159.60	11.898	0.21497	-0.012	55.334	0.6889
21.10	708.2	-239.92	-139.67	13.099	0.21551	-0.010	60.770	0.6062
31.01	706.9	-149.90	-139.32	0.580	0.22379	-0.010	2.580	0.2438
31.02	706.6	-149.89	-113.22	1.796	0.22433	-0.010	7.995	0.2180
31.03	706.7	-149.90	-89.58	2.782	0.22427	-0.009	12.394	0.2055
31.04	706.9	-149.89	-63.76	3.756	0.22412	-0.007	16.750	0.1945
31.05	706.9	-149.85	-49.73	4.233	0.22416	-0.006	18.878	0.1885
41.01	706.5	-200.02	-194.95	0.657	0.21923	-0.001	2.996	0.5910
41.02	706.3	-200.03	-193.11	0.971	0.21954	-0.001	4.421	0.6388
41.03	706.3	-199.96	-190.63	1.379	0.21994	-0.002	6.268	0.6718
41.08	706.0	-199.89	-179.63	7.250	0.22003	-0.009	32.940	1.6259
41.09	706.0	-199.99	-175.15	7.679	0.21790	-0.010	35.229	1.4182
41.10	706.0	-199.96	-164.70	8.598	0.21951	-0.008	39.159	1.1106
18.01	799.4	-240.52	-230.48	0.683	0.22229	-0.001	3.071	0.3059
18.02	799.3	-240.51	-210.32	2.235	0.22193	-0.0	10.069	0.3335
18.03	801.2	-240.49	-185.20	5.654	0.22211	-0.003	25.454	0.4604
19.01	797.9	-239.79	-179.91	8.380	0.21338	-0.007	39.267	0.6558
19.02	798.3	-239.74	-174.46	9.606	0.21335	-0.003	45.021	0.6897

TABLE B-1 (Continued)

Run No.	Inlet Press. (psia)	Inlet Temp. (°F)	Outlet Temp. (°F)	Power (Btu/min)	Flow (lb/min)	Corr. (Btu/lb)	$\Delta \underline{H}p$ (Btu/lb)	$\left(\frac{\Delta \underline{H}}{\Delta T}\right)_p$ (Btu/lb-°F)
19.03	800.3	-239.76	-177.08	9.152	0.21375	-0.004	42.810	0.6830
19.04	797.9	-239.74	-168.93	10.336	0.21338	-0.001	48.437	0.6840
19.05	798.9	-239.74	-171.87	10.000	0.21357	-0.001	46.821	0.6899
20.01	798.0	-239.69	-156.97	10.657	0.19987	-0.002	53.316	0.6445
20.02	800.0	-239.70	-142.29	11.577	0.20058	-0.001	57.719	0.5925
32.01	799.1	-149.76	-138.99	0.685	0.22815	-0.007	2.995	0.2781
32.02	799.6	-149.78	-113.83	2.016	0.22835	-0.006	8.824	0.2454
32.03	799.5	-149.74	-90.25	3.078	0.22820	-0.006	13.484	0.2267
32.04	799.5	-149.72	-64.14	4.093	0.22824	-0.004	17.931	0.2095
32.05	799.5	-149.74	-48.76	4.662	0.22801	-0.003	20.445	0.2025
42.01	800.2	-209.97	-199.91	0.981	0.22956	-0.0	4.275	0.4249
42.02	800.9	-209.94	-189.79	2.329	0.23079	-0.001	10.091	0.5008
42.03	800.0	-209.97	-187.11	2.875	0.23052	-0.001	12.469	0.5454
42.04	800.1	-209.94	-184.95	3.494	0.23050	-0.006	15.153	0.6064
42.05	799.5	-209.93	-183.93	3.958	0.23035	-0.009	17.175	0.6606
42.06	800.2	-209.94	-182.99	4.612	0.23062	-0.011	19.989	0.7417
42.07	799.7	-209.94	-181.80	5.708	0.23034	-0.029	24.751	0.8796
42.08	800.2	-209.94	-180.91	6.292	0.23065	-0.030	27.251	0.9387
42.09	800.2	-209.91	-178.98	7.063	0.23062	-0.015	30.610	0.9897
42.10	799.8	-209.91	-174.75	7.999	0.22956	-0.014	34.831	0.9906
42.11	800.0	-209.91	-169.55	8.807	0.23069	-0.010	38.168	0.9457
42.12	799.6	-209.91	-159.27	9.829	0.22629	-0.009	43.425	0.8575
42.13	800.4	-209.91	-149.44	10.537	0.23074	-0.008	45.657	0.7550
40.01	950.9	-180.61	-178.71	0.431	0.22977	-0.002	1.874	0.9865
40.02	950.3	-180.46	-176.48	1.001	0.22962	-0.003	4.358	1.0949
40.03	951.0	-180.46	-174.47	1.673	0.22972	-0.003	7.279	1.2151
40.04	951.1	-180.48	-172.34	2.421	0.22665	-0.011	10.670	1.3108
40.05	950.1	-180.45	-170.44	3.006	0.22769	-0.010	13.193	1.3179
40.06	950.5	-180.44	-168.32	3.569	0.22795	-0.011	15.647	1.2910
40.07	950.5	-180.45	-166.33	4.023	0.22869	-0.010	17.582	1.2452
9.01	1142.7	-50.49	-40.79	0.415	0.23180	-0.002	1.789	0.1844
9.02	1141.7	-50.48	-5.25	1.847	0.23185	-0.001	7.965	0.1761
9.03	1141.1	-50.51	30.14	3.164	0.23182	-0.001	13.646	0.1692
9.04	1143.2	-50.49	73.16	4.688	0.23201	-0.001	20.203	0.1634
9.05	1142.7	-50.46	100.65	5.624	0.23216	-0.001	24.223	0.1603
9.06	1142.4	-50.48	109.95	5.932	0.23169	-0.001	25.601	0.1596
9.07	1142.3	-50.46	120.15	6.271	0.23182	-0.001	27.050	0.1585
15.01	1141.1	-240.18	-230.64	0.621	0.22085	0.0	2.810	0.2945
15.02	1143.0	-240.28	-209.79	2.112	0.22123	0.0	9.547	0.3131
15.03	1143.8	-240.25	-180.03	4.896	0.22114	-0.001	22.141	0.3677
15.04	1143.2	-240.25	-164.55	7.446	0.22105	-0.002	33.683	0.4450
16.01	1143.5	-240.35	-230.18	0.628	0.21018	0.0	2.990	0.2940
16.02	1141.8	-240.34	-209.94	1.976	0.20955	0.0	9.429	0.3102
17.01	1141.2	-240.35	-180.12	4.842	0.21925	-0.001	22.082	0.3666
17.02	1142.7	-240.35	-164.94	7.298	0.21959	-0.003	33.232	0.4407
17.03	1141.3	-240.41	-160.02	8.232	0.21882	-0.008	37.614	0.4679
17.04	1143.5	-240.35	-154.83	9.111	0.21908	-0.007	41.578	0.4862
17.05	1141.4	-240.41	-149.78	9.828	0.21855	-0.007	44.961	0.4961

TABLE B-1 (Continued)

Run No.	Inlet Press. (psia)	Inlet Temp. (°F)	Outlet Temp. (°F)	Power (Btu/min)	Flow (lb/min)	Corr. (Btu/lb)	$\Delta \underline{H}p$ (Btu/lb)	$\left(\frac{\Delta \underline{H}}{\Delta T}\right)_p$ (Btu/lb-°F)
17.06	1142.2	-240.37	-140.50	10.824	0.21871	-0.005	49.486	0.4955
37.01	1143.9	-180.20	-174.76	0.701	0.21174	0.0	3.313	0.6091
37.02	1144.1	-180.13	-169.65	1.484	0.21098	0.0	7.032	0.6709
37.03	1144.1	-180.13	-166.68	2.025	0.21136	0.0	9.579	0.7122
37.04	1144.1	-180.15	-165.57	2.246	0.21193	0.0	10.598	0.7269
37.05	1144.3	-180.17	-163.07	2.735	0.21159	0.0	12.925	0.7558
37.06	1144.4	-180.17	-159.78	3.345	0.21134	0.0	15.829	0.7763
37.07	1143.7	-180.16	-154.56	4.191	0.21154	-0.002	19.810	0.7738
37,08	1144.1	-180.13	-149.97	4.811	0.21133	-0.002	22.764	0.7548
33.01	1143.9	-149.75	-139.09	1.108	0.21120	-0.004	5.243	0.4918
33.02	1143.1	-149.74	-113.52	2.911	0.21158	-0.003	13.754	0.3797
33.03	1143.9	-149.70	-88.99	4.186	0.21172	-0.003	19.767	0.3256
33.04	1143.7	-149.71	-63.69	5.308	0.21172	-0.003	25.070	0.2914
33.05	1143.3	-149.74	-41.34	6.185	0.21154	-0.002	29.238	0.2697
43.01	1144.4	70.04	79.77	0.346	0.23792	-0.001	1.453	0.1493
43.02	1143.4	70.00	99.92	1.055	0.23883	-0.001	4.415	0.1476
43.03	1143.2	70.03	125.12	1.926	0.23874	-0.001	8.065	0.1464
43.04	1143.8	70.03	150.04	2.776	0.23959	-0.001	11.585	0.1448
43.05	1143.6	69.77	169.47	3.432	0.23898	-0.001	14.360	0.1440
13.01	1370.4	-240.28	-230.30	0.658	0.22818	0.0	2.883	0.2889
13.02	1369.2	-240.27	-211.00	2.020	0.22812	0.0	8.854	0.3025
13.03	1374.3	-240.25	-180.20	4.633	0.22856	-0.0	20.269	0.3375
13.04	1371.4	-240.23	-158.98	7.190	0.22810	-0.002	31.520	0.3879
13.05	1371.8	-240.24	-157.05	7.493	0.22842	-0.001	32.804	0.3943
13.06	1370.3	-240.18	-155.03	7.776	0.22781	-0.001	34.135	0.4009
13.07	1370.2	-240.23	-152.76	8.128	0.22809	-0.002	35.635	0.4074
13.08	1371.1	-240.31	-148.51	8.715	0.22719	-0.002	38.356	0.4178
14.01	1371.2	-240.23	-144.70	8.766	0.21558	-0.004	40.656	0.4256
14.02	1372.2	-240.22	-140.50	9.288	0.21644	-0.005	42.907	0.4303
14.03	1372.1	-240.38	-137.48	9.624	0.21598	-0.004	44.556	0.4330
14.04	1371.0	-240.22	-134.87	9.866	0.21483	-0.005	45.920	0.4359
14.05	1372.0	-240.24	-129.23	10,413	0.21517	-0.003	48.390	0.4359
36.01	1372.3	-170.17	-164.67	0.661	0.21435	-0.001	3.084	0.5607
36.02	1372.7	-170.25	-160.46	1.222	0.21483	-0.002	5.688	0.5810
36.03	1372.5	-170.21	-158.73	1.452	0.21495	-0.002	6.753	0.5883
36.04	1372.3	-170.23	-156.11	1.829	0.21579	-0.002	8.472	0.6000
36.05	1371.9	-170.21	-153.81	2.167	0.21721	-0.002	9.973	0.6081
36.06	1372.1	-170.19	-152.39	2.366	0.21765	-0.003	10.867	0.6105
36.07	1372.9	-170.21	-150.72	2.608	0.21789	-0.004	11.964	0.6138
36.08	1372.9	-170.18	-145.33	3.317	0.21812	-0.004	15.205	0.6119
36.09	1372.3	-170.23	-141.10	3.831	0.21791	-0.005	17.576	0.6034
36.10	1372.7	-170.13	-130.11	4.994	0.21770	-0.004	22.938	0.5732
36.11	1373.0	-170.10	-110.42	6.559	0.21721	-0.003	30.193	0.5059
36.12	1372.4	-170.14	-89.90	7.837	0.21741	-0.003	36.042	0.4492
36.13	1372.3	-170.11	-64.02	9.126	0.21708	-0.003	42.036	0.3962
36.14	1372.4	-170.11	-55.64	9.526	0.21685	-0.003	43.924	0.3837
12.01	1716.3	-240.38	-231.39	0.520	0.20742	0.004	2.510	0.2792
12.02	1717.9	-240.36	-210.84	1.789	0.20775	0.001	8.615	0.2918

TABLE B-1 (Concluded)

Run No.	Inlet Press. (psia)	Inlet Temp. (°F)	Outlet Temp. (°F)	Power (Btu/min)	Flow (lb/min)	Corr. (Btu/lb)	$\Delta\underline{H}p$ (Btu/lb)	$\left(\frac{\Delta H}{\Delta T}\right)_p$ (Btu/lb-°F)
12.03	1717.1	-240.37	-179.83	3.958	0.20759	-0.009	19.057	0.3148
12.04	1716.2	-240.35	-150.20	6.612	0.20821	-0.055	31.700	0.3516
12.05	1716.9	-240.45	-144.17	7.210	0.20793	-0.054	34.620	0.3596
34.01	1715.2	-159.52	-154.22	0.485	0.19930	-0.001	2.434	0.4592
34.02	1715.0	-159.57	-148.08	1.077	0.19912	-0.001	5.410	0.4708
34.03	1714.4	-159.50	-144.30	1.448	0.19993	-0.001	7.243	0.4765
34.04	1716.0	-159.50	-139.60	1.907	0.20004	-0.001	9.532	0.4790
34.05	1715.8	-159.52	-134.77	2.368	0.20000	-0.001	11.839	0.4783
34.06	1714.8	-159.52	-123.78	3.377	0.19972	-0.001	16.906	0.4730
34.07	1715.4	-159.55	-109.20	4.536	0.19940	-0.002	22.749	0.4518
34.08	1714.6	-159.49	-89.42	5.832	0.19963	-0.002	29.211	0.4169
34.09	1715.2	-159.52	-65.05	7.149	0.20027	-0.002	35.693	0.3778
34.10	1714.8	-159.51	-53.42	7.678	0.19947	-0.002	38.489	0.3628
8.01	1999.0	-50.52	-40.67	0.541	0.23090	-0.0	2.341	0.2376
8.02	1999.5	-50.49	-5.55	2.341	0.23628	-0.0	9.908	0.2205
8.03	1999.6	-50.49	29.93	3.956	0.23672	-0.0	16.710	0.2078
8.04	2003.1	-50.43	72.71	5.791	0.23961	-0.0	24.170	0.1963
8.05	2002.1	-50.45	99.52	6.835	0.23924	-0.0	28.571	0.1905
8.06	2001.2	-50.42	109.74	7.229	0.23917	-0.0	30.224	0.1887
8.07	2000.3	-50.42	120.43	7.631	0.23904	-0.0	31.925	0.1869
11.01	2001.2	-240.12	-230.42	0.620	0.23315	0.002	2.660	0.2743
11.02	2001.0	-240.11	-210.19	1.982	0.23289	-0.0	8.510	0.2844
11.03	2002.0	-240.09	-180.13	4.200	0.23295	-0.007	18.024	0.3006
11.04	2000.8	-240.06	-148.96	6.852	0.23263	-0.014	29.439	0.3231
11.07	1998.8	-240.04	-134.52	8.247	0.23234	-0.032	35.465	0.3361
35.01	2001.0	-140.09	-134.36	0.515	0.21347	-0.0	2.413	0.4212
35.02	2000.6	-140.07	-129.51	0.955	0.21372	-0.001	4.467	0.4230
35.03	2001.2	-140.09	-125.63	1.305	0.21390	-0.001	6.101	0.4219
35.04	2001.4	-140.07	-114.75	2.250	0.21410	-0.001	10.508	0.4150
35.05	2000.4	-140.06	-89.11	4.209	0.21426	-0.001	19.642	0.3855
35.06	2000.6	-140.02	-65.02	5.667	0.21364	-0.001	26.527	0.3537
35.07	2000.0	-140.07	-44.86	6.737	0.21340	-0.001	31.569	0.3316
45.01	1999.4	70.26	80.22	0.384	0.22960	-0.0	1.670	0.1677
45.02	2001.2	70.31	100.79	1.181	0.23504	-0.0	5.023	0.1648
45.03	1999.3	70.31	126.32	2.166	0.23838	-0.0	9.088	0.1623
45.04	1998.3	70.31	150.41	3.095	0.24184	-0.0	12.798	0.1598
45.05	1999.4	70.25	171.26	3.874	0.24202	-0.0	16.007	0.1585

TABLE B-2

BASIC ISOTHERMAL DATA FOR ARGON

Run No.	Inlet Temp. (°F)	Inlet Press. (psia)	Press. Drop (psid)	Power (Btu/min)	Flow (lb/min)	Corr. (Btu/lb)	ΔH_T (Btu/lb)	$\left(\frac{\Delta H}{\Delta P}\right)_T$ (Btu/lb-psid)
49.02	-208.88	1801.3	200.73	0.008	0.16165	-0.012	0.036	-0.00018
49.03	-208.92	1601.8	201.49	0.017	0.16257	-0.014	0.089	-0.00044
49.04	-208.89	1400.4	198.29	0.031	0.16393	-0.030	0.162	-0.00082
49.05	-208.89	1199.1	211.74	0.050	0.16760	-0.035	0.263	-0.00124
49.06	-208.89	1003.1	221.13	0.065	0.17069	0.020	0.402	-0.00182
49.07	-208.89	798.8	223.78	0.105	0.17813	0.023	0.615	-0.00275
50.01	-191.21	1996.4	97.80	0.018	0.32183	0.006	0.061	-0.00062
50.03	-191.19	1795.7	103.87	0.037	0.32591	0.010	0.124	-0.00119
50.05	-191.17	1597.5	109.12	0.071	0.33469	-0.009	0.204	-0.00187
50.07	-191.20	1397.6	115.50	0.102	0.34174	0.015	0.312	-0.00270
50.09	-191.17	1196.1	100.50	0.127	0.31504	0.010	0.414	-0.00412
50.11	-191.20	1014.2	84.79	0.164	0.28259	0.020	0.601	-0.00709
50.12	-191.17	936.1	96.19	0.274	0.29929	0.007	0.923	-0.00960
50.13	-191.18	845.1	96.40	0.415	0.29431	0.033	1.443	-0.01497
50.15	-191.17	635.4	234.24	2.542	0.22383	0.004	11.361	-0.04850
50.16	-191.21	439.9	175.36	0.706	0.13922	0.003	5.073	-0.02893
51.01	-168.24	1995.5	87.98	0.075	0.28547	0.018	0.280	-0.00318
51.03	-168.23	1796.8	99.46	0.129	0.30158	0.016	0.442	-0.00444
51.05	-168.20	1598.4	99.68	0.184	0.29408	0.027	0.654	-0.00656
51.07	-168.31	1397.7	105.37	0.346	0.29411	0.063	1.240	-0.01177
51.08	-168.25	1298.3	113.03	0.622	0.29643	0.040	2.139	-0.01892
51.09	-168.22	1200.6	114.54	0.919	0.28631	0.020	3.229	-0.02819
51.10	-168.20	1098.0	122.84	1.873	0.27176	0.021	6.911	-0.05626
51.11	-168.26	999.5	128.60	2.025	0.24225	0.046	8.404	-0.06535
51.12	-168.25	898.2	128.02	1.349	0.20971	0.027	6.461	-0.05047
51.13	-168.22	797.1	126.39	0.891	0.18174	0.0	4.901	-0.03878
51.14	-168.23	697.0	139.92	0.736	0.16791	0.005	4.386	-0.03135
51.15	-168.16	596.9	241.81	1.120	0.18390	0.003	6.096	-0.02521
51.16	-168.25	401.2	232.47	0.624	0.12993	-0.010	4.791	-0.02061
47.01	-58.02	2001.4	254.93	0.285	0.11459	0.018	2.509	-0.00984
47.02	-58.02	1803.7	229.39	0.235	0.10116	0.002	2.324	-0.01013
47.03	-57.99	1604.7	208.26	0.196	0.09055	0.008	2.170	-0.01042
47.04	-57.99	1404.0	231.76	0.214	0.08681	0.002	2.468	-0.01065
47.05	-57.98	1204.7	227.74	0.194	0.07941	-0.002	2.439	-0.01071
47.06	-57.99	1002.8	223.91	0.167	0.07045	0.005	2.369	-0.01058
47.07	-58.03	803.3	265.96	0.181	0.06623	0.009	2.747	-0.01033
47.08	-57.99	609.6	195.33	0.096	0.04929	0.006	1.963	-0.01005
47.09	-57.99	432.0	242.87	0.100	0.04215	0.008	2.392	-0.00985
52.01	166.95	1998.7	209.69	0.147	0.21644	0.002	0.681	-0.00325
52.02	166.92	1801.4	192.31	0.124	0.19611	0.005	0.638	-0.00332
52.03	166.94	1604.7	201.41	0.130	0.18855	0.001	0.691	-0.00343
52.04	166.88	1411.8	213.90	0.136	0.18090	0.004	0.755	-0.00353
52.05	166.47	1207.5	233.31	0.147	0.17262	-0.003	0.847	-0.00363
52.06	166.65	1008.0	245.52	0.145	0.15889	0.003	0.916	-0.00373
52.07	166.62	798.5	260.09	0.141	0.14105	-0.003	0.994	-0.00382
52.08	166.85	601.8	280.38	0.133	0.12112	0.004	1.102	-0.00393
52.09	166.82	430.5	199.34	0.068	0.08566	0.007	0.801	-0.00402

TABLE B-3

BASIC ISOBARIC DATA FOR C_2F_6

Run No.	Inlet Press. (psia)	Inlet Temp. (°F)	Outlet Temp. (°F)	Power (Btu/min)	Flow (lb/min)	Corr. (Btu/lb)	ΔH_p (Btu/lb)	$\left(\frac{\Delta H}{\Delta T}\right)_p$ (Btu/lb-°F)
1.01	248.6	0.04	13.73	0.017	0.00399	-0.001	4.169	0.3046
1.02	248.6	0.04	21.05	0.026	0.00399	-0.001	6.524	0.3106
1.03	248.6	0.04	25.29	0.032	0.00399	-0.001	7.972	0.3157
1.04	248.6	0.04	26.13	0.036	0.00399	0.002	8.982	0.3442
1.05	248.6	0.04	26.24	0.040	0.00399	0.010	10.053	0.3837
1.06	248.6	0.04	26.25	0.047	0.00399	0.014	11.770	0.4489
2.01	248.8	24.98	27.06	0.003	0.00399	-0.001	0.754	0.3618
2.02	248.7	24.98	26.39	0.002	0.00399	-0.001	0.482	0.3411
2.03	248.7	24.98	26.75	0.002	0.00399	-0.001	0.611	0.3461
2.04	248.8	24.98	27.08	0.004	0.00399	-0.001	1.086	0.5183
2.05	248.8	24.98	27.09	0.007	0.00399	-0.002	1.697	0.8030
2.06	248.8	24.98	27.09	0.009	0.00399	-0.002	2.180	1.0372
2.07	248.8	24.98	27.11	0.016	0.00399	-0.005	3.990	1.8752
2.08	248.8	24.98	27.11	0.041	0.00399	0.016	10.326	4.8561
2.09	248.8	24.98	27.10	0.091	0.00399	0.049	22.813	10.7362
2.10	248.8	24.98	27.09	0.108	0.00399	0.021	27.149	12.8708
2.11	248.8	24.98	33.87	0.127	0.00399	0.004	31.857	3.5845
2.12	248.8	24.98	41.32	0.135	0.00399	0.002	33.844	2.0722
2.13	248.8	24.98	49.20	0.143	0.00399	0.008	35.887	1.4819
13.01	247.2	67.65	86.24	0.174	0.03991	-0.018	4.334	0.2331
13.02	247.1	67.65	120.87	0.491	0.03991	-0.042	12.263	0.2304
14.01	246.7	122.16	135.21	0.120	0.03991	-0.015	3.000	0.2299
14.02	246.6	122.16	159.79	0.348	0.03991	-0.042	8.668	0.2303
14.03	246.7	122.16	173.11	0.471	0.03991	-0.039	11.752	0.2306
23.01	247.2	176.26	190.95	0.136	0.03991	-0.030	3.379	0.2300
23.02	247.2	176.26	234.30	0.534	0.03991	-0.001	13.377	0.2305
23.03	247.3	176.26	247.73	0.658	0.03991	0.022	16.510	0.2310
28.01	247.0	55.88	68.08	0.117	0.03991	-0.007	2.928	0.2400
4.01	432.1	-0.02	10.22	0.126	0.04095	0.001	3.069	0.2997
4.02	432.1	-0.02	25.35	0.320	0.04095	-0.006	7.814	0.3080
4.03	432.1	-0.02	41.62	0.542	0.04095	-0.001	13.229	0.3177
4.04	432.2	-0.02	47.68	0.635	0.04095	-0.001	15.498	0.3249
16.01	431.0	122.11	133.22	0.121	0.04095	-0.021	2.929	0.2636
16.02	431.0	122.11	154.94	0.347	0.04095	-0.017	8.453	0.2575
16.03	430.9	122.11	176.72	0.569	0.04095	-0.017	13.885	0.2543
27.01	431.9	55.94	59.28	0.067	0.04095	0.030	1.669	0.4996
27.02	432.0	55.94	62.94	0.161	0.04095	0.008	3.934	0.5620
27.03	432.1	55.94	65.51	0.269	0.04095	0.078	6.635	0.6933
27.04	432.2	55.94	65.87	0.469	0.04095	0.246	11.691	1.1773
27.05	432.3	55.94	67.23	0.739	0.04095	0.208	18.257	1.6171
27.06	432.2	55.94	65.85	0.383	0.04095	0.120	9.461	0.9546
27.07	432.5	55.94	72.16	0.898	0.04095	0.156	22.095	1.3622
27.08	432.4	55.94	87.11	1.146	0.04095	0.086	28.065	0.9004
29.01	431.7	68.00	70.11	0.070	0.04095	0.071	1.782	0.8446
29.02	431.8	68.00	82.48	0.320	0.04095	0.052	7.877	0.5440
29.03	431.8	68.00	119.88	0.785	0.04095	0.051	19.223	0.3705
12.01	489.7	67.65	71.33	0.103	0.04121	-0.008	2.486	0.6756
12.02	489.9	67.65	72.84	0.162	0.04121	-0.010	3.911	0.7535

TABLE B-3 (Continued)

Run No.	Inlet Press. (psia)	Inlet Temp. (°F)	Outlet Temp. (°F)	Power (Btu/min)	Flow (lb/min)	Corr. (Btu/lb)	ΔH_p (Btu/lb)	$\left(\frac{\Delta H}{\Delta T}\right)_p$ (Btu/lb-°F)
12.03	489.9	67.65	74.20	0.239	0.04121	-0.012	5.790	0.8839
12.04	490.0	67.65	75.78	0.383	0.04121	-0.012	9.281	1.1416
12.05	489.9	67.65	77.91	0.529	0.04121	-0.006	12.838	1.2512
12.06	489.9	67.65	77.12	0.484	0.04121	-0.009	11.736	1.2393
12.07	489.9	67.65	79.74	0.608	0.04121	-0.007	14.747	1.2197
12.08	489.9	67.65	87.74	0.814	0.04121	0.004	19.753	0.9832
12.09	489.9	67.65	110.83	1.152	0.04121	0.007	27.966	0.6476
12.10	489.9	67.65	121.11	1.278	0.04121	0.007	31.010	0.5801
30.01	598.1	68.00	77.77	0.188	0.04163	0.013	4.530	0.4636
30.02	598.2	68.00	83.43	0.325	0.04163	0.030	7.845	0.5084
30.03	598.2	68.00	85.59	0.386	0.04163	0.041	9.315	0.5296
30.04	598.4	68.00	88.44	0.473	0.04163	0.062	11.434	0.5594
30.05	598.4	68.00	91.36	0.573	0.04163	0.073	13.831	0.5921
30.06	598.5	68.00	96.76	0.730	0.04163	0.140	17.686	0.6149
30.07	598.5	68.00	106.48	0.953	0.04163	0.095	22.984	0.5973
30.08	598.5	68.00	120.49	1.182	0.04163	0.078	28.467	0.5423
10.01	699.7	67.65	75.30	0.122	0.04195	-0.002	2.911	0.3806
10.02	699.7	67.65	83.97	0.274	0.04196	-0.002	6.534	0.4003
10.03	699.8	67.65	91.16	0.415	0.04195	-0.001	9.884	0.4204
10.04	699.7	67.65	96.54	0.534	0.04195	-0.002	12.725	0.4404
10.05	699.7	67.65	101.03	0.639	0.04195	-0.003	15.228	0.4562
10.06	699.6	67.65	98.80	0.587	0.04195	-0.0	13.996	0.4493
10.07	699.6	67.65	97.69	0.560	0.04195	-0.001	13.341	0.4441
10.08	699.7	67.65	104.63	0.726	0.04195	-0.003	17.313	0.4682
10.09	699.7	67.65	111.28	0.876	0.04195	-0.001	20.883	0.4786
10.10	699.8	67.65	121.54	1.081	0.04195	0.004	25.773	0.4783
9.01	839.0	67.57	75.91	0.119	0.04195	-0.001	2.833	0.3396
9.02	839.1	67.57	91.85	0.364	0.04195	-0.002	8.668	0.3570
9.03	839.1	67.57	105.55	0.599	0.04195	-0.0	14.283	0.3761
9.04	839.1	67.57	100.60	0.511	0.04195	-0.001	12.184	0.3689
9.05	839.1	67.57	113.06	0.737	0.04195	-0.001	17.578	0.3864
9.06	839.1	67.57	110.02	0.681	0.04195	-0.001	16.231	0.3823
9.07	839.1	67.57	116.27	0.802	0.04195	-0.002	19.112	0.3924
9.08	839.2	67.57	121.35	0.897	0.04195	-0.002	21.376	0.3975
17.01	1048.6	122.09	123.94	0.030	0.04269	-0.002	0.702	0.3792
17.02	1048.6	122.09	128.04	0.097	0.04269	-0.001	2.265	0.3807
17.03	1048.6	122.09	132.67	0.173	0.04269	-0.002	4.042	0.3821
17.04	1048.6	122.09	149.91	0.455	0.04269	0.016	10.668	0.3835
17.05	1048.7	122.09	175.19	0.846	0.04269	0.024	19.831	0.3735
17.06	1048.7	134.02	138.10	0.067	0.04269	0.019	1.581	0.3876
19.01	1398.4	122.11	132.25	0.145	0.04322	0.001	3.357	0.3311
19.02	1398.3	122.11	145.00	0.330	0.04322	0.002	7.638	0.3337
19.03	1398.3	122.11	149.69	0.399	0.04322	0.003	9.227	0.3346
19.04	1398.4	122.11	165.34	0.630	0.04322	0.001	14.583	0.3373
19.05	1398.4	122.11	175.76	0.783	0.04322	0.002	18.128	0.3379
19.06	1398.4	160.11	167.76	0.113	0.04322	0.002	2.615	0.3418
6.01	1968.7	0.02	10.61	0.133	0.04501	0.001	2.949	0.2785
6.02	1967.7	0.02	41.53	0.524	0.04501	-0.001	11.631	0.2802

TABLE B-3 (Concluded)

Run No.	Inlet Press. (psia)	Inlet Temp. (°F)	Outlet Temp. (°F)	Power (Btu/min)	Flow (lb/min)	Corr. (Btu/lb)	ΔH_p (Btu/lb)	$\left(\frac{\Delta H}{\Delta T}\right)_p$ (Btu/lb-°F)
6.03	1968.8	0.02	68.95	0.875	0.04501	-0.002	19.445	0.2821
7.01	1968.7	67.61	77.30	0.126	0.04501	0.001	2.791	0.2880
7.02	1969.0	67.61	92.20	0.320	0.04501	0.0	7.114	0.2893
7.03	1969.2	67.61	122.01	0.715	0.04501	0.0	15.879	0.2919
20.01	1968.9	122.93	134.74	0.159	0.04501	-0.0	3.524	0.2984
20.02	1968.9	122.93	163.61	0.552	0.04501	0.0	12.265	0.3015
20.03	1968.9	122.93	175.60	0.718	0.04501	0.001	15.954	0.3029
21.01	1969.5	176.20	181.02	0.067	0.04501	0.0	1.491	0.3094
21.02	1969.5	176.20	188.52	0.171	0.04501	0.001	3.808	0.3091
21.03	1969.5	176.20	213.76	0.524	0.04501	0.004	11.647	0.3101
21.04	1969.6	176.20	230.37	0.756	0.04501	0.009	16.809	0.3103
21.05	1969.5	176.20	248.93	1.013	0.04501	0.009	22.517	0.3096

TABLE B-4

BASIC ISOTHERMAL DATA FOR C_2F_6

Run No.	Inlet Temp. (°F)	Inlet Press. (psia)	Press. Drop (psid)	Power (Btu/min)	Flow (lb/min)	Corr. (Btu/lb)	ΔH_T (Btu/lb)	$\left(\frac{\Delta H}{\Delta P}\right)_T$ (Btu/lb-psid)
3.01	-0.07	247.3	22.68	0.001	0.03990	0.0	0.023	-0.00100
3.02	-0.08	432.1	23.24	0.0	0.04095	0.0	0.011	-0.00049
5.01	-0.03	720.3	23.72	0.0	0.04201	-0.0	0.003	-0.00014
5.02	-0.03	992.7	24.26	0.0	0.04259	-0.004	-0.002	0.00009
5.03	-0.02	1460.9	25.11	0.0	0.04334	-0.009	-0.009	0.00036
5.04	-0.02	1968.7	25.88	0.0	0.04501	-0.015	-0.015	0.00059
11.01	67.60	699.0	28.20	0.008	0.04195	0.0	0.186	-0.00658
11.02	67.62	533.5	29.07	0.023	0.04139	0.007	0.552	-0.01900
11.03	67.60	404.3	94.22	0.204	0.04081	-0.003	4.996	-0.05303
11.04	67.60	367.5	123.67	0.208	0.04062	0.008	5.130	-0.04148
11.05	67.58	384.5	109.58	0.204	0.04071	-0.006	5.016	-0.04578
8.01	67.56	1969.1	28.07	0.0	0.04502	0.018	0.018	-0.00066
8.02	67.57	1496.3	27.72	0.001	0.04341	0.0	0.028	-0.00102
8.03	67.57	990.7	27.71	0.002	0.04259	0.0	0.050	-0.00179
8.04	67.54	839.1	27.81	0.003	0.04230	0.002	0.078	-0.00279
15.01	122.05	430.8	130.52	0.128	0.04094	0.011	3.132	-0.02400
15.02	122.06	613.1	67.48	0.107	0.04169	-0.013	2.564	-0.03800
15.03	122.06	765.8	44.29	0.071	0.04213	-0.019	1.655	-0.03736
15.04	122.06	918.4	35.99	0.032	0.04246	-0.033	0.709	-0.01970
15.05	122.06	1015.3	33.76	0.019	0.04263	-0.004	0.431	-0.01276
18.01	122.06	1213.6	31.66	0.009	0.04293	0.008	0.219	-0.00692
18.02	122.07	1398.2	31.11	0.005	0.04322	0.011	0.131	-0.00420
18.03	122.05	1613.1	31.07	0.003	0.04374	0.008	0.072	-0.00232
18.04	122.06	1814.0	31.04	0.002	0.04438	-0.003	0.053	-0.00171
18.05	122.06	1969.0	31.01	0.002	0.04508	0.003	0.038	-0.00123
22.01	176.15	1928.9	25.15	0.004	0.03792	-0.007	0.094	-0.00372
22.02	176.16	1613.3	26.20	0.006	0.03696	-0.003	0.157	-0.00599
22.03	176.16	1420.5	27.56	0.009	0.03661	-0.006	0.233	-0.00846
22.04	176.16	1219.9	30.06	0.014	0.03634	-0.010	0.374	-0.01244
22.05	176.17	1013.3	35.63	0.022	0.03607	-0.003	0.609	-0.01710
22.06	176.17	813.9	46.58	0.033	0.03575	-0.003	0.924	-0.01983
22.07	176.16	516.1	80.46	0.050	0.03497	-0.005	1.438	-0.01787
22.08	176.14	364.7	150.09	0.081	0.03436	0.006	2.377	-0.01584
24.01	246.78	473.5	123.85	0.043	0.03481	-0.002	1.235	-0.00997
24.02	246.77	713.6	73.13	0.031	0.03553	-0.002	0.874	-0.01195
24.03	246.65	913.1	55.44	0.025	0.03592	0.001	0.689	-0.01243
24.04	246.66	1013.2	49.64	0.021	0.03607	0.002	0.596	-0.01200
24.05	246.71	1413.2	36.48	0.012	0.03660	-0.005	0.316	-0.00867
24.06	246.65	1873.2	30.96	0.006	0.03722	0.004	0.164	-0.00530
24.07	246.73	1721.2	32.05	0.008	0.03770	-0.002	0.203	-0.00633

APPENDIX C

CORRECTED BASIC DATA

TABLE C-1

$\bar{C}p$ VALUES FOR ARGON

PRESSURE (PSIA)	INLET TEMP. (°F)	OUTLET TEMP. (°F)	$\bar{C}_P$ (BTU/LB-°F)
286.	-200.29	-189.87	0.1853
	-200.30	-146.36	0.1680
	-200.30	-121.14	0.1622
	-200.29	-93.61	0.1579
	-100.53	-80.23	0.1412
	-100.48	-50.42	0.1394
	-100.49	-20.76	0.1380
	-100.46	9.37	0.1369
	-100.49	33.78	0.1361
	-100.55	50.58	0.1355
	-50.34	-4.65	0.1355
	-50.32	30.23	0.1341
	-50.35	73.26	0.1330
	-50.46	100.46	0.1323
	-50.43	110.16	0.1323
	-50.51	119.93	0.1321
	70.26	99.50	0.1301
	70.26	125.68	0.1297
	70.28	149.46	0.1294
	99.95	170.73	0.1288
	99.75	190.13	0.1286
	99.71	218.28	0.1285
	-223.91	-220.71	0.2556
	-208.70	-192.39	0.1952
	-220.10	-208.70	0.2278
	-189.87	-146.36	0.1640
	-189.87	-169.48	0.1706
	-146.36	-121.14	0.1498
	-121.14	-93.61	0.1407

TABLE C-1 (Continued)

PRESSURE (PSIA)	**INLET TEMP. (°F)**	**OUTLET TEMP. (°F)**	$\overline{C_p}$ **(BTU/LB-°F)**
457.	-240.09	-229.98	0.3228
	-240.08	-215.03	0.3551
	-240.08	-210.65	0.3687
	-240.09	-209.52	0.3730
	-240.08	-208.35	0.3778
	-149.84	-140.31	0.1804
	-149.86	-114.05	0.1712
	-149.89	-89.82	0.1650
	-149.85	-63.46	0.1605
	-149.86	-52.75	0.1591
	-229.98	-215.03	0.3767
	-229.98	-209.52	0.3976
	-229.98	-207.87	0.4172
	-215.03	-210.65	0.4463
	-215.03	-209.52	0.4543
	-215.03	-208.35	0.4627
	-210.65	-209.52	0.4970
	-210.65	-208.35	0.5300
	-210.05	-207.87	0.5888
	-209.52	-207.87	0.6600
	-208.35	-207.87	1.0438
	-206.64	-204.25	0.4887
	-205.53	-201.00	0.3830
	-204.25	-192.47	0.3052
	-205.49	-201.00	0.3873
	-201.00	-174.61	0.2477
	-192.47	-174.61	0.2384
	-192.47	-155.47	0.2213
	-174.61	-155.47	0.2054
	-174.61	-139.72	0.1919
	-140.31	-114.05	0.1679
	-89.82	-63.46	0.1502
	-63.46	-52.75	0.1476

TABLE C-1 (Continued)

PRESSURE (PSIA)	INLET TEMP. (°F)	OUTLET TEMP. (°F)	$\overline{C_P}$ (BTU/LB-°F)
571.	-240.00	-229.91	0.3160
	-239.96	-209.97	0.3535
	-239.93	-201.49	0.3877
	-239.82	-200.19	0.3963
	-239.89	-198.87	0.4068
	-240.01	-198.23	0.4321
	-149.97	-140.23	0.2047
	-149.92	-112.83	0.1904
	-149.94	-89.92	0.1824
	-149.89	-64.22	0.1749
	-149.90	-53.89	0.1723
	-229.91	-209.97	0.3723
	-229.91	-200.19	0.4249
	-229.91	-198.87	0.4367
	-229.91	-198.23	0.4740
	-209.97	-201.49	0.5146
	-209.97	-200.19	0.5323
	-209.97	-198.87	0.5523
	-201.49	-200.19	0.6277
	-201.49	-198.87	0.6744
	-200.49	-198.23	0.9905
	-200.19	-198.87	0.7008
	-200.19	-198.23	1.2179
	-198.87	-198.23	2.2844
	-196.56	-195.74	0.8000
	-196.56	-194.10	0.6638
	-196.56	-184.35	0.4822
	-196.56	-163.56	0.3574
	-196.56	-140.22	0.2978
	-196.01	-194.10	0.6560
	-195.74	-194.10	0.5957
	-195.74	-184.35	0.4593
	-194.10	-184.35	0.4364
	-194.10	-163.56	0.3327
	-184.35	-163.56	0.2841
	-184.35	-140.22	0.2467
	-163.56	-140.22	0.2134
	-112.83	-89.92	0.1690
	-112.83	-64.22	0.1630
	-89.92	-64.22	0.1578
	-64.22	-53.89	0.1506

TABLE C-1 (Continued)

PRESSURE (PSIA)	INLET TEMP. (°F)	OUTLET TEMP. (°F)	$\overline{C_p}$ (BTU/LB-°F)
706.	-239.90	-229.87	0.3129
	-239.89	-207.46	0.3458
	-239.89	-188.83	0.4889
	-239.90	-188.57	0.5177
	-239.95	-195.70	0.3883
	-149.90	-139.32	0.2438
	-149.89	-113.22	0.2180
	-149.90	-89.58	0.2055
	-149.89	-63.76	0.1945
	-149.85	-49.73	0.1885
	-194.95	-190.63	0.7655
	-63.76	-49.73	0.1608
	-188.83	-188.57	4.6732
	-188.57	-185.86	5.9693
	-188.96	-186.97	8.2814
	-229.87	-207.46	0.3618
	-207.46	-195.70	0.4976
	-195.70	-188.83	1.1776
	-194.95	-193.11	0.7364
	-193.11	-188.96	1.2783
	-190.63	-188.96	2.0078
	-177.87	-159.60	0.3129
	-187.86	-186.97	2.6573
	-186.97	-185.05	1.4229
	-185.05	-179.63	0.7659
	-179.63	-175.15	0.4971
	-175.15	-164.70	0.3778
	-89.58	-63.76	0.1677

TABLE C-1 (Continued)

PRESSURE (PSIA)	INLET TEMP. (°F)	OUTLET TEMP. (°F)	$\overline{C_p}$ (BTU/LB-°F)
800.	-240.52	-230.48	0.3059
	-240.51	-210.32	0.3335
	-240.49	-185.20	0.4604
	-239.79	-179.91	0.6558
	-239.74	-174.46	0.6897
	-239.76	-177.08	0.6830
	-239.74	-168.93	0.6840
	-239.74	-171.87	0.6899
	-239.69	-156.97	0.6445
	-239.70	-142.29	0.5925
	-149.76	-138.99	0.2781
	-149.78	-113.83	0.2454
	-149.74	-90.25	0.2267
	-149.72	-64.14	0.2095
	-149.74	-48.76	0.2025
	-209.97	-199.91	0.4249
	-209.94	-181.80	0.8796
	-209.94	-180.91	0.9387
	-209.91	-178.98	0.9897
	-209.91	-174.75	0.9906
	-209.91	-169.55	0.9457
	-209.91	-149.44	0.7550
	-230.48	-210.32	0.3474
	-179.91	-177.08	1.2339
	-177.08	-174.46	0.8954
	-171.87	-156.97	0.4561
	-187.11	-184.95	1.2477
	-184.95	-183.93	1.9853
	-183.93	-182.99	2.9904
	-182.99	-181.80	3.9319
	-181.80	-180.91	2.9034
	-180.91	-178.98	1.7627
	-178.98	-174.75	1.0319
	-90.25	-64.14	0.1769
	-64.14	-48.76	0.1657
950.	-180.61	-178.71	0.9865
	-180.46	-176.48	1.0949
	-180.46	-174.47	1.2151
	-180.48	-172.34	1.3108
	-180.45	-170.44	1.3179
	-180.44	-168.32	1.2910
	-180.45	-166.33	1.2452
	-178.71	-176.48	1.1731
	-176.48	-174.47	1.4408
	-174.47	-172.34	1.5864
	-172.34	-170.44	1.3584
	-170.44	-168.32	1.1632
	-168.32	-166.33	0.9668

TABLE C-1 (Continued)

PRESSURE (PSIA)	**INLET TEMP. (°F)**	**OUTLET TEMP. (°F)**	$\overline{C_p}$ **(BTU/LB-°F)**
1143.	-240.18	-230.64	0.2945
	-240.28	-209.79	0.3131
	-240.25	-180.03	0.3677
	-240.25	-164.55	0.4450
	-240.35	-230.18	0.2940
	-240.35	-180.12	0.3666
	-240.35	-164.94	0.4407
	-240.41	-160.02	0.4679
	-240.35	-154.83	0.4862
	-240.41	-149.78	0.4961
	-240.37	-140.50	0.4955
	-180.20	-174.76	0.6091
	-180.13	-169.65	0.6709
	-180.13	-166.68	0.7122
	-180.15	-165.57	0.7269
	-180.17	-163.07	0.7558
	-180.17	-159.78	0.7763
	-180.16	-154.56	0.7738
	-180.13	-149.97	0.7548
	-149.75	-139.09	0.4918
	-149.74	-113.52	0.3797
	-149.70	-88.99	0.3256
	-149.71	-63.69	0.2914
	-149.74	-41.34	0.2697
	-50.49	-40.79	0.1844
	-50.48	-5.25	0.1761
	-50.51	30.14	0.1692
	-50.49	73.16	0.1634
	-50.46	100.65	0.1603
	-50.48	109.95	0.1596
	-50.46	120.15	0.1585
	70.04	79.77	0.1493
	70.00	99.92	0.1476
	70.03	125.12	0.1464
	70.03	150.04	0.1448
	69.77	169.47	0.1440
	-230.18	-209.94	0.3179
	-209.94	-180.12	0.4242
	-160.02	-149.78	0.7175
	-154.83	-149.78	0.6661
	-174.76	-169.65	0.7348
	-169.65	-166.68	0.8576
	-165.57	-163.07	0.9268
	-163.07	-159.78	0.8833
	-159.78	-149.97	0.7090
	-139.09	-113.52	0.3332
	-113.52	-88.99	0.2450
	-88.99	-63.69	0.2096
	-63.69	-41.34	0.1861
	-5.25	30.14	0.1604
	30.14	73.16	0.1523
	150.04	169.47	0.1409

TABLE C-1 (Continued)

PRESSURE (PSIA)	**INLET TEMP. (°F)**	**OUTLET TEMP. (°F)**	$\overline{C_P}$ **(BTU/LB-°F)**
1371.	-240.28	-230.30	0.2889
	-240.27	-211.00	0.3025
	-240.25	-180.20	0.3375
	-240.23	-158.98	0.3879
	-240.24	-157.05	0.3943
	-240.18	-155.03	0.4009
	-240.23	-152.76	0.4074
	-240.31	-148.51	0.4178
	-240.23	-144.70	0.4256
	-240.22	-140.50	0.4303
	-240.38	-137.48	0.4330
	-240.22	-134.87	0.4359
	-240.24	-129.23	0.4359
	-170.17	-164.67	0.5607
	-170.25	-160.46	0.5810
	-170.21	-158.73	0.5883
	-170.23	-156.11	0.6000
	-170.21	-153.81	0.6081
	-170.19	-152.39	0.6105
	-170.21	-150.72	0.6138
	-170.18	-145.33	0.6119
	-170.23	-141.10	0.6034
	-170.13	-130.11	0.5732
	-170.10	-110.42	0.5059
	-170.14	-89.90	0.4492
	-170.11	-64.02	0.3962
	-170.11	-55.64	0.3837
	-230.30	-211.00	0.3096
	-211.00	-180.20	0.3673
	-180.20	-158.98	0.5355
	-144.70	-137.48	0.5445
	-140.50	-134.87	0.4996
	-164.67	-160.46	0.6050
	-160.46	-156.11	0.6464
	-158.73	-156.11	0.6542
	-156.11	-153.81	0.6580
	-152.39	-150.72	0.6333
	-150.72	-141.10	0.6064
	-141.10	-130.11	0.4805
	-145.33	-110.42	0.4277
	-130.11	-110.42	0.3672
	-110.42	-89.90	0.2840
	-64.02	-55.64	0.2233

TABLE C-1 (Continued)

PRESSURE (PSIA)	INLET TEMP. (°F)	OUTLET TEMP. (°F)	$\overline{C_p}$ (BTU/LB-°F)
1714.	-240.38	-231.39	0.2792
	-240.36	-210.84	0.2918
	-240.37	-179.83	0.3148
	-240.35	-150.20	0.3516
	-240.45	-144.17	0.3596
	-159.52	-154.22	0.4592
	-159.57	-148.08	0.4708
	-159.50	-144.30	0.4765
	-159.50	-139.60	0.4790
	-159.52	-134.77	0.4783
	-159.52	-123.78	0.4730
	-159.55	-109.20	0.4518
	-159.49	-89.42	0.4169
	-159.52	-65.05	0.3778
	-159.51	-53.42	0.3628
	-231.39	-210.84	0.2973
	-210.84	-179.83	0.3364
	-179.83	-150.20	0.4268
	-154.22	-148.08	0.4805
	-148.08	-144.30	0.4926
	-144.30	-139.60	0.4902
	-139.60	-134.77	0.4754
	-134.77	-109.20	0.4261
	-123.78	-109.20	0.3998
	-109.20	-89.42	0.3281
	-89.42	-65.05	0.2654
	-65.05	-53.42	0.2408

TABLE C-1 (Concluded)

PRESSURE (PSIA)	INLET TEMP. (oF)	OUTLET TEMP. (oF)	$\overline{C_p}$ (BTU/LB-oF)
2000.	-240.12	-230.42	0.2743
	-240.11	-210.19	0.2844
	-240.09	-180.13	0.3006
	-240.06	-148.96	0.3231
	-240.04	-134.52	0.3361
	-140.09	-134.36	0.4212
	-140.07	-129.51	0.4230
	-140.09	-125.63	0.4219
	-140.07	-114.75	0.4150
	-140.06	-89.11	0.3855
	-140.02	-65.02	0.3537
	-140.07	-44.86	0.3316
	-50.52	-40.67	0.2376
	-50.49	-5.55	0.2205
	-50.49	29.93	0.2078
	-50.43	72.71	0.1963
	-50.45	99.52	0.1905
	-50.42	109.74	0.1887
	-50.42	120.43	0.1869
	70.26	80.22	0.1677
	70.31	100.79	0.1648
	70.31	126.32	0.1623
	70.31	150.41	0.1598
	70.25	171.26	0.1585
	-230.42	-210.19	0.2884
	-210.19	-180.13	0.3156
	-180.13	-148.96	0.3651
	-148.96	-134.52	0.4143
	-144.71	-139.33	0.4128
	-125.63	-114.75	0.4085
	-114.75	-65.02	0.3210
	-89.11	-65.02	0.2877
	-65.02	-44.86	0.2432
	-40.67	-5.55	0.2156
	-5.55	29.93	0.1917
	150.41	171.26	0.1533

TABLE C-2

$\bar{\mu}$ VALUES FOR ARGON

TEMPERATURE (°F)	INLET PRESS. (PSIA)	PRESS. DROP (PSID)	$\bar{\mu}$ (°F/PSID)
-240.	419.7	164.5	0.00028
	574.8	188.8	-0.00018
	918.5	186.7	-0.00088
	1095.6	179.1	-0.00114
	1265.5	171.5	-0.00139
	1407.0	149.5	-0.00162
	1605.3	185.0	-0.00188
	1803.4	194.2	-0.00212
	2000.5	174.9	-0.00240

TABLE C-3

$\bar{\Phi}$ VALUES FOR ARGON

TEMPERATURE (°F)	INLET PRESS. (PSIA)	PRESS. DROP (PSID)	$\bar{\phi}$ (BTU/LB-PSID)
-208.9	1801.3	200.7	-0.00018
	798.8	223.8	-0.00275
	1003.1	221.1	-0.00182
	1199.1	211.7	-0.00124
	1400.4	198.3	0.0
	1601.8	201.5	-0.00044
-191.2	439.9	175.4	-0.02893
	635.4	234.2	-0.04850
	845.1	96.4	-0.01497
	936.1	96.2	-0.00960
	1014.2	84.8	-0.00709
	1196.1	100.5	-0.00412
	1397.6	115.5	-0.00270
	1597.5	109.1	-0.00187
	1795.7	103.9	-0.00119
	1996.4	97.8	-0.00062

TABLE C-3 (Concluded)

TEMPERATURE (°F)	INLET PRESS. (PSIA)	PRESS. DROP (PSID)	$\bar{\Phi}$ (BTU/LB-PSID)
-168.3	401.2	232.5	-0.02061
	596.9	241.8	-0.02521
	697.0	139.9	-0.03135
	797.1	126.4	-0.03878
	898.2	128.0	-0.05047
	999.5	128.6	-0.06535
	1098.0	122.8	-0.05626
	1200.6	114.5	-0.02819
	1298.3	113.0	-0.01892
	1397.7	105.4	-0.01177
	1598.4	99.7	-0.00656
	1796.8	99.5	-0.00444
	1995.5	88.0	-0.00318
-58.	432.0	242.9	-0.00985
	609.6	195.3	-0.01005
	803.3	266.0	-0.01033
	1002.8	223.9	-0.01058
	1204.7	227.7	-0.01071
	1404.0	231.8	-0.01065
	1604.7	208.3	-0.01042
	1803.7	229.4	-0.01013
167.	430.5	199.3	-0.00402
	601.8	280.4	-0.00393
	798.5	260.1	-0.00382
	1008.0	245.5	-0.00373
	1207.5	233.3	-0.00363
	1411.8	213.9	-0.00353
	1604.7	201.4	-0.00343
	1801.4	192.3	-0.00332
	1998.7	209.7	-0.00325

TABLE C-4

ENTHALPY TRAVERSE DATA FOR ARGON

Pressure = 286. psia		Pressure = 457. psia		Pressure = 571. psia	
Temperature (°F)	$\Delta\underline{H}$* (Btu/lb)	Temperature (°F)	$\Delta\underline{H}$* (Btu/lb)	Temperature (°F)	$\Delta\underline{H}$* (Btu/lb)
-230.06	3.353	-215.03	8.870	-201.49	14.999
-229.24	3.640	-210.65	10.825	-200.19	15.841
-227.51	4.286	-209.52	11.373	-198.87	16.766
-226.75	4.994	-208.35	11.961	-198.00	17.450
-226.73	6.684	-207.99	13.178	-198.23	18.228
-226.75	27.994	-207.97	14.462	-198.04	21.491
-226.72	47.341	-207.97	36.659	-198.01	27.905
-226.75	49.739	-207.96	43.594	-197.97	35.362
-225.14	52.630	-207.97	47.889	-197.97	40.598
-223.91	52.498	-206.64	49.390	-197.99	44.236
-220.71	53.766	-205.53	49.910	-197.97	45.243
		-205.25	50.069	-196.56	46.358
		-204.25	50.558	-196.01	46.738
		-201.00	51.583	-195.74	47.014
				-194.10	47.991

*$\Delta H = 0$ at -240.°F

TABLE C-5

$\bar{C}p$ VALUES FOR C_2F_6

PRESSURE (PSIA)	**INLET TEMP. (°F)**	**OUTLET TEMP. (°F)**	**$\bar{C}_p$ (BTU/LB-°F)**
247.	0.04	13.73	0.3046
	0.04	21.05	0.3106
	0.04	25.29	0.3157
	67.65	86.24	0.2331
	67.65	120.87	0.2304
	122.16	135.21	0.2299
	122.16	159.79	0.2303
	122.16	173.11	0.2306
	176.26	190.95	0.2300
	176.26	234.30	0.2305
	176.26	247.73	0.2310
	55.88	68.08	0.2400
	13.73	21.05	0.3220
	21.05	25.29	0.3390
	25.29	26.39	0.3499
	26.39	26.75	0.3550
	28.01	33.87	0.2913
	33.87	41.32	0.2697
	41.32	49.20	0.2573
	86.24	120.87	0.2290
	135.21	159.79	0.2305
	159.79	173.11	0.2300
	190.95	234.30	0.2310
	234.30	247.73	0.2320
432.	-0.02	10.22	0.2997
	-0.02	25.35	0.3080
	-0.02	41.62	0.3177
	-0.02	47.68	0.3249
	122.11	133.22	0.2636
	122.11	154.94	0.2575
	122.11	176.72	0.2543
	55.94	59.28	0.4996
	55.94	62.94	0.5620
	55.94	65.51	0.6933
	68.00	70.11	0.8446
	68.00	82.48	0.5440
	68.00	119.88	0.3705
	10.22	25.35	0.3128
	25.35	41.62	0.3340
	41.62	47.68	0.3708
	55.94	59.28	0.4996
	59.28	62.94	0.6170
	62.94	65.51	1.0530
	67.23	72.16	0.7999
	72.16	87.11	0.4250
	70.11	82.48	0.4925
	82.48	119.88	0.3021
	133.22	154.94	0.2543
	154.94	176.72	0.2494

TABLE C-5 (Continued)

PRESSURE (PSIA)	INLET TEMP. (°F)	OUTLET TEMP. (°F)	$\overline{C}_p$ (BTU/LB-°F)
437.	55.96	61.80	0.4999
	55.96	65.17	0.5782
	55.95	66.21	0.6404
	55.96	66.83	0.7317
	55.97	67.08	0.8518
	55.95	67.19	1.0400
	55.96	67.27	1.1931
	55.97	67.53	1.3367
	56.00	68.40	1.4470
	56.11	69.58	1.4099
	61.80	65.17	0.7148
	65.17	66.21	1.1918
	66.21	66.83	2.2229
	66.83	67.08	5.7079
	67.08	67.19	20.4450
	67.19	67.27	22.0190
	67.27	67.53	7.5757
	67.53	68.40	2.8704
	68.40	69.58	0.8859
442.	55.95	61.85	0.4953
	55.96	65.43	0.5620
	55.96	66.62	0.6163
	55.96	67.46	0.6908
	55.96	67.86	0.7951
	55.96	68.06	0.9653
	55.96	68.34	1.1418
	55.96	68.76	1.2591
	55.96	69.96	1.3032
	55.96	71.41	1.2768
	61.85	65.43	0.6719
	65.43	66.62	1.0472
	66.62	67.46	1.6306
	67.46	67.86	3.8156
	67.86	68.06	10.9965
	68.06	68.34	8.8466
	68.34	68.76	4.6887
	68.76	69.96	1.7800
	69.96	71.41	1.0226

TABLE C-5 (Continued)

PRESSURE (PSIA)	INLET TEMP. (°F)	OUTLET TEMP. (°F)	$\overline{C_p}$ (BTU/LB-°F)
490.	67.65	71.33	0.6756
	67.65	72.84	0.7535
	67.65	74.20	0.8839
	67.65	75.78	1.1416
	67.65	77.91	1.2512
	67.65	77.12	1.2393
	67.65	79.74	1.2197
	67.65	87.74	0.9832
	67.65	110.83	0.6476
	67.65	121.11	0.5801
	71.33	72.84	0.9435
	72.84	74.20	1.3818
	74.20	75.78	2.2103
	75.78	77.12	1.8345
	77.12	77.91	1.3938
	77.91	79.74	1.0449
	79.74	87.74	0.6250
	87.74	110.83	0.3576
	110.83	121.11	0.2935
598.	68.00	77.77	0.4636
	68.00	83.43	0.5084
	68.00	85.59	0.5296
	68.00	88.44	0.5594
	68.00	91.36	0.5921
	68.00	96.76	0.6149
	68.00	106.48	0.5973
	68.00	120.49	0.5423
	77.77	83.43	0.5860
	83.43	85.59	0.6816
	85.59	88.44	0.7426
	88.44	91.36	0.8208
	91.36	96.76	0.7068
	96.76	106.48	0.5496
	106.48	120.49	0.3883

TABLE C-5 (Continued)

PRESSURE (PSIA)	INLET TEMP. (°F)	OUTLET TEMP. (°F)	$\overline{C_p}$ (BTU/LB-°F)
700.	67.65	75.30	0.3806
	67.65	83.97	0.4003
	67.65	91.16	0.4204
	67.65	96.54	0.4404
	67.65	101.03	0.4562
	67.65	98.80	0.4493
	67.65	97.69	0.4441
	67.65	104.63	0.4682
	67.65	111.28	0.4786
	67.65	121.54	0.4783
	75.30	83.97	0.4168
	83.97	91.16	0.4684
	91.16	96.54	0.5247
	96.54	97.69	0.5538
	98.80	101.03	0.5751
	101.03	104.63	0.5725
	97.69	98.80	0.5627
	104.63	111.28	0.5314
	111.28	121.54	0.4777
839.	67.57	75.91	0.3396
	67.57	91.85	0.3570
	67.57	105.55	0.3761
	67.57	100.60	0.3689
	67.57	113.06	0.3864
	67.57	110.02	0.3823
	67.57	116.27	0.3924
	67.57	121.35	0.3975
	75.91	91.85	0.3661
	91.85	100.60	0.4011
	100.60	105.55	0.4237
	105.55	110.02	0.4387
	110.02	113.06	0.4505
	113.06	116.27	0.4603
	116.27	121.35	0.4581

TABLE C-5 (Concluded)

PRESSURE (PSIA)	INLET TEMP. (°F)	OUTLET TEMP. (°F)	$\bar{C}_p$ (BTU/LB-°F)
1049.	122.09	123.94	0.3792
	122.09	128.04	0.3807
	122.09	132.67	0.3821
	122.09	149.91	0.3835
	122.09	175.19	0.3735
	134.02	138.10	0.3876
	123.94	128.04	0.3817
	128.04	132.67	0.3836
	132.67	149.91	0.3843
	149.91	175.19	0.3625
1398.	122.11	132.25	0.3311
	122.11	145.00	0.3337
	122.11	149.69	0.3346
	122.11	165.34	0.3373
	122.11	175.76	0.3379
	160.11	167.76	0.3418
	132.25	145.00	0.3358
	145.00	149.69	0.3394
	149.69	165.34	0.3421
	165.34	175.76	0.3412
1969.	0.02	10.61	0.2785
	0.02	41.53	0.2802
	0.02	68.95	0.2821
	67.61	77.30	0.2880
	67.61	92.20	0.2893
	67.61	122.01	0.2919
	122.93	134.74	0.2984
	122.93	163.61	0.3015
	122.93	175.60	0.3029
	176.20	181.02	0.3094
	176.20	188.52	0.3091
	176.20	213.76	0.3101
	176.20	230.37	0.3103
	176.20	248.93	0.3096
	10.61	41.53	0.2808
	41.53	68.95	0.2850
	77.30	92.20	0.2902
	92.20	122.01	0.2941
	134.74	163.61	0.3025
	163.61	175.60	0.3070
	181.02	188.52	0.3093
	188.52	213.76	0.3107
	213.76	230.37	0.3105
	230.37	248.93	0.3080

TABLE C-6

$\bar{\Phi}$ VALUES FOR C_2F_6

TEMPERATURE (°F)	INLET PRESS. (PSIA)	PRESS. DROP (PSID)	$\bar{\Phi}$ (BTU/LB-PSID)
0.	247.3	22.7	-0.00100
	432.1	23.2	-0.00049
	720.3	23.7	-0.00014
	992.7	24.3	0.00009
	1460.9	25.1	0.00036
	1968.7	25.9	0.00059
68.	384.5	109.6	-0.04578
	367.5	123.7	-0.04148
	404.3	94.2	-0.05303
	533.5	29.1	-0.01900
	699.0	28.2	-0.00658
	839.1	27.8	-0.00279
	990.7	27.7	-0.00179
	1496.3	27.7	-0.00102
	1969.1	28.1	-0.00066
122.	430.8	130.5	-0.02400
	613.1	67.5	-0.03800
	765.8	44.3	-0.03736
	918.4	36.0	-0.01970
	1015.3	33.8	-0.01276
	1213.6	31.7	-0.00692
	1398.2	31.1	-0.00420
	1613.1	31.1	-0.00232
	1814.0	31.0	-0.00171
	1969.0	31.0	-0.00123
176.	364.7	150.1	-0.01584
	516.1	80.5	-0.01787
	813.9	46.6	-0.01983
	1013.3	35.6	-0.01710
	1219.9	30.1	-0.01244
	1420.5	27.6	-0.00846
	1613.3	26.2	-0.00599
	1928.9	25.1	-0.00372
247.	473.5	123.8	-0.00997
	713.6	73.1	-0.01195
	913.1	55.4	-0.01243
	1013.2	49.6	-0.01200
	1413.2	36.5	-0.00867
	1873.2	31.0	-0.00530
	1721.2	32.0	-0.00633

TABLE C-7

ENTHALPY TRAVERSE DATA FOR C_2F_6

Pressure = 247. psia		Pressure = 432. psia	
Temperature (°F)	$\Delta \underline{H}$* (Btu/lb)	Temperature (°F)	$\Delta \underline{H}$** (Btu/lb)
11.93	4.169	59.36	1.644
19.25	6.524	61.77	2.924
23.49	7.972	63.01	3.865
25.26	8.620	64.15	4.568
25.29	9.563	65.32	5.730
25.30	11.856	65.60	6.576
25.31	18.192	65.65	6.579
25.31	30.679	65.77	7.075
25.32	35.015	65.91	7.485
26.50	38.202	65.96	8.450
32.07	39.723	65.96	9.473
39.52	41.710	65.97	11.688
47.40	43.753	66.00	13.516
		66.05	14.785
		66.24	15.743
		66.74	16.787
		67.33	18.260
		67.70	18.268

*$\Delta \underline{H}$ = 0. at 0.°F

**$\Delta \underline{H}$ = 0. at 55.97°F

REFERENCES

1. Angus, S., Armstrong, B., "International Thermodynamic Tables of the Fluid State, Argon, 1971", Butterworths, London, 1971.

2. Bird, R. B. et al., Transport Phenomena, John Wiley & Sons, Inc., 1960.

3. Bhirud, V. L., Powers, J. E., "Thermodynamic Properties of a 5 mole Percent Propane in Methane Mixture," University of Michigan, August, 1969.

4. Bird, R. B., Brock, J. R., A.I. Ch. E. J., 5, 436 (1959).

5. Carl, R. F., Pitzer, K. S., Ind. Eng. Chem., 50(2), 265 (1958).

6. Carnahan, B. et al., "Applied Numerical Methods," John Wiley & Sons, Inc., 1969.

7. Clusius, K., Z. Phys. Chem., B31, 459 (1936).

8. Clusius, K., Frank, A., Z. Phys. Chem., B42, 395 (1939).

9. Carney, R. A., et al., J. Mole. Spec., 7, 209 (1961).

10. Din, F., "Thermodynamic Functions of Gases," 2, Butterworths Scientific Publications, London, 1956.

11. E. I. du Pont de Nemours, "Thermodynamic Properties of 'Freon-116' Refrigerant," Wilmington, Dela. (1968).

12. Dymond, J. H., Smith, E. B., "A Compilation of Second and Third Virial Coefficients," Univ. Oxford (1964).

13. Douslin, D. R. et al., J. Chem. Thermodyn., 1 (3), 305 (1969).

14. Edmister, W. C., Petroleum Refiner, 27, 113, 314, 609 (1948).

15. Eucken, A., Verh. Deut. Phys. Ges., 18, 4 (1916).

16. Eucken, A., Hauck, F., Z. Phys. Chem., 134, 161 (1928).

17. Eubank, P. T., Smith, J. M., A.I.Ch.E.J., 8, 117 (1962).

18. Furtado, A. W., Ph.D. Thesis, Univ. of Mich., 1973.

19. Faulkner, R. C., Ph.D. Thesis, Univ. of Mich., 1959.

20. Flynn, G. P. et al., J. Chem. Phys, 51, 3860 (1969).

21. Grigor, A. F., Steele, W. A., J. Phys. Chem. Liq., 1, 129 (1968).

22. Gosman, A. L. et al., "Thermodynamic Properties of Argon from the Triple Point to 300K at Pressures to 1000 Atmospheres," NSRDS-NBS27, 1969.

23. Hall, L. A. et al., "A Bibliography of Thermophysical Properties of Argon from 0 to 300°K," NBS Technical Note 217, June, 1964.

24. Hilsenrath, J. et al., "Table of Thermal Properties of Gases," NBS Circ. No. 564 (1955).

25. Jones, Jr., M. L., Ph.D. Thesis, Univ. of Mich, 1961.

26. Kaganir, M. G., J. Ph. Ch. (Russian), 32, 1958.

27. Leong, K. S., "List of Experimental Specific Heat Determinations of A.M. Sirota," Technical Report No. 19, Univ. of Glasgow, 1966.

28. Leong, K. S., "List of Experimental Determinations of the Specific Enthalpy, Specific Heat and Joule-Thomson Coefficients of Steam," Technical Report No. 20, Univ. of Glasgow, 1966.

29. Lenoir, J. M. et al., A Paper Presented at 34th Midyear Meeting of A.P.I., Chicago, Ill., 1969.

30. Leland, T. W., Chappelear, P.S., Ind. Eng. Chem., 60 (7), 85 (1968).

31. Lee, A. L. et al., A.I.Ch.E.J., 10 (5), 694 (1964).

32. Lydersen, A. L. et al., Eng. Expt. Stat. Rept., 4, The Univ. of Wisconsin, Oct., 1955.

33. Lard, E. W., Horn, R. C., Anal. Chem., 32 (7), 878 (1960).

34. Miyazaki, T., Ph.D. Thesis, Univ. of Mich. 1973.

35. Mage, D. T., Ph.D. Thesis, Univ. of Mich. 1964.

36. Manker, E. A., Ph.D. Thesis, Univ. of Mich. 1964.

37. Mather, A. E., Ph.D. Thesis, Univ. of Mich. 1967.

38. Michels, A. et al., Physica, 24, 769 (1958).

39. Michels, A. et al., Physica, 15, 689 (1949).

40. Montgomery, J. B., Devries, T., J. Am. Chem. Soc., 64, 2372 (1942).

41. Pace, E. L., Aston, J. G., J. Am. Chem. Soc., 70, 566 (1948).

42. Powers, J. E., Proceedings Natural Gas Processors Association 48th Convention, 1969.

43. Pitzer, K. S., et al., J. Am. Chem. Soc., 77, 3433 (1955).

44. Pope, G. A., Ph.D. Thesis, Rice Univ., 1971.

45. Powers, J. E., Private Communications, 1971-1973.

46. Riedel, L., Chem-Ing. Tech., 26, 83 (1954).

47. Rivikin, S. L., Gukov, V. M., Teploenergetika, 15 (10), 72 (1968).

48. Reid, R. C., Sherwood, T. K., "The Properties of Gases and Liquids," McGraw-Hill, Inc., 2nd ed., 1968.

49. Roebuck, J. R., Osterberg, H., Phys. Rev., 46 (2), 785 (1934).

50. Rossini, F. D. *et al.*, "Selected Values of Physical and Thermodynamic Properties of Hydrocarbons and Related Compounds," Carnegie Press, Pittsburgh, Pa., 1953.

51. Sirota, A. M. *et al.*, Teploenergetika, 1960 (7).

52. Sirota, A. M., Shrago, Z. Kh., Teploenergetika, 15 (3), 1968.

53. Sherwood, T. K., J. Chem. Eng. Data, 7, 47 (1962).

54. "Selected Values of Properties of Chemical Compounds," Thermodynamic Research Center Data Project, Texas A & M Univ., Dec., 1967.

55. Vukalovich, M. P., Altunin, V. V., "Thermophysical Properties of Carbon Dioxide," Collets Ltd., London & Wellingborough, 1968.

56. Vasserman, A. A., Rabinovich, V. A., "Thermophysical Properties of Liquid Air and Its Components," Israel Program for Scientific Translations, Jerusalem, 1970.

57. Vasserman, A. A. *et al.*, "Thermophysical Properties of Air Components," Israel Program for Scientific Translations, Jerusalem, 1971.

58. Underwriters Laboratories Report.

59. Weiss, A. H., Joffee, J., Ind. Eng. Chem., 49, 120 (1957).

60. Walker, P. A., Ph.D. Thesis, Univ. of London, 1956.

61. Yesavage, V. F., Ph.D. Thesis, Univ. of Mich. 1968.